Synthesis and biochemical evaluation of multifunctional acetylcholinesterase inhibitor hybrids for treatment of Alzheimer's disease

by

Todd J. Eckroat

A dissertation submitted in partial fulfillment
of the requirements for the degree of
Doctor of Philosophy
(Medicinal Chemistry)
in the University of Michigan
2014

Doctoral committee:

Associate Professor Sylvie Garneau-Tsodikova, University of Kentucky, Co-Chair
Research Professor Scott D. Larsen, Co-Chair
Assistant Professor Mi Hee Lim
Professor Henry I. Mosberg
Assistant Professor Matthew B. Soellner

To my parents:

Thank you for all your love, prayers, and support.

Acknowledgements

First, I would like to thank my Ph.D. adviser, Dr. Sylvie Garneau-Tsodikova, for giving me the opportunity to join her lab and work with her over these past years. I am appreciative of all that she has taught me about science, writing, presenting, and life, and I am grateful for the monetary support and intellectual guidance she has provided. She has provided an excellent example of a successful scientist which I hope to emulate in my future career. I am also grateful that she allowed me the opportunity to move with her from the University of Michigan to the University of Kentucky. I would also like to thank my committee members: Dr. Scott Larsen, Dr. Mi He Lim, Dr. Henry Mosberg, and Dr. Matthew Soellner. I am grateful for the excellent guidance, direction, and support that they have provided throughout the course of my Ph.D. studies.

Over the course of my Ph.D. studies, I have had the opportunity to work with a remarkable group of people in the Garneau-Tsodikova lab. I would like to thank all of them for being great friends and a source of intellectual and social support. A few current and former members deserve special recognition. Dr. Keith Green has been a great resource over the years, from teaching me as 1st year rotator to answering science questions on a day-to-day basis and everything in between. The biochemical work presented in this dissertation would not have been possible without his skill and hard work. He is a remarkable scientist and valued friend. Dr. Jacob Houghton was also a great resource during his time in the lab, especially when it came to chemistry questions. He was also instrumental in getting the tacrine-mefenamic acid project up and running. Joshua Bornstein made significant contributions to the tacrine-mefenamic acid and tacrine linker projects presented in this dissertation, both synthetically and biochemically. He is a valued friend, and he could always be counted on for a laugh. Working with him made my time in the lab more enjoyable. Christopher Jones made important contributions to the tacrine-mefenamic acid and tacrine linker projects during his time in the lab. Rebecca Reed also made important

contributions to the tacrine linker project during her rotation in the lab. Dr. Abdelrahman Mayhoub was a great source of knowledge with regards to organic chemistry during his time in the lab, and his molecular modelling was essential to the tacrine-metal-Aβ project.

The work presented in this dissertation would not have been possible without the help of collaborators. I would like to thank Dr. Mi Hee Lim and the Lim lab for their collaboration on the metal-Aβ studies. In particular, I would like to thank Akiko Kochi for her work on the metal binding, Aβ, and BBB permeability studies presented in chapter 4. The results of these studies were essential to this dissertation, and I am appreciative of her hard work. I would also like to thank Dr. Mayland Chang at the University of Notre Dame for her collaboration on metabolism studies of selected compounds.

I would like to thank all of the people in the Life Sciences Institute, College of Pharmacy, and Department of Medicinal Chemistry at the University of Michigan that I have had the pleasure of working with during the course of my Ph.D. studies. In particular, I would like to thank Dr. George Garcia and Mark Nelson for their help, support, and guidance during the final stage of my Ph.D. studies. I am grateful that both went out of their way to help me get through a difficult stage. I would also like to thank Dr. Matthew Soellner for allowing me to rotate in his lab for a semester as a 1st year student. It was great experience, and I learned a lot. Dr. Scott Woehler was invaluable in providing NMR support in the College of Pharmacy.

Finally, I would like to thank my family and friends for their support throughout my life, particularly during the challenging time of graduate school. I would like to thank my parents, Larry and Cozella Eckroat, for their continuous love, prayers, and support. I could not ask for better parents. I would not be who I am today without them. I would like to thank my sister and brother-in-law, Andrea and Randy Konkol, and my nieces, Lauren and Meghan Konkol, for their love, support, and ability to bring a smile to my face. I have truly been blessed with a great family. I would also like to thank my girlfriend, Meagan Cauble, for her love and support during the last two years. Meeting her was a blessing, and I do not think I could have completed my Ph.D. without her by my side.

Preface

This dissertation is composed of five chapters and describes my Ph.D. studies aimed at the synthesis and biochemical evaluation of multifunction acetylcholinesterase (AChE) inhibitor hybrids for treatment of Alzheimer's disease (AD). Chapter 1 serves as an introduction to AD and describes the scope of the disease, its pathological hallmarks, and current treatments. Chapter 2 describes two series of tacrine- and 6-chlorotacrine-mefenamic acid hybrids. Several compounds that showed remarkable inhibition of AChE were identified from these series (Bornstein, J. J.; **Eckroat, T. J.**; Houghton, J. L.; Jones, C. K.; Green, K. D.; Garneau-Tsodikova, S. *Med Chem Commun* **2011**, *2*, 406-412.). Chapter 3 investigates the role of linker moieties in bifunctional tacrine hybrids through the synthesis of 6-chlorotacrine analogs and comparison to 6-chlortacrine-mefenamic acid hybrids in AChE inhibition assays (**Eckroat, T. J.**; Green, K. D.; Reed, R. A.; Bornstein, J. J.; Garneau-Tsodikova, S. *Bioorg Med Chem* **2013**, *21*, 3614-3623.). Chapter 4 describes the synthesis of a novel 6-chlorotacrine-metal-Aβ modulator hybrid. In addition to strong inhibition of AChE and BChE under various conditions, this compound showed the ability to interact with metal ions involved in AD, control metal-free and metal-induced Aβ aggregate assembly, and disaggregate preformed metal-free and metal-associated Aβ aggregates (Kochi, A.*; **Eckroat, T. J.***; Green, K. D.; Mayhoub, A. S.; Lim, M. H.; Garneau-Tsodikova, S. *Chem Sci* **2013**, *4*, 4137-4145. *Denotes equal contribution.). Chapter 5 suggests various future directions for these projects.

Table of Contents

Dedication……...ii

Acknowledgments……iii

Preface……v

List of Figures……x

List of Tables……xiv

List of Abbreviations……xv

Abstract…… xviii

Chapter

1. Alzheimer's disease (AD): background, epidemiology, pathological hallmarks, current treatments, and the multifunctional approach to treatment
   - 1.1. Background and epidemiology of AD……1
   - 1.2. Pathological hallmarks of AD……4
   - 1.3. Current treatments for AD……...6
   - 1.4. Multifunctional approach for treatment of AD……8
   - 1.5. References……...9
2. Tacrine-mefenamic acid hybrids for inhibition of acetylcholinesterase
   - 2.1. Abstract……13
   - 2.2. Introduction……...13
   - 2.3. Results and discussion……...15
     - 2.3.1. Synthesis……..15
     - 2.3.2. Biochemical evaluation……... 17
       - 2.3.2.1. AChE inhibition……..17
       - 2.3.2.2. Molecular modeling……21
   - 2.4. Conclusion……....24
   - 2.5. Materials and instrumentation……...24
   - 2.6. Methods…… 25

2.6.1. Chemical methods……...25
2.6.1.1. General procedure for the synthesis of 9-chlorotacrine derivatives….25
2.6.1.2. General procedure for attachment of amine linkers to tacrine and 6-chlorotacrine……...26
2.6.1.3. General procedure for esterification for the preparation of mefenamic acid linkers……..33
2.6.1.4. General procedure for attachment of linkers to mefenamic acid…….34
2.6.1.5. General procedure for ester hydrolysis of mefenamic acid linkers…..36
2.6.1.6. General procedure for coupling of tacrine and 6-chlorotacrine to mefenamic acid……...37
2.6.2. Biochemical and computational methods……71
2.6.2.1. *In vitro* AChE assay……71
2.6.2.2. Studies of the mode of inhibition……72
2.6.2.3. *In vitro* AChE ROS inactivation assay……72
2.6.2.4. Molecular modeling……73
2.7. References……73
3. Investigation of the role of linker moieties in bifunctional tacrine hybrids
3.1. Abstract……76
3.2. Introduction……...76
3.3. Results and discussion……...79
3.3.1. Synthesis……..79
3.3.2. Biochemical evaluation……... 80
3.3.2.1. Molecular modeling……80
3.3.2.2. AChE inhibition……..81
3.4. Conclusion……90
3.5. Materials and instrumentation……...91
3.6. Methods……..... 92
3.6.1. Chemical methods……... 92
3.6.1.1. Preparation of N^1-(6-chloro-1,2,3,4-tetrahydroacridin-9-yl)pentane-1,5-diamine……92

3.6.1.2. General procedure for attachment of alkyl amine linkers to 6-chlorotacrine……...93
3.6.1.3. General procedure for attachment of amino alcohol linkers to 6-chlorotacrine……...96
3.6.2. Biochemical and computational methods……97
3.6.2.1. *In vitro* AChE assay……97
3.6.2.2. Studies of the mode of inhibition……97
3.6.2.3. *In vitro* AChE ROS inactivation assay……98
3.6.2.4. Molecular modeling……98
3.7. References……99
3.8. Appendix……102
4. A novel hybrid of 6-chlorotacrine and metal-amyloid-β modulator for inhibition of acetylcholinesterase and metal-induced amyloid-β aggregation
4.1. Abstract……...111
4.2. Introduction……111
4.3. Results and discussion……113
4.3.1. Hybrid design and synthesis……...113
4.3.2. Biochemical evaluation…… 115
4.3.2.1. AChE inhibition……115
4.3.2.2. BChE inhibition……116
4.3.2.3. Effect of metals and Aβ on AChE inhibition……118
4.3.2.4. Effect of metals and Aβ on BChE inhibition……120
4.3.2.5. Metal binding……120
4.3.2.6. Aβ aggregation inhibition……123
4.3.2.7. Disaggregation of Aβ aggregates……125
4.3.2.8. Molecular modeling……..126
4.3.2.9. Blood-brain barrier (BBB) permeability……...127
4.4. Conclusion……..128
4.5. Materials and instrumentation……129
4.6. Methods…….. 130
4.6.1. Chemical methods…… 130

4.6.1.1. Preparation of 6-chloro-1,2,3,4-tetrahydroacridin-9-amine……..130
4.6.1.2. Preparation of N^1-((6-bromopyridin-2-yl)methyl)-N^4,N^4-dimethylbenzene-1,4-diamine……..130
4.6.1.3. Preparation of N^1-((6-((10-aminodecyl)amino)pyridin-2-yl)methyl)-N^4,N^4-dimethylbenzene-1,4-diamine……131
4.6.1.4. Preparation of 2-bromo-6-(1,3-dioxolan-2-yl)pyridine……131
4.6.1.5. Preparation of N^1-(6-(1,3-dioxolan-2-yl)pyridin-2-yl)-N^{10}-(6-chloro-1,2,3,4-tetrahydroacridin-9-yl)decane-1,10-diamine……... 132
4.6.1.6. Preparation of 6-((10-((6-chloro-1,2,3,4-tetrahydroacridin-9-yl)amino)decyl)amino)picolinaldehyde……... 133
4.6.1.7. Preparation of N^1-((6-((10-((6-chloro-1,2,3,4-tetrahydroacridin-9-yl)amino)decyl)amino)pyridin-2-yl)methyl)-N^4,N^4-dimethylbenzene-1,4-diamine……...133
4.6.2. Biochemical, biophysical, and computational methods……134
4.6.2.1. *In vitro* AChE and BChE assay……134
4.6.2.2. *In vitro* AChE and BChE ROS inactivation assay……134
4.6.2.3. Metal binding studies by UV-Vis and NMR spectroscopy……135
4.6.2.4. Aβ peptide experiments……135
4.6.2.5. Gel electrophoresis with Western blotting……136
4.6.2.6. Transmission electron microscopy (TEM)……136
4.6.2.7. Effect of metals and Aβ peptide on AChE and BChE inhibition…...137
4.6.2.8. Molecular modeling……..137
4.6.2.9. Parallel artificial membrane permeability assay adapted for blood-brain barrier (PAMPA-BBB)……139
4.7. References……...139
4.8. Appendix……143
5. Future directions ……...……145

List of Figures

Chapter 1

1.1. Percentage changes in selected causes of death from 2000-2010……2
1.2. Biochemical reactions catalyzed by ChAT and AChE……...5
1.3. Structures of FDA approved AD drugs……..6

Chapter 2

2.1. Structures of tacrine (**1**) and mefenamic acid (**2**)……..14
2.2. Synthetic schemes for the preparation of **A.** tacrine-containing portion of bifunctional molecules, **B.** mefenamic acid-containing portion of Series B of bifunctional compounds, **C.** Series A of tacrine- and 6-chlorotacrine-mefenamic acid bifunctional molecules, and **D.** Series B of tacrine- and 6-chlorotacrine-mefenamic acid bifunctional molecules……16
2.3. Representative examples of IC_{50} curves (**A**-**C**) and ROS IC_{50} curves (**D**-**E**) for selected compounds from Series A (**10b** and **10c**) and Series B (**13l**)……...21
2.4. Representative plot showing the non-competitive inhibition with respect to acetylthiocholine (ATC) for **10e** using four concentrations each of inhibitor and ATC……21
2.5. A selection of hybrid molecules docked in *Tc*AChE showing **A**. the interaction of the 6-chlorotacrine moiety of compounds **11c** (yellow) and **13m** (orange) with Trp84, Phe330, and His440 in the CAS, **B.** the proximity of the mefenamic acid moiety in compounds **10c** (yellow), **11e** (blue), and **13j** (magenta) to Tyr70 and Trp279 of the PAS, and **C.** the proximity of the mefenamic acid moiety of compounds **11c** (yellow) and **13m** (orange) to Trp279 and Tyr residues (70, 121, and 334) near the PAS…….....22

Chapter 3

3.1. **A.** Structures of tacrine (**1**), mefenamic acid (**2**), mefenamic acid with linkers (**9b-d**), and 6-chlorotacrine-mefenamic acid hybrids (**11a-f** and **13f-h**, **13j-l**, **13n-p**). **B.** Synthetic scheme for the preparation of 6-chlorotacrine amine linkers (**6b-i**), methyl linkers (**14a-f**), and hydroxyl linkers (**15a-b**)……..79

3.2. A selection of linker molecules docked in *Tc*AChE showing **A.** the interaction of 6-chlorotacrine amine linkers **6d** (magenta), **6f** (pink), **6g** (green), **6h** (yellow), and **6i** (orange) with residues Trp84, Phe330, and His440 near the CAS and Gln69, Tyr70, Asp72, and Gln74 near the PAS, **B.** the interaction of 6-chlorotacrine hydroxyl linkers **15a** (white) and **15b** (turquoise) with residues Trp84, Phe330, and His440 and Tyr70 and Asp72, **C.** a comparison of the binding of 6-carbon amine linker **6d** (magenta), 6-carbon methyl linker **14c** (yellow), and 6-carbon hydroxyl linker **15b** (turquoise) showing the proximity of the terminal functional group to Gln69, Tyr70, and Asp72, and **D.** a comparison of the binding of 6-chlorotacrine-mefenamic acid hybrid **11f** (orange) and 12-carbon amine linker **6i** (yellow) showing the proximity of the mefenamic acid moiety of **11f** with Tyr70, Trp279, and Tyr334 near the PAS and the terminal amine group of **6i** with Tyr70, Asp72, and Gln74…….80

3.3. Representative examples of IC_{50} curves (**A-D**) for selected 6-chlorotacrine with linkers (compounds **6d**, **6g**, **14c**, and **15b**). Inset in panels **A-D** are representative plots showing the non-competitive inhibition with respect to acetylthiocholine (ATC) for compounds **6d**, **6g**, **14c**, and **15b** using various concentrations of inhibitor and ATC……85

3.4. ^{1}H NMR in $CDCl_3$ for compound **6c**……..102

3.5. ^{13}C NMR in $CDCl_3$ for compound **6c**…….102

3.6. ^{1}H NMR in $CDCl_3$ for compound **14a**……103

3.7. ^{13}C NMR in $CDCl_3$ for compound **14a**……..103

3.8. ^{1}H NMR in $CDCl_3$ for compound **14b**……...104

3.9. ^{13}C NMR in $CDCl_3$ for compound **14b**……..104

3.10. ^{1}H NMR in $CDCl_3$ for compound **14c**……..105

3.11. ^{13}C NMR in $CDCl_3$ for compound **14c**…….105

3.12. ^{1}H NMR in $CDCl_3$ for compound **14d**……106
3.13. ^{13}C NMR in $CDCl_3$ for compound **14d**……106
3.14. ^{1}H NMR in $CDCl_3$ for compound **14e**……107
3.15. ^{13}C NMR in $CDCl_3$ for compound **14e**……107
3.16. ^{1}H NMR in $CDCl_3$ for compound **14f**……108
3.17. ^{13}C NMR in $CDCl_3$ for compound **14f**……108
3.18. ^{1}H NMR in $CDCl_3$ for compound **15a**……109
3.19. ^{13}C NMR in $CDCl_3$ for compound **15a**……109
3.20. ^{1}H NMR in $CDCl_3$ for compound **15b**……110
3.21. ^{13}C NMR in $CDCl_3$ for compound **15b**……110

Chapter 4

4.1. Structures of 6-chlorotacrine (**16**), 6-chlorotacrine linker (**6h**), N^1,N^1-dimethyl-N^4-(pyridin-2-ylmethyl)benzene-1,4-diamine, metal-Aβ modulator (**17**), metal-Aβ modulator linker (**18**), and hybrid of 6-chlorotacrine-metal-Aβ modulator (**19**)…… 113
4.2. Synthetic schemes for the preparation of **A.** 6-chlorotacrine (**16**), **B.** metal-Aβ modulator linker (**18**), and **C.** hybrid of 6-chlorotacrine-metal-Aβ modulator (**19**)…… 114
4.3. Metal binding studies of **A.** cpd **16**, **B.** cpd **6h**, **C.** cpd **18**, and **D.** cpd **19** with $CuCl_2$ (left) or $ZnCl_2$ (middle) by UV-Vis. **C** and **D.** right panel = Zn^{2+} binding of **18** or **19** by ^{1}H NMR. NMR spectra of **18** or **19** (black, 2.0 mM) with $ZnCl_2$ (red, 3.2 mM) in CD_3OD at rt……121
4.4. Metal binding studies of **19** with **A.** $CuCl_2$ or **B.** $ZnCl_2$ in the absence and presence of Aβ and/or AChE at pH 6.6 (Cu^{2+}) and 7.4 (Zn^{2+}), monitored by UV-Vis. Spectra of Aβ, **19**, [Aβ + **19**], [Aβ + MCl_2], [MCl_2 + **19**], and [Aβ + MCl_2 + **19** ± AChE] are depicted in black, light blue, orange, red, dark blue, and purple, respectively……...122
4.5. *In vitro* studies of the influence of **6h** and **16-19** on metal-free and metal-associated $Aβ_{1-40}$ aggregation with and without AChE. **A.** Scheme of the inhibition experiment. **B.** Visualization of various-sized Aβ species in the absence (left) and presence (right)

of AChE by gel electrophoresis with Western blot (anti-Aβ antibody, 6E10). **C.** TEM images of the 24 h incubated samples……124
4.6. Disaggregation studies using **6h** and **16-19** with and without AChE. **A.** Scheme of the disaggregation experiment. **B.** Visualization of various-sized $A\beta_{1-40}$ species in the absence (left) and presence (right) of AChE by gel electrophoresis with Western blot (anti-Aβ antibody, 6E10)……..126
4.7. Hybrid **19** docked with $A\beta_{1-40}$-*Tc*AChE complex. **A.** Interaction of **19** with *Tc*AChE (grey) and $A\beta_{1-40}$ (yellow/orange). **B.** Close-up of important interactions between **19** and W84, H440, and F330 (grey) from *Tc*AChE and H6, H13, and H14 (yellow) from $A\beta_{1-40}$……127
4.8. ^{1}H NMR in $CDCl_3$ for compound **18**……..143
4.9. ^{13}C NMR in $CDCl_3$ for compound **18**……143
4.10. ^{1}H NMR in $CDCl_3$ for compound **19**……144
4.11. ^{13}C NMR in $CDCl_3$ for compound **19**……..144

List of Tables

Chapter 2

2.1. Inhibition of *Ee*AChE activity by tacrine-mefenamic acid hybrids……..20

Chapter 3

3.1. Inhibition of *Ee*AChE activity by 6-chlorotacrine with linkers generated in this study……... 81

3.2. Comparison of inhibition of *Ee*AChE activity by combination of 6-chlorotacrine with linkers with mefenamic acid (**2**) or **9b-d** and by covalently linked 6-chlorotacrine-mefenamic acid hybrids……..86

Chapter 4

4.1. Inhibition of *Ee*AChE and *es*BChE activity by compounds **6h** and **16-19** and effect of M^{2+} and Aβ on IC_{50} of hybrid **19** under various conditions……..117

4.2. Values (MW, *c*log*P*, HBA, HBD, PSA, logBB, and -logP_e) for compounds **6h** and **16-19**…….128

List of Abbreviations

Aβ	Amyloid-β
ACh	Acetylcholine
AChE	Acetylcholinesterase
AChEi	Acetylcholinesterase inhibitor
AcOH	Acetic acid
AD	Alzheimer's disease
aq.	Aqueous
ATC	Acetylthiocholine
BBB	Blood-brain barrier
BChE	Butyrylcholinesterase
BSA	Bovine serum albumin
BTC	Butyrylthiocholine
CAS	Catalytic active site
CDC	Centers for Disease Control and Prevention
ChAT	Choline acetyltransferase
ChE	Cholinesterase
*c*logP	Calculated logarithm of octanol-H_2O partition coefficient
CNS	Central nervous system
DCC	*N*,*N'*-Dicylcohexylcarbodiimide
DETAPAC	Diethylenetriaminepentaacetic acid
DIPEA	Diisopropylethylamine
DMF	*N*,*N*-Dimethylformamide
DTNB	5,5'-Dithiobis(2-nitrobenzoic acid)
EAA	Excitatory amino acid
EDAC	*N*-(3-Dimethylaminopropyl)-*N'*-ethylcarbodiimide

eq	Equivalents
Et_3N	Triethylamine
EtOAc	Ethyl acetate
EtOH	Ethanol
FT-IR	Fourier transform infrared spectroscopy
HBA	Hydrogen bond acceptor
HBD	Hydrogen bond donor
HEPES	2-(4-(2-hydroxyethyl)piperazin-1-yl)ethanesulfonic acid
HIV	Human immunodeficiency virus
HOBt	Hydroxybenzotriazole
IC_{50}	Half maximal inhibitory concentration
LCMS	Liquid chromatography mass spectrometry
logBB	-0.0148 x PSA + 0.152 x *c*log*P* + 0.130
MeOH	Methanol
MW	Molecular weight
NFT	Neurofibrillary tangle
NMDAR	*N*-Methyl-D-aspartate receptor
NMR	Nuclear magnetic resonance spectroscopy
NSAID	Non-steroidal anti-inflammatory drug
PAMPA	Parallel artificial membrane permeability assay
PAS	Peripheral anionic site
PDB	Protein data bank
PET	Positron emission tomography
PSA	Polar surface area
ppm	Parts-per-million
PVDF	Polyvinylidene fluoride
R_f	Retention factor
ROS	Reactive oxygen species
rt	Room temperature
SAR	Structure activity relationship
SP	Senile plaque

SPECT	Single-photon emission computed tomography
TBS	Tris-buffered saline
TBS-T	Tris-buffere saline containing 0.1% Tween-20
TEM	Transmission electron microscopy
THF	Tetrahydrofuran
TLC	Thin layer chromatography
UV-Vis	UV-Visible spectroscopy

Abstract

Alzheimer's disease (AD) places a significant and dramatically increasing burden on society. While pathological hallmarks of this neurodegenerative disorder are known, the exact cause remains unclear. Acetylcholinesterase inhibitors (AChEis) may help with cognitive symptoms, but they are incapable of reversing disease progression. The multifunctional hybrid approach towards new AD treatments aims to combine two molecules, one of which is usually an AChEi, with beneficial properties for AD into a single chemical entity showing enhanced properties and capable of attacking multiple facets of the disease. Using this approach, several such hybrids were synthesized and characterized biochemically.

Tacrine was the first AChEi approved for the treatment of AD. Mefenamic acid is a non-steroidal anti-inflammatory drug capable of inactivating AChE through radicals generated in the presence of reactive oxygen species (ROS). Various tacrine- and 6-chlorotacrine-mefenamic acid hybrids were synthesized. Several were potent AChEis with low nanomolar IC_{50} values under standard conditions and in the presence ROS, the most potent being **13m** ($IC_{50} = 0.418 \pm 0.025$ nM, ROS $IC_{50} = 0.009 \pm 0.003$ nM). Compared to tacrine, **13m** exhibited >100-fold increase in potency under standard conditions and >20,000-fold increase in the presence of ROS.

Subsequent studies investigated the role of the linker and the need for covalent linkage of mefenamic acid in regards to AChE inhibition. Results suggest the mefenamic acid moiety in an amine-linked tacrine-mefenamic acid hybrid may not contribute to AChE inhibition under standard conditions, and the linker moiety alone may be responsible for the increase in potency. However, in the presence of ROS, there may be some advantage to amine-linked tacrine-mefenamic acid hybrids.

Additionally, 6-chlorotacrine-metal-amyloid-β modulator hybrid **19** was synthesized. **19** displayed potent inhibition of AChE (IC_{50} = 2.37 ± 0.29 nM) and butyrylcholinesterase (IC_{50} = 2.01 ± 0.12 nM). Inhibition was largely retained in the presence of ROS, Cu^{2+}/Zn^{2+}, and amyloid-β (Aβ). **19** showed remarkable multifunctionality through interaction with Cu^{2+}/Zn^{2+}, control of metal-free and metal-induced Aβ aggregate assembly, and disaggregation of preformed metal-free and metal-associated Aβ aggregates. A particularly promising compound, **19** represents one of the few tacrine hybrids designed to specifically target the interplay of AChE/Aβ/metals.

Chapter 1

Alzheimer's disease (AD): background, epidemiology, pathological hallmarks, current treatments, and the multifunctional approach to treatment

1.1. Background and epidemiology of AD

Despite the fact that it has been over 100 years since the progressive, neurodegenerative disorder known as Alzheimer's disease (AD) was first formally described in the scientific literature, there is still much we do not know about this devastating disease. The exact cause and sequence of events leading to disease onset and progression has eluded researchers despite the identification of numerous factors that are known to play a role. Current pharmacological treatments for AD may offer some relief from the well-known cognitive symptoms. However, research efforts to develop a drug that is able to halt or reverse disease progression remain ongoing. The burden that AD places on humanity, in terms of sheer number of people affected, is at its highest level ever and only expected to get worse. Clearly, research into understanding and treating the AD problem is an important endeavor, and this dissertation describes one approach.

AD is named for the German neuropathologist and clinician, Alois Alzheimer (b. 1864 d. 1915), who first reported on the disease.[1] Alzheimer's clinical work with dementia patient Auguste Deter, and subsequent post mortem examination of her brain and spinal cord tissues, led to his 1906 lecture in which he described his findings on the disease that now bears his name. Alzheimer's initial report included a symptomatic description of cognitive failures, as well as descriptions and drawings of senile plaques (SPs) and neurofibrillary tangles (NFTs). The official eponym "Alzheimer's disease" was first applied in a textbook by psychiatrist Emil Kraepelin in 1910, but research into understanding causes, symptoms, and treatments has only gained momentum over the last 30 years.[1,2] Today, the SPs and

NFTs first described by Alois Alzheimer are well recognized by doctors and researchers as pathological hallmarks of AD and potential targets for therapeutic intervention.

Over a century has passed since Alzheimer's initial report, and the scope of the disease has grown immensely. Consider that, in the United States alone, AD is estimated to affect a total of 5.2 million Americans, 96% of which are age 65 and older. Put another way, one in nine people age 65 and older suffer from AD, a prevalence that jumps to one in three when considering the population age 85 and older. By the year 2050, it is expected that nearly 1 million new cases of AD will be diagnosed annually, and the total number of people age 65 and older suffering from AD is projected to approach 14 million.[2] Globally, it is estimated that over 24 million people are suffering from AD.[3]

AD represents the 6th leading cause of death across all ages in the United States. Based on preliminary data, the Centers for Disease Control and Prevention (CDC) listed AD as the underlying cause of death for 84,691 people in 2011.[4] However, many people die after being diagnosed with and experiencing complications from AD, but other acute conditions (*e.g.* pneumonia), not AD, may be listed as the primary cause of death. Thus, the true number of deaths caused by AD is probably higher than the listed value. In addition, while this number is currently still well behind the numbers listed for other leading causes of death such as heart disease and cancer (both well over 500,000 people), it will likely grow significantly as the incidence of AD increases in the coming decades.[2,4] It should also be noted that AD showed a 68% increase in the number of deaths caused between the years 2000 and 2010 (Fig. 1.1). This is a dramatic

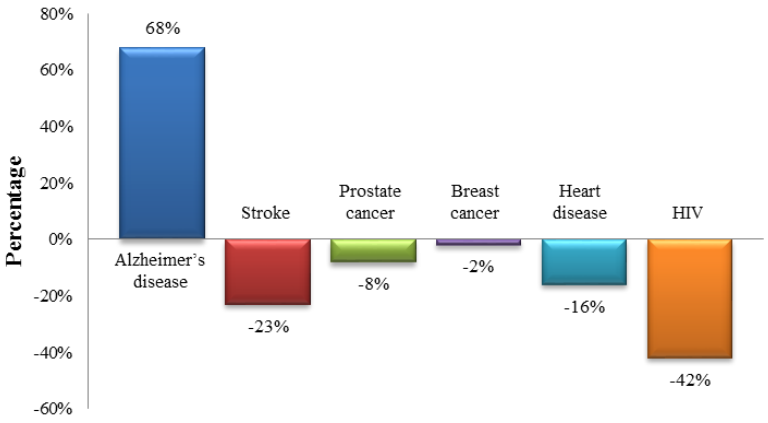

Fig. 1.1. Percentage changes in selected causes of death from 2000-2010. Reproduced from ref. 2.

increase, especially when compared to the percentage changes in other selected causes of death such as heart disease, stroke, prostate cancer, breast cancer, and human immunodeficiency virus (HIV), which showed decreases ranging from 2-42%.[2]

Age is the single biggest risk factor for developing AD, as the disease is seen primarily in individuals age 65 and over.[2,3,5] In fact, the dramatic projected rise in the incidence of AD can most likely be attributed to the ever increasing age of the population. For example, the average life expectancy at birth for someone born in 1900 was approximately 49 years, but for someone born in 2008 it was approximately 78 years.[6] Other risk factors for developing AD have been identified including cerebrovascular disease, diabetes, obesity, hypertension, dyslipidemia, depression, smoking, traumatic head injury, genetics, and family history.[2,3]

Symptoms of AD can be divided into three primary groups: (1) cognitive failures, (2) psychiatric and behavioral disturbances, and (3) difficulties in performing tasks of daily living.[2,5] Cognitive failures include things such as memory loss, language difficulties, and challenges in planning or solving problems. This group of symptoms, in particular the ability to remember new information, is usually the first to appear. The second group includes symptoms such as agitation, depression, and hallucinations. The third group of symptoms is the most severe, usually occurring in advanced stages of the disease, and prevents patients from being able to perform tasks such as eating, bathing, or dressing without assistance. It can also prevent those suffering from AD from being able to recognize family members or even speak. The progression from mild AD to severe AD varies between individual cases, but it is generally on the timescale of years.[5]

Postmortem histopathological examination of brain tissue is currently the only way to firmly confirm AD.[7] In view of the limited accessibility to living brain and other central nervous system (CNS) tissues, AD is currently diagnosed by the patient's primary care physician, and the process typically involves a mental state assessment through cognitive tests, physical and neurological examination, examination of family, medical, and psychiatric history, as well as interviews with the patient and family members or other

close individuals.[2,5,7] These diagnostic tools are problematic, especially in the early stages of the disease, due to the lack absolute sensitivity and accuracy. Therefore, as pathological hallmarks such as amyloid-β (Aβ) plaques (see section 1.2) precede the onset of dementia and cognitive decline in AD patients by years or even decades, their detection by nuclear imaging techniques such as positron emission tomography (PET) or single-photon emission computed tomography (SPECT) represents a promising new presymptomatic diagnostic tool for AD.[8-12]

1.2. Pathological hallmarks of AD

Billions of neurons are found in a healthy adult brain. These neurons are interconnected through an even greater number of synapses. Synapses are specialized junctions in which information flows in chemical pulses from a releasing neuron to a detecting neuron. The chemical flow of information is carried out by neurotransmitters (*e.g.* acetylcholine (ACh), dopamine, serotonin, glycine, opioid peptides). The interconnectivity of neurons through synapses and neurotransmitters is the biochemical basis of memories, emotions, thoughts, sensations, movements and skills. AD, through various mechanisms, leads to malfunctioning neurons and synapses.[2]

In general, AD is characterized by significant neurodegeneration and neuronal atrophy in the brain. Several specific pathological hallmarks of AD have been identified, and they include decreased cholinergic neurons and ACh levels, plaques caused by aggregation of the Aβ peptide, NFTs associated with irregular phosphorylation of the tau protein, inflammation and increased oxidative stress from reactive oxygen species (ROS), and dyshomeostasis of metal ions such as Cu^{2+} and Zn^{2+}.[2,13-21] Observation of these hallmarks has led to several hypotheses in attempts to explain the underlying cause of the disease. However, the exact cause and timeframe of events leading to AD remains unknown, and it is likely multifactorial and involves a complex array of factors.

ACh is known to play a role in learning and memory,[22-24] and the reduction of activity at cholinergic neurons in the brains of AD patients has been known for some time.[25,26] These facts led to the cholinergic hypothesis of AD, first proposed in 1982, in which cholinergic

deficit was seen as the primary cause of the disease. Although it has been met with some skepticism, the cholinergic hypothesis remains important in understanding AD today, and it has led to various treatments for AD (see section 1.3) aimed at restoring the cholinergic deficit.[15,27-29]

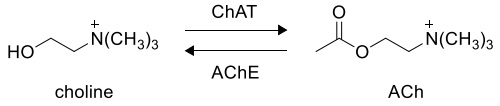

Fig. 1.2. Biochemical reactions catalyzed by ChAT and AChE.

Two enzymes play major roles in controlling brain ACh levels: choline acetyltransferase (ChAT) and acetylcholinesterase (AChE) (Fig. 1.2). ChAT catalyzes the synthesis of ACh from choline and acetyl-CoA, and levels of ChAT can be decreased by as much as 90% in individuals with severe AD when compared to normal.[30] AChE catalyzes the hydrolysis of ACh to choline and acetate, and its action is important for terminating synaptic transmission mediated by ACh. Butyrylcholinesterase (BChE), a related enzyme, is capable of catalyzing the same reaction. Of note, BChE levels are known to increase in AD patients, which may further exacerbate the problems caused by decreased ChAT levels.[30] Structurally, AChE is known to contain features that include a peripheral anionic site (PAS) near the exterior of the enzyme at the entrance of a gorge that leads to the catalytic active site (CAS) in the interior of the enzyme. The CAS contains the catalytic triad of serine, histidine, and glutamate that is responsible for the enzymatic reaction. The gorge leading to the CAS is about 20 Å long and lined with conserved aromatic amino acid residues. The PAS near the exterior of the enzyme also consists largely of aromatic residues, and it is thought to serve as a low affinity binding site to concentrate ACh at the gorge opening.[31-33] Interestingly, the PAS also plays a role in promoting the aggregation of Aβ peptides, another hallmark of AD.[34-37]

Aβ is a peptide processed from the amyloid precursor protein (APP) by β-secretase and γ-secretase enzymes.[38] The presence and possible role Aβ peptide aggregates in AD is well characterized in the literature, and the accumulation of extracellular Aβ plaques and Aβ oligomers is thought be essential for AD (the amyloid hypothesis of AD) as these aggregates interfere with communication between neurons and contribute to neuronal death, possibly through oxidative stress and mitochondrial dysfunction.[2,13,39-43] The

amyloid hypothesis of AD is supported by the fact that most common genetic mutations leading to AD are related to Aβ processing. Mutations in genes encoding APP and presenilin 1/2 (part of γ-secretase) are responsible for early-onset autosomal dominant AD, while the apolipoprotein E ε4 allele is a major risk factor for late-onset AD.[13,17,44,45] Metal ions, such as Cu^{2+} and Zn^{2+}, are known to interact with Aβ peptides, promote their aggregation, and increase neurotoxicity.[19,21,46-51] In addition, through their interaction with Aβ, these metal ions may lead to the production of ROS which, along with inflammatory responses, have also been implicated in the onset and progression of AD.[19,52-57]

Although not relevant to the work presented in subsequent chapters of this dissertation, a brief mention of tau pathology related to AD is warranted. Tau is a protein associated with microtubules that interacts with the neuronal cytoskeleton to help facilitate intracellular signaling processes. In a hyperphosphorylated state, tau can aggregate to form intracellular NFTs leading to microtubule dissociation, compromised axonal transport, and diminished synaptic function, and there is evidence that tau may act synergistically with Aβ to produce neuronal dysfunction.[13,58]

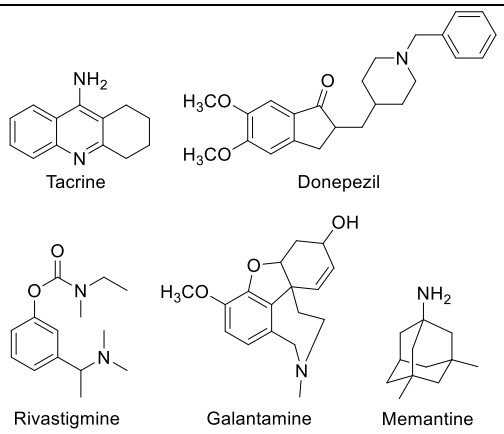

Fig. 1.3. Structures of FDA approved AD drugs.

1.3. Current treatments for AD

Current pharmacological therapies for AD are largely centered on AChE inhibitors (AChEis), which aim to decrease the rate of synaptic ACh decomposition leading to increased cholinergic transmission and improved cognitive function. Four out of the five drugs approved by the FDA for the treatment of AD (tacrine, donepezil, rivastigmine, and galantamine) are AChEis (Fig. 1.3), with the outlier being an *N*-methyl-D-aspartate receptor (NMDAR) antagonist (memantine). Although these have had moderate success, they only treat symptoms of AD, and, while symptomatic treatment is beneficial, it leaves much to be desired and offers little

hope for reducing projected cases of AD as AChEis are incapable of directly halting or reversing disease progression.[59]

Tacrine was the first AChEi approved for AD in 1993 for mild to moderate AD,[60] and it is known to be a potent inhibitor of BChE in addition to AChE. While still used widely for research purposes, tacrine is no longer used clinically because of poor pharmacokinetics that requires dosing four times a day and numerous side effects.[61] The most severe side effect was hepatotoxicity, most likely caused by metabolism to a hydroxylated analog followed by additional metabolism to a reactive quinone-like compound.[62,63]

Donepezil, which is marketed under the trade name Aricept®, is the most commonly prescribed AChEi for AD as it accounts for over 50% of the entire sales market of drugs for AD and is used in more than 75 countries and regions worldwide.[64] In the United States, studies have shown that over 60% of patients being treated with an AChEi for AD received donepezil while the remainder was nearly evenly split between those receiving galantamine and rivastigmine.[65] Donepezil was first approved by the FDA in 1996 for the treatment of mild to moderate AD.[66] Additionally, in 2007, it was approved for severe AD making it the only AChEi approved for the entire clinical spectrum of the disease.[67,68] Compared to its predecessor tacrine, donepezil shows a better pharmacological profile by exhibiting better oral bioavailability, longer duration of action, and fewer adverse events in patients. In particular, donepezil shows significantly less hepatotoxicity.[62,64] Overall, despite some controversy, numerous clinical studies in recent years have shown that donepezil is effective for the treatment of AD.[69-75]

Rivastigmine and galantamine were approved by the FDA for mild to moderate AD in 2000 and 2001, respectively. Both show better pharmacological profiles than tacrine, similar to that of donepezil.[61] Memantine was approved in 2003 for the treatment of moderate to severe AD. As an NMDAR antagonist, memantine works by partially protecting neurons from toxicity due to excessive glutamate release,[76] and evidence shows that memantine may have added benefits when use in combination with an AChEi.[77-79]

1.4. Multifunctional approach for treatment of AD

As mentioned above, current treatments for AD only address symptoms and are incapable of directly halting or reversing disease progression. This clearly indicates the need for new and improved therapeutics. In addition to offering improved treatment, the development of new and improved therapeutics for the treatment of AD can offer tools to aid in the understanding of the complex biochemical events surrounding the development and progression of AD. The work described in this dissertation employs a hybrid strategy towards the development of new therapeutics for AD relying on chemically linking a known AChEi with another compound capable of exerting other properties which are beneficial to the treatment of AD to create a bifunctional or multifunctional hybrid compound. This allows one hybrid to attack multiple facets of the disease at once. As evidenced through numerous examples in the literature, this has been a popular strategy over the past 15-20 years.[32,80-93]

Although the use of tacrine has been severely limited since its inception due to hepatotoxicity, it is often the AChEi of choice for designing multifunctional hybrids due to its AChE inhibitory properties and the ease at which synthetic derivatives such as the 9-chloro derivative,[88] which is susceptible to nucleophilic substitution for generating linked compounds, can be generated. By linking tacrine with another compound to create a multifunctional hybrid, it is possible to not only increase potency towards AChE inhibition but to also attack the multifactorial nature of AD. For example, a heptylene-linked tacrine dimer was shown to be 150-fold more potent than tacrine. This large increase in potency was likely due to the fact that the compound was capable of simultaneously binding to the CAS and PAS of the enzyme.[32,80] As another example, tacrine-8-hydroxyquinoline hybrids were shown to be potent inhibitors of AChE and antioxidants with low cell toxicity and the ability to complex copper ions, as well as the predicted ability to be able to disrupt AChE-mediated Aβ aggregation. The best compound from this series showed a remarkable 700-fold greater potency towards human AChE than tacrine.[81] Other examples will be discussed in subsequent chapters for comparison purposes.

Specifically, this dissertation describes the synthesis and biochemical evaluation of novel AChEi-ROS scavenger hybrid scaffolds and novel AChEi-metal-Aβ modulator hybrid scaffolds. Chapter 2 describes two series of tacrine- and 6-chlorotacrine-mefenamic acid hybrids. Several compounds that showed remarkable inhibition of AChE were identified from these series. Chapter 3 investigates the role of linker moieties in bifunctional tacrine hybrids through the synthesis of 6-chlorotacrine analogs and comparison to 6-chlortacrine-mefenamic acid hybrids in AChE inhibition assays. Chapter 4 describes the synthesis of a novel 6-chlorotacrine-metal-Aβ modulator hybrid. In addition to strong inhibition of AChE and BChE under various conditions, this compound showed the ability to interact with metal ions involved in AD, control metal-free and metal-induced Aβ aggregate assembly, and disaggregate preformed metal-free and metal-associated Aβ aggregates. Chapter 5 suggests various future directions for these projects.

1.5. References

(1) Ramirez-Bermudez, J. *Arch Med Res* **2012**, *43*, 595-599.
(2) Thies, W.; Bleiler, L. *Alzheimers Dement* **2013**, *9*, 208-245.
(3) Mayeux, R.; Stern, Y. *Cold Spring Harb Perspect Med* **2012**, *2*, a006239.
(4) Hoyert, D. L.; Xu, J. *National vital statistics reports* **2012**, *61*, no. 6.
(5) Burns, A.; Iliffe, S. *BMJ* **2009**, *338*, 467-471.
(6) Arias, E. *National vital statistics reports* **2012**, *61*, no. 3.
(7) Ono, M.; Saji, H. *J Pharmacol Sci* **2012**, *118*, 338-344.
(8) Klohs, J.; Rudin, M. *Neuroscientist* **2011**, *17*, 539-559.
(9) Rowe, C. C.; Ackerman, U.; Browne, W.; Mulligan, R.; Pike, K. L.; O'Keefe, G.; Tochon-Danguy, H.; Chan, G.; Berlangieri, S. U.; Jones, G.; Dickinson-Rowe, K. L.; Kung, H. P.; Zhang, W.; Kung, M. P.; Skovronsky, D.; Dyrks, T.; Holl, G.; Krause, S.; Friebe, M.; Lehman, L.; Lindemann, S.; Dinkelborg, L. M.; Masters, C. L.; Villemagne, V. L. *Lancet Neurol* **2008**, *7*, 129-135.
(10) Pike, K. E.; Savage, G.; Villemagne, V. L.; Ng, S.; Moss, S. A.; Maruff, P.; Mathis, C. A.; Klunk, W. E.; Masters, C. L.; Rowe, C. C. *Brain* **2007**, *130*, 2837-2844.
(11) Risacher, S. L.; Saykin, A. J. *Semin Neurol* **2013**, *33*, 386-416.
(12) Eckroat, T. J.; Mayhoub, A. S.; Garneau-Tsodikova, S. *Beilstein J Org Chem* **2013**, *9*, 1012-1044.
(13) Oboudiyat, C.; Glazer, H.; Seifan, A.; Greer, C.; Isaacson, R. S. *Semin Neurol* **2013**, *33*, 313-329.
(14) Castellani, R. J.; Perry, G. *Arch Med Res* **2012**, *43*, 694-698.
(15) Contestabile, A. *Behav Brain Res* **2011**, *221*, 334-340.
(16) Musial, A.; Bajda, M.; Malawska, B. *Curr Med Chem* **2007**, *14*, 2654-2679.
(17) Alonso Vilatela, M. E.; Lopez-Lopez, M.; Yescas-Gomez, P. *Arch Med Res* **2012**, *43*, 622-631.

(18) Pritchard, S. M.; Dolan, P. J.; Vitkus, A.; Johnson, G. V. *J Cell Mol Med* **2011**, *15*, 1621-1635.
(19) Jomova, K.; Vondrakova, D.; Lawson, M.; Valko, M. *Mol Cell Biochem* **2010**, *345*, 91-104.
(20) Budimir, A. *Acta Pharm* **2011**, *61*, 1-14.
(21) Pithadia, A. S.; Lim, M. H. *Curr Opin Chem Biol* **2012**, *16*, 67-73.
(22) Drachman, D. A.; Leavitt, J. *Arch Neurol* **1974**, *30*, 113-121.
(23) Drachman, D. A. *Neurology* **1977**, *27*, 783-790.
(24) Bartus, R. T. *Pharmacol Biochem Behav* **1978**, *9*, 833-836.
(25) Davies, P.; Maloney, A. J. *Lancet* **1976**, *2*, 1403.
(26) Perry, E. K.; Tomlinson, B. E.; Blessed, G.; Perry, R. H.; Cross, A. J.; Crow, T. T. *Lancet* **1981**, *2*, 149.
(27) Craig, L. A.; Hong, N. S.; McDonald, R. J. *Neurosci Biobehav Rev* **2011**, *35*, 1397-1409.
(28) Pepeu, G.; Giovannini, M. G. *Chem Biol Interact* **2010**, *187*, 403-408.
(29) Sugimoto, H. *Chem Biol Interact* **2008**, *175*, 204-208.
(30) Giacobini, E. *Int J Geriatr Psychiatry* **2003**, *18*, S1-5.
(31) Dvir, H.; Silman, I.; Harel, M.; Rosenberry, T. L.; Sussman, J. L. *Chem Biol Interact* **2010**, *187*, 10-22.
(32) Rydberg, E. H.; Brumshtein, B.; Greenblatt, H. M.; Wong, D. M.; Shaya, D.; Williams, L. D.; Carlier, P. R.; Pang, Y. P.; Silman, I.; Sussman, J. L. *J Med Chem* **2006**, *49*, 5491-5500.
(33) Bourne, Y.; Radic, Z.; Kolb, H. C.; Sharpless, K. B.; Taylor, P.; Marchot, P. *Chem Biol Interact* **2005**, *157-158*, 159-165.
(34) Inestrosa, N. C.; Alvarez, A.; Perez, C. A.; Moreno, R. D.; Vicente, M.; Linker, C.; Casanueva, O. I.; Soto, C.; Garrido, J. *Neuron* **1996**, *16*, 881-891.
(35) Alvarez, A.; Alarcon, R.; Opazo, C.; Campos, E. O.; Munoz, F. J.; Calderon, F. H.; Dajas, F.; Gentry, M. K.; Doctor, B. P.; De Mello, F. G.; Inestrosa, N. C. *J Neurosci* **1998**, *18*, 3213-3223.
(36) De Ferrari, G. V.; Canales, M. A.; Shin, I.; Weiner, L. M.; Silman, I.; Inestrosa, N. C. *Biochemistry* **2001**, *40*, 10447-10457.
(37) Bartolini, M.; Bertucci, C.; Cavrini, V.; Andrisano, V. *Biochem Pharmacol* **2003**, *65*, 407-416.
(38) Kreft, A. F.; Martone, R.; Porte, A. *J Med Chem* **2009**, *52*, 6169-6188.
(39) Hardy, J. A.; Higgins, G. A. *Science* **1992**, *256*, 184-185.
(40) Haass, C.; Selkoe, D. J. *Nat Rev Mol Cell Biol* **2007**, *8*, 101-112.
(41) Jakob-Roetne, R.; Jacobsen, H. *Angew Chem Int Ed Engl* **2009**, *48*, 3030-3059.
(42) Kurz, A.; Perneczky, R. *J Alzheimers Dis* **2011**, *24 Suppl 2*, 61-73.
(43) Wang, Y. J.; Zhou, H. D.; Zhou, X. F. *Drug Discov Today* **2006**, *11*, 931-938.
(44) Rao, A. T.; Degnan, A. J.; Levy, L. M. *AJNR Am J Neuroradiol* **2013**.
(45) Tanzi, R. E.; Bertram, L. *Cell* **2005**, *120*, 545-555.
(46) Drew, S. C.; Barnham, K. J. *Acc Chem Res* **2011**, *44*, 1146-1155.
(47) Faller, P.; Hureau, C. *Dalton Trans* **2009**, 1080-1094.
(48) Hureau, C. *Coord Chem Rev* **2012**, *256*, 2164-2174.
(49) Hureau, C.; Dorlet, P. *Coord Chem Rev* **2012**, *256*, 2175-2187.
(50) Savelieff, M. G.; Lee, S.; Liu, Y.; Lim, M. H. *ACS Chem Biol* **2013**, *8*, 856-865.

(51) Scott, L. E.; Orvig, C. *Chem Rev* **2009**, *109*, 4885-4910.
(52) McGeer, P. L.; McGeer, E. G. *Neurobiol Aging* **2007**, *28*, 639-647.
(53) McGeer, P. L.; Rogers, J.; McGeer, E. G. *J Alzheimers Dis* **2006**, *9*, 271-276.
(54) McGeer, P. L.; Schulzer, M.; McGeer, E. G. *Neurology* **1996**, *47*, 425-432.
(55) Joo, Y.; Kim, H. S.; Woo, R. S.; Park, C. H.; Shin, K. Y.; Lee, J. P.; Chang, K. A.; Kim, S.; Suh, Y. H. *Mol Pharmacol* **2006**, *69*, 76-84.
(56) Szekely, C. A.; Town, T.; Zandi, P. P. *Subcell Biochem* **2007**, *42*, 229-248.
(57) Quintanilla, R. A.; Orellana, J. A.; von Bernhardi, R. *Arch Med Res* **2012**, *43*, 632-644.
(58) Ittner, L. M.; Gotz, J. *Nat Rev Neurosci* **2011**, *12*, 65-72.
(59) Schliebs, R.; Arendt, T. *J Neural Transm* **2006**, *113*, 1625-1644.
(60) Davis, K. L.; Powchik, P. *Lancet* **1995**, *345*, 625-630.
(61) Mehta, M.; Adem, A.; Sabbagh, M. *Int J Alzheimers Dis* **2012**, *2012*, 728983.
(62) Ames, D. J.; Bhathal, P. S.; Davies, B. M.; Fraser, J. R. E. *Lancet* **1988**, *331*, 887.
(63) Pirmohamed, M.; Madden, S.; Park, B. K. *Clin Pharmacokinet* **1996**, *31*, 215-230.
(64) Takeda, M.; Tanaka, T.; Okochi, M. *Psychiatry Clin Neurosci* **2011**, *65*, 399-404.
(65) Mucha, L.; Shaohung, S.; Cuffel, B.; McRae, T.; Mark, T. L.; Del Valle, M. *J Manag Care Pharm* **2008**, *14*, 451-461.
(66) Black, S. E.; Doody, R.; Li, H.; McRae, T.; Jambor, K. M.; Xu, Y.; Sun, Y.; Perdomo, C. A.; Richardson, S. *Neurology* **2007**, *69*, 459-469.
(67) Winblad, B.; Jelic, V. *Alzheimer Dis Assoc Disord* **2004**, *18 Suppl 1*, S2-8.
(68) Jelic, V.; Darreh-Shori, T. *Clinical Medicine Insights: Therapeutics* **2010**, *2*, 771-788.
(69) Wallin, A. K.; Andreasen, N.; Eriksson, S.; Batsman, S.; Nasman, B.; Ekdahl, A.; Kilander, L.; Grut, M.; Ryden, M.; Wallin, A.; Jonsson, M.; Olofsson, H.; Londos, E.; Wattmo, C.; Eriksdotter Jonhagen, M.; Minthon, L. *Dement Geriatr Cogn Disord* **2007**, *23*, 150-160.
(70) Atri, A.; Molinuevo, J. L.; Lemming, O.; Wirth, Y.; Pulte, I.; Wilkinson, D. *Alzheimers Res Ther* **2013**, *5*, 6.
(71) Cummings, J. L.; Geldmacher, D.; Farlow, M.; Sabbagh, M.; Christensen, D.; Betz, P. *CNS Neurosci Ther* **2013**, *19*, 294-301.
(72) Sozio, P.; Cerasa, L. S.; Marinelli, L.; Di Stefano, A. *Neuropsychiatr Dis Treat* **2012**, *8*, 361-368.
(73) Takeda, A.; Loveman, E.; Clegg, A.; Kirby, J.; Picot, J.; Payne, E.; Green, C. *Int J Geriatr Psychiatry* **2006**, *21*, 17-28.
(74) Tariot, P.; Salloway, S.; Yardley, J.; Mackell, J.; Moline, M. *BMC Res Notes* **2012**, *5*, 283.
(75) Yang, Y. H.; Chen, C. H.; Chou, M. C.; Li, C. H.; Liu, C. K.; Chen, S. H. *J Clin Psychopharmacol* **2013**, *33*, 351-355.
(76) Parsons, C. G.; Stoffler, A.; Danysz, W. *Neuropharmacology* **2007**, *53*, 699-723.
(77) Patel, L.; Grossberg, G. T. *Drugs Aging* **2011**, *28*, 539-546.
(78) Sobow, T. *Expert Rev Neurother* **2010**, *10*, 693-702.
(79) Rountree, S. D.; Chan, W.; Pavlik, V. N.; Darby, E. J.; Siddiqui, S.; Doody, R. S. *Alzheimers Res Ther* **2009**, *1*, 7.
(80) Carlier, P. R.; Han, Y. F.; Chow, E. S.; Li, C. P.; Wang, H.; Lieu, T. X.; Wong, H. S.; Pang, Y. P. *Bioorg Med Chem* **1999**, *7*, 351-357.

(81) Fernandez-Bachiller, M. I.; Perez, C.; Gonzalez-Munoz, G. C.; Conde, S.; Lopez, M. G.; Villarroya, M.; Garcia, A. G.; Rodriguez-Franco, M. I. *J Med Chem* **2010**, *53*, 4927-4937.
(82) Fernandez-Bachiller, M. I.; Perez, C.; Campillo, N. E.; Paez, J. A.; Gonzalez-Munoz, G. C.; Usan, P.; Garcia-Palomero, E.; Lopez, M. G.; Villarroya, M.; Garcia, A. G.; Martinez, A.; Rodriguez-Franco, M. I. *ChemMedChem* **2009**, *4*, 828-841.
(83) Fernandez-Bachiller, M. I.; Perez, C.; Monjas, L.; Rademann, J.; Rodriguez-Franco, M. I. *J Med Chem* **2012**, *55*, 1303-1317.
(84) Bornstein, J. J.; Eckroat, T. J.; Houghton, J. L.; Jones, C. K.; Green, K. D.; Garneau-Tsodikova, S. *Med Chem Commun* **2011**, *2*, 406-412.
(85) Fang, L.; Kraus, B.; Lehmann, J.; Heilmann, J.; Zhang, Y.; Decker, M. *Bioorg Med Chem Lett* **2008**, *18*, 2905-2909.
(86) Camps, P.; Formosa, X.; Galdeano, C.; Munoz-Torrero, D.; Ramirez, L.; Gomez, E.; Isambert, N.; Lavilla, R.; Badia, A.; Clos, M. V.; Bartolini, M.; Mancini, F.; Andrisano, V.; Arce, M. P.; Rodriguez-Franco, M. I.; Huertas, O.; Dafni, T.; Luque, F. J. *J Med Chem* **2009**, *52*, 5365-5379.
(87) Camps, P.; Formosa, X.; Munoz-Torrero, D.; Petrignet, J.; Badia, A.; Clos, M. V. *J Med Chem* **2005**, *48*, 1701-1704.
(88) Hu, M. K.; Wu, L. J.; Hsiao, G.; Yen, M. H. *J Med Chem* **2002**, *45*, 2277-2282.
(89) Mao, F.; Huang, L.; Luo, Z.; Liu, A.; Lu, C.; Xie, Z.; Li, X. *Bioorg Med Chem* **2012**, *20*, 5884-5892.
(90) Marco-Contelles, J.; Leon, R.; de los Rios, C.; Samadi, A.; Bartolini, M.; Andrisano, V.; Huertas, O.; Barril, X.; Luque, F. J.; Rodriguez-Franco, M. I.; Lopez, B.; Lopez, M. G.; Garcia, A. G.; Carreiras Mdo, C.; Villarroya, M. *J Med Chem* **2009**, *52*, 2724-2732.
(91) Wang, Y.; Wang, F.; Yu, J. P.; Jiang, F. C.; Guan, X. L.; Wang, C. M.; Li, L.; Cao, H.; Li, M. X.; Chen, J. G. *Bioorg Med Chem* **2012**, *20*, 6513-6522.
(92) Kochi, A.; Eckroat, T. J.; Green, K. D.; Mayhoub, A. S.; Lim, M. H.; Garneau-Tsodikova, S. *Chem Sci* **2013**, *4*, 4137-4145.
(93) Chen, Y.; Sun, J.; Huang, Z.; Liao, H.; Peng, S.; Lehmann, J.; Zhang, Y. *Bioorg Med Chem* **2013**, *21*, 2462-2470.

Note:

A portion of this chapter was adapted from a published review article: **Eckroat, T. J.**; Mayhoub, A. S.; Garneau-Tsodikova, S. *Beilstein J Org Chem* **2013**, *9*, 1012-1044.

Chapter 2

Tacrine-mefenamic acid hybrids for inhibition of acetylcholinesterase

2.1. Abstract

Alzheimer's disease (AD) is a complex syndrome characterized by the degeneration of the brain and central nervous system that may be caused by an assortment of genetic and environmental factors. Consequently, a conjunctive approach targeting multiple affecters of AD could lead to improved drug candidates for the treatment of AD. A convergent chemical synthetic approach yielded a series of tacrine-mefenamic acid hybrids that were evaluated for their ability to inhibit acetylcholinesterase (AChE). A majority of the compounds tested showed low nanomolar IC_{50} values, an improvement over the parent compound, tacrine, suggesting that they could be effective in increasing cholinergic function. Additionally, an assay to evaluate the compounds upon exposure to reactive oxygen species (ROS) was performed, the results of which may suggest a role for the mefenamic acid moiety in the inhibition of AChE. Molecular modeling studies were performed to rationalize the experimental results.

2.2. Introduction

Alzheimer's disease (AD) is a progressive neurodegenerative disorder characterized by the atrophy of cholinergic neurons in areas of the brain vital for cognitive function, leading to symptoms that range from memory loss to the loss of motor abilities and eventually death. Pathologies associated with AD include the degeneration of brain cells due to the development of plaques and tangles associated with the aggregation of the protein fragment amyloid-β (Aβ) and the irregular phosphorylation of the Tau protein, respectively. Additionally, concurrent deficits in excitatory amino acid (EAA) transmission *via* acetylcholine (ACh) are observed due to substantial deficits in choline acetyltransferase (ChAT),[1-3] the enzyme responsible for the formation of ACh in the brain.

One of the primary pharmacological strategies employed in the treatment of AD has been inhibition of cholinesterases (ChEs). These therapies aim to decrease the rate of decomposition of ACh at synapses in the brain thereby raising the potential for increased levels of EAA transmission and improved cognitive function. This strategy has proved moderately successful, yielding potent reversible acetylcholinesterase inhibitors (AChEis) such as tacrine (**1**) (Fig. 2.1), donepezil, and galantamine, as well as substrate mimics such as neostigmine and pyridostigmine, all of which have shown benefit in the management of AD symptoms to varying degrees. However, despite the moderate clinical successes that have been observed, it has been suggested that these treatments, highlighted by clinical studies of donepezil, are not cost-effective and that an alternative approach may provide better outcomes.[4,5] Nonetheless, interest in developing improved ChE inhibitors for treatment of AD has increased recently, likely due to the body of empirical evidence showing the benefits of ChE inhibitors in AD patients as well as the lack of successful alternative approaches.

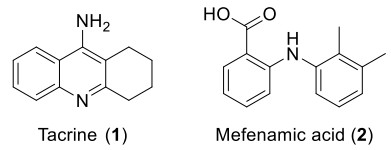

Fig. 2.1. Structures of tacrine (**1**) and mefenamic acid (**2**).

Other factors responsible for the onset and progression of AD have been identified, including inflammatory responses and the resultant increased oxidative stress in the form of free-radicals. The increase in oxidative stress related to the natural decline in an aging body's defense mechanisms often precedes the onset of the previously mentioned indications associated with AD. There is substantial epidemiological evidence linking the development of AD to inflammatory processes in the brain[6] as well as evidence that treatment with non-steroidal anti-inflammatory drugs (NSAIDs) may improve cognition and delay the progression of AD.[7-10] Given this information, it is evident that treatment of only a single determinant of the pathology of AD is not an effective approach. Furthermore, the evidence implies that treatment of multiple determinants of the disease, especially those related to oxidative stress, may provide synergistic effects.

One solution to this type of problem that has recently emerged is a conjunctive approach in which two biologically active molecules with similar or dissimilar mechanisms of action

are combined into a single molecule to improve potency and/or exhibit multiple modes of action, resulting in a synergistic effect. Tacrine-based dimers and hybrids with improved pharmacological properties have been the target of a number of discovery efforts in the past decade, leading in several cases to compounds with desirable synergy and improved potency.[11-15]

Based on the potential of reported tacrine-based molecules, we decided to take a similar approach in identifying compounds with the potential to serve as multi-functioning therapeutics. The ability of NSAIDS such as mefenamic acid (**2**) (Fig. 2.1) to inactivate enzymes, including AChE, in the presence of peroxidases and their potential for AD treatment has been well-characterized in the literature.[9,16-18] Studies have shown that mefenamic acid is capable of decreasing the occurrence of free-radicals and attenuating Aβ peptide-induced neurotoxicity while improving cognitive impairments.[10] Additionally, it has been suggested that AChE may accelerate the formation of stable amyloid fibrils and stable Aβ complexes.[19] This role is attributed to the peripheral anionic site (PAS) as propidium iodide, a PAS binding molecule, has proved effective in reducing Aβ aggregation while there are no similar reports implicating catalytic active site (CAS) inhibitors.[20] The numerous desirable properties of mefenamic acid led us to believe that it would be an ideal scaffold to incorporate into a series of tacrine-based hybrid molecules aimed at both the CAS and PAS, taking advantage of tacrine's affinity for the CAS and using it to guide the mefenamic acid portion of the molecules to the PAS. This type of strategy has been widely discussed in the literature and was recently reviewed.[21]

Herein, we report the synthesis and evaluation of a series of tacrine- and 6-chlorotacrine-mefenamic acid hybrid molecules aimed at combining the AChE inhibitor properties of tacrine with the antioxidant and AChE modulating properties of mefenamic acid into a single, dual-action molecule for the treatment of AD. This conjunctive medicinal chemistry approach led to the identification of nanomolar and sub-nanomolar inhibitors of AChE.

2.3. Results and discussion

2.3.1. Synthesis

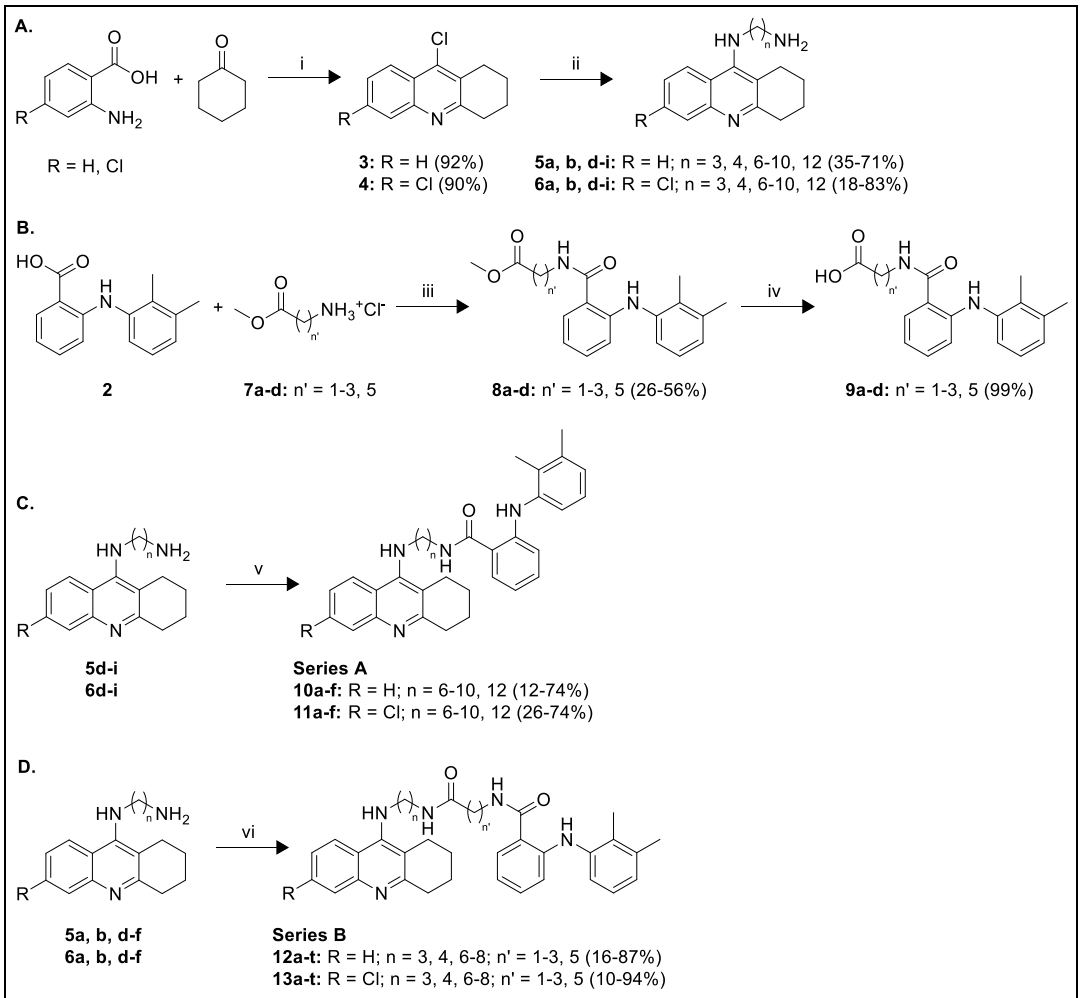

Fig. 2.2. Synthetic schemes for the preparation of **A.** tacrine-containing portion of bifunctional molecules, **B.** mefenamic acid-containing portion of Series B of bifunctional compounds, **C.** Series A of tacrine- and 6-chlorotacrine-mefenamic acid bifunctional molecules, and **D.** Series B of tacrine- and 6-chlorotacrine-mefenamic acid bifunctional molecules. *Reagents and conditions*: (i) $POCl_3$, Δ. (ii) $H_2N(CH_2)_nNH_2$ (3 eq), 1-pentanol, Δ. (iii) DCC (3 eq), HOBt (3 eq), DIPEA (7 eq), DMF. (iv) 1 M NaOH (H_2O), THF. (v) **2**, EDAC·HCl (1.1 eq), HOBt (1.1 eq), Et_3N (1.8 eq), DMF. (vi) **9a-d**, EDAC·HCl (1.1 eq), HOBt (1.1 eq), Et_3N (1.8 eq), DMF.

Figure 2.2 illustrates the convergent synthetic approach to the synthesis of tacrine-based bifunctional inhibitors of AChE comprised of mefenamic acid (**2**) connected to tacrine (**1**) or 6-chlorotacrine *via* a hydrophobic linker moiety which in some cases (Series B) contains an amide functionality. This approach allows for the fine tuning of the linker region in order to assess the optimal spacing between the two active molecules. The starting compounds 9-chlorotacrine (**3**) and 6,9-dichlorotacrine (**4**) were synthesized as previously reported (Fig. 2.2A).[22] The tacrine-containing portion of the bifunctional molecules (Series A and B) was prepared by an established method.[23] Nucleophilic aromatic substitution of

various diamines at the 9-Cl position of tacrine derivatives **3** and **4** gave **5a, b, d-i** and **6a, b, d-i** in yields from 18-83% (Fig. 2.2A). The mefenamic acid-containing portion of the bifunctional molecules of Series B was prepared by coupling methyl esters **7a-d** to **2** to yield **8a-d** in low to moderate yield. The subsequent hydrolysis of esters **8a-d** yielded compounds **9a-d** quantitatively (Fig. 2.2B). Compound **7a** was commercially available whereas **7b-d** were prepared using stoichiometric hydrochloric acid in methanol followed by evaporation of the solvents to yield the HCl salts in quantitative yield. The coupling of **5a, b, d-i** and **6a, b, d-i** with mefenamic acid or with **9a-d** gave compounds **10a-f** and **11a-f** (Series A) as well as compounds **12a-t** and **13a-t** (Series B), respectively (Fig. 2.2C,D). After purification by chromatographic techniques, the final bifunctional inhibitors were obtained in varying yields, 10-94%.

2.3.2. Biochemical evaluation

2.3.2.1. AChE inhibition

In order to evaluate the potential of the bifunctional compounds as therapeutic agents for the symptoms of AD, their IC_{50} values were determined *via* two biochemical assays (Table 2.1 and Fig. 2.3). The first assay, which employed the method of Ellman,[24] was used to determine the inhibitory potential of each molecule towards AChE from *Electrophorus electricus* (*Ee*AChE). All compounds of interest were incubated in the presence of the enzyme for 10 min before initiation of the enzymatic reaction with acetylcholine, allowing for binding of the potential inhibitors. Additionally, a ROS inhibition assay was performed according to the method of Muraoka and Miura to assess the potential of ROS-induced inactivation of AChE.[16] The compounds of interest were incubated in the presence of horseradish peroxidase and hydrogen peroxide prior to incubation with AChE in order to generate radical species. It is thought that mefenamic acid radical species generated by peroxidases that are triggered during inflammatory responses are capable of effectively inactivating AChE.[16] We hypothesized that by inhibiting the enzyme with tacrine while simultaneously using the tacrine moiety to direct the mefenamic acid radical to the vicinity of the AChE active site, we may see a synergistic effect evidenced by a decrease in the IC_{50} value relative to that obtained without ROS. In fact, this trend was observed for most of the tested compounds. All ROS IC_{50} values were within one order of magnitude or showed

improvement relative to their performance using the Ellman method. Interestingly, this trend is opposite of that seen with the parent compound, tacrine, suggesting the mefenamic acid moiety is contributing to the increased potency of the molecules.

An additional set of experiments were completed in which the assays were performed with a 1:1 equimolar ratio of mefenamic acid and tacrine in order to confirm that linking these two molecules was indeed beneficial. The results reported in Table 2.1 show that the best inhibitors did in fact outperform a 1:1 mixture, with compound **13m** being over 150-fold and 9300-fold more potent in the *Ee*AChE and ROS assays, respectively. These results confirm that linking the two molecules yields more potent inhibitors than concurrent exposure to the two parent compounds.

Series A showed an overall better performance in the assays, consistently yielding potent compounds, particularly in the ROS assay. All compounds tested were in the low nanomolar range with several molecules that were active at picomolar concentrations, showing drastic improvement over tacrine (AChE IC_{50} = 52.4 ± 7.3 nM, ROS AChE IC_{50} = 183 ± 21 nM). The data for Series A indicate that compounds with a 6-chlorotacrine moiety are more potent than their non-chlorinated tacrine counterparts, a trend observed in similar studies with tacrine hybrids.[12,15,25] A linker region comprised of 8 to 10 aliphatic carbons between the amine and amide nitrogen atoms of the respective parent molecules was found to be ideal for this series as several of these compounds showed sub-nanomolar IC_{50} values, the best being compounds **11c** and **11e** (Table 2.1).

Close examination of the data for Series B revealed several trends. The 6-chlorotacrine derivatives consistently outperformed their non-halogenated counterparts, similarly to Series A, a trend observed in a number of other studies.[12,15,25] Previous studies have also shown that the 6-Cl moiety may cause an increase in selectivity for AChE over butyrylcholinesterase (BChE), thus decreasing the occurrence of unwanted side effects.[11,12,15] An optimal length for the amide containing methylene linker between **1** and **2** was determined to be about 10 atoms, which was determined by direct comparison after adding the total number of methylene units to the amide atoms (n + n' + 2 = number of

atoms in linker). An optimal length for the methylene linker between tacrine and the amide nitrogen was determined to be n = 7 by a direct comparison of all molecules with a value of n = 3, 4, 5, 6, 7, and 8. Without exception, all compounds with n = 7 showed IC_{50} values below 50 nM. Following these two trends led to the most potent compound **13m** (AChE IC_{50} = 0.418 ± 0.025 nM, ROS AChE IC_{50} = 0.009 ± 0.003 nM). This compound exhibits >100-fold increase in potency in the AChE assay and >20,000-fold increase in the AChE ROS assay compared to the parent compound, tacrine (**1**).

In order to investigate the mode of inhibition of the tacrine-mefenamic acid hybrids, representative compounds from each series were selected and evaluated at constant inhibitor concentration and varying substrate concentrations. Surprisingly, Lineweaver-Burk analysis of the most potent compounds suggested that those inhibitors are non-competitive (Fig. 2.4). This is an interesting result considering what is known about tacrine's competitive mode of inhibition with regards to the natural acetylcholine substrate. A more likely scenario than the observed non-competitive inhibition, given what is known of tacrine, is that mixed inhibition is observed to some degree, but the non-competitive aspect dominates under the given reaction conditions. The inhibition assay indicated that tacrine acted as a competitive inhibitor. It may not be ruled out as a possibility that tacrine is interacting with the CAS, disrupting the enzyme function, and in fact, analysis of a selection of weaker inhibitors (data not shown) indicated mixed inhibition patterns in a Lineweaver-Burk analysis. Studies of similar compounds, in which a class of hydrocarbon-linked tacrine dimers were co-crystallized with AChE from *Torpedo californica* (*Tc*AChE), suggested that the tacrine moieties may also interact *via* π-π stacking with the heterocyclic residues of the PAS.[26] Given this crystallographic evidence, another plausible scenario in which the reported compounds interact with the PAS, but do not form additional contacts with the CAS, could explain this non-competitive pattern of inhibition. Interestingly, a recent study of tacrine-ferulic acid hybrids showed a similar non-competitive inhibition profile,[27] while many other hybrids' mode of inhibition was not reported, but rather assigned based on docking studies. However, the exact mode of interaction may not be strictly defined based on the current study, and will be the target of future research efforts with this interesting set of compounds.

Table 2.1. Inhibition of *Ee*AChE activity by tacrine-mefenamic acid hybrids.

Compound[a]	Series	R	n	n'	IC_{50} (nM)	ROS IC_{50} (nM)
1					52.4 ± 7.3	183 ± 21
2					> 1.25 mM	6120 ± 680
1 and 2 (1:1 mix)					68.7 ± 3.8	83.9 ± 0.4
3					> 25 μM	
4					> 50 μM	
Neostigmine					4.6 ± 1.0	
Pyridostigmine					82.0 ± 1.5	
10a	**A**	H	6		2.24 ± 0.11	0.129 ± 0.030
10b	**A**	H	7		1.39 ± 0.21	25.2 ± 4.5
10c	**A**	H	8		75.5 ± 19.2	0.045 ± 0.015
10d	**A**	H	9		1.54 ± 0.17	15.1 ± 0.2
10e	**A**	H	10		385 ± 48	0.908 ± 0.267
10f	**A**	H	12		50.9 ± 1.4	6.94 ± 1.42
11a	**A**	Cl	6		7230 ± 187	1.02 ± 0.36
11b	**A**	Cl	7		1380 ± 340	29.8 ± 4.0
11c	**A**	Cl	8		0.495 ± 0.064	1.49 ± 0.30
11d	**A**	Cl	9		6.94 ± 0.66	6.72 ± 0.78
11e	**A**	Cl	10		0.776 ± 0.108	1.85 ± 0.11
11f	**A**	Cl	12		2360 ± 830	16.2 ± 1.8
12a	**B**	H	3	1	87.3 ± 33.6	47.5 ± 11.5
12b	**B**	H	3	2	3800 ± 280	7.92 ± 1.96
12c	**B**	H	3	3	3730 ± 253	23.0 ± 9.0
12d	**B**	H	3	5	811 ± 70	20.2 ± 6.5
12e	**B**	H	4	1	262 ± 68	53.6 ± 3.8
12f	**B**	H	4	2	426 ± 86	2.43 ± 0.36
12g	**B**	H	4	3	89.7 ± 11.3	14.6 ± 2.4
12h	**B**	H	4	5	1860 ± 290	34.0 ± 9.0
12i	**B**	H	6	1	18.3 ± 4.0	54.8 ± 4.7
12j	**B**	H	6	2	985 ± 95	40.2 ± 8.4
12k	**B**	H	6	3	195 ± 27	29.9 ± 11.1
12l	**B**	H	6	5	1440 ± 197	34.0 ± 2.4
12m	**B**	H	7	1	5.55 ± 1.21	15.3 ± 6.6
12n	**B**	H	7	2	13.9 ± 1.4	1.02 ± 0.36
12o	**B**	H	7	3	8.09 ± 0.91	44.6 ± 1.2
12p	**B**	H	7	5	3.60 ± 0.16	3.66 ± 0.24
12q	**B**	H	8	1	3.30 ± 0.75	17.2 ± 4.3
12r	**B**	H	8	2	8.58 ± 1.42	4.07 ± 0.56
12s	**B**	H	8	3	17.4 ± 6.2	14.6 ± 5.2
12t	**B**	H	8	5	18.7 ± 5.0	6.26 ± 1.79
13a	**B**	Cl	3	1	28.1 ± 5.2	3.10 ± 0.94
13b	**B**	Cl	3	2	20.3 ± 1.4	21.3 ± 3.3
13c	**B**	Cl	3	3	7.13 ± 0.41	1.03 ± 0.22
13d	**B**	Cl	3	5	1.65 ± 0.33	7.85 ± 2.45
13e	**B**	Cl	4	1	156 ± 34	89.4 ± 6.2
13f	**B**	Cl	4	2	2470 ± 98	33.0 ± 9.3
13g	**B**	Cl	4	3	13.6 ± 1.8	12.4 ± 1.8
13h	**B**	Cl	4	5	37.4 ± 9.4	0.299 ± 0.067
13i	**B**	Cl	6	1	7.65 ± 0.24	3.46 ± 0.49
13j	**B**	Cl	6	2	1.14 ± 0.31	2.96 ± 0.41
13k	**B**	Cl	6	3	41.7 ± 11.5	15.6 ± 1.5
13l	**B**	Cl	6	5	2.94 ± 0.45	7.39 ± 1.51
13m	**B**	Cl	7	1	0.418 ± 0.025	0.009 ± 0.003
13n	**B**	Cl	7	2	6.67 ± 1.82	10.0 ± 1.6
13o	**B**	Cl	7	3	7.91 ± 0.69	6.55 ± 1.66
13p	**B**	Cl	7	5	11.1 ± 1.1	13.4 ± 3.9
13q	**B**	Cl	8	1	39.8 ± 3.3	18.1 ± 3.7
13r	**B**	Cl	8	2	18.3 ± 5.5	4.97 ± 0.26
13s	**B**	Cl	8	3	17.0 ± 3.0	6.59 ± 0.83
13t	**B**	Cl	8	5	80.1 ± 16.6	8.67 ± 0.73

[a] See Fig. 2.2 for chemical structures.

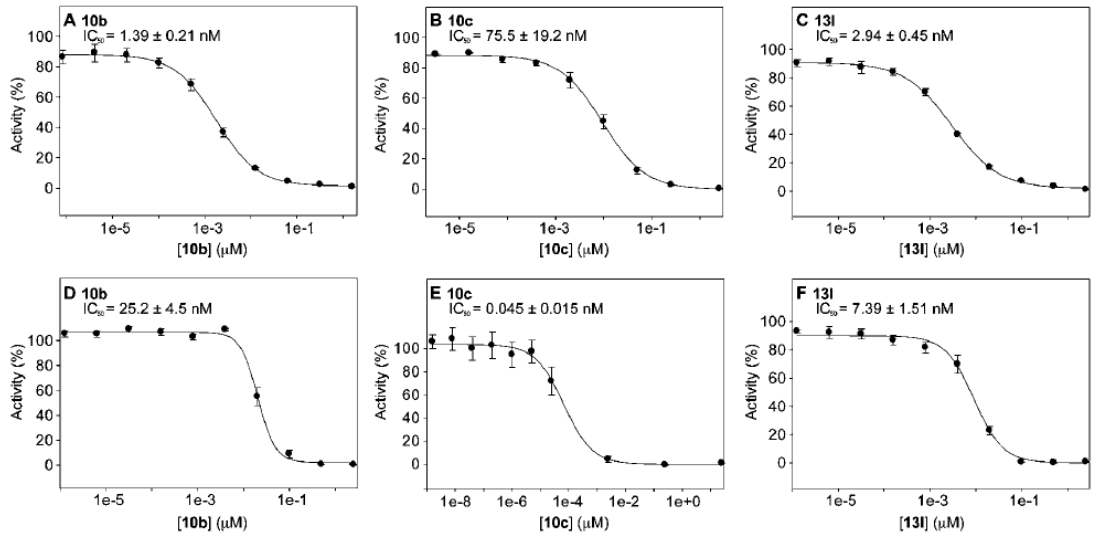

Fig. 2.3. Representative examples of IC_{50} curves (**A**-**C**) and ROS IC_{50} curves (**D**-**E**) for selected compounds from Series A (**10b** and **10c**) and Series B (**13l**).

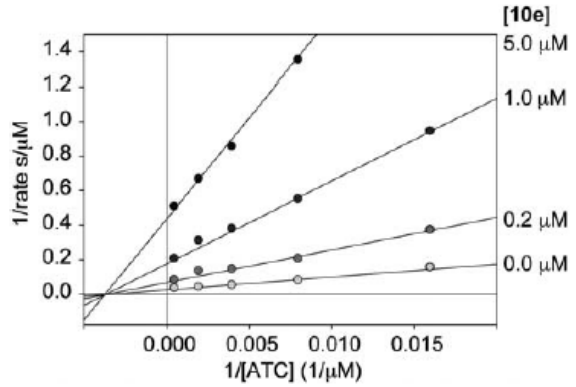

Fig. 2.4. Representative plot showing the non-competitive inhibition with respect to acetylthiocholine (ATC) for **10e** using four concentrations each of inhibitor and ATC.

2.3.2.2. Molecular modeling

In order to elucidate the trends observed in the inhibition data, molecular modeling experiments were performed with a selection of the most potent molecules. A structure of *Tc*AChE complexed with tacrine (PDB: 1ACJ)[28] was used for the modeling studies. Although the following results remain speculative in the absence of crystallographic data, they do provide a basis for rationalizing the observed trends. Our goal was to visualize the interactions of the three sections of our inhibitors with their suspected regions of interaction in the *Tc*AChE active site: the tacrine moiety, the linker region, and the mefenamic acid moiety with the CAS, the mid-gorge region, and the PAS, respectively. Modeling was performed using AutoDock. The best scoring conformations in terms of energetics were selected after 100 docking iterations focused around the active site (see experimental section for further details). Models of several tacrine-mefenamic acid hybrids were constructed, all of which suggested strong interactions between the energy minimized hybrids and the enzyme complex. A selection

of these results are depicted in Fig. 2.5.

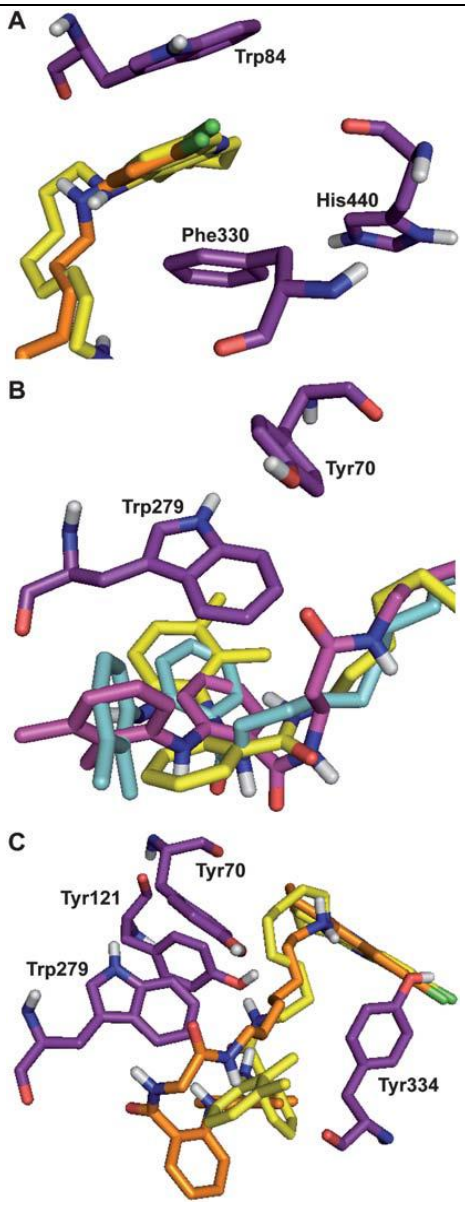

Fig. 2.5. A selection of hybrid molecules docked in *Tc*AChE showing **A**. the interaction of the 6-chlorotacrine moiety of compounds **11c** (yellow) and **13m** (orange) with Trp84, Phe330, and His440 in the CAS, **B.** the proximity of the mefenamic acid moiety in compounds **10c** (yellow), **11e** (blue), and **13j** (magenta) to Tyr70 and Trp279 of the PAS, and **C.** the proximity of the mefenamic acid moiety of compounds **11c** (yellow) and **13m** (orange) to Trp279 and Tyr residues (70, 121, and 334) near the PAS. Oxygen, nitrogen, and hydrogen atoms are shown in red, blue, and white, respectively.

The energy-minimized complexes of all molecules modeled predicted that the tacrine portion would be situated in the CAS. In accordance with similar docking studies of tacrine containing molecules, the quinoline ring system is stacked between Trp84 and Phe330 while the nitrogen atom of the ring is positioned such that it indicates the formation of a hydrogen bond with the backbone carbonyl of His440 (Fig. 2.5A). This is consistent with previous docking studies that used tacrine-based molecules with *Tc*AChE[25,29] and suggests that these tacrine-mefenamic acid hybrids could be capable of acting as substrate competitive inhibitors like tacrine (Fig. 2.5A-C). We suspect that the non-competitive or mixed-mode of inhibition may arise from additional beneficial interactions that are not predicted by these modeling experiments.

The methylene linker portion of both series spans the active-site gorge, allowing the tacrine and mefenamic acid moieties to interact with the CAS and PAS, respectively. There are

approximately 16 Å between the two binding sites from the quinolone ring nitrogen atom,[30] and a similar distance is observed in the *Tc*AChE structure used in this study. As mentioned, a linker length of approximately 10 atoms showed the strongest inhibition in the biochemical assays. This trend is not perfectly defined across the two series of inhibitors with regards to inhibition data, and the same is true of the modeling studies, which fail to further elucidate specific beneficial interactions. Yet, it is quite clear that a linker length of approximately 8-10 atoms, with or without an amide bond, would allow for the mefenamic acid portion to interact with the PAS if the tacrine moiety bound in the CAS.

A great deal of variability in the orientation of the mefenamic acid moiety was observed in the molecules docked. Variations in the interactions of the linker section may explain the inconsistencies observed with the mefenamic acid moiety. One trend that is immediately apparent is the ability of the tacrine moiety, if bound in the CAS, to direct the mefenamic acid to the vicinity of the PAS (Fig. 2.5B). Mefenamic acid is thought to deactivate AChE through a free-radical mechanism, not through specific interaction or modification of the CAS.[16] Our modeling studies showed that the mefenamic acid moiety would be in close proximity to Trp279 as well as tyrosines (Tyr70, 121, and 334) near the PAS (Fig. 2.5C), which may have two implications.

Since IC_{50} values were dependent on the enzyme concentration, it was hypothesized that the low IC_{50} values observed in the ROS assay may be due to the inactivation of some amount of the enzyme by radicals through interaction with tyrosine or tryptophan residues proximal to the PAS, which provides another possible explanation for the non-competitive or mixed-mode of inhibition (Fig. 2.5B,C). It is known that AChE has an adhesion function, located at the PAS, that governs AChE's interactions with Aβ and is believed to induce Aβ fibril formation.[19,31,32] Perturbation of the PAS by a number of small molecules and antibodies has been shown to inhibit Aβ fibril formation, presumably by blocking the interaction at the PAS.[19,33] Consequently, we believe that the tacrine-mefenamic acid hybrids reported herein may be capable of disrupting Aβ fibril formation and further experiments will be carried out to determine whether or not this is the case.

2.4. Conclusion

Tacrine-mefenamic acid hybrid molecules were synthesized *via* an easily accessible, convergent synthetic route and evaluated as inhibitors of AChE in two biochemical assays. The compounds appeared to act as non-competitive or mixed-mode inhibitors with respect to acetylthiocholine in the instances tested, and most were capable of inducing a half-maximal enzymatic response at low nanomolar concentrations with instances of picomolar IC_{50} values observed. One plausible explanation is that mixed inhibition is observed with a predominantly non-competitive mode of inhibition being observed for the most potent inhibitors tested. Several sub-nanomolar inhibitors were identified and selected for molecular modeling experiments. Taken together, the results suggest that the tacrine portion of the inhibitors may be capable of binding in the AChE CAS, spanning the active-site gorge *via* a methylene-based linker, and positioning the mefenamic acid moiety to interact with the PAS. While there is some discrepancy between the modeling studies and analysis of the mode of inhibition, these compounds provide the framework for the development of novel AChE inhibitors that may be capable of alleviating the symptoms of AD associated with a decrease in cholinergic function and may also be capable of diminishing Aβ aggregation to the extent that AChE is involved. Along with a more thorough investigation aimed at determining the mechanism by which AChE function is reduced by these inhibitors, further optimization studies aimed at improving potency and determining the possible secondary effects of the hybrid molecules are currently underway.

2.5. Materials and instrumentation

All reagents were purchased from Sigma-Aldrich (St. Louis, MO, USA) and used without further purification. Reactions were monitored by TLC (Merck, Silica gel 60 F_{254}). Visualization was achieved using one or more of the following methods: UV absorption by fluorescence quenching, a cerium-molybdate stain ($(NH_4)_2Ce(NO_3)_6$ (5 g), $(NH_4)_6Mo_7O_{24}•4H_2O$ (120 g), H_2SO_4 (80 mL), H_2O (720 mL)), a ninhydrin stain (ninhydrin (1.5 g), *n*-butanol (100 mL), AcOH (3 mL)), a $KMnO_4$ stain ($KMnO_4$ (1.5 g), K_2CO_3 (10 g), NaOH (1.25 mL 10%), H_2O (200 mL)), a bromocresol green stain (bromocresol green (0.04 g), EtOH (100 mL, absolute), slowly drip NaOH (0.1 M) until the solution just turns pale blue), or Dragendorff's reagent (solution A: $BiNO_3$ (0.17 g) in

AcOH (2 mL), H_2O (8 mL); solution B: KI (4 g) in AcOH (10 mL) and H_2O (20 mL). Solutions A and B were mixed and diluted to 100 mL with H_2O). Compounds were purified by SiO_2 flash chromatography (Dynamic Adsorbents Inc., Flash Silica Gel 32-63u). ^1H NMR and ^{13}C NMR spectra were recorded on Bruker Avance™ DPX 300 or 500 or Varian 400 MHz spectrometers. Liquid chromatography mass spectrometry (LCMS) was performed on a Shimadzu LCMS- 2019EV equipped with a SPD-20AV UV-Vis detector and a LC-20AD liquid chromatograph. IR measurements were taken by using a Perkin-Elmer SpectrumBX FT-IR system. Analyses by UV-Vis assays were done on a multimode SpectraMax M5 plate reader using 96-well plates (Fisher Scientific). Molecular modeling was performed using AutoDock 4.2 and Cygwin 1.7.

2.6. Methods

2.6.1. Chemical methods

2.6.1.1. General procedure for the synthesis of 9-chlorotacrine derivatives

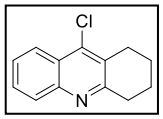

9-Chloro-1,2,3,4-tetrahydroacridine (3). The known compound **3**[22] was prepared using the following procedure. To a mixture of anthranilic acid (5.00 g, 36.5 mmol, 1 eq) and cyclohexanone (4.0 mL, 38.6 mmol, 1.1 eq) at 0 °C was carefully added $POCl_3$ (20 mL, 214.5 mmol, 5.9 eq). After being refluxed for 2 h, the reaction was cooled down to rt and concentrated under reduced pressure. The crude product was diluted with EtOAc (100 mL) and neutralized with a 10% aq. K_2CO_3 solution. The organic layer was washed with brine (2x100 mL), dried ($MgSO_4$), filtered, and concentrated under reduced pressure. Further purification by flash column chromatography (SiO_2; 5:1/hexane:EtOAc, R_f 0.59 (2:1/hexane:EtOAc)) gave **3** (7.30 g, 92%) as a light yellow powder: ^1H NMR ($CDCl_3$, 400 MHz) δ 8.10 (dd, 1H, J_1 = 8.0 Hz, J_2 = 1.6 Hz), 7.94 (d, 1H, J = 8.8 Hz), 7.62 (ddd, 1H, J_1 = 8.8 Hz, J_2 = 7.2 Hz, J_3 = 1.6 Hz), 7.48 (ddd, 1H, J_1 = 8.0 Hz, J_2 = 7.2 Hz, J_3 = 1.2 Hz), 3.08 (t, 2H, J = 6.8 Hz), 2.95 (t, 2H, J = 6.8 Hz), 1.91 (m, 4H); ^{13}C NMR ($CDCl_3$, 100 MHz) δ 159.4, 146.5, 141.5, 129.2, 128.8, 128.5, 126.5, 125.3, 123.6, 34.1, 27.4, 22.61, 22.57; *m/z* calcd for $C_{13}H_{12}ClN$: 217.07; found 218.15 $[M+H]^+$.

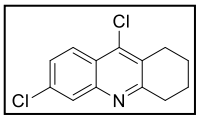

6,9-Dichloro-1,2,3,4-tetrahydroacridine (4). The known compound **4**[22] was prepared as described for the synthesis of **3**. Reaction of 2-amino-4-chlorobenzoic acid (5.00 g, 29.2 mmol, 1 eq), cyclohexanone (3.02 mL, 29.2 mmol, 1 eq), and $POCl_3$ (20 mL, 215 mmol, 5.9 eq) yielded, after purification by flash column chromatography (SiO_2; 5:1/hexane:EtOAc, R_f 0.76 (2:1/hexane:EtOAc)), **4** (6.62 g, 90%) as a light yellow powder: ^{1}H NMR ($CDCl_3$, 300 MHz) δ 8.08 (d, 1H, J = 9.0 Hz), 7.97 (d, 1H, J = 2.0 Hz), 7.47 (dd, 1H, J_1 = 9.0 Hz, J_2 = 2.0 Hz), 3.11 (t, 2H, J = 6.4 Hz), 3.00 (t, 2H, J = 6.4 Hz), 1.96 (m, 4H); ^{13}C NMR ($CDCl_3$, 75 MHz) δ 160.9, 147.0, 141.4, 135.2, 129.2, 127.6, 127.4, 125.2, 123.9, 34.2, 27.5, 22.5; *m/z* calcd for $C_{13}H_{11}Cl_2N$: 252.14; found 253.95 $[M+H]^+$.

2.6.1.2. General procedure for attachment of amine linkers to tacrine and 6-chlorotacrine

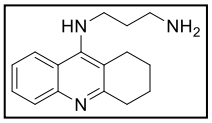

***N*^{1}-(1,2,3,4-Tetrahydroacridin-9-yl)propane-1,3-diamine (5a).** 9-Chloro-1,2,3,4-tetrahydroacridine (**3**) (0.4 g, 1.84 mmol, 1 eq), 1,3-diaminopropane (0.7 mL, 8.38 mmol, 3.65 eq) and 1-pentanol (3 mL) were combined and heated to reflux for 48 h. The reaction was cooled to rt, diluted with CH_2Cl_2 (50 mL), and washed with 10% aq. KOH (2x50 mL), H_2O (2x50 mL), and brine (50 mL). The organic layer was dried ($MgSO_4$), filtered, and concentrated *in vacuo* to afford the crude product, which was purified by flash column chromatography (SiO_2; 7:3/CH_2Cl_2:MeOH with NH_4OH (7 mL/L of solvent), R_f 0.05) to afford **5a** (310 mg, 66%) as a yellow oil: ^{1}H NMR ($CDCl_3$, 300 MHz) δ 8.04 (dd, 1H, J_1 = 8.6 Hz, J_2 = 0.8 Hz), 7.98 (d, 1H, J = 8.4 Hz), 7.56 (m, 1H), 7.33 (m, 1H), 3.68 (t, 2H, J = 6.5 Hz), 3.07 (m, 2H), 2.93 (t, 2H, J = 6.3 Hz), 2.70 (m, 2H), 2.34 (br s, 2H), 1.90 (m, 4H), 1.82 (p, 2H, J = 6.4 Hz), 1.45 (br s, 1H); ^{13}C NMR ($CDCl_3$, 125 MHz) δ 158.4, 151.0, 147.4, 128.6, 128.3, 123.5, 122.9, 120.2, 115.9, 48.1, 40.5, 34.4, 34.0, 25.1, 23.1, 22.8; *m/z* calcd for $C_{16}H_{21}N_3$: 255.17; found 256.00 $[M+H]^+$.

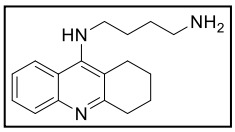

***N*^{1}-(1,2,3,4-Tetrahydroacridin-9-yl)butane-1,4-diamine (5b)**. Compound **5b** was prepared as described for the synthesis of **5a**. The reaction of 9-chloro-1,2,3,4-tetrahydroacridine (**3**) (0.5 g, 2.30 mmol,

1 eq), 1,4-diaminobutane (0.803 mL, 8.00 mmol, 3.48 eq), and 1-pentanol (3.5 mL) yielded, after purification by flash column chromatography (SiO_2; 7:3/CH_2Cl_2:MeOH with NH_4OH (7 mL/L of solvent), R_f 0.05), **5b** (345 mg, 56%) as a yellow solid: ^1H NMR ($CDCl_3$, 300 MHz) δ 7.75 (t, 2H, *J* = 8.4 Hz), 7.35 (t, 1H, *J* = 7.6 Hz), 7.13 (t, 1H, *J* = 7.6 Hz), 3.89 (br s, 1H), 3.25 (t, 2H, *J* = 7.1 Hz), 2.87 (t, 2H, *J* = 6.0 Hz), 2.49 (m, 4H), 1.70 (m, 4H), 1.45 (p, 2H, *J* = 7.4 Hz), 1.28 (p, 2H, *J* = 7.4 Hz), 1.08 (br s, 2H); ^{13}C NMR ($CDCl_3$, 75 MHz) δ 158.3, 150.5, 147.4, 128.7, 128.0, 123.3, 122.8, 120.1, 115.8, 49.1, 41.7, 34.0, 30.8, 29.0, 24.7, 22.9, 22.7; *m/z* calcd for $C_{17}H_{23}N_3$: 269.19; found 282.25 $[M+2Li]^+$.

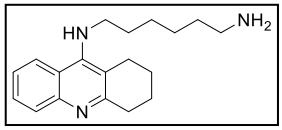

***N*^{1}-(1,2,3,4-Tetrahydroacridin-9-yl)hexane-1,6-diamine (5d).** Compound **5d** was prepared as described for the synthesis of **5a**. The reaction of 9-chloro-1,2,3,4-tetrahydroacridine (**3**) (0.84 g, 2.30 mmol, 1 eq), 1,6-diaminohexane (2.31 mL, 15.9 mmol, 4.2 eq), and 1-pentanol (5 mL) yielded, after purification by flash column chromatography (SiO_2; 7:3/CH_2Cl_2:MeOH with NH_4OH (7 mL/L of solvent), R_f 0.10), **5d** (452 mg, 56%) as a yellow solid: ^1H NMR ($CDCl_3$, 300 MHz) δ 7.90 (d, 1H, *J* = 8.5 Hz), 7.85 (d, 1H, *J* = 8.6 Hz), 7.49 (t, 1H, *J* = 7.6 Hz), 7.28 (t, 1H, *J* = 7.6 Hz), 3.89 (br s, 1H), 3.41 (t, 2H, *J* = 7.1 Hz), 3.01 (m, 2H), 2.61 (m, 4H), 1.85 (m, 4H), 1.59 (m, 4H), 1.35 (m, 6H); ^{13}C NMR ($CDCl_3$, 75 MHz) δ 158.4, 150.7, 147.5, 128.8, 128.2, 123.5, 122.8, 120.2, 115.9, 49.4, 42.0, 34.1, 33.5, 31.7, 26.8, 26.6, 24.8, 23.0, 22.8; *m/z* calcd for $C_{19}H_{27}N_3$: 297.22; found 298.05 $[M+H]^+$.

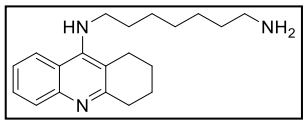

***N*^{1}-(1,2,3,4-Tetrahydroacridin-9-yl)heptane-1,7-diamine (5e)**. Compound **5e** was prepared as described for the synthesis of **5a**. The reaction of 9-chloro-1,2,3,4-tetrahydroacridine (**3**) (250 mg, 1.15 mmol, 1 eq), 1,7-diaminoheptane (449 mg, 3.45 mmol, 3 eq), and 1-pentanol (3 mL) yielded, after purification by flash column chromatography (SiO_2; 7:3/CH_2Cl_2:MeOH with NH_4OH (7 mL/L of solvent), R_f 0.13), **5e** (144 mg, 40%) as a yellow oil: ^1H NMR ($CDCl_3$, 500 MHz) δ 7.91 (d, 1H, *J* = 8.5 Hz), 7.86 (d, 1H, *J* = 8.5 Hz), 7.50 (t, 1H, *J* = 7.4 Hz), 7.29 (t, 1H, *J* = 7.7 Hz), 3.93 (br s, 1H), 3.41 (t, 2H, *J* = 7.2 Hz), 3.01 (m, 2H), 2.65 (br s, 4H), 2.48 (br s, 2H), 1.86 (m, 4H), 1.59 (p, 2H, *J* = 7.0 Hz), 1.40 (br p, 2H), 1.32 (br p,

2H), 1.27 (m, 4H); ^{13}C NMR ($CDCl_3$, 125 MHz) δ 158.4, 150.7, 147.5, 128.7, 128.2, 123.5, 122.9, 120.2, 115.8, 49.4, 41.9, 34.0, 33.1, 31.7, 29.2, 26.9, 26.7, 24.8, 23.0, 22.8; *m/z* calcd for $C_{20}H_{29}N_3$: 311.24; found 312.10 $[M+H]^+$.

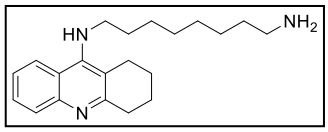

***N*^{1}-(1,2,3,4-Tetrahydroacridin-9-yl)octane-1,8-diamine (5f).** Compound **5f** was prepared as described for the synthesis of **5a**. The reaction of 9-chloro-1,2,3,4-tetrahydroacridine (**3**) (250 mg, 1.15 mmol, 1 eq), 1,8-diaminooctane (498 mg, 3.45 mmol, 3 eq), and 1-pentanol (3 mL) yielded, after purification by flash column chromatography (SiO_2; 7:3/CH_2Cl_2:MeOH with NH_4OH (7 mL/L of solvent), R_f 0.10), **5f** (208 mg, 56%) as a yellow oil: ^{1}H NMR ($CDCl_3$, 500 MHz) δ 7.92 (d, 1H, *J* = 8.5 Hz), 7.87 (d, 1H, *J* = 8.4 Hz), 7.51 (t, 1H, *J* = 7.1 Hz), 7.30 (t, 1H, *J* = 7.3 Hz), 3.91 (br s, 1H), 3.41 (t, 2H, *J* = 6.9 Hz), 3.02 (m, 2H), 2.67 (m, 4H), 1.87 (m, 4H), 1.58 (p, 2H, *J* = 7.1 Hz), 1.44 (br p, 2H), 1.31 (br p, 2H), 1.25 (br s, 6H); ^{13}C NMR ($CDCl_3$, 125 MHz) δ 158.4, 150.7, 147.5, 128.8, 128.2, 123.5, 122.8, 120.2, 115.8, 49.4, 41.6, 34.1, 31.7, 29.3, 26.9, 26.8, 24.8, 23.1, 22.8; *m/z* calcd for $C_{21}H_{31}N_3$: 325.25; found 326.00 $[M+H]^+$.

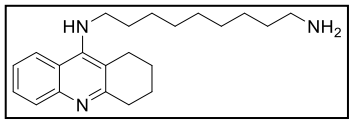

***N*^{1}-(1,2,3,4-Tetrahydroacridin-9-yl)nonane-1,9-diamine (5g).** Compound **5g** was prepared as described for the synthesis of **5a**. The reaction of 9-chloro-1,2,3,4-tetrahydroacridine (**3**) (250 mg, 1.15 mmol, 1 eq), 1,9-diaminononane (546 mg, 3.45 mmol, 3 eq), and 1-pentanol (3 mL) yielded, after purification by flash column chromatography (SiO_2; 7:3/CH_2Cl_2:MeOH with NH_4OH (7 mL/L of solvent), R_f 0.08), **5g** (276 mg, 71%) as a yellow oil: ^{1}H NMR ($CDCl_3$, 500 MHz) δ 7.85 (d, 1H, *J* = 8.5 Hz), 7.80 (d, 1H, *J* = 8.4 Hz), 7.42 (t, 1H, *J* = 7.3 Hz), 7.21 (t, 1H, *J* = 7.4 Hz), 3.91 (br s, 1H), 3.76 (br s, 1H) 3.34 (m, 2H) 2.94 (m, 2H), 2.61 (t, 2H, *J* = 7.0 Hz), 2.56 (m, 2H), 1.77 (br s, 4H), 1.50 (p, 2H, *J* = 7.1 Hz), 1.38 (br p, 2H), 1.23 (br p, 2H), 1.15 (br s, 8H); ^{13}C NMR ($CDCl_3$, 125 MHz) δ 158.2, 150.8, 147.3, 128.4, 128.2, 123.4, 122.9, 120.1, 115.6, 49.3, 41.5, 33.9, 32.2, 31.6, 29.4, 29.22, 29.19, 26.79, 26.75, 24.7, 23.0, 22.7; *m/z* calcd for $C_{22}H_{33}N_3$: 339.27; found 340.10 $[M+H]^+$.

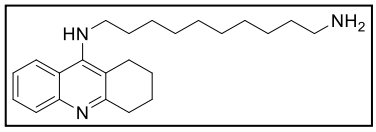

***N*^{1}-(1,2,3,4-Tetrahydroacridin-9-yl)decane-1,10-diamine (5h).** Compound **5h** was prepared as described for the synthesis of **5a**. The reaction of 9-chloro-1,2,3,4-tetrahydroacridine (**3**) (250 mg, 1.15 mmol, 1 eq), 1,10-diaminodecane (595 mg, 3.45 mmol, 3 eq), and 1-pentanol (3 mL) yielded, after purification by flash column chromatography (SiO_2; 7:3/CH_2Cl_2:MeOH with NH_4OH (7 mL/L of solvent), R_f 0.09), **5h** (143 mg, 35%) as a yellow oil: ^{1}H NMR ($CDCl_3$, 500 MHz) δ 7.92 (d, 1H, *J* = 8.5 Hz), 7.87 (d, 1H, *J* = 8.5 Hz), 7.51 (t, 1H, *J* = 7.4 Hz), 7.30 (t, 1H, *J* = 7.6 Hz), 3.92 (br s, 1H), 3.43 (t, 2H, *J* = 7.1 Hz) 3.02 (m, 2H), 2.64 (m, 4H), 1.87 (m, 4H), 1.80 (very br s, 2H), 1.60 (p, 2H, *J* = 7.4 Hz), 1.39 (br p, 2H), 1.33 (m, 2H), 1.24 (br s, 10H); ^{13}C NMR ($CDCl_3$, 125 MHz) δ 158.4, 150.7, 147.5, 128.8, 128.2, 123.5, 122.9, 120.2, 115.8, 49.5 , 42.1, 34.1, 33.5, 31.8, 29.49, 29.46, 29.43, 29.3, 26.91, 26.85, 24.8, 23.1, 22.8; *m/z* calcd for $C_{23}H_{35}N_3$: 353.28; found 354.15 $[M+H]^+$.

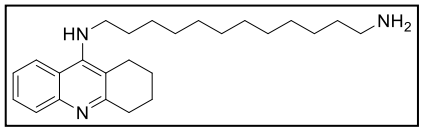

***N*^{1}-(1,2,3,4-Tetrahydroacridin-9-yl)dodecane-1,12-diamine (5i).** Compound **5i** was prepared as described for the synthesis of **5a**. The reaction of 9-chloro-1,2,3,4-tetrahydroacridine (**3**) (250 mg, 1.15 mmol, 1 eq), 1,12-diaminododecane (691 mg, 3.45 mmol, 3 eq), and 1-pentanol (3 mL) yielded, after purification by flash column chromatography (SiO_2; 7:3/CH_2Cl_2:MeOH with NH_4OH (7 mL/L of solvent), R_f 0.11), **5i** (313 mg, 71%) as a yellow oil: ^{1}H NMR ($CDCl_3$, 500 MHz) δ 7.96 (d, 1H, *J* = 8.5 Hz), 7.90 (d, 1H, *J* = 8.5 Hz), 7.54 (t, 1H, *J* = 7.6 Hz), 7.34 (t, 1H, *J* = 7.6 Hz), 3.96 (br s, 1H), 3.47 (t, 2H, *J* = 6.8 Hz) 3.06 (m, 2H), 2.71 (m, 2H), 2.67 (t, 2H, *J* = 7.1 Hz), 1.92 (m, 4H), 1.65 (p, 2H, *J* = 7.0 Hz), 1.39 (m, 4H), 1.26 (m, 16H); ^{13}C NMR ($CDCl_3$, 125 MHz) δ 158.4, 150.8, 147.5, 128.8, 128.2, 123.5, 122.9, 120.2, 115.8, 49.6, 42.3, 34.1, 33.8, 31.8, 29.6, 29.56 , 29.53, 29.50, 29.41, 29.37, 26.94, 26.90, 24.8, 23.1, 22.8; *m/z* calcd for $C_{25}H_{39}N_3$: 381.31; found 382.10 $[M+H]^+$.

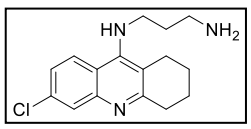

***N*^{1}-(6-Chloro-1,2,3,4-tetrahydroacridin-9-yl)propane-1,3-diamine (6a).** Compound **6a** was prepared as described for the synthesis of **5a**. The reaction of 6,9-dichloro-1,2,3,4-

tetrahydroacridine (**4**) (756 mg, 3 mmol, 1 eq), 1,3-diaminopropane (1.00 mL, 12 mmol, 4 eq), and 1-pentanol (6 mL) yielded, after purification by flash column chromatography (SiO_2; 7:3/CH_2Cl_2:MeOH with NH_4OH (7 mL/L of solvent), R_f 0.13), **6a** (703 mg, 81%) as a yellow oil: ^{1}H NMR ($CDCl_3$, 500 MHz) δ 7.96 (d, 1H, J = 9.1 Hz), 7.90 (d, 1H, J = 1.9 Hz), 7.27 (dd, 1H, J_1 = 9.1 Hz, J_2 = 1.9 Hz), 5.03 (br s, 1H), 3.65 (t, 2H, J = 6.4 Hz), 3.04 (br s, 2H), 2.94 (t, 2H, J = 6.4 Hz), 2.70 (br s, 2H), 1.92 (br s, 4H), 1.82 (p, 2H, J = 6.4 Hz), 1.58 (br s, 2H); ^{13}C NMR ($CDCl_3$, 125 MHz) δ 159.5, 151.1, 148.2, 133.9, 127.5, 124.7, 124.1, 118.3, 115.7, 48.5, 40.6, 34.0, 25.0, 23.0, 22.7; *m/z* calcd for $C_{16}H_{20}ClN_3$: 289.13; found 289.95 $[M+H]^+$.

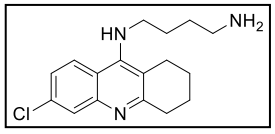

***N*^{1}-(6-Chloro-1,2,3,4-tetrahydroacridin-9-yl)butane-1,4-diamine (6b).** Compound **6b** was prepared as described for the synthesis of **5a**. The reaction of 6,9-dichloro-1,2,3,4-tetrahydroacridine (**4**) (756 mg, 3 mmol, 1 eq), 1,4-diaminobutane (1.21 mL, 12 mmol, 4 eq), and 1-pentanol (6 mL) yielded, after purification by flash column chromatography (SiO_2; 7:3/CH_2Cl_2:MeOH with NH_4OH (7 mL/L of solvent), R_f 0.13), **6b** (758 mg, 83%) as a yellow oil: ^{1}H NMR ($CDCl_3$, 500 MHz) δ 7.89 (d, 1H, J = 9.1 Hz), 7.87 (d, 1H, J = 1.5 Hz), 7.26 (dd, 1H, J_1 = 9.1 Hz, J_2 = 1.5 Hz), 4.07 (br s, 1H), 3.49 (t, 2H, J = 7.1 Hz), 3.02 (br s, 2H), 2.75 (t, 2H, J = 6.9 Hz), 2.67 (br s, 2H), 1.91 (bt t, 4H), 1.71 (p, 2H, J = 7.5 Hz), 1.55 (p, 2H, J = 7.3 Hz), 1.49 (br s, 2H); ^{13}C NMR ($CDCl_3$, 125 MHz) δ 159.6, 150.7, 148.2, 133.9, 127.6, 124.6, 124.2, 118.5, 115.9, 49.5, 41.8, 34.1, 30.9, 29.2, 24.7, 22.9, 22.7; *m/z* calcd for $C_{17}H_{22}ClN_3$: 303.15; found 304.05 $[M+H]^+$.

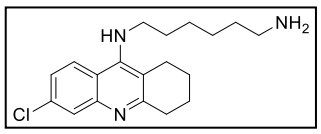

***N*^{1}-(6-Chloro-1,2,3,4-tetrahydroacridin-9-yl)hexane-1,6-diamine (6d).** Compound **6d** was prepared as described for the synthesis of **5a**. The reaction of 6,9-dichloro-1,2,3,4-tetrahydroacridine (**4**) (756 mg, 3 mmol, 1 eq), 1,6-diaminohexane (1.74 mL, 12 mmol, 4 eq), and 1-pentanol (6 mL) yielded, after purification by flash column chromatography (SiO_2; 7:3/CH_2Cl_2:MeOH with NH_4OH (7 mL/L of solvent), R_f 0.13), **6d** (830 mg, 83%) as a yellow oil: ^{1}H NMR ($CDCl_3$, 500 MHz) δ 7.89 (d, 1H, J = 9.1 Hz), 7.87 (d, 1H, J = 1.5 Hz), 7.26 (dd, 1H, J_1 = 9.1 Hz, J_2 = 1.5 Hz), 3.98 (br s, 1H), 3.47 (t, 2H, J = 7.0 Hz),

3.02 (br s, 2H), 2.69 (t, 2H, J = 7.0 Hz), 2.65 (br s, 2H), 2.23 (br s, 2H), 1.91 (br t, 4H), 1.65 (p, 2H, J = 7.0 Hz), 1.46 (p, 2H, J = 7.3 Hz), 1.37 (m, 4H); ^{13}C NMR ($CDCl_3$, 125 MHz) δ 159.5, 150.8, 148.1, 133.9, 127.5, 124.6, 124.2, 118.4, 115.7, 49.5, 41.9, 34.0, 33.2, 31.8, 26.8, 26.6, 24.6, 22.9, 22.6; *m/z* calcd for $C_{19}H_{26}ClN_3$: 331.18; found 331.95 $[M+H]^+$.

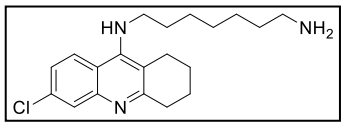

***N*^{1}-(6-Chloro-1,2,3,4-tetrahydroacridin-9-yl)heptane-1,7-diamine (6e)**. Compound **6e** was prepared as described for the synthesis of **5a**. The reaction of 6,9-dichloro-1,2,3,4-tetrahydroacridine (**4**) (250 mg, 0.99 mmol, 1 eq), 1,7-diaminoheptane (388 mg, 2.98 mmol, 3 eq), and 1-pentanol (3 mL) yielded, after purification by flash column chromatography (SiO_2; 7:3/CH_2Cl_2:MeOH with NH_4OH (7 mL/L of solvent), R_f 0.11), **6e** (61 mg, 18%) as a yellow oil: ^{1}H NMR ($CDCl_3$, 500 MHz) δ 7.86 (d, 1H, J = 9.3 Hz), 7.85 (s, 1H), 7.22 (dd, 1H, J_1 = 9.0 Hz, J_2 = 1.4 Hz), 3.93 (br s, 1H), 3.43 (m, 2H), 2.99 (br s, 2H), 2.64 (m, 4H), 1.88 (m, 4H), 1.62 (p, 2H, J = 7.0 Hz), 1.50 (br s, 2H), 1.38 (m, 4H), 1.29 (m, 4H); ^{13}C NMR ($CDCl_3$, 125 MHz) δ 159.5, 150.7, 148.2, 133.8, 127.6, 124.6, 124.1, 118.4, 115.7, 49.6, 42.1, 34.1, 33.6, 31.7, 29.2, 26.87, 26.77, 24.6, 22.9, 22.7; *m/z* calcd for $C_{20}H_{28}ClN_3$: 345.20; found 345.95 $[M+H]^+$.

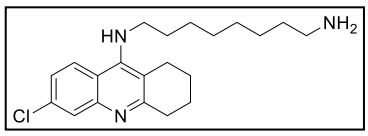

***N*^{1}-(6-Chloro-1,2,3,4-tetrahydroacridin-9-yl)octane-1,8-diamine (6f)**. Compound **6f** was prepared as described for the synthesis of **5a**. The reaction of 6,9-dichloro-1,2,3,4-tetrahydroacridine (**4**) (250 mg, 0.99 mmol, 1 eq), 1,8-diaminooctane (429 mg, 2.98 mmol, 3 eq), and 1-pentanol (3 mL) yielded, after purification by flash column chromatography (SiO_2; 7:3/CH_2Cl_2:MeOH with NH_4OH (7 mL/L of solvent), R_f 0.13), **6f** (232 mg, 65%) as a yellow oil: ^{1}H NMR ($CDCl_3$, 500 MHz) δ 7.86 (d, 1H, J = 9.4 Hz), 7.85 (s, 1H), 7.23 (dd, 1H, J_1 = 9.0 Hz, J_2 = 1.9 Hz), 3.93 (br s, 1H), 3.44 (m, 2H), 2.99 (br t, 2H), 2.64 (m, 4H), 1.88 (m, 4H), 1.71 (br s, 2H), 1.61 (p, 2H, J = 7.1 Hz), 1.40 (br p, 2H), 1.33 (br p, 2H), 1.27 (br s, 6H); ^{13}C NMR ($CDCl_3$, 125 MHz) δ 159.5, 150.8, 148.2, 133.8, 127.6, 124.6, 124.1, 118.4, 115.7, 49.6, 42.1, 34.1, 33.5, 31.8, 29.33, 29.28, 26.82, 26.75, 24.5, 22.9, 22.7; *m/z* calcd for $C_{21}H_{30}ClN_3$: 359.21; found 359.95 $[M+H]^+$.

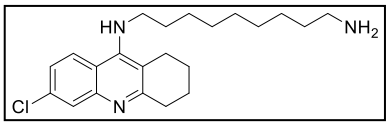

***N*[1]-(6-Chloro-1,2,3,4-tetrahydroacridin-9-yl)nonane-1,9-diamine (6g).** Compound **6g** was prepared as described for the synthesis of **5a**. The reaction of 6,9-dichloro-1,2,3,4-tetrahydroacridine (**4**) (250 mg, 0.99 mmol, 1 eq), 1,9-diaminononane (471 mg, 2.98 mmol, 3 eq), and 1-pentanol (3 mL) yielded, after purification by flash column chromatography (SiO_2; 7:3/CH_2Cl_2:MeOH with NH_4OH (7 mL/L of solvent), R_f 0.15), **6g** (237 mg, 64%) as a yellow oil: ^{1}H NMR ($CDCl_3$, 500 MHz) δ 7.84 (d, 1H, J = 9.1 Hz), 7.83 (s, 1H), 7.20 (dd, 1H, J_1 = 9.5 Hz, J_2 = 2.0 Hz), 3.91 (br s, 1H), 3.41 (br t, 2H), 2.97 (br s, 2H), 2.64 (t, 2H, J = 7.1 Hz), 2.60 (br s, 2H), 1.86 (m, 4H), 1.78 (very br s, 2H), 1.59 (p, 2H, J = 7.0 Hz), 1.39 (br p, 2H), 1.31 (br p, 2H), 1.24 (br s, 8H); ^{13}C NMR ($CDCl_3$, 125 MHz) δ 159.5, 150.7, 148.2, 133.8, 127.6, 124.6, 124.0, 118.4, 115.6, 49.6, 42.1, 34.1, 33.4, 31.7, 29.4, 29.3, 29.2, 26.85, 26.81, 24.5, 22.9, 22.7; *m/z* calcd for $C_{22}H_{32}ClN_3$: 373.23; found 374.00 $[M+H]^+$.

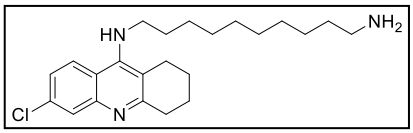

***N*[1]-(6-Chloro-1,2,3,4-tetrahydroacridin-9-yl)decane-1,10-diamine (6h).** Compound **6h** was prepared as described for the synthesis of **5a**. The reaction of 6,9-dichloro-1,2,3,4-tetrahydroacridine (**4**) (250 mg, 0.99 mmol, 1 eq), 1,10-diaminodecane (513 mg, 2.98 mmol, 3 eq), and 1-pentanol (3 mL) yielded, after purification by flash column chromatography (SiO_2; 7:3/CH_2Cl_2:MeOH with NH_4OH (7 mL/L of solvent), R_f 0.15), **6h** (190 mg, 49%) as a yellow oil: ^{1}H NMR ($CDCl_3$, 500 MHz) δ 7.81 (d, 1H, J = 7.0 Hz), 7.80 (s, 1H), 7.17 (dd, 1H, J = 9.0 Hz, J_2 = 2.1 Hz), 3.89 (br t, 1H), 3.39 (q, 2H, J = 6.7 Hz), 2.95 (br s, 2H), 2.60 (m, 4H), 1.83 (m, 4H), 1.56 (p, 2H, J = 7.1 Hz), 1.36 (br p, 4H), 1.30 (br p, 2H), 1.21 (m, 10H); ^{13}C NMR ($CDCl_3$, 125 MHz) δ 159.5, 150.7, 148.2, 133.7, 127.6, 124.6, 124.0, 118.3, 115.6, 49.5, 42.2, 34.1, 33.7, 31.7, 29.45, 29.41, 29.3, 26.8, 24.5, 22.9, 22.6; *m/z* calcd for $C_{23}H_{34}ClN_3$: 387.24; found 388.05 $[M+H]^+$.

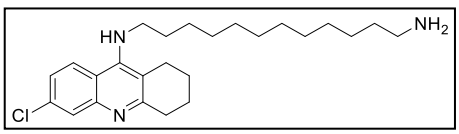

***N*[1]-(6-Chloro-1,2,3,4-tetrahydroacridin-9-yl)dodecane-1,12-diamine (6i).** Compound **6i** was prepared as described for the synthesis of **5a**. The

reaction of 6,9-dichloro-1,2,3,4-tetrahydroacridine (**4**) (250 mg, 0.99 mmol, 1 eq), 1,12-diaminododecane (596 mg, 2.98 mmol, 3 eq), and 1-pentanol (3 mL) yielded, after purification by flash column chromatography (SiO_2; 7:3/CH_2Cl_2:MeOH with NH_4OH (7 mL/L of solvent), R_f 0.15), **6i** (207 mg, 50%) as a yellow oil: ^{1}H NMR ($CDCl_3$, 500 MHz) δ 7.80 (d, 1H, J = 6.9 Hz), 7.79 (d, 1H, J = 1.8 Hz), 7.16 (dd, 1H, J_1 = 9.1 Hz, J_2 = 1.8 Hz), 3.88 (br t, 1H), 3.37 (br q, 2H), 2.94 (br s, 2H), 2.62 (t, 2H, J = 7.1 Hz), 2.56 (br s, 2H), 1.82 (m, 4H), 1.55 (p, 2H, J = 7.1 Hz), 1.36 (br p, 2H), 1.28 (br p, 2H), 1.18 (m, 16H); ^{13}C NMR ($CDCl_3$, 125 MHz) δ 159.4, 150.7, 148.2, 133.7, 127.6, 124.6, 123.9, 118.3, 115.6, 49.5, 42.0, 34.1, 33.4, 31.7, 29.57, 29.52, 29.48, 29.46, 29.45, 29.3, 26.8, 24.5, 22.9, 22.6; *m/z* calcd for $C_{25}H_{38}ClN_3$: 415.28; found 416.10 $[M+H]^+$.

2.6.1.3. General procedure for esterification for the preparation of mefenamic acid linkers

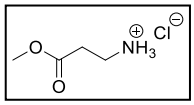

3-Methoxy-3-oxopropan-1-aminium chloride (7b). β-Alanine (3.00 g, 33.7 mmol, 1 eq) was dissolved in MeOH (60 mL). HCl (3.05 mL of 12.1 M, 37.1 mmol, 1.1 eq) was added dropwise. The reaction mixture was stirred for 18 h at rt before being concentrated under reduced pressure. The residue was redissolved in MeOH (50 mL) and concentrated under reduced pressure to yield **7b** (4.66 g, 99%) as a white powder: ^{1}H NMR (DMSO-d6, 300 MHz) δ 8.29 (s, 3H), 3.62 (s, 3H), 2.98 (t, 2H, J = 4.3 Hz), 2.73 (t, 2H, J = 4.3 Hz); ^{13}C NMR (DMSO-d6, 75 MHz) δ 171.2, 52.2, 35.0, 31.7; IR (CD_3OD cast): ν 3033 (NH_3^+), 1740 (C=O), 1597, 1570, 1526, 1424, 1349, 1228 (C-O), 1007, 797 cm^{-1}.

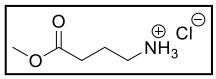

4-Methoxy-4-oxobutan-1-aminium chloride (7c). Compound **7c** was prepared as described for the synthesis of **7b**. Reaction of γ-aminobutyric acid (3.48 g, 33.7 mmol, 1 eq) and HCl (3.05 mL of 12 M, 37.1 mmol, 1.1 eq) yielded **7c** (5.12 g, 99%) as a white powder: ^{1}H NMR (DMSO-d6, 500 MHz) δ 8.26 (s, 3H), 3.59 (s, 3H), 2.77 (m, 2H), 2.43 (t, 2H, J = 7.5 Hz), 1.82 (p, 2H, J = 7.5 Hz); ^{13}C NMR (DMSO-d6, 75 MHz) δ 173.1, 51.9, 38.4, 30.6, 22.8; IR (CD_3OD cast): ν 2956 (NH_3^+), 1733 (C=O), 1600, 1518, 1430, 1386, 1295, 1215 (C-O), 1155, 970 cm^{-1}.

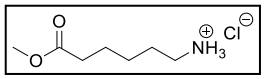

6-Methoxy-6-oxohexan-1-aminium chloride (7d). Compound **7d** was prepared as described for the synthesis of **7b**. Reaction of 6-aminocaproic acid (3.50 g, 26.7 mmol, 1 eq) and HCl (2.3 mL of 12.1 M, 27.8 mmol, 1.04 eq) yielded **7d** (4.80 g, 99%) as a white powder: ^{1}H NMR (DMSO-d6, 300 MHz) δ 8.07 (s, 3H), 3.59 (s, 3H), 2.72 (m, 2H), 2.30 (t, 2H, *J* = 7.3 Hz), 1.54 (m, 4H), 1.30 (m, 2H); ^{13}C NMR ($CDCl_3$, 75 MHz) δ 173.9, 51.6, 39.7, 33.6, 27.2, 25.9, 24.2; IR (CD_3OD cast): ν 2950 (NH_3^+), 1732 (C=O), 1623, 1582, 1516, 1426, 1315, 1253, 1196 (C-O), 1155, 978 cm^{-1}.

2.6.1.4. General procedure for attachment of linkers to mefenamic acid

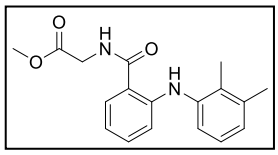

Methyl 2-(2-((2,3-dimethylphenyl)amino)benzamido)acetate (8a). Under anhydrous conditions, mefenamic acid (1.09 g, 4.5 mmol, 1 eq) and DCC (2.79 g, 13.5 mmol, 3 eq) were dissolved in DMF (45 mL). HOBt hydrate (1.82 g, 13.5 mmol, 3 eq) and DIPEA (5.49 mL, 31.5 mmol, 7 eq) were added, followed by glycine methyl ester hydrochloride (**7a**) (1.70 g, 13.5 mmol, 3 eq). The reaction progress was monitored by TLC for product formation (1:1/hexane:EtOAc, R_f 0.57). After stirring for 72 h at rt, the reaction mixture was diluted in EtOAc (150 mL). The organic mixture was successively washed with H_2O (90 mL) and brine (100 mL), dried ($MgSO_4$), filtered, and concentrated under reduced pressure. Further purification by flash column chromatography (SiO_2; 3:1/hexane:EtOAc, R_f 0.24) gave **8a** (793 mg, 56%) as an orange oil: ^{1}H NMR ($CDCl_3$, 500 MHz) δ 9.18 (s, 1H), 7.53 (d, 1H, *J* = 7.9 Hz), 7.25 (t, 1H, *J* = 7.8 Hz), 7.18 (d, 1H, *J* = 7.9 Hz), 7.10 (t, 1H, *J* = 7.7 Hz), 6.99 (d, 1H, *J* = 7.4 Hz), 6.91 (d, 1H, *J* = 8.5 Hz), 6.73 (t, 1H, *J* = 7.5 Hz), 6.71 (br s, 1H), 4.26 (d, 2H, *J* = 5.0 Hz), 3.84 (s, 3H), 2.35 (s, 3H), 2.21 (s, 3H); ^{13}C NMR ($CDCl_3$, 75 MHz) δ 170.6, 169.6, 147.5, 139.3, 138.1, 132.7, 131.2, 127.7, 125.9, 125.8, 121.4, 116.7, 115.6, 114.8, 52.5, 41.6, 20.7, 13.9; *m/z* calcd for $C_{18}H_{20}N_2O_3$: 312.15; found 312.90 $[M+H]^+$.

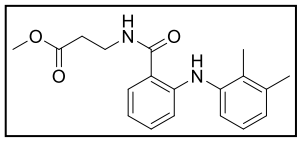

Methyl 3-(2-((2,3-dimethylphenyl)amino)benzamido)propanoate (8b). Compound **8b** was prepared as described for the synthesis of **8a**. The reaction of mefenamic acid (967 mg, 4.0 mmol, 1 eq), DCC (2.48 g, 12.0 mmol, 3 eq),

DMF (40 mL), HOBt hydrate (1.62 g, 12.0 mmol, 3 eq), DIPEA (4.88 mL, 28.0 mmol, 7 eq) and **7b** (1.67 g, 12.0 mmol, 3 eq) was monitored by TLC for product formation (1:1/hexane:EtOAc, R_f 0.73). Purification by flash column chromatography (SiO_2; 3:1/hexane:EtOAc, R_f 0.35) gave **8b** (338 mg, 26%) as a yellow oil: ^{1}H NMR ($CDCl_3$, 300 MHz) δ 9.32 (s, 1H), 7.46 (d, 1H, *J* = 7.9 Hz), 7.24 (m, 2H), 7.11 (t, 1H, *J* = 7.7 Hz), 7.01 (s, 1H), 6.99 (d, 1H, *J* = 7.6 Hz), 6.96 (d, 1H, *J* = 8.5 Hz), 6.70 (t, 1H, *J* = 7.5 Hz), 3.75 (m, 5H), 2.69 (t, 2H, *J* = 6.0 Hz), 2.38 (s, 3H), 2.25 (s, 3H); ^{13}C NMR ($CDCl_3$, 125 MHz) δ 173.3, 169.6, 147.2, 139.5, 138.1, 132.4, 130.9, 127.5, 125.8, 125.6, 120.9, 116.8, 116.5, 114.8, 51.9, 35.1, 33.8, 20.7, 13.9; *m/z* calcd for $C_{19}H_{22}N_2O_3$: 326.16; found 327.00 $[M+H]^+$.

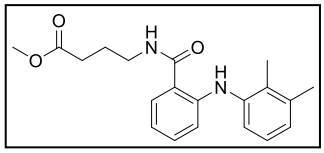

Methyl 4-(2-((2,3-dimethylphenyl)amino)benzamido)butanoate (8c). Compound **8c** was prepared as described for the synthesis of **8a**. The reaction of mefenamic acid (725 mg, 3 mmol, 1 eq), DCC (1.86 g, 9 mmol, 3 eq), DMF (30 mL), HOBt hydrate (1.22 g, 9 mmol, 3 eq), DIPEA (3.66 mL, 21 mmol, 7 eq) and **7c** (1.37 g, 9 mmol, 3 eq) was monitored by TLC for product formation (1:1/hexane:EtOAc, R_f 0.69). Purification by flash column chromatography (SiO_2; 3:1/hexane:EtOAc, R_f 0.30) gave **8c** (362 mg, 36%) as a yellow oil: ^{1}H NMR (DMSO-d6, 300 MHz) δ 9.62 (s, 1H), 8.58 (t, 1H, *J* = 4.9 Hz), 7.66 (d, 1H, *J* = 7.9 Hz), 7.22 (t, 1H, *J* = 7.9 Hz), 7.09 (d, 1H, *J* = 7.9 Hz), 7.04 (m, 1H), 6.89 (d, 1H, *J* = 7.4 Hz), 6.86 (d, 1H, *J* = 8.7 Hz), 6.72 (t, 1H, *J* = 7.4 Hz), 3.58 (s, 3H), 3.30 (q, 2H, *J* = 5.9 Hz), 2.38 (t, 2H, *J* = 7.3 Hz), 2.25 (s, 3H), 2.10 (s, 3H), 1.81 (p, 2H, *J* = 7.0 Hz); ^{13}C NMR (DMSO-d6, 75 MHz) δ 173.6, 169.6, 146.6, 139.7, 138.1, 132.3, 129.7, 129.1, 126.2, 125.4, 120.0, 117.5, 117.2, 114.3, 51.7, 38.8, 31.2, 24.8, 20.7, 13.9; *m/z* calcd for $C_{20}H_{24}N_2O_3$: 340.18; found 341.00 $[M+H]^+$.

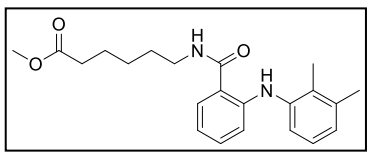

Methyl 6-(2-((2,3-dimethylphenyl)amino)benzamido)hexanoate (8d). Compound **8d** was prepared as described for the synthesis of **8a**. The reaction of mefenamic acid (725 mg, 3 mmol, 1 eq), DCC (1.86 g, 9 mmol, 3

eq), DMF (30 mL), HOBt hydrate (1.22 g, 9 mmol, 3 eq), DIPEA (3.66 mL, 21 mmol, 7 eq), and **7d** (1.63 g, 9 mmol, 3 eq) was monitored by TLC for product formation (1:1/hexane:EtOAc, R_f 0.73). Purification by flash column chromatography (SiO_2; 3:1/hexane:EtOAc, R_f 0.35) gave **8d** (389 mg, 35%) as an orange oil: ^{1}H NMR (DMSO-d6, 300 MHz) δ 9.61 (s, 1H), 8.54 (t, 1H, *J* = 5.4 Hz), 7.64 (d, 1H, *J* = 7.9 Hz), 7.22 (t, 1H, *J* = 7.8 Hz), 7.09 (d, 1H, *J* = 7.9 Hz), 7.04 (t, 1H, *J* = 7.7 Hz), 6.89 (d, 1H, *J* = 7.2 Hz), 6.86 (d, 1H, *J* = 8.4 Hz), 6.72 (t, 1H, *J* = 7.5 Hz), 3.57 (s, 3H), 3.25 (q, 2H, *J* = 6.5 Hz), 2.29 (t, 2H, *J* = 7.5 Hz), 2.26 (s, 3H), 2.10 (s, 3H), 1.54 (m, 4H), 1.31 (m, 2H); ^{13}C NMR (DMSO-d6, 75 MHz) δ 173.8, 169.4, 146.5, 139.8, 138.1, 132.2, 129.6, 129.0, 126.2, 125.4, 119.9, 117.8, 117.2, 114.4, 51.6, 39.2, 33.7, 29.2, 26.4, 24.7, 20.7, 13.9; *m/z* calcd for $C_{22}H_{28}N_2O_3$: 368.21; found 369.05 $[M+H]^+$.

2.6.1.5. General procedure for ester hydrolysis of mefenamic acid linkers

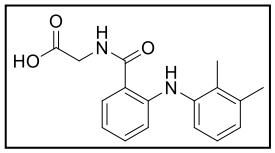

2-(2-((2,3-Dimethylphenyl)amino)benzamido)acetic acid (9a). 1 M NaOH (70 mL) was added to **8a** (793 mg, 2.4 mmol) dissolved in THF (30 mL). After stirring for 48 h at 40 °C, the reaction mixture was cooled to 0 °C and acidified to pH 1-2 using 1 M HCl. The product was extracted from the reaction mixture using EtOAc (2x200 mL), dried ($MgSO_4$), and concentrated under reduced pressure to yield **9a** (759 mg, 99%) as a pale yellow powder: ^{1}H NMR ($CDCl_3$, 300 MHz) δ 9.12 (br s, 1H), 7.51 (d, 1H, *J* = 7.8 Hz), 7.25 (t, 1H, *J* = 7.8 Hz), 7.17 (d, 1H, *J* = 7.8 Hz), 7.10 (t, 1H, *J* = 7.6 Hz), 6.99 (d, 1H, *J* = 7.4 Hz), 6.90 (d, 1H, *J* = 8.5 Hz), 6.73 (m, 2H), 4.29 (d, 2H, *J* = 3.0 Hz), 2.34 (s, 3H), 2.20 (s, 3H); ^{13}C NMR ($CDCl_3$, 75 MHz) δ 174.0, 170.0, 147.6, 139.2, 138.1, 132.9, 131.3, 127.7, 126.0, 125.8, 121.5, 116.8, 115.3, 114.9, 41.6, 20.7, 13.9; *m/z* calcd for $C_{17}H_{18}N_2O_3$: 298.13; found 299.05 $[M+H]^+$.

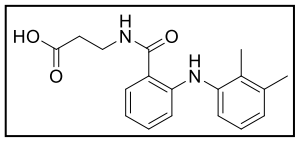

3-(2-((2,3-Dimethylphenyl)amino)benzamido)propanoic acid (9b). Compound **9b** was prepared as described for the synthesis of **9a**. The reaction of **8b** (338 mg, 1.04 mmol, 1 eq) in THF (30 mL) with 1 M NaOH (70 mL) yielded **9b** (323 mg, 99%) as a pink powder: ^{1}H NMR ($CDCl_3$, 300 MHz) δ 9.16 (s, 1H), 7.42 (dd, 1H, J_1 = 7.8 Hz, J_2 = 1.2 Hz), 7.23 (m, 2H), 7.10 (t, 1H, *J* = 7.6 Hz), 6.98 (d, 1H, *J* = 7.4 Hz), 6.94 (d, 1H, *J* = 8.4 Hz), 6.90 (m, 1H),

6.70 (t, 1H, J = 7.3 Hz), 3.73 (q, 2H, J = 5.9 Hz), 2.74 (t, 2H, J = 5.8 Hz), 2.35 (s, 3H), 2.22 (s, 3H); ^{13}C NMR ($CDCl_3$, 75 MHz) δ 177.0, 169.8, 147.3, 139.4, 138.1, 132.5, 130.9, 127.4, 125.8, 125.7, 121.0, 116.8, 116.3, 114.9, 34.9, 33.7, 20.7, 13.9; *m/z* calcd for $C_{18}H_{20}N_2O_3$: 312.15; found 313.10 $[M+H]^+$.

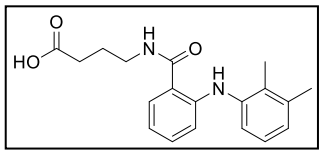

4-(2-((2,3-Dimethylphenyl)amino)benzamido)butanoic acid (9c). Compound **9c** was prepared as described for the synthesis of **9a**. The reaction of **8c** (360 mg, 1.06 mmol, 1 eq) in THF (30 mL) with 1 M NaOH (70 mL) yielded **9c** (346 mg, 99%) as a pink powder: ^{1}H NMR ($CDCl_3$, 300 MHz) δ 9.19 (s, 1H), 7.41 (d, 1H, J = 6.8 Hz), 7.23 (td, 1H, J_1 = 7.2 Hz, J_2 = 1.2 Hz), 7.17 (d, 1H, J = 7.7 Hz), 7.08 (t, 1H, J = 7.7 Hz), 6.97 (d, 1H, J = 7.5 Hz), 6.93 (d, 1H, J = 8.5 Hz), 6.70 (t, 1H, J = 7.5 Hz), 6.49 (br t, 1H), 3.54 (q, 2H, J = 6.5 Hz), 2.52 (t, 2H, J = 6.9 Hz), 2.34 (s, 3H), 2.20 (s, 3H), 2.00 (p, 2H, J = 6.8 Hz); ^{13}C NMR ($CDCl_3$, 75 MHz) δ 177.5, 170.1, 147.2, 139.4, 138.1, 132.4, 130.9, 127.3, 125.8, 125.7, 121.0, 116.8, 116.4, 114.9, 39.2, 31.5, 24.6, 20.7, 13.9; *m/z* calcd for $C_{19}H_{22}N_2O_3$: 326.16; found 327.00 $[M+H]^+$.

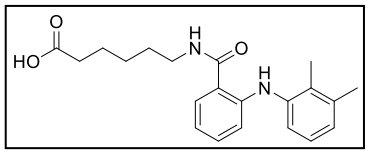

6-(2-((2,3-Dimethylphenyl)amino)benzamido)hexanoic acid (9d). Compound **9d** was prepared as described for the synthesis of **9a**. The reaction of **8d** (382 mg, 1.04 mmol, 1 eq) in THF (30 mL) with 1 M NaOH (70 mL) yielded **9d** (368 mg, 99%) as a pink powder: ^{1}H NMR ($CDCl_3$, 300 MHz) δ 9.16 (s, 1H), 7.41 (d, 1H, J = 7.8 Hz), 7.23 (d, 1H, J = 7.3 Hz), 7.19 (t, 1H, J = 8.4 Hz), 7.08 (t, 1H, J = 7.6 Hz), 6.95 (d, 1H, J = 7.1 Hz), 6.94 (d, 1H, J = 8.5 Hz), 6.70 (t, 1H, J = 7.5 Hz), 6.28 (br t, 1H), 3.45 (q, 2H, J = 6.6 Hz), 2.38 (t, 2H, J = 7.4 Hz), 2.34 (s, 3H), 2.21 (s, 3H), 1.68 (m, 4H), 1.46 (m, 2H); ^{13}C NMR ($CDCl_3$, 75 MHz) δ 179.3, 169.8, 147.0, 139.5, 138.1, 132.2, 130.8, 127.3, 125.7, 125.5, 120.7, 117.1, 116.8, 114.9, 39.6, 33.9, 29.3, 26.4, 24.3, 20.7, 13.9; *m/z* calcd for $C_{21}H_{26}N_2O_3$: 354.19; found 354.95 $[M+H]^+$.

2.6.1.6. General procedure for coupling of tacrine and 6-chlorotacrine to mefenamic acid

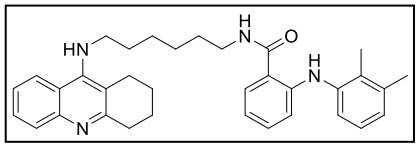

2-((2,3-Dimethylphenyl)amino)-*N*-(6-((1,2,3,4-tetrahydroacridin-9-yl)amino)hexyl)benzamide (10a). Under anhydrous conditions, EDAC hydrochloride (40 mg, 0.209 mmol, 1.1 eq) and HOBt hydrate (32 mg, 0.209 mmol, 1.1 eq) were added to mefenamic acid (**2**) (46 mg, 0.190 mmol, 1 eq) in DMF (3 mL). After 3 min, **5d** (57 mg, 0.190 mmol, 1 eq) dissolved in DMF (1 mL) was added to the reaction mixture. After 5 min, Et_3N (47 μL, 0.342 mmol, 1.8 eq) was added and the reaction mixture was stirred for 72 h at rt before dilution with CH_2Cl_2 (100 mL). The organic mixture was successively washed with 1 M HCl (80 mL), 1 M NaOH (90 mL), H_2O (100 mL), and brine (100 mL), dried ($MgSO_4$), filtered, and concentrated under reduced pressure. Further purification by flash column chromatography (SiO_2; 9:1/CH_2Cl_2:MeOH with NH_4OH (7 mL/L of solvent), R_f 0.29) gave **10a** (97 mg, 74%) as a pale yellow powder: ^{1}H NMR ($CDCl_3$, 500 MHz) δ 9.20 (s, 1H), 7.97 (d, 1H, *J* = 8.5 Hz), 7.93 (d, 1H, *J* = 8.5 Hz), 7.57 (t, 1H, *J* = 7.4 Hz), 7.40 (d, 1H, *J* = 7.6 Hz), 7.36 (t, 1H, *J* = 7.6 Hz), 7.22 (t, 1H, *J* = 7.8 Hz), 7.18 (d, 1H, *J* = 7.9 Hz), 7.08 (t, 1H, *J* = 7.6 Hz), 6.96 (m, 2H), 6.70 (t, 1H, *J* = 7.4 Hz), 6.22 (br t, 1H), 3.99 (very br s, 1H), 3.51 (t, 2H, *J* = 7.2 Hz), 3.44 (q, 2H, *J* = 6.7 Hz), 3.08 (br t, 2H), 2.73 (br t, 2H), 2.34 (s, 3H), 2.22 (s, 3H), 1.94 (m, 4H), 1.70 (p, 2H, *J* = 7.0 Hz), 1.65 (p, 2H, *J* = 6.9 Hz), 1.46 (m, 4H); ^{13}C NMR ($CDCl_3$, 125 MHz) δ 169.7, 158.5, 150.7, 147.5, 147.0, 139.6, 138.1, 132.2, 130.8, 128.8, 128.3, 127.2, 125.7, 125.6, 123.7, 122.8, 120.8, 120.3, 117.1, 116.8, 116.0, 114.9, 49.4, 39.6, 34.1, 31.7, 29.6, 26.7, 26.6, 24.8, 23.1, 22.8, 20.7, 13.9; *m/z* calcd for $C_{34}H_{40}N_4O$: 520.32; found 521.25 $[M+H]^+$.

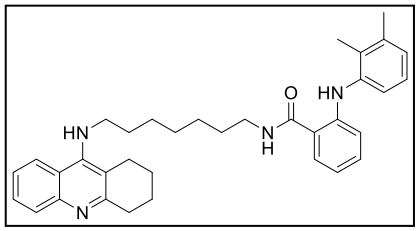

2-((2,3-Dimethylphenyl)amino)-*N*-(7-((1,2,3,4-tetrahydroacridin-9-yl)amino)heptyl)benzamide (10b). Compound **10b** was prepared as described for the synthesis of **10a**. The reaction of mefenamic acid (**2**) (57 mg, 0.235 mmol, 1 eq), EDAC hydrochloride (50 mg, 0.259 mmol, 1.1 eq), HOBt hydrate (40 mg, 0.259 mmol, 1.1 eq), **5e** (88 mg, 0.282 mmol, 1.2 eq), and Et_3N (59 μL, 0.423 mmol, 1.8 eq) in DMF (4 mL) yielded, after purification by flash column chromatography (SiO_2; 9:1/CH_2Cl_2:MeOH with NH_4OH (7 mL/L of solvent), R_f 0.32), **10b** (44 mg, 40%) as a pale yellow solid: ^{1}H NMR ($CDCl_3$, 500 MHz)

δ 9.22 (s, 1H), 7.97 (d, 1H, *J* = 8.5 Hz), 7.92 (d, 1H, *J* = 8.4 Hz), 7.56 (t, 1H, *J* = 7.0 Hz), 7.42 (d, 1H, *J* = 7.9 Hz), 7.35 (t, 1H, *J* = 7.2 Hz), 7.21 (t, 1H, *J* = 7.2 Hz), 7.18 (d, 1H, *J* = 7.9 Hz), 7.08 (t, 1H, *J* = 7.6 Hz), 6.95 (d, 2H, *J* = 7.8 Hz), 6.69 (t, 1H, *J* = 7.2 Hz), 6.35 (br t, 1H), 3.98 (very br s, 1H), 3.49 (t, 2H, *J* = 7.2 Hz), 3.42 (q, 2H, *J* = 7.0 Hz), 3.07 (br t, 2H), 2.72 (br t, 2H), 2.33 (s, 3H), 2.22 (s, 3H), 1.93 (m, 4H), 1.67 (p, 2H, *J* = 6.3 Hz), 1.60 (p, 2H, *J* = 6.3 Hz), 1.39 (br s, 6H); ^{13}C NMR ($CDCl_3$, 125 MHz) δ 169.7, 158.5, 150.8, 147.5, 147.0, 139.6, 138.0, 132.1, 130.7, 128.7, 128.3, 127.3, 125.7, 125.5, 123.6, 122.9, 120.7, 120.3, 117.2, 116.7, 115.9, 114.9, 49.4, 39.7, 34.1, 31.7, 29.6, 29.0, 26.9, 26.8, 24.8, 23.1, 22.8, 20.7, 13.9; *m/z* calcd for $C_{35}H_{42}N_4O$: 534.34; found 535.25 $[M+H]^+$.

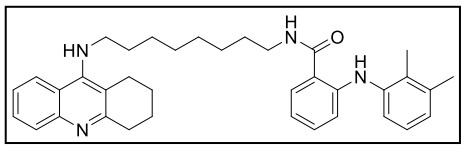

2-((2,3-Dimethylphenyl)amino-*N*-(8-((1,2,3,4-tetrahydroacridin-9-yl)amino)octyl)benzamide (10c). Compound **10c** was prepared as described for the synthesis of **10a**. The reaction of mefenamic acid (**2**) (43 mg, 0.177 mmol, 1 eq), EDAC hydrochloride (37 mg, 0.194 mmol, 1.1 eq), HOBt hydrate (30 mg, 0.194 mmol, 1.1 eq), **5f** (69 mg, 0.212 mmol, 1.2 eq), and Et_3N (44 μL, 0.318 mmol, 1.8 eq) in DMF (3 mL) yielded, after purification by flash column chromatography (SiO_2; 9:1/CH_2Cl_2:MeOH with NH_4OH (7 mL/L of solvent), R_f 0.42), **10c** (17 mg, 17%) as a pale yellow oil: ^{1}H NMR ($CDCl_3$, 500 MHz) δ 9.21 (s, 1H), 8.00 (d, 2H, *J* = 8.6 Hz), 7.59 (t, 1H, *J* = 7.7 Hz), 7.43 (d, 1H, *J* = 7.3 Hz), 7.38 (t, 1H, *J* = 7.7 Hz), 7.22 (t, 1H, *J* = 7.8 Hz), 7.18 (d, 1H, *J* = 7.9 Hz), 7.08 (t, 1H, *J* = 7.6 Hz), 6.96 (d, 2H, *J* = 8.1 Hz), 6.70 (t, 1H, *J* = 7.4 Hz), 6.26 (br t, 1H), 4.21 (very br s, 1H), 3.56 (t, 2H, *J* = 7.1 Hz), 3.43 (q, 2H, *J* = 6.8 Hz), 3.12 (br t, 2H), 2.71 (br t, 2H), 2.34 (s, 3H), 2.22 (s, 3H), 1.94 (m, 4H, *J* = 3.1 Hz), 1.70 (p, 2H, *J* = 7.1 Hz), 1.62 (p, 2H, *J* = 6.7 Hz), 1.37 (m, 8H); ^{13}C NMR ($CDCl_3$, 125 MHz) δ 169.7, 157.5, 151.5, 147.0, 146.3, 139.6, 138.1, 132.1, 130.7, 128.9, 127.6, 127.3, 125.7, 125.5, 123.8, 123.1, 120.7, 119.6, 117.2, 116.8, 115.1, 114.9, 49.4, 39.8, 33.2, 31.7, 29.6, 29.2, 29.1, 26.9, 26.8, 24.6, 22.9, 22.5, 20.7, 13.9; *m/z* calcd for $C_{36}H_{44}N_4O$: 548.35; found 549.30 $[M+H]^+$.

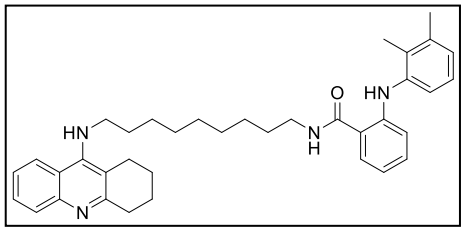

2-((2,3-Dimethylphenyl)amino)-*N*-(9-((1,2,3,4-tetrahydroacridin-9-yl)amino)nonyl)benzamide (10d). Compound **10d** was prepared as described for the synthesis of **10a**. The reaction of mefenamic acid (**2**) (45 mg, 0.185 mmol, 1 eq), EDAC hydrochloride (39 mg, 0.204 mmol, 1.1 eq), HOBt hydrate (31 mg, 0.204 mmol, 1.1 eq), **5g** (76 mg, 0.222 mmol, 1.2 eq), and Et_3N (46 μL, 0.333 mmol, 1.8 eq) in DMF (4 mL) yielded, after purification by flash column chromatography (SiO_2; 9:1/CH_2Cl_2:MeOH with NH_4OH (7 mL/L of solvent), R_f 0.37), **10d** (39 mg, 37%) as an orange solid: ^1H NMR ($CDCl_3$, 500 MHz) δ 9.22 (s, 1H), 7.98 (d, 1H, *J* = 8.5 Hz), 7.93 (d, 1H, *J* = 8.4 Hz), 7.57 (t, 1H, *J* = 7.1 Hz), 7.43 (d, 1H, *J* = 7.8 Hz), 7.36 (t, 1H, *J* = 7.3 Hz), 7.22 (t, 1H, *J* = 7.3 Hz), 7.18 (d, 1H, *J* = 7.9 Hz), 7.08 (t, 1H, *J* = 7.6 Hz), 6.95 (d, 2H, *J* = 8.0 Hz), 6.70 (t, 1H, *J* = 7.4 Hz), 6.30 (br t, 1H), 4.00 (very br s, 1H), 3.51 (t, 2H, *J* = 7.2 Hz), 3.43 (q, 2H, *J* = 7.0 Hz), 3.09 (br s, 2H), 2.73 (br s, 2H), 2.34 (s, 3H), 2.22 (s, 3H), 1.94 (br s, 4H), 1.67 (p, 2H, *J* = 7.2 Hz), 1.62 (p, 2H, *J* = 7.4 Hz), 1.39 (m, 4H), 1.32 (br s, 6H); ^{13}C NMR ($CDCl_3$, 125 MHz) δ 169.7, 158.3, 150.9, 147.4, 147.0, 139.6, 138.0, 132.1, 130.7, 128.6, 128.4, 127.3, 125.7, 125.5, 123.6, 122.9, 120.7, 120.2, 117.3, 116.7, 115.7, 114.9, 49.5, 39.8, 34.0, 31.8, 29.6, 29.4, 29.24, 29.16, 26.94, 26.86, 24.8, 23.1, 22.8, 20.7, 13.9; *m/z* calcd for $C_{37}H_{46}N_4O$: 562.37; found 563.45 $[M+H]^+$.

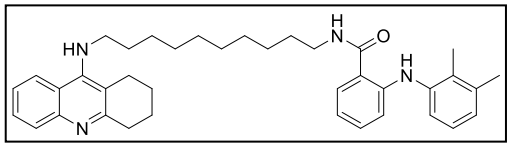

2-((2,3-Dimethylphenyl)amino-*N*-(10-((1,2,3,4-tetrahydroacridin-9-yl)amino)decyl)benzamide (10e). Compound **10e** was prepared as described for the synthesis of **10a**. The reaction of mefenamic acid (**2**) (35 mg, 0.146 mmol, 1 eq), EDAC hydrochloride (31 mg, 0.160 mmol, 1.1 eq), HOBt hydrate (24 mg, 0.160 mmol, 1.1 eq), **5h** (62 mg, 0.175 mmol, 1.2 eq), and Et_3N (37 μL, 0..263 mmol, 1.8 eq) in DMF (3 mL) yielded, after purification by flash column chromatography (SiO_2; 9:1/CH_2Cl_2:MeOH with NH_4OH (7 mL/L of solvent), R_f 0.42), **10e** (10 mg, 12%) as a pale yellow oil: ^1H NMR ($CDCl_3$, 500 MHz) δ 9.21 (s, 1H), 8.00 (d, 1H, *J* = 8.7 Hz), 7.98 (d, 1H, *J* = 11.5 Hz), 7.59 (t, 1H, *J* = 7.3 Hz), 7.42 (d, 1H, *J* = 7.8 Hz), 7.38 (t, 1H, *J* = 7.5 Hz), 7.22 (t, 1H, *J* = 7.6 Hz), 7.19 (d, 1H, *J* = 8.0 Hz), 7.08 (t, 1H, *J* =

7.6 Hz), 6.96 (d, 2H, *J* = 8.2 Hz), 6.70 (t, 1H, *J* = 7.4 Hz), 6.23 (br t, 1H), 4.11 (br s, 1H), 3.55 (t, 2H, *J* = 7.0 Hz), 3.44 (q, 2H, *J* = 6.8 Hz), 3.11 (br s, 2H), 2.72 (br s, 2H), 2.34 (s, 3H), 2.22 (s, 3H), 1.95 (m, 4H), 1.69 (p, 2H, *J* = 7.1 Hz), 1.63 (p, 2H, *J* = 7.3 Hz), 1.40 (m, 4H), 1.31 (m, 8H); ^{13}C NMR ($CDCl_3$, 125 MHz) δ 169.7, 157.9, 151.3, 147.0, 146.7, 139.6, 138.1, 132.1, 130.7, 128.7, 128.1, 127.3, 125.7, 125.5, 123.7, 123.0, 120.7, 119.8, 117.3, 116.7, 115.3, 114.9, 49.5, 39.8, 33.5, 31.8, 29.6, 29.41, 29.38, 29.28, 29.24, 27.0, 26.9, 24.7, 23.0, 22.6, 20.7, 13.9; *m/z* calcd for $C_{38}H_{48}N_4O$: 576.38; found 577.30 $[M+H]^+$.

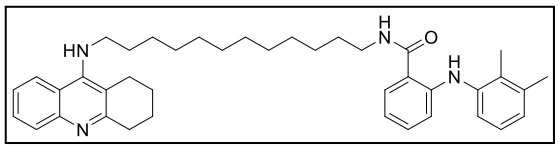

2-((2,3-Dimethylphenyl)amino)-*N*-(12-((1,2,3,4-tetrahydroacridin-9-yl)amino)dodecyl)benzamide (10f). Compound **10f** was prepared as described for the synthesis of **10a**. The reaction of mefenamic acid (**2**) (57 mg, 0.236 mmol, 1 eq), EDAC hydrochloride (50 mg, 0.259 mmol, 1.1 eq), HOBt hydrate (40 mg, 0.259 mmol, 1.1 eq), **5i** (108 mg, 0.283 mmol, 1.2 eq), and Et_3N (59 μL, 0.425 mmol, 1.8 eq) in DMF (4 mL) yielded, after purification by flash column chromatography (SiO_2; 9:1/CH_2Cl_2:MeOH with NH_4OH (7 mL/L of solvent), R_f 0.38), **10f** (27 mg, 19%) as a pale yellow powder: ^{1}H NMR ($CDCl_3$, 500 MHz) δ 9.21 (s, 1H), 7.99 (d, 1H, *J* = 8.5 Hz), 7.93 (d, 1H, *J* = 8.5 Hz), 7.57 (t, 1H, *J* = 7.3 Hz), 7.41 (d, 1H, *J* = 7.8 Hz), 7.36 (t, 1H, *J* = 7.5 Hz), 7.22 (t, 1H, *J* = 7.7 Hz), 7.19 (d, 1H, *J* = 8.0 Hz), 7.08 (t, 1H, *J* = 7.7 Hz), 6.95 (d, 2H, *J* = 8.8 Hz), 6.70 (t, 1H, *J* = 7.6 Hz), 6.27 (br t, 1H), 4.00 (very br s, 1H), 3.51 (t, 2H, *J* = 7.2 Hz), 3.44 (q, 2H, *J* = 6.8 Hz), 3.09 (br s, 2H), 2.73 (br s, 2H), 2.34 (s, 3H), 2.23 (s, 3H), 1.94 (m, 4H), 1.68 (p, 2H, *J* = 7.4 Hz), 1.63 (p, 2H, *J* = 7.3 Hz), 1.40 (m, 4H), 1.29 (m, 12H); ^{13}C NMR ($CDCl_3$, 125 MHz) δ 169.7, 158.4, 150.9, 147.4, 147.0, 139.6, 138.0, 132.1, 130.8, 128.6, 128.3, 127.3, 125.7, 125.5, 123.6, 122.9, 120.7, 120.2, 117.3, 116.7, 115.7, 114.9, 49.6, 39.9, 34.0, 31.8, 29.72, 29.67, 29.52, 29.51, 29.49, 29.4, 29.3, 27.0, 26.9, 24.8, 23.1, 22.8, 20.7, 13.9; *m/z* calcd for $C_{40}H_{52}N_4O$: 604.41; found 605.40 $[M+H]^+$.

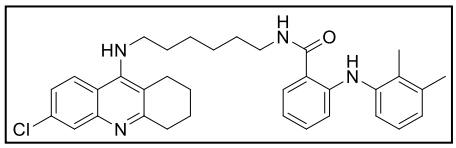

***N*-(6-((6-Chloro-1,2,3,4-tetrahydroacridin-9-yl)amino)hexyl)-2-((2,3-dimethylphenyl)amino)benzamide (11a).**

Compound **11a** was prepared as described for the synthesis of **10a**. The reaction of mefenamic acid (**2**) (57 mg, 0.238 mmol, 1 eq), EDAC hydrochloride (41 mg, 0.262 mmol, 1.1 eq), HOBt hydrate (35 mg, 0.262 mmol, 1.1 eq), **6d** (95 mg, 0.285 mmol, 1.2 eq), and Et_3N (60 μL, 0.428 mmol, 1.8 eq) in DMF (4 mL) yielded, after purification by flash column chromatography (SiO_2; 9:1/CH_2Cl_2:MeOH with NH_4OH (7 mL/L of solvent), R_f 0.48), **11a** (97 mg, 74%) as a pale yellow powder: ^{1}H NMR ($CDCl_3$, 500 MHz) δ 9.21 (br s, 1H), 7.90 (d, 1H, *J* = 8.6 Hz), 7.89 (s, 1H), 7.40 (d, 1H, *J* = 7.9 Hz), 7.26 (d, 1H, *J* = 9.6 Hz), 7.21 (t, 1H, *J* = 7.4 Hz), 7.17 (d, 1H, *J* = 8.0 Hz), 7.07 (t, 1H, *J* = 7.7 Hz), 6.95 (d, 2H, *J* = 8.2 Hz), 6.67 (t, 1H, *J* = 7.5 Hz), 6.40 (br t, 1H), 3.99 (br s, 1H), 3.48 (br t, 2H), 3.43 (q, 2H, *J* = 6.7 Hz), 3.03 (br s, 2H), 2.66 (br s, 2H), 2.33 (s, 3H), 2.21 (s, 3H), 1.91 (br s, 4H), 1.65 (m, 4H), 1.44 (m, 4H); ^{13}C NMR ($CDCl_3$, 125 MHz) δ 169.8, 159.6, 150.8, 148.2, 147.0, 139.6, 138.1, 133.9, 132.2, 130.7, 127.6, 127.3, 125.7, 125.5, 124.6, 124.2, 120.6, 118.4, 117.2, 116.8, 115.8, 114.9, 49.5, 39.6, 34.1, 31.7, 29.6, 26.7, 26.6, 24.6, 22.9, 22.7, 20.7, 13.9; *m/z* calcd for $C_{34}H_{39}ClN_4O$: 554.28; found 555.20 $[M+H]^+$.

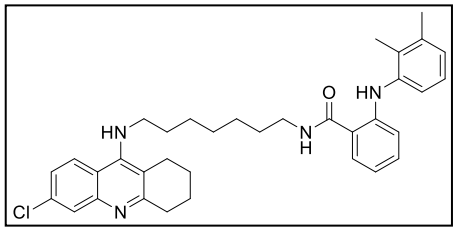

***N*-(7-((6-Chloro-1,2,3,4-tetrahydroacridin-9-yl)amino)heptyl)-2-((2,3-dimethylphenyl)amino)benzamide (11b)**. Compound **11b** was prepared as described for the synthesis of **10a**. The reaction of mefenamic acid (**2**) (30 mg, 0.123 mmol, 1 eq), EDAC hydrochloride (26 mg, 0.136 mmol, 1.1 eq), HOBt hydrate (21 mg, 0.136 mmol, 1.1 eq), **6e** (57 mg, 0.148 mmol, 1.2 eq), and Et_3N (31 μL, 0.222 mmol, 1.8 eq) in DMF (3 mL) yielded, after purification by flash column chromatography (SiO_2; 9:1/CH_2Cl_2:MeOH with NH_4OH (7 mL/L of solvent), R_f 0.50), **11b** (29 mg, 41%) as a pale yellow oil: ^{1}H NMR ($CDCl_3$, 500 MHz) δ 9.20 (s, 1H), 7.91 (d, 1H, *J* = 7.1 Hz), 7.90 (d, 1H, *J* = 1.9 Hz), 7.41 (d, 1H, *J* = 7.8 Hz), 7.28 (dd, 1H, J_1 = 8.9 Hz, J_2 = 1.9 Hz), 7.22 (t, 1H, *J* = 7.6 Hz), 7.18 (d, 1H, *J* = 7.6 Hz), 7.08 (t, 1H, *J* = 7.6 Hz), 6.95 (d, 2H, *J* = 8.2 Hz), 6.70 (t, 1H, *J* = 7.5 Hz), 6.27 (br t, 1H), 3.98 (br s, 1H), 3.49 (t, 2H, *J* = 7.4 Hz), 3.43 (q, 2H, *J* = 6.8 Hz), 3.04 (br s, 2H), 2.68 (br s, 2H), 2.33 (s, 3H), 2.22 (s, 3H), 1.92 (m, 4H), 1.67 (p, 2H, *J* = 7.1 Hz), 1.62 (p, 2H, *J* = 6.9 Hz), 1.40 (br s, 6H); ^{13}C NMR ($CDCl_3$, 125 MHz) δ 169.7, 159.5, 150.9, 148.1, 147.0, 139.6, 138.1, 134.0,

132.2, 130.7, 127.5, 127.2, 125.7, 125.5, 124.6, 124.2, 120.7, 118.4, 117.2, 116.8, 115.8, 114.9, 49.6, 39.7, 34.0, 31.7, 29.6, 29.0, 26.9, 26.8, 24.6, 22.9, 22.7, 20.7, 13.9; *m/z* calcd for $C_{35}H_{41}ClN_4O$: 568.30; found 569.20 $[M+H]^+$.

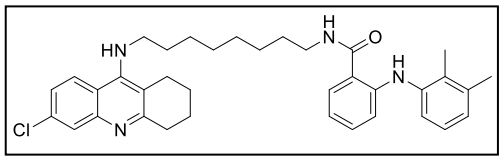

***N*-(8-((6-Chloro-1,2,3,4-tetrahydroacridin-9-yl)amino)octyl)-2-((2,3-dimethylphenyl)amino)benzamide (11c).** Compound **11c** was prepared as described for the synthesis of **10a**. The reaction of mefenamic acid (**2**) (38 mg, 0.158 mmol, 1 eq), EDAC hydrochloride (33 mg, 0.173 mmol, 1.1 eq), HOBt hydrate (26 mg, 0.173 mmol, 1.1 eq), **6f** (68 mg, 0.189 mmol, 1.2 eq), and Et_3N (40 μL, 0.284 mmol, 1.8 eq) in DMF (3 mL) yielded, after purification by flash column chromatography (SiO_2; 9:1/CH_2Cl_2:MeOH with NH_4OH (7 mL/L of solvent), R_f 0.79), **11c** (24 mg, 26%) as a pale yellow oil: ^{1}H NMR ($CDCl_3$, 500 MHz) δ 9.20 (s, 1H), 7.92 (d, 1H, J = 9.6 Hz), 7.90 (s, 1H), 7.42 (d, 1H, J = 7.8 Hz), 7.28 (dd, 1H, J_1 = 9.0 Hz, J_2 = 1.9 Hz), 7.22 (t, 1H, J = 8.2 Hz), 7.18 (d, 1H, J = 7.9 Hz), 7.08 (t, 1H, J = 7.6 Hz), 6.96 (d, 2H, J = 8.2 Hz), 6.70 (t, 1H, J = 7.5 Hz), 6.26 (br t, 1H), 3.98 (br s, 1H), 3.49 (t, 2H, J = 7.1 Hz), 3.43 (q, 2H, J = 6.6 Hz), 3.04 (br s, 2H), 2.68 (br s, 2H), 2.34 (s, 3H), 2.22 (s, 3H), 1.93 (m, 4H), 1.67 (p, 2H, J = 7.3 Hz), 1.62 (p, 2H, J = 7.1 Hz), 1.38 (m, 8H); ^{13}C NMR ($CDCl_3$, 125 MHz) δ 169.7, 159.5, 150.9, 148.2, 147.0, 139.6, 138.1, 134.0, 132.1, 130.7, 127.6, 127.2, 125.7, 125.5, 124.7, 124.2, 120.7, 118.4, 117.2, 116.7, 115.7, 114.9, 49.6, 39.8, 34.0, 31.8, 29.6, 29.20, 29.16, 26.9, 26.8, 24.6, 22.9, 22.7, 20.7, 13.9; *m/z* calcd for $C_{36}H_{43}ClN_4O$: 582.31; found 583.20 $[M+H]^+$.

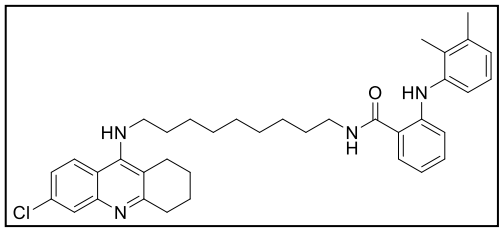

***N*-(9-((6-chloro-1,2,3,4-tetrahydroacridin-9-yl)amino)nonyl)-2-(2,3-dimethylphenyl)amino)benzamide (11d).** Compound **11d** was prepared as described for the synthesis of **10a**. The reaction of mefenamic acid (**2**) (38 mg, 0.159 mmol, 1 eq), EDAC hydrochloride (34 mg, 0.175 mmol, 1.1 eq), HOBt hydrate (27 mg, 0.175 mmol, 1.1 eq), **6g** (71 mg, 0.191 mmol, 1.2 eq), and Et_3N (40 μL, 0.287 mmol, 1.8 eq) in DMF (3 mL) yielded, after purification by flash column

chromatography (SiO_2; 9:1/CH_2Cl_2:MeOH with NH_4OH (7 mL/L of solvent), R_f 0.53), **11d** (42 mg, 44%) as a pale yellow oil: ^1H NMR ($CDCl_3$, 500 MHz) δ 9.23 (s, 1H), 7.91 (d, 1H, *J* = 10.6 Hz), 7.90 (s, 1H), 7.42 (d, 1H *J* = 7.8 Hz), 7.27 (d, 1H, *J* = 10.7 Hz), 7.21 (t, 1H, *J* = 7.5 Hz), 7.18 (d, 1H, *J* = 8.5 Hz), 7.07 (t, 1H, *J* = 7.6 Hz), 6.95 (d, 2H, *J* = 8.1 Hz), 6.68 (t, 1H, *J* = 7.5 Hz), 6.36 (br t, 1H), 4.01 (br s, 1H), 3.49 (t, 2H, *J* = 6.9 Hz), 3.43 (q, 2H, *J* = 6.8 Hz), 3.03 (br s, 2H), 2.67 (br s, 2H), 2.33 (s, 3H), 2.22 (s, 3H), 1.92 (m, 4H), 1.68-1.58 (m, 4H), 1.35 (m, 12H); ^{13}C NMR ($CDCl_3$, 125 MHz) δ 169.7, 159.4, 150.9, 148.1, 147.0, 139.6, 138.0, 134.0, 132.1, 130.7, 127.5, 127.3, 125.7, 125.5, 124.7, 124.2, 120.7, 118.4, 117.3, 116.7, 115.6, 114.9, 49.6, 39.8, 34.0, 31.8, 29.6, 29.4, 29.22, 29.16, 26.9, 26.8, 24.6, 22.9, 22.7, 20.7, 13.9; *m/z* calcd for $C_{37}H_{45}ClN_4O$: 596.32; found 597.20 $[M+H]^+$.

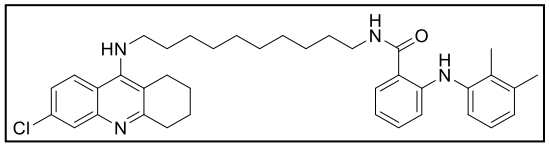

***N*-(10-((6-chloro-1,2,3,4-tetrahydroacridin-9-yl)amino)decyl)-2-((2,3-dimethylphenyl)amino)benzamide** (**11e**). Compound **11e** was prepared as described for the synthesis of **10a**. The reaction of mefenamic acid (**2**) 35 mg, 0.146 mmol, 1 eq), EDAC hydrochloride (31 mg, 0.160 mmol, 1.1 eq), HOBt hydrate (24 mg, 0.160 mmol, 1.1 eq), **6h** (68 mg, 0.175 mmol, 1.2 eq), and Et_3N (37 μL, 0.263 mmol, 1.8 eq) in DMF (3 mL) yielded, after purification by flash column chromatography (SiO_2; 9:1/CH_2Cl_2:MeOH with NH_4OH (7 mL/L of solvent), R_f 0.69), **11e** (35 mg, 39%) as a pale yellow oil: ^1H NMR ($CDCl_3$, 500 MHz) δ 9.21 (s, 1H), 7.93 (d, 1H, *J* = 9.5 Hz), 7.92 (d, 1H, *J* = 2.1 Hz), 7.42 (d, 1H, *J* = 7.8 Hz), 7.28 (dd, 1H, J_1 = 9.0 Hz, J_2 = 2.1 Hz), 7.22 (t, 1H, *J* = 7.6 Hz), 7.18 (d, 1H, *J* = 8.0 Hz), 7.08 (t, 1H, *J* = 7.6 Hz), 6.95 (d, 2H, *J* = 8.2 Hz), 6.69 (t, 1H, *J* = 7.4 Hz), 6.30 (br t, 1H), 4.09 (very br s, 1H), 3.52 (t, 2H, *J* = 7.2 Hz), 3.44 (q, 2H, *J* = 6.8 Hz), 3.04 (br s, 2H), 2.67 (br s, 2H), 2.34 (s, 3H), 2.22 (s, 3H), 1.93 (m, 4H), 1.67 (p, 2H, *J* = 7.4 Hz), 1.62 (p, 2H, *J* = 7.3 Hz), 1.38 (m, 4H), 1.30 (m, 8H); ^{13}C NMR ($CDCl_3$, 125 MHz) δ 169.7, 159.1, 151.1, 147.7, 147.0, 139.6, 138.0, 134.2, 132.1, 130.7, 127.3, 127.1, 125.7, 125.5, 124.7, 124.3, 120.7, 118.2, 117.3, 116.7, 115.4, 114.9, 49.6, 39.8, 33.7, 31.8, 29.6, 29.40, 29.38, 29.26, 29.24, 27.0, 26.8, 24.5, 22.9, 22.6, 20.7, 13.9; *m/z* calcd for $C_{38}H_{47}ClN_4O$: 610.34; found 611.30 $[M+H]^+$.

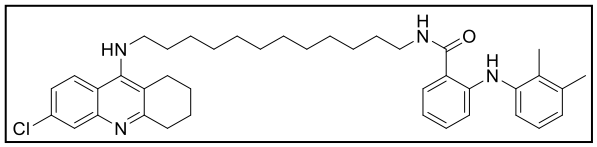

***N*-(12-((6-Chloro-1,2,3,4-tetrahydroacridin-9-yl)amino)dodecyl)-2-((2,3-dimethylphenyl)amino)benzamide (11f).** Compound **11f** was prepared as described for the synthesis of **10a**. The reaction of mefenamic acid (**2**) (32 mg, 0.131 mmol, 1 eq), EDAC hydrochloride (28 mg, 0.144 mmol, 1.1 eq), HOBt hydrate (22 mg, 0.144 mmol, 1.1 eq), **6i** (66 mg, 0.157 mmol, 1.2 eq), and Et_3N (33 μL, 0..234 mmol, 1.8 eq) in DMF (3 mL) yielded, after purification by flash column chromatography (SiO_2; 9:1/CH_2Cl_2:MeOH with NH_4OH (7 mL/L of solvent), R_f 0.51), **11f** (43 mg, 55%) as a pale yellow oil: ^{1}H NMR ($CDCl_3$, 500 MHz) δ 9.22 (s, 1H), 7.91 (d, 1H, *J* = 9.3 Hz), 7.90 (s, 1H), 7.41 (d, 1H, *J* = 7.8 Hz), 7.28 (d, 1H, *J* = 9.0 Hz), 7.21 (t, 1H, *J* = 7.5 Hz), 7.18 (d, 1H, *J* = 8.6 Hz), 7.08 (t, 1H, *J* = 7.6 Hz), 6.95 (d, 2H, *J* = 8.2 Hz), 6.69 (t, 1H, *J* = 7.4 Hz), 6.31 (br t, 1H), 3.99 (br s, 1H), 3.50 (t, 2H, *J* = 6.9 Hz), 3.44 (q, 2H, *J* = 6.6 Hz), 3.04 (br s, 2H), 2.68 (br s, 2H), 2.34 (s, 3H), 2.22 (s, 3H), 1.93 (m, 4H), 1.69-1.60 (m, 4H), 1.33 (m, 18H); ^{13}C NMR ($CDCl_3$, 125 MHz) δ 169.7, 159.5, 150.9, 148.2, 147.0, 139.6, 138.0, 134.0, 132.1, 130.7, 127.6, 127.3, 125.7, 125.5, 124.7, 124.2, 120.7, 118.4, 117.3, 116.7, 115.6, 114.9, 49.6, 39.9, 34.1, 31.8, 29.7, 29.53, 29.49, 29.3, 27.0, 26.9, 24.6, 23.0, 22.7, 20.7, 13.9; *m/z* calcd for $C_{40}H_{51}ClN_4O$: 638.37; found 639.35 $[M+H]^+$.

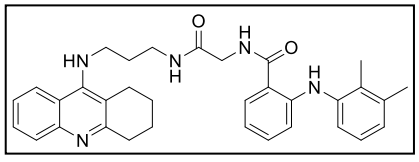

2-((2,3-Dimethylphenyl)amino)-*N*-(2-oxo-2-((3-((1,2,3,4-tetrahydroacridin-9-yl)amino)propyl)amino)ethyl)benzamide (12a). Compound **12a** was prepared as described for the synthesis of **10a**. The reaction of **9a** (78 mg, 0.261 mmol, 1 eq), EDAC hydrochloride (55 mg, 0.287 mmol, 1.1 eq), HOBt hydrate (44 mg, 0.287 mmol, 1.1 eq), **5a** (80 mg, 0.313 mmol, 1.2 eq), and Et_3N (65 μL, 0.470 mmol, 1.8 eq) in DMF (4 mL) yielded, after purification by flash column chromatography (SiO_2; 9:1/CH_2Cl_2:MeOH with NH_4OH (7 mL/L of solvent), R_f 0.28), **12a** (38 mg, 41%) as a white powder: ^{1}H NMR ($CDCl_3$, 500 MHz) δ 9.19 (s, 1H), 8.00 (d, 1H, *J* = 8.4 Hz), 7.93 (d, 1H, *J* = 8.4 Hz), 7.55 (t, 1H, *J* = 7.5 Hz), 7.51 (d, 1H, *J* = 7.5 Hz), 7.35 (t, 1H, *J* = 7.5 Hz), 7.22 (t, 2H, *J* = 7.2 Hz), 7.12 (d, 1H, *J* = 7.8 Hz), 7.07 (t, 1H, *J* = 7.6 Hz), 6.97 (d,

1H, *J* = 7.3 Hz), 6.88 (d, 1H, *J* = 8.5 Hz), 6.84 (br t, 1H), 6.65 (t, 1H, *J* = 7.4 Hz), 4.91 (br s, 1H), 4.14 (d, 2H, *J* = 5.3 Hz), 3.52 (m, 2H), 3.48 (q, 2H, *J* = 6.2 Hz), 3.05 (m, 2H), 2.71 (m, 2H), 2.32 (s, 3H), 2.19 (s, 3H), 1.88 (m, 4H), 1.83 (p, 2H, *J* = 6.3 Hz); ^{13}C NMR ($CDCl_3$, 125 MHz) δ 170.2, 170.0, 151.1, 147.6, 146.3, 139.2, 138.1, 136.4, 132.9, 131.1, 129.9, 128.7, 127.8, 126.0, 125.9, 124.1, 122.6, 121.3, 120.0, 116.9, 116.3, 115.3, 115.0, 45.4, 43.7, 37.0, 33.4, 31.2, 25.0, 22.9, 22.5, 20.7, 13.9; *m/z* calcd for $C_{33}H_{37}N_5O_2$: 535.29; found 536.25 $[M+H]^+$.

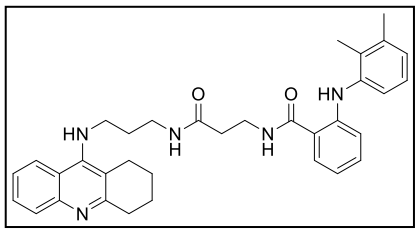

2-((2,3-Dimethylphenyl)amino)-*N*-(3-oxo-3-((3-((1,2,3,4-tetrahydroacridin-9-yl)amino)propyl)amino)propyl)benzamide (12b). Compound **12b** was prepared as described for the synthesis of **10a**. The reaction of **9b** (83 mg, 0.264 mmol, 1 eq), EDAC hydrochloride (56 mg, 0.291 mmol, 1.1 eq), HOBt hydrate (44 mg, 0.291 mmol, 1.1 eq), **5a** (80 mg, 0.317 mmol, 1.2 eq), and Et_3N (66 μL, 0.474 mmol, 1.8 eq) in DMF (4 mL) yielded, after purification by flash column chromatography (SiO_2; 9:1/CH_2Cl_2:MeOH with NH_4OH (7 mL/L of solvent), R_f 0.19), **12b** (46 mg, 32%) as a white powder: ^{1}H NMR ($CDCl_3$, 500 MHz) δ 9.30 (s, 1H), 7.99 (d, 1H, *J* = 8.5 Hz), 7.90 (d, 1H, *J* = 8.5 Hz), 7.54 (t, 1H, *J* = 7.6 Hz), 7.45 (d, 1H, *J* = 7.9 Hz), 7.33 (m, 2H), 7.20 (t, 1H, *J* = 7.8 Hz), 7.16 (d, 1H, *J* = 7.9 Hz), 7.07 (t, 1H, *J* = 7.7 Hz), 6.96 (d, 1H, *J* = 7.4 Hz), 6.93 (d, 1H, *J* = 8.5 Hz), 6.64 (m, 2H), 4.78 (br t, 1H,), 3.74 (q, 2H, *J* = 5.9 Hz), 3.48 (q, 2H, *J* = 6.2 Hz), 3.42 (q, 2H, *J* = 6.3 Hz), 3.05 (t, 2H, *J* = 5.9 Hz), 2.73 (t, 2H, *J* = 5.7 Hz), 2.56 (t, 2H, *J* = 5.9 Hz), 2.32 (s, 3H), 2.20 (s, 3H), 1.89 (m, 4H), 1.79 (p, 2H, *J* = 6.4 Hz); ^{13}C NMR ($CDCl_3$, 125 MHz) δ 172.5, 169.9, 158.3, 150.7, 147.2, 147.0, 139.5, 138.1, 132.4, 130.8, 128.5, 128.3, 127.6, 125.8, 125.6, 123.9, 122.6, 120.8, 120.3, 116.9, 116.44, 116.42, 114.9, 45.4, 36.7, 35.8, 35.5, 33.8, 31.4, 25.1, 23.0, 22.7, 20.7, 13.9; *m/z* calcd for $C_{34}H_{39}N_5O_2$: 549.31; found 550.20 $[M+H]^+$.

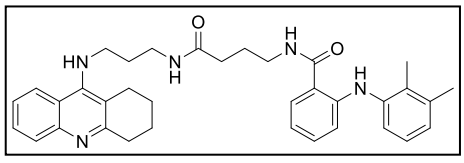

2-((2,3-Dimethylphenyl)amino)-*N*-(4-oxo-4-((3-((1,2,3,4-tetrahydroacridin-9-yl)amino)propyl)amino)butyl)benzamide (12c).

Compound **12c** was prepared as described for the synthesis of **10a**. The reaction of **9c** (85 mg, 0.261 mmol, 1 eq), EDAC hydrochloride (55 mg, 0.287 mmol, 1.1 eq), HOBt hydrate (44 mg, 0.287 mmol, 1.1 eq), **5a** (80 mg, 0.313 mmol, 1.2 eq), and Et_3N (65 μL, 0.470 mmol, 1.8 eq) in DMF (4 mL) yielded, after purification by flash column chromatography (SiO_2; 9:1/CH_2Cl_2:MeOH with NH_4OH (7 mL/L of solvent), R_f 0.19), **12c** (52 mg, 35%) as a white powder: ^{1}H NMR ($CDCl_3$, 500 MHz) δ 9.30 (s, 1H), 8.02 (d, 1H, J = 8.2 Hz), 7.90 (d, 1H, J = 8.2 Hz), 7.54 (ddd, 1H, J_1 = 7.6 Hz, J_2 = 7.0 Hz, J_3 = 1.0 Hz), 7.50 (dd, 1H, J_1 = 7.9 Hz, J_2 = 1.3 Hz), 7.33 (ddd, 1H, J_1 = 7.6 Hz, J_2 = 7.1 Hz, J_3 = 1.0 Hz), 7.18 (m, 3H), 7.07 (t, 1H, J = 7.7 Hz), 6.95 (m, 2H), 6.85 (t, 1H, J = 5.9 Hz), 6.67 (m, 1H), 4.83 (br t, 1H), 3.50 (m, 4H), 3.41 (q, 2H, J = 6.3 Hz), 3.04 (t, 2H, J = 6.1 Hz), 2.74 (t, 2H, J = 5.9 Hz), 2.35 (t, 2H, J = 6.5 Hz), 2.32 (s, 3H), 2.20 (s, 3H), 1.97 (p, 2H, J = 6.3 Hz), 1.89 (m, 4H), 1.79 (p, 2H, J = 6.4 Hz); ^{13}C NMR ($CDCl_3$, 125 MHz) δ 173.8, 170.3, 158.3, 150.7, 147.1, 147.0, 139.5, 138.1, 132.3, 130.7, 128.5, 128.3, 127.6, 125.8, 125.6, 123.9, 122.7, 120.7, 120.3, 116.9, 116.6, 116.4, 114.9, 45.4, 39.4, 36.7, 34.0, 33.8, 31.4, 25.4, 25.1, 23.0, 22.7, 20.7, 13.9; *m/z* calcd for $C_{35}H_{41}N_5O_2$: 563.33; found 564.30 $[M+H]^+$.

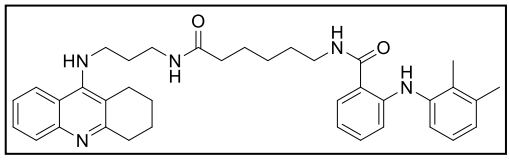

2-((2,3-Dimethylphenyl)amino)-*N*-(6-oxo-6-((3-((1,2,3,4-tetrahydroacridin-9-yl)amino)propyl)amino)hexyl)benzamide (12d). Compound **12d** was prepared as described for the synthesis of **10a**. The reaction of **9d** (104 mg, 0.294 mmol, 1 eq), EDAC hydrochloride (62 mg, 0.323 mmol, 1.1 eq), HOBt hydrate (50 mg, 0.323 mmol, 1.1 eq), **5a** (90 mg, 0.352 mmol, 1.2 eq), and Et_3N (73 μL, 0.529 mmol, 1.8 eq) in DMF (4 mL) yielded, after purification by flash column chromatography (SiO_2; 9:1/CH_2Cl_2:MeOH with NH_4OH (7 mL/L of solvent), R_f 0.19), **12d** (58 mg, 33%) as a pale yellow: ^{1}H NMR ($CDCl_3$, 300 MHz) δ 9.24 (s, 1H), 8.04 (d, 1H, J = 8.5 Hz), 7.89 (d, 1H, J = 8.4 Hz), 7.53 (d, 1H, J = 7.2 Hz), 7.49 (t, 1H, J = 9.0 Hz), 7.32 (t, 1H, J = 7.6 Hz), 7.15 (m, 2H), 7.04 (t, 1H, J = 7.6 Hz), 6.91 (m, 2H), 6.82 (t, 1H, J = 5.5 Hz), 6.76 (t, 1H, J = 5.8 Hz), 6.62 (t, 1H, J = 7.5 Hz), 5.30 (br s, 1H), 3.50 (m, 2H), 3.38 (m, 4H), 3.02 (m, 2H), 2.71 (m, 2H), 2.30 (s, 3H), 2.23 (m, 2H), 2.21 (s, 3H), 1.86 (m, 4H), 1.76-1.58 (m, 6H), 1.38 (m, 2H); ^{13}C NMR ($CDCl_3$, 75 MHz) δ 174.2, 169.9, 157.4, 151.4, 146.9, 146.0, 139.6, 138.1, 132.1, 130.6, 128.9, 127.6, 127.1, 125.7, 125.5,

124.0, 123.0, 120.5, 119.7, 117.1, 116.8, 115.6, 114.8, 45.0, 39.4, 36.34, 36.28, 33.1, 31.4, 29.1, 26.4, 25.2, 25.0, 22.9, 22.5, 20.7, 13.9; *m/z* calcd for $C_{37}H_{45}N_5O_2$: 591.36; found 592.35 $[M+H]^+$.

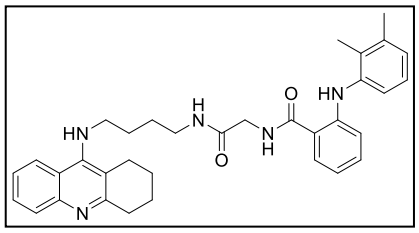

2-((2,3-Dimethylphenyl)amino)-*N*-(2-oxo-2-((4-((1,2,3,4-tetrahydroacridin-9-yl)amino)butyl)amino)ethyl)benzamide (12e). Compound **12e** was prepared as described for the synthesis of **10a**. The reaction of **9a** (83 mg, 0.278 mmol, 1 eq), EDAC hydrochloride (59 mg, 0.306 mmol, 1.1 eq), HOBt hydrate (47 mg, 0.306 mmol, 1.1 eq), **5b** (90 mg, 0.334 mmol, 1.2 eq), and Et_3N (70 μL, 0.500 mmol, 1.8 eq) in DMF (4 mL) yielded, after purification by flash column chromatography (SiO_2; 9:1/CH_2Cl_2:MeOH with NH_4OH (7 mL/L of solvent), R_f 0.29), **12e** (54 mg, 36%) as a white powder: ^1H NMR ($CDCl_3$, 500 MHz) δ 9.23 (s, 1H), 7.91 (t, 2H, *J* = 9.1 Hz), 7.57 (d, 2H, *J* = 6.6 Hz), 7.53 (t, 1H, *J* = 7.2 Hz), 7.31 (t, 1H, *J* = 7.3 Hz), 7.19 (t, 1H, *J* = 7.4 Hz), 7.12 (d, 1H, *J* = 7.9 Hz), 7.05 (t, 2H, *J* = 7.3 Hz), 6.95 (d, 1H, *J* = 7.4 Hz), 6.86 (d, 1H, *J* = 8.4 Hz), 6.65 (t, 1H, *J* = 7.3 Hz), 4.10 (d, 3H, *J* = 5.2 Hz), 3.46 (br s, 2H), 3.31 (q, 2H, *J* = 6.6 Hz), 3.03 (t, 2H, *J* = 5.4 Hz), 2.64 (t, 2H, *J* = 5.9 Hz), 2.29 (s, 3H), 2.15 (s, 3H), 1.87 (m, 4H), 1.66 (m, 2H), 1.61 (m, 2H); ^{13}C NMR ($CDCl_3$, 125 MHz) δ 170.2, 169.4, 158.1, 150.9, 147.6, 146.9, 139.3, 138.1, 132.8, 131.2, 128.6, 128.00, 127.98, 126.0, 125.9, 123.8, 122.9, 121.4, 120.1, 116.8, 116.0, 115.4, 114.8, 48.8, 43.7, 39.2, 33.6, 28.8, 27.0, 24.8, 22.9, 22.6, 20.6, 13.9; *m/z* calcd for $C_{34}H_{39}N_5O_2$: 549.31; found 550.25 $[M+H]^+$.

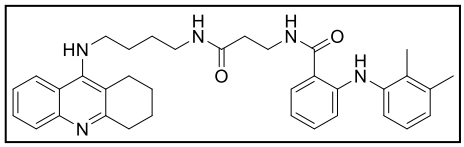

2-((2,3-Dimethylphenyl)amino)-*N*-(3-oxo-3-((4-((1,2,3,4-tetrahydroacridin-9-yl)amino)butyl)amino)propyl)benzamide (12f). Compound **12f** was prepared as described for the synthesis of **10a**. The reaction of **9b** (75 mg, 0.2404 mmol, 1 eq), EDAC hydrochloride (50.7 mg, 0.2644 mmol, 1.1 eq), HOBt hydrate (40.5 mg, 0.2644 mmol, 1.1 eq), **5b** (127.2 mg, .4722 mmol, 1.96 eq), and Et_3N (60 μL, 0.4327 mmol, 1.8 eq) in DMF (3 mL) yielded, after purification by flash column chromatography (SiO_2; 9:1/CH_2Cl_2:MeOH with NH_4OH (7 mL/L of solvent), R_f 0.19), **12f**

(65 mg, 48%) as a pink powder: ^{1}H NMR ($CDCl_3$, 300 MHz) δ 9.32 (s, 1H), 7.92 (d, 1H, *J* = 6.0 Hz), 7.90 (d, 1H, *J* = 7.1 Hz), 7.53 (t, 1H, *J* = 7.6 Hz), 7.46 (d, 1H, *J* = 7.9 Hz), 7.40 (t, 1H, *J* = 5.6 Hz), 7.32 (t, 1H, *J* = 7.7 Hz), 7.18 (t, 1H, *J* = 7.0 Hz), 7.14 (d, 1H, *J* = 5.0 Hz), 7.05 (t, 1H, *J* = 7.7 Hz), 6.93 (d, 1H, *J* = 4.9 Hz), 6.91 (d, 1H, *J* = 8.4 Hz), 6.65 (t, 1H, *J* = 7.5 Hz), 6.60 (t, 1H, *J* = 5.9 Hz), 4.17 (br s, 1H), 3.69 (q, 2H, *J* = 5.8 Hz), 3.46 (m, 2H), 2.28 (q, 2H, *J* = 6.3 Hz), 3.03 (br t, 2H), 2.64 (br t, 2H), 2.51 (t, 2H, *J* = 5.8 Hz), 2.30 (s, 3H), 2.18 (s, 3H), 1.87 (m, 4H), 1.64 (m, 4H); ^{13}C NMR ($CDCl_3$, 75 MHz) δ 171.9, 169.8, 157.8, 151.0, 147.2, 146.6, 139.5, 138.1, 132.3, 130.7, 128.7, 127.8, 127.7, 125.8, 125.6, 123.9, 122.9, 120.7, 119.9, 116.8, 116.5, 115.8, 114.8, 48.7, 39.1, 35.8, 35.4, 33.5, 28.9, 27.0, 24.7, 22.9, 22.6, 20.7, 13.9; *m/z* calcd for $C_{35}H_{41}N_5O_2$: 563.33; found 564.30 $[M+H]^+$.

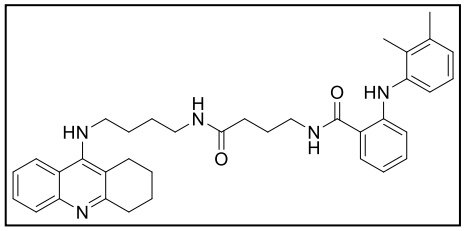

2-((2,3-Dimethylphenyl)amino)-*N*-(4-oxo-4-((4-((1,2,3,4-tetrahydroacridin-9-yl)amino)butyl)amino)butyl)benzamide (12g). Compound **12g** was prepared as described for the synthesis of **10a**. The reaction of **9c** (114 mg, 0.348 mmol, 1 eq), EDAC hydrochloride (73 mg, 0.383 mmol, 1.1 eq), HOBt hydrate (59 mg, 0.383 mmol, 1.1 eq), **5b** (122 mg, 0.453 mmol, 1.3 eq), and Et_3N (87 μL, 0.627 mmol, 1.8 eq) in DMF (4 mL) yielded, after purification by flash column chromatography (SiO_2; 9:1/CH_2Cl_2:MeOH with NH_4OH (7 mL/L of solvent), R_f 0.14), **12g** (32 mg, 16%) as a pink solid: ^{1}H NMR ($CDCl_3$, 300 MHz) δ 9.33 (s, 1H), 7.94 (d, 1H, *J* = 8.5 Hz), 7.91 (d, 1H, *J* = 8.4 Hz), 7.53 (t, 2H, *J* = 8.0 Hz), 7.32 (t, 1H, *J* = 7.5 Hz), 7.26 (br t, 1H), 7.18 (t, 1H, *J* = 7.4 Hz), 7.14 (d, 1H, *J* = 7.9 Hz), 7.04 (t, 1H, *J* = 7.7 Hz), 6.92 (m, 2H), 6.74 (br t, 1H), 6.69 (t, 1H, *J* = 7.3 Hz), 4.28 (br s, 1H), 3.48 (m, 4H), 3.31 (m, 2H), 3.04 (m, 2H), 2.65 (m, 2H), 2.32 (m, 5H), 2.17 (s, 3H), 1.93 (m, 2H), 1.87 (m, 4H), 1.70 (m, 2H), 1.61 (m, 2H); ^{13}C NMR ($CDCl_3$, 75 MHz) δ 173.2, 170.3, 157.6, 151.2, 147.1, 146.3, 139.6, 138.1, 132.3, 130.6, 128.8, 127.8, 127.5, 125.8, 125.6, 123.9, 123.0, 120.7, 119.8, 116.9, 116.6, 115.7, 114.8, 48.8, 39.4, 39.2, 34.1, 33.3, 28.9, 27.0, 25.2, 24.7, 22.9, 22.5, 20.7, 13.9; *m/z* calcd for $C_{36}H_{43}N_5O_2$: 577.34; found 578.30 $[M+H]^+$.

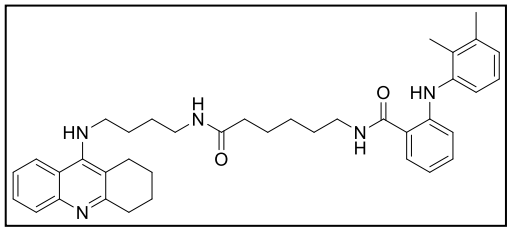

2-((2,3-Dimethylphenyl)amino)-*N*-(6-oxo-6-((4-((1,2,3,4-tetrahydroacridin-9-yl)amino)butyl)amino)hexyl)benzamide (12h). Compound **12h** was prepared as described for the synthesis of **10a**. The reaction of **9d** (80 mg, 0.226 mmol, 1 eq), EDAC hydrochloride (47.6 mg, 0.248 mmol, 1.1 eq), HOBt hydrate (38 mg, 0.248 mmol, 1.1 eq), **5b** (102 mg, 0.377 mmol, 1.7 eq), and Et_3N (57 μL, 0.406 mmol, 1.8 eq) in DMF (4 mL) yielded, after purification by flash column chromatography (SiO_2; 9:1/CH_2Cl_2:MeOH with NH_4OH (7 mL/L of solvent), R_f 0.17), **12h** (43 mg, 31%) as a pink powder: ^{1}H NMR ($CDCl_3$, 300 MHz) δ 9.23 (s, 1H), 7.91 (t, 2H, J = 8.7 Hz), 7.53 (td, 1H, J_1 = 7.6 Hz, J_2 = 1.2 Hz), 7.45 (dd, 1H, J_1 = 7.9 Hz, J_2 = 1.3 Hz), 7.32 (td, 1H, J_1 = 7.4 Hz, J_2 = 1.1 Hz), 7.17 (td, 1H, J_1 = 7.8 Hz, J_2 = 1.4 Hz), 7.14 (d, 1H, J = 7.6 Hz), 7.04 (t, 1H, J = 7.7 Hz), 6.93 (br s, 1H), 6.90 (br s, 1H), 6.65 (m, 2H), 5.99 (t, 1H, J = 5.7 Hz), 4.10 (br s, 1H), 3.46 (m, 2H), 3.39 (q, 2H, J = 6.8 Hz), 3.24 (q, 2H, J = 6.5 Hz), 3.03 (br t, 2H), 2.66 (br t, 2H), 2.30 (s, 3H), 2.18 (s, 3H), 2.14 (t, 2H, J = 7.3 Hz), 1.88 (m, 4H), 1.62 (m, 8H), 1.36 (m, 2H); ^{13}C NMR ($CDCl_3$, 75 MHz) δ 173.1, 169.9, 158.0, 150.9, 146.9, 146.7, 139.6, 138.1, 132.1, 130.6, 128.6, 127.9, 127.6, 125.7, 125.5, 123.8, 122.9, 120.6, 120.0, 117.1, 116.8, 115.9, 114.8, 48.8, 39.3, 39.0, 36.3, 33.5, 29.1, 28.9, 27.1, 26.3, 25.0, 24.8, 22.9, 22.6, 20.7, 13.9; *m/z* calcd for $C_{38}H_{47}N_5O_2$: 605.37; found 606.30 $[M+H]^+$.

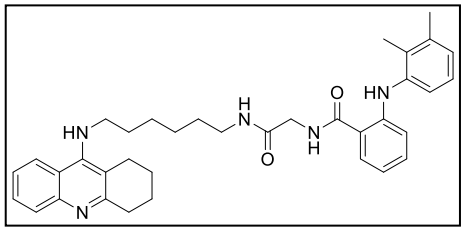

2-((2,3-Dimethylphenyl)amino)-*N*-(2-oxo-2-((6-((1,2,3,4-tetrahydroacridin-9-yl)amino)hexyl)amino)ethyl)benzamide (12i). Compound **12i** was prepared as described for the synthesis of **10a**. The reaction of **9a** (73 mg, 0.246 mmol, 1 eq), EDAC hydrochloride (52 mg, 0.270 mmol, 1.1 eq), HOBt hydrate (41 mg, 0.270 mmol, 1.1 eq), **5d** (88 mg, 0.295 mmol, 1.2 eq), and Et_3N (62 μL, 0.442 mmol, 1.8 eq) in DMF (4 mL) yielded, after purification by flash column chromatography (SiO_2; 9:1/CH_2Cl_2:MeOH with NH_4OH (7 mL/L of solvent), R_f 0.30), **12i** (123 mg, 87%) as a pale yellow powder: ^{1}H NMR ($CDCl_3$, 500 MHz) δ 9.21 (s, 1H), 7.95 (d, 1H, J = 8.5 Hz), 7.93 (d, 1H, J = 8.4 Hz), 7.55 (m, 2H), 7.35 (t, 1H, J = 7.6 Hz), 7.21 (m, 2H), 7.15 (d, 1H,

J = 7.9 Hz), 7.08 (t, 1H, *J* = 7.6 Hz), 6.97 (d, 1H, *J* = 7.3 Hz), 6.88 (d, 1H, *J* = 8.4 Hz), 6.69 (t, 1H, *J* = 7.5 Hz), 6.37 (br t, 1H), 4.09 (d, 2H, *J* = 4.9 Hz), 4.08 (br s, 1H), 3.46 (m, 2H), 3.30 (q, 2H, *J* = 6.3 Hz), 3.08 (br t, 2H), 2.70 (br t, 2H), 2.32 (s, 3H), 2.19 (s, 3H), 1.93 (m, 4H), 1.63 (p, 2H, *J* = 7.0 Hz), 1.53 (p, 2H, *J* = 7.0 Hz), 1.38 (m, 4H); ^{13}C NMR ($CDCl_3$, 125 MHz) δ 170.1, 169.0, 158.2, 150.9, 147.6, 147.2, 139.3, 138.1, 132.8, 131.2, 128.5, 128.4, 127.8, 126.0, 125.9, 123.7, 122.9, 121.4, 120.1, 116.8, 115.8, 115.4, 114.9, 49.3, 43.7, 39.4, 33.8, 31.6, 29.4, 26.53, 26.50, 24.8, 23.0, 22.7, 20.7, 13.9; *m/z* calcd for $C_{36}H_{43}N_5O_2$: 577.34; found 578.25 $[M+H]^+$.

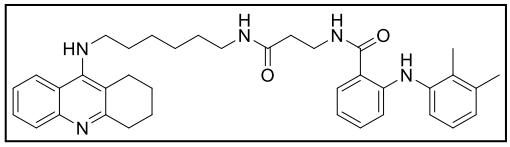

2-((2,3-Dimethylphenyl)amino)-*N*-(3-oxo-3-((6-((1,2,3,4-tetrahydroacridin-9-yl)amino)hexyl)amino)propyl)benzamide (12j). Compound **12j** was prepared as described for the synthesis of **10a**. The reaction of **9b** (85 mg, 0.272 mmol, 1 eq), EDAC hydrochloride (57 mg, 0.299 mmol, 1.1 eq), HOBt hydrate (46 mg, 0.299 mmol, 1.1 eq), **5d** (110 mg, 0.369 mmol, 1.36 eq), and Et_3N (68 μL, 0.490 mmol, 1.8 eq) in DMF (4 mL) yielded, after purification by flash column chromatography (SiO_2; 9:1/CH_2Cl_2:MeOH with NH_4OH (7 mL/L of solvent), R_f 0.50), **12j** (113 mg, 70%) as a pale yellow powder: ^{1}H NMR ($CDCl_3$, 500 MHz) δ 9.34 (s, 1H), 7.95 (d, 1H, *J* = 8.5 Hz), 7.91 (d, 1H, *J* = 8.5 Hz), 7.55 (t, 1H, *J* = 7.6 Hz), 7.46 (d, 1H, *J* = 7.8 Hz), 7.40 (br t, 1H), 7.34 (t, 1H, *J* = 7.6 Hz), 7.18 (m, 2H), 7.06 (t, 1H, *J* = 7.7 Hz), 6.93 (t, 2H, *J* = 8.6 Hz), 6.66 (t, 1H, *J* = 7.5 Hz), 6.33 (br t, 1H), 4.04 (br s, 1H), 3.70 (q, 2H, *J* = 5.7 Hz), 3.46 (br t, 2H), 3.24 (q, 2H, *J* = 6.6 Hz), 3.06 (br t, 2H), 2.69 (br t, 2H), 2.51 (t, 2H, *J* = 5.8 Hz), 2.32 (s, 3H), 2.20 (s, 3H), 1.91 (br s, 4H), 1.61 (p, 2H, *J* = 7.1 Hz), 1.49 (p, 2H, *J* = 7.1 Hz), 1.34 (m, 4H); ^{13}C NMR ($CDCl_3$, 75 MHz) δ 171.7, 169.8, 158.2, 150.9, 147.2, 139.5, 138.1, 132.3, 130.8, 128.5, 128.4, 127.7, 125.8, 125.6, 123.7, 122.9, 120.8, 120.1, 116.8, 116.5, 115.8, 114.8, 49.3, 39.4, 35.8, 35.5, 33.8, 31.6, 29.5, 26.6, 26.5, 24.8, 23.0, 22.7, 20.7, 13.9; *m/z* calcd for $C_{37}H_{45}N_5O_2$: 591.36; found 592.35 $[M+H]^+$.

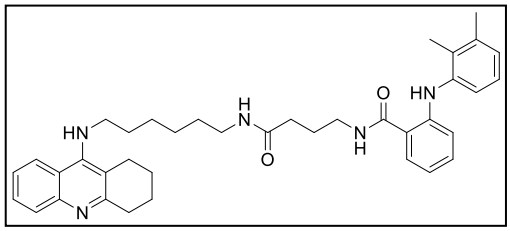

2-((2,3-Dimethylphenyl)amino)-*N*-(4-oxo-4-((6-((1,2,3,4-tetrahydroacridin-9-yl)amino)hexyl)amino)butyl)benzamide (12k). Compound **12k** was prepared as described for the synthesis of **10a**. The reaction of **9c** (70 mg, 0.214 mmol, 1 eq), EDAC hydrochloride (45 mg, 0.236 mmol, 1.1 eq), HOBt hydrate (36 mg, 0.236 mmol, 1.1 eq), **5d** (77 mg, 0.257 mmol, 1.2 eq), and Et_3N (54 μL, 0.386 mmol, 1.8 eq) in DMF (4 mL) yielded, after purification by flash column chromatography (SiO_2; 9:1/CH_2Cl_2:MeOH with NH_4OH (7 mL/L of solvent), R_f 0.19), **12k** (46 mg, 35%) as a pink powder: ^{1}H NMR ($CDCl_3$, 300 MHz) δ 9.38 (s, 1H), 7.96 (d, 1H, J = 8.5 Hz), 7.92 (d, 1H, J = 8.5 Hz), 7.55 (t, 1H, J = 7.6 Hz), 7.51 (d, 1H, J = 7.9 Hz), 7.34 (t, 1H, J = 7.6 Hz), 7.30 (t, 1H, J = 5.1 Hz), 7.18 (m, 2H), 7.06 (t, 1H, J = 7.7 Hz), 6.93 (d, 2H, J = 8.1 Hz), 6.68 (t, 1H, J = 7.5 Hz), 6.53 (br t, 1H), 4.11 (br s, 1H), 3.47 (m, 4H), 3.23 (q, 2H, J = 6.5 Hz), 3.06 (br t, 2H), 2.68 (br t, 2H), 2.30 (m, 5H), 2.20 (s, 3H), 1.94 (m, 2H, J = 6.4 Hz), 1.90 (m, 4H), 1.63 (p, 2H, J = 7.0 Hz), 1.49 (p, 2H, J = 6.9 Hz), 1.34 (m, 4H); ^{13}C NMR ($CDCl_3$, 75 MHz) δ 173.1, 170.2, 158.0, 151.1, 147.1, 146.9, 139.6, 138.1, 132.2, 130.6, 128.6, 128.0, 127.8, 125.8, 125.5, 123.7, 123.0, 120.7, 119.9, 116.9, 116.6, 115.5, 114.8, 49.2, 39.5, 39.4, 34.1, 33.6, 31.6, 29.5, 26.6, 26.5, 25.2, 24.7, 23.0, 22.6, 20.7, 13.9; *m/z* calcd for $C_{38}H_{47}N_5O_2$: 605.37; found 606.30 $[M+H]^+$.

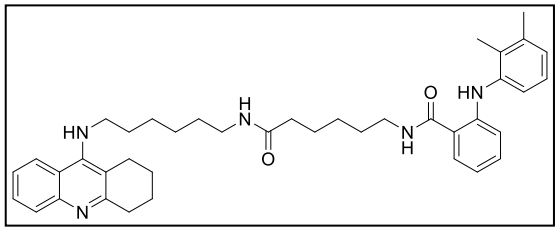

2-((2,3-Dimethylphenyl)amino)-*N*-(6-oxo-6-((6-((1,2,3,4-tetrahydroacridin-9-yl)amino)hexyl)amino)hexyl)benzamide (12l). Compound **12l** was prepared as described for the synthesis of **10a**. The reaction of **9d** (88 mg, 0.247 mmol, 1 eq), EDAC hydrochloride (42 mg, 0.272 mmol, 1.1 eq), HOBt hydrate (37 mg, 0.272 mmol, 1.1 eq), **5d** (90 mg, 0.302 mmol, 1.2 eq), and Et_3N (62 μL, 0.445 mmol, 1.8 eq) in DMF (4 mL) yielded, after purification by flash column chromatography (SiO_2; 9:1/CH_2Cl_2:MeOH with NH_4OH (7 mL/L of solvent), R_f 0.56), **12l** (97 mg, 62%) as a pale yellow powder: ^{1}H NMR ($CDCl_3$, 500 MHz) δ 9.27 (s, 1H), 7.95 (d, 1H, J = 9.1 Hz), 7.89 (d, 1H, J = 8.5 Hz), 7.52 (t, 1H, J = 7.2 Hz), 7.47 (d, 1H, J = 7.8

Hz), 7.31 (t, 1H, J = 7.4 Hz), 7.14 (m, 2H), 7.02 (t, 1H, J = 7.6 Hz), 6.95 (t, 1H, J = 5.5 Hz), 6.90 (m, 2H), 6.62 (t, 1H, J = 7.4 Hz), 6.27 (t, 1H, J = 5.5 Hz), 4.18 (br s, 1H), 3.45 (t, 2H, J = 7.0 Hz), 3.38 (q, 2H, J = 6.7 Hz), 3.17 (q, 2H, J = 6.6 Hz), 3.02 (br t, 2H), 2.65 (br t, 2H), 2.28 (s, 3H), 2.17 (s, 3H), 2.13 (t, 2H, J = 7.4 Hz), 1.87 (br s, 4H), 1.61 (m, 6H), 1.44 (m, 2H), 1.35 (m, 4H), 1.25 (m, 2H); ^{13}C NMR ($CDCl_3$, 125 MHz) δ 173.1, 169.9, 157.9, 151.1, 146.9, 146.8, 139.6, 138.0, 132.0, 130.5, 128.6, 128.0, 127.7, 125.7, 125.4, 123.7, 123.1, 120.5, 119.9, 117.2, 116.8, 115.5, 114.7, 49.2, 39.4, 39.2, 36.3, 33.6, 31.6, 29.5, 29.1, 26.6, 26.5, 26.4, 25.1, 24.7, 23.0, 22.6, 20.7, 13.9; *m/z* calcd for $C_{40}H_{51}N_5O_2$: 633.40; found 634.35 $[M+H]^+$.

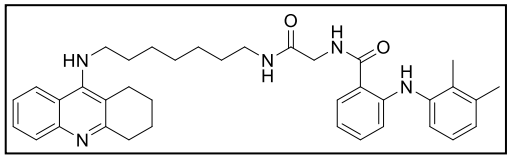

2-((2,3-Dimethylphenyl)amino)-*N*-(2-oxo-2-((7-((1,2,3,4-tetrahydroacridin-9-yl)amino)heptyl)amino)ethyl)benzamide (12m). Compound **12m** was prepared as described for the synthesis of **10a**. The reaction of **9a** (56 mg, 0.186 mmol, 1 eq), EDAC hydrochloride (39 mg, 0.205 mmol, 1.1 eq), HOBt hydrate (31 mg, 0.205 mmol, 1.1 eq), **5e** (70 mg, 0.223 mmol, 1.2 eq), and Et_3N (47 μL, 0.335 mmol, 1.8 eq) in DMF (4 mL) yielded, after purification by flash column chromatography (SiO_2; 9:1/CH_2Cl_2:MeOH with NH_4OH (7 mL/L of solvent), R_f 0.29), **12m** (35 mg, 32%) as a pale yellow powder: ^{1}H NMR ($CDCl_3$, 500 MHz) δ 9.24 (s, 1H), 7.97 (d, 1H, J = 8.3 Hz), 7.93 (d, 1H, J = 8.4 Hz), 7.56 (m, 2H), 7.36 (m, 2H), 7.21 (td, 1H, J_1 = 7.2 Hz, J_2 = 1.2 Hz), 7.15 (d, 1H, J = 7.8 Hz), 7.07 (t, 1H, J = 7.6 Hz), 6.96 (d, 1H, J = 7.4 Hz), 6.88 (d, 1H, J = 8.4 Hz), 6.67 (t, 1H, J = 7.2 Hz), 6.55 (t, 1H, J = 5.5 Hz), 4.11 (d, 2H, J = 5.2 Hz), 3.48 (t, 2H, J = 7.2 Hz), 3.27 (q, 2H, J = 6.8 Hz), 3.07 (br s, 2H), 2.70 (br s, 2H), 2.32 (s, 3H), 2.18 (s, 3H), 1.92 (m, 4H), 1.63 (p, 2H, J = 7.2 Hz), 1.48 (br p, 2H, J = 6.4 Hz), 1.33 (m, 7H); ^{13}C NMR ($CDCl_3$, 125 MHz) δ 170.1, 169.0, 157.9, 151.2, 147.6, 146.8, 139.3, 138.1, 132.7, 131.2, 128.6, 128.0, 127.9, 125.9, 125.8, 123.7, 123.0, 121.4, 119.9, 116.8, 115.53, 115.48, 114.8, 49.3, 43.6, 39.6, 33.6, 31.6, 29.3, 28.9, 26.70, 26.65, 24.7, 23.0, 22.6, 20.7, 13.9; *m/z* calcd for $C_{37}H_{45}N_5O_2$: 591.36; found 592.30 $[M+H]^+$.

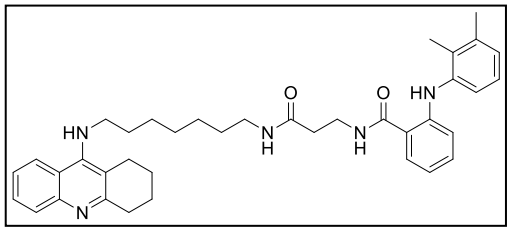

2-((2,3-Dimethylphenyl)amino)-*N*-(3-oxo-3-((7-((1,2,3,4-tetrahydroacridin-9-yl)amino)heptyl)amino)propyl)benzamide (12n). Compound **12n** was prepared as described for the synthesis of **10a**. The reaction of **9b** (56 mg, 0.178 mmol, 1 eq), EDAC hydrochloride (38 mg, 0.196 mmol, 1.1 eq), HOBt hydrate (30 mg, 0.196 mmol, 1.1 eq), **5e** (67 mg, 0.214 mmol, 1.2 eq), and Et_3N (45 μL, 0.320 mmol, 1.8 eq) in DMF (4 mL) yielded, after purification by flash column chromatography (SiO_2; 9:1/CH_2Cl_2:MeOH with NH_4OH (7 mL/L of solvent), R_f 0.24), **12n** (50 mg, 47%) as a pale yellow powder: ^{1}H NMR ($CDCl_3$, 500 MHz) δ 9.34 (s, 1H), 7.96 (d, 1H, J = 8.5 Hz), 7.91 (d, 1H, J = 8.5 Hz), 7.56 (t, 1H, J = 7.2 Hz), 7.45 (d, 1H, J = 7.9 Hz), 7.34 (m, 2H), 7.19 (t, 1H, J = 7.6 Hz), 7.17 (d, 1H, J = 7.4 Hz), 7.07 (t, 1H, J = 7.6 Hz), 6.95 (d, 1H, J = 7.6 Hz), 6.92 (d, 1H, J = 8.4 Hz), 6.67 (t, 1H, J = 7.4 Hz), 6.10 (t, 1H, J = 5.3 Hz), 4.02 (br s, 1H), 3.72 (q, 2H, J = 5.8 Hz), 3.48 (t, 2H, J = 7.2 Hz), 3.23 (q, 2H, J = 6.7 Hz), 3.07 (br s, 2H), 2.71 (br s, 2H), 2.52 (t, 2H, J = 5.8 Hz), 2.33 (s, 3H), 2.21 (s, 3H), 1.92 (m, 4H), 1.63 (p, 2H, J = 7.0 Hz), 1.46 (br p, 2H, J = 6.8 Hz), 1.32 (m, 6H); ^{13}C NMR ($CDCl_3$, 125 MHz) δ 171.7, 169.8, 158.3, 150.9, 147.3, 147.2, 139.6, 138.0, 132.3, 130.8, 128.4, 127.7, 125.8, 125.6, 123.7, 122.9, 120.8, 120.1, 116.8, 116.5, 115.8, 114.7, 49.4, 39.5, 35.8, 35.5, 33.9, 31.7, 29.4, 28.9, 26.7, 24.8, 23.0, 22.8, 20.7, 13.9; *m/z* calcd for $C_{38}H_{47}N_5O_2$: 605.37; found 606.35 $[M+H]^+$.

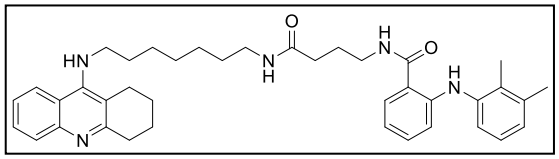

2-((2,3-Dimethylphenyl)amino)-*N*-(4-oxo-4-((7-((1,2,3,4-tetrahydroacridin-9-yl)amino)heptyl)amino)butyl)benzamide (12o). Compound **12o** was prepared as described for the synthesis of **10a**. The reaction of **9c** (61 mg, 0.188 mmol, 1 eq), EDAC hydrochloride (40 mg, 0.207 mmol, 1.1 eq), HOBt hydrate (32 mg, 0.207 mmol, 1.1 eq), **5e** (70 mg, 0.226 mmol, 1.2 eq), and Et_3N (47 μL, 0.338 mmol, 1.8 eq) in DMF (4 mL) yielded, after purification by flash column chromatography (SiO_2; 9:1/CH_2Cl_2:MeOH with NH_4OH (7 mL/L of solvent), R_f 0.40), **12o** (27 mg, 23%) as a pale yellow powder: ^{1}H NMR ($CDCl_3$, 500 MHz) δ 9.36 (s, 1H), 7.96 (d, 1H, J = 8.3 Hz), 7.92 (d, 1H, J = 8.4 Hz), 7.56 (t, 1H, J = 7.2 Hz), 7.49 (dd, 1H, J_1 =

7.9 Hz, J_2 = 1.2 Hz), 7.35 (t, 1H, J = 8.0 Hz), 7.20 (td, 1H, J_1 = 7.2 Hz, J_2 = 1.2 Hz), 7.17 (d, 1H, J = 8.0 Hz), 7.15 (br t, 1H, J = 5.4 Hz), 7.07 (t, 1H, J = 7.7 Hz), 6.94 (m, 2H), 6.70 (t, 1H, J = 7.3 Hz), 6.25 (br t, 1H), 4.00 (very br s, 1H), 3.49 (p, 4H, J = 6.6 Hz), 3.23 (q, 2H, J = 6.7 Hz), 3.07 (br t, 2H), 2.71 (br t, 2H), 2.32 (m, 5H), 2.21 (s, 3H), 1.97 (p, 2H, J = 6.3 Hz) 1.93 (m, 4H), 1.63 (p, 2H, J = 7.4 Hz), 1.46 (br p, 2H, J = 6.7 Hz), 1.31 (m, 6H); ^{13}C NMR ($CDCl_3$, 125 MHz) δ 173.0, 170.2, 158.3, 150.9, 147.3, 147.2, 139.6, 138.1, 132.2, 130.7, 128.5, 128.4, 127.6, 125.7, 125.5, 123.6, 122.9, 120.7, 120.1, 116.9, 116.6, 115.8, 114.8, 49.4, 39.6, 39.5, 34.2, 33.9, 31.7, 29.4, 28.9, 26.8, 26.7, 25.1, 24.8, 23.0, 22.8, 20.7, 13.9; *m/z* calcd for $C_{39}H_{49}N_5O_2$: 619.39; found 620.30 $[M+H]^+$.

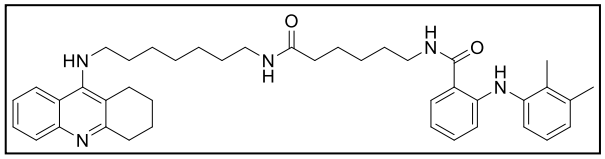

2-((2,3-Dimethylphenyl)amino)-*N*-(6-oxo-6-((7-((1,2,3,4-tetrahydroacridin-9-yl)amino)heptyl)amino)hexyl)benzamide (12p). Compound **12p** was prepared as described for the synthesis of **10a**. The reaction of **9d** (53 mg, 0.148 mmol, 1 eq), EDAC hydrochloride (31 mg, 0.163 mmol, 1.1 eq), HOBt hydrate (25 mg, 0.163 mmol, 1.1 eq), **5e** (55 mg, 0.178 mmol, 1.2 eq), and Et_3N (37 μL, 0.266 mmol, 1.8 eq) in DMF (4 mL) yielded, after purification by flash column chromatography (SiO_2; 9:1/CH_2Cl_2:MeOH with NH_4OH (7 mL/L of solvent), R_f 0.23), **12p** (35 mg, 37%) as a pale yellow powder: ^{1}H NMR ($CDCl_3$, 500 MHz) δ 9.24 (s, 1H), 7.97 (d, 1H, J = 8.5 Hz), 7.92 (d, 1H, J = 8.4 Hz), 7.57 (t, 1H, J = 7.5 Hz), 7.45 (d, 1H, J = 7.6 Hz), 7.36 (t, 1H, J = 7.6 Hz), 7.21 (t, 1H, J = 7.6 Hz), 7.17 (d, 1H, J = 7.9 Hz), 7.07 (t, 1H, J = 7.6 Hz), 6.94 (d, 2H, J = 8.4 Hz), 6.68 (t, 1H, J = 7.5 Hz), 6.48 (br t, 1H), 5.66 (br t, 1H), 4.02 (very br s, 1H), 3.49 (t, 2H, J = 7.2 Hz), 3.44 (q, 2H, J = 6.7 Hz), 3.21 (q, 2H, J = 6.7 Hz), 3.07 (br s, 2H), 2.71 (br s, 2H), 2.33 (s, 3H), 2.21 (s, 3H), 2.18 (t, 2H, J = 7.3 Hz), 1.93 (m, 4H), 1.68 (m, 6H), 1.37 (m, 10H); ^{13}C NMR ($CDCl_3$, 125 MHz) δ 172.8, 169.8, 158.3, 150.9, 147.3, 147.0, 139.6 , 138.1, 132.1, 130.7, 128.5, 128.4, 127.4, 125.7, 125.5, 123.6, 122.9, 120.6, 120.1, 117.2, 116.8, 115.8, 114.9, 49.4, 39.4, 36.4, 33.9, 31.7, 29.6, 29.2, 28.9, 26.8, 26.7, 26.4, 25.0, 24.8, 23.0, 22.8, 20.7, 13.9; *m/z* calcd for $C_{41}H_{53}N_5O_2$: 647.42; found 648.30 $[M+H]^+$.

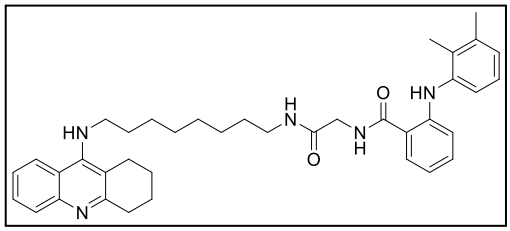

2-((2,3-Dimethylphenyl)amino)-*N*-(2-oxo-2-((8-((1,2,3,4-tetrahydroacridin-9-yl)amino)octyl)amino)ethyl)benzamide (12q). Compound **12q** was prepared as described for the synthesis of **10a**. The reaction of **9a** (44 mg, 0.146 mmol, 1 eq), EDAC hydrochloride (31 mg, 0.161 mmol, 1.1 eq), HOBt hydrate (25 mg, 0.161 mmol, 1.1 eq), **5f** (57 mg, 0.175 mmol, 1.2 eq), and Et_3N (37 μL, 0.263 mmol, 1.8 eq) in DMF (4 mL) yielded, after purification by flash column chromatography (SiO_2; 9:1/CH_2Cl_2:MeOH with NH_4OH (7 mL/L of solvent), R_f 0.30), **12q** (36 mg, 41%) as a pale yellow powder: ^{1}H NMR ($CDCl_3$, 500 MHz) δ 9.24 (s, 1H), 7.97 (d, 1H, *J* = 8.2 Hz), 7.91 (d, 1H, *J* = 8.3 Hz), 7.56 (m, 2H), 7.35 (m, 2H), 7.21 (t, 1H, *J* = 7.3 Hz), 7.16 (d, 1H, *J* = 7.8 Hz), 7.08 (t, 1H, *J* = 7.6 Hz), 6.97 (d, 1H, *J* = 7.4 Hz), 6.88 (d, 1H, *J* = 8.4 Hz), 6.68 (t, 1H, *J* = 7.2 Hz), 6.51 (br t, 1H, *J* = 5.4 Hz), 4.11 (d, 2H, *J* = 5.2 Hz), 3.99 (very br s, 1H), 3.48 (t, 2H, *J* = 7.2 Hz), 3.27 (q, 2H, *J* = 6.8 Hz), 3.07 (br s, 2H), 2.71 (br s, 2H), 2.33 (s, 3H), 2.19 (s, 3H), 1.93 (m, 4H), 1.64 (p, 2H, *J* = 7.1 Hz), 1.48 (br p, 2H), 1.35 (br p, 2H), 1.28 (br s, 6H); ^{13}C NMR ($CDCl_3$, 125 MHz) δ 170.1, 168.9, 158.3, 150.9, 147.6, 147.3, 139.3, 138.1, 132.7, 131.2, 128.5, 128.4, 127.9, 125.9, 125.8, 123.6, 123.0, 121.5, 120.1, 116.8, 115.7, 115.5, 114.8, 49.4, 43.6, 39.6, 33.9, 31.8, 29.4, 29.14, 29.08, 26.8, 26.7, 24.8, 23.1, 22.8, 20.7, 14.0; *m/z* calcd for $C_{38}H_{47}N_5O_2$: 605.37; found 606.30 $[M+H]^+$.

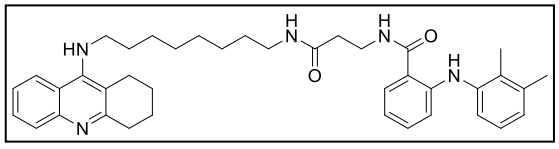

2-((2,3-Dimethylphenyl)amino)-*N*-(3-oxo-3-((8-((1,2,3,4-tetrahydroacridin-9-yl)amino)octyl)amino)propyl)benzamide (12r). Compound **12r** was prepared as described for the synthesis of **10a**. The reaction of **9b** (54 mg, 0.172 mmol, 1 eq), EDAC hydrochloride (36 mg, 0.189 mmol, 1.1 eq), HOBt hydrate (29 mg, 0.189 mmol, 1.1 eq), **5f** (67 mg, 0.206 mmol, 1.2 eq), and Et_3N (43 μL, 0.310 mmol, 1.8 eq) in DMF (4 mL) yielded, after purification by flash column chromatography (SiO_2; 9:1/CH_2Cl_2:MeOH with NH_4OH (7 mL/L of solvent), R_f 0.39), **12r** (30 mg, 28%) as a pale yellow powder: ^{1}H NMR ($CDCl_3$, 500 MHz) δ 9.34 (s, 1H), 7.97 (d, 1H, *J* = 8.5 Hz), 7.91 (d, 1H, *J* = 8.5 Hz), 7.56 (t, 1H, *J* = 7.1 Hz), 7.45 (d, 1H, *J* = 6.8 Hz), 7.34 (m, 2H), 7.19 (m, 2H), 7.07 (t, 1H, *J* = 7.6 Hz), 6.94 (t, 2H, *J* = 9.2 Hz), 6.68 (t,

1H, *J* = 7.2 Hz), 6.10 (t, 1H, *J* = 5.3 Hz), 4.00 (very br s, 1H), 3.72 (q, 2H, *J* = 5.8 Hz), 3.49 (t, 2H, *J* = 7.2 Hz), 3.24 (q, 2H, *J* = 6.8 Hz), 3.07 (br t, 2H), 2.71 (br t, 2H), 2.52 (t, 2H, *J* = 5.9 Hz), 2.33 (s, 3H), 2.21 (s, 3H), 1.93 (m, 4H), 1.64 (p, 2H, *J* = 7.1 Hz), 1.46 (br p, 2H, *J* = 6.7 Hz), 1.35 (br p, 2H), 1.27 (br s, 6H); ^{13}C NMR ($CDCl_3$, 125 MHz) δ 171.7, 169.8, 158.3, 150.9, 147.3, 147.2, 139.6, 138.0, 132.3, 130.8, 128.5, 128.4, 127.7, 125.7, 125.5, 123.6, 122.9, 120.8, 120.1, 116.8, 116.5, 115.7, 114.7, 49.4, 39.6, 35.8, 35.5, 33.9, 31.8, 29.5, 29.14, 29.10, 26.78, 26.75, 24.8, 23.1, 22.8, 20.7, 13.9; *m/z* calcd for $C_{39}H_{49}N_5O_2$: 619.39; found 620.35 $[M+H]^+$.

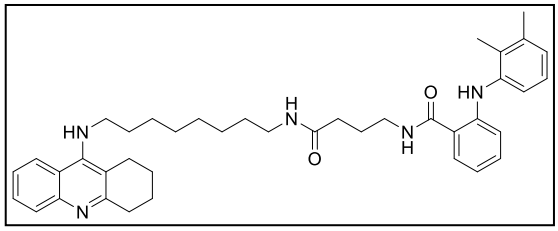

2-((2,3-Dimethylphenyl)amino)-*N*-(4-oxo-4-((8-((1,2,3,4-tetrahydroacridin-9-yl)amino)octyl)amino)butyl)benzamide (**12s**). Compound **12s** was prepared as described for the synthesis of **10a**. The reaction of **9c** (61 mg, 0.187 mmol, 0.87 eq), EDAC hydrochloride (45 mg, 0.237 mmol, 1.1 eq), HOBt hydrate (36 mg, 0.237 mmol, 1.1 eq), **5f** (84 mg, 0.258 mmol, 1.2 eq), and Et_3N (54 μL, 0.387 mmol, 1.8 eq) in DMF (3 mL) yielded, after purification by flash column chromatography (SiO_2; 9:1/CH_2Cl_2:MeOH with NH_4OH (7 mL/L of solvent), R_f 0.44), **12s** (60 mg, 51%) as a yellow oil: ^{1}H NMR ($CDCl_3$, 500 MHz) δ 9.38 (s, 1H), 7.99 (d, 1H, *J* = 8.5 Hz), 7.95 (d, 1H, *J* = 8.4 Hz), 7.56 (t, 1H, *J* = 8.0 Hz), 7.52 (d, 1H, *J* = 7.9 Hz), 7.34 (m, 2H), 7.18 (t, 1H, *J* = 8.4 Hz), 7.16 (d, 1H, *J* = 7.2 Hz), 7.06 (t, 1H, *J* = 7.6 Hz), 6.93 (m, 2H), 6.67 (t, 1H, *J* = 7.8 Hz), 6.53 (t, 1H, *J* = 5.2 Hz), 4.23 (br s, 1H), 3.52 (t, 2H, *J* = 7.1 Hz), 3.48 (q, 2H, *J* = 8.4 Hz), 3.22 (q, 2H, *J* = 6.7 Hz), 3.07 (br s, 2H), 2.69 (br s, 2H), 2.32 (m, 5H), 2.20 (s, 3H), 1.96 (p, 2H, *J* = 6.5 Hz), 1.91 (m, 4H), 1.65 (p, 2H, *J* = 7.1 Hz), 1.46 (br p, 2H), 1.36 (br p, 2H), 1.27 (br s, 6H); ^{13}C NMR ($CDCl_3$, 125 MHz) δ 173.1, 170.2, 157.6, 151.5, 147.1, 146.5, 139.7, 138.0, 132.2, 130.6, 128.8, 127.8, 127.6, 125.7, 125.5, 123.8, 123.1, 120.7, 119.7, 116.9, 116.7, 115.2, 114.8, 49.3, 39.6, 39.5, 34.2, 33.3, 31.6, 29.5, 29.11, 29.07, 26.8, 26.7, 25.2, 24.6, 22.9, 22.5, 20.7, 13.9; *m/z* calcd for $C_{40}H_{51}N_5O_2$: 633.40; found 634.65 $[M+H]^+$.

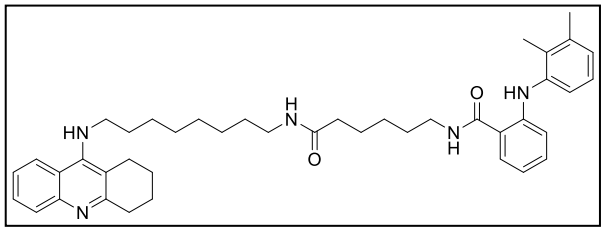

2-((2,3-Dimethylphenyl)amino)-*N*-(6-oxo-6-((8-((1,2,3,4-tetrahydroacridin-9-yl)amino)octyl)amino)hexyl)benzamide (**12t**). Compound **12t** was prepared as described for the synthesis of **10a**. The reaction of **9d** (63 mg, 0.177 mmol, 0.80 eq), EDAC hydrochloride (47 mg, 0.244 mmol, 1.1 eq), HOBt hydrate (37 mg, 0.244 mmol, 1.1 eq), **5f** (87 mg, 0.266 mmol, 1.2 eq), and Et_3N (57 μL, 0.399 mmol, 1.8 eq) in DMF (3 mL) yielded, after purification by flash column chromatography (SiO_2; 9:1/CH_2Cl_2:MeOH with NH_4OH (7 mL/L of solvent), R_f 0.31), **12t** (70 mg, 60%) as a yellow oil: ^{1}H NMR ($CDCl_3$, 500 MHz) δ 9.25 (s, 1H), 7.99 (d, 1H, *J* = 8.5 Hz), 7.91 (d, 1H, *J* = 8.4 Hz), 7.55 (t, 1H, *J* = 7.6 Hz), 7.46 (d, 1H, *J* = 7.5 Hz), 7.34 (t, 1H, *J* = 7.7 Hz), 7.18 (t, 1H, *J* = 8.0 Hz), 7.16 (d, 1H, *J* = 7.9 Hz), 7.06 (d, 1H, *J* = 7.7 Hz), 6.93 (d, 2H, *J* = 8.1 Hz), 6.70 (t, 1H, *J* = 5.4 Hz), 6.66 (t, 1H, *J* = 7.4 Hz), 5.95 (t, 1H, *J* = 5.5 Hz), 4.08 (br s, 1H), 3.49 (t, 2H, *J* = 6.9 Hz), 3.42 (q, 2H, *J* = 6.7 Hz), 3.19 (q, 2H, *J* = 6.6 Hz), 3.05 (m, 2H), 2.69 (m, 2H), 2.31 (s, 3H), 2.20 (s, 3H), 2.16 (t, 2H, *J* = 7.4 Hz), 1.91 (m, 4H), 1.64 (m, 6H), 1.40 (m, 6H), 1.27 (m, 6H); ^{13}C NMR ($CDCl_3$, 125 MHz) δ 173.0, 169.9, 158.1, 151.1, 147.1, 146.9, 139.6, 138.0, 132.1, 130.6, 128.5, 128.3, 127.6, 125.7, 125.4, 123.6, 123.0, 120.6, 120.0, 117.2, 116.8, 115.6, 114.8, 49.4, 39.5, 39.4, 36.4, 33.8, 31.7, 29.6, 29.2, 29.15, 29.10, 26.79, 26.76, 26.4, 25.1, 24.7, 23.0, 22.7, 20.7, 13.9; *m/z* calcd for $C_{42}H_{55}N_5O_2$: 661.44; found 662.40 $[M+H]^+$.

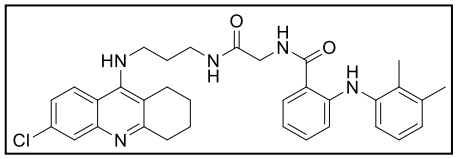

***N*-(2-((3-((6-Chloro-1,2,3,4-tetrahydroacridin-9-yl)amino)propyl)amino)-2-oxoethyl)-2-((2,3-dimethylphenyl)amino)benzamide (13a).** Compound **13a** was prepared as described for the synthesis of **10a**. The reaction of **9a** (64 mg, 0.213 mmol, 1 eq), EDAC hydrochloride (45 mg, 0.234 mmol, 1.1 eq), HOBt hydrate (36 mg, 0.234 mmol, 1.1 eq), **6a** (74 mg, 0.255 mmol, 1.2 eq), and Et_3N (53 μL, 0.383 mmol, 1.8 eq) in DMF (4 mL) yielded, after purification by flash column chromatography (SiO_2; 9:1/CH_2Cl_2:MeOH with NH_4OH (7 mL/L of solvent), R_f 0.48), **13a** (65 mg, 53%) as a pale yellow powder: ^{1}H NMR ($CDCl_3$, 500 MHz) δ 9.18 (s, 1H), 7.90 (d, 1H, *J* = 9.1 Hz), 7.84 (s, 1H), 7.52 (d, 1H, *J* = 7.9 Hz), 7.45 (t, 1H, *J* = 5.2 Hz), 7.21 (m, 2H), 7.13 (t,

1H, *J* = 6.0 Hz), 7.09 (br s, 1H), 7.06 (t, 1H, *J* = 7.8 Hz), 6.97 (d, 1H, *J* = 7.2 Hz), 6.87 (d, 1H, *J* = 8.5 Hz), 6.63 (t, 1H, *J* = 7.5 Hz), 4.76 (br t, 1H), 4.13 (d, 2H, *J* = 5.2 Hz), 3.45 (p, 4H, *J* = 6.6 Hz), 2.99 (t, 2H, *J* = 6.0 Hz), 2.67 (t, 2H, *J* = 5.8 Hz), 2.30 (s, 3H), 2.14 (s, 3H), 1.86 (m, 4H), 1.79 (p, 2H, *J* = 6.2 Hz); ^{13}C NMR ($CDCl_3$, 125 MHz) δ 170.3, 170.1, 159.7, 150.6, 147.8, 147.6, 139.2, 138.2, 134.0, 132.9, 131.1, 127.8, 127.3, 126.1, 125.9, 124.5, 124.2, 121.4, 118.6, 116.9, 116.6, 115.2, 115.0, 45.4, 43.8, 36.8, 33.9, 31.2, 24.9, 22.9, 22.6, 20.7, 13.9; *m/z* calcd for $C_{33}H_{36}ClN_5O_2$: 569.26; found 570.20 $[M+H]^+$.

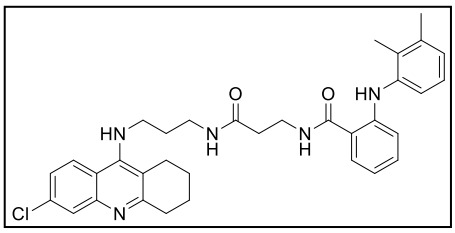

***N*-(3-((3-((6-Chloro-1,2,3,4-tetrahydroacridin-9-yl)amino)propyl)amino)-3-oxopropyl)-2-((2,3-dimethylphenyl)amino)benzamide (13b).** Compound **13b** was prepared as described for the synthesis of **10a**. The reaction of **9b** (73 mg, 0.234 mmol, 1 eq), EDAC hydrochloride (49 mg, 0.257 mmol, 1.1 eq), HOBt hydrate (39 mg, 0.257 mmol, 1.1 eq), **6a** (81 mg, 0.280 mmol, 1.2 eq), and Et_3N (59 μL, 0.420 mmol, 1.8 eq) in DMF (4 mL) yielded, after purification by flash column chromatography (SiO_2; 9:1/CH_2Cl_2:MeOH with NH_4OH (7 mL/L of solvent), R_f 0.33), **13b** (70 mg, 51%) as a white powder: ^{1}H NMR ($CDCl_3$, 500 MHz) δ 9.28 (s, 1H), 7.90 (d, 1H, *J* = 9.0 Hz), 7.81 (s, 1H), 7.55 (br t, 1H), 7.46 (d, 1H, *J* = 7.7 Hz), 7.26 (br t, 1H), 7.19 (d, 1H, *J* = 9.1 Hz), 7.17 (d, 1H, *J* = 8.0 Hz), 7.12 (d, 1H, *J* = 7.9 Hz), 7.04 (t, 1H, *J* = 7.7 Hz), 6.92 (d, 1H, *J* = 7.4 Hz), 6.89 (d, 1H, *J* = 8.4 Hz), 6.61 (t, 1H, *J* = 7.4 Hz), 4.89 (br s, 1H), 3.71 (q, 2H, *J* = 5.3 Hz), 3.43 (q, 2H, *J* = 5.8 Hz), 3.37 (q, 2H, *J* = 5.8 Hz), 2.97 (br s, 2H), 2.66 (br t, 2H), 2.56 (br t, 2H), 2.29 (s, 3H), 2.16 (s, 3H), 1.84 (br s, 4H), 1.74 (br p, 2H, *J* = 5.8 Hz); ^{13}C NMR ($CDCl_3$, 125 MHz) δ 172.8, 169.9, 159.5, 150.7, 147.7, 147.2, 139.5, 138.1, 134.0, 132.3, 130.7, 127.7, 127.0, 125.8, 125.6, 124.4, 124.3, 120.8, 118.5, 116.9, 116.5, 116.2, 114.8, 45.2, 36.5, 36.0, 35.5, 33.9, 33.8, 31.3, 22.9, 22.6, 20.7, 13.9; *m/z* calcd for $C_{34}H_{38}ClN_5O_2$: 583.27; found 584.20 $[M+H]^+$.

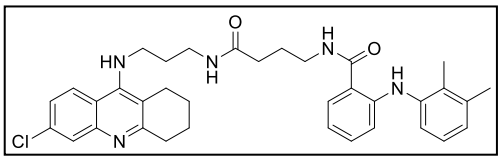

***N*-(4-((3-((6-Chloro-1,2,3,4-tetrahydroacridin-9-yl)amino)propyl)amino)-4-oxobutyl)-2-((2,3-dimethylphenyl)amino)benzamide (13c).**

Compound **13c** was prepared as described for the synthesis of **10a**. The reaction of **9c** (84 mg, 0.257 mmol, 1 eq), EDAC hydrochloride (54 mg, 0.283 mmol, 1.1 eq), HOBt hydrate (43 mg, 0.283 mmol, 1.1 eq), **6a** (95 mg, 0.327 mmol, 1.2 eq), and Et_3N (64 μL, 0.555 mmol, 1.8 eq) in DMF (4 mL) yielded, after purification by flash column chromatography (SiO_2; 9:1/CH_2Cl_2:MeOH with NH_4OH (7 mL/L of solvent), R_f 0.54), **13c** (77 mg, 50%) as a white powder: ^{1}H NMR ($CDCl_3$, 300 MHz) δ 9.26 (s, 1H), 7.94 (d, 1H, J = 9.1 Hz), 7.85 (d, 1H, J = 2.0 Hz), 7.48 (d, 1H, J = 7.1 Hz), 7.24 (dd, 1H, J_1 = 9.0 Hz, J_2 = 2.0 Hz), 7.17 (m, 2H), 7.08 (br s, 1H), 7.06 (t, 1H, J = 7.6 Hz), 6.81 (t, 1H, J = 5.8 Hz), 6.67 (t, 1H, J = 7.5 Hz), 4.87 (t, 1H, J = 6.5 Hz), 3.48 (m, 4H), 3.39 (q, 2H), 3.00 (m, 2H), 2.71 (br t, 2H), 2.36 (m, 2H), 2.31 (s, 3H), 2.18 (s, 3H), 1.96 (m, 2H), 1.88 (m, 4H), 1.77 (m, 2H); ^{13}C NMR ($CDCl_3$, 75 MHz) δ 173.9, 170.4, 159.7, 150.6, 148.0, 147.1, 139.5, 138.1, 133.9, 132.4, 130.6, 127.5, 127.4, 125.8, 125.6, 124.4, 124.3, 120.7, 118.6, 116.9, 116.54, 116.49, 114.9, 45.3, 39.4, 36.6, 34.0, 25.6, 25.5, 25.03, 24.95, 22.9, 22.7, 20.7, 13.9; *m/z* calcd for $C_{35}H_{40}ClN_5O_2$: 597.29; found 598.25 $[M+H]^+$.

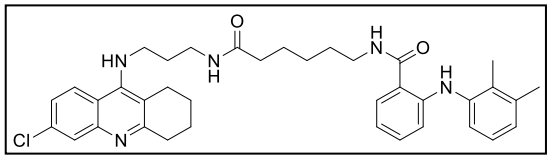

***N*-(6-((3-((6-Chloro-1,2,3,4-tetrahydroacridin-9-yl)amino)propyl)amino)-6-oxohexyl)-2-((2,3-dimethylphenyl)amino)benzamide (13d).** Compound **13d** was prepared as described for the synthesis of **10a**. The reaction of **9d** (83 mg, 0.235 mmol, 1 eq), EDAC hydrochloride (50 mg, 0.259 mmol, 1.1 eq), HOBt hydrate (40 mg, 0.259 mmol, 1.1 eq), **6a** (82 mg, 0.282 mmol, 1.2 eq), and Et_3N (60 μL, 0.423 mmol, 1.8 eq) in DMF (4 mL) yielded, after purification by flash column chromatography (SiO_2; 9:1/CH_2Cl_2:MeOH with NH_4OH (7 mL/L of solvent), R_f 0.28), **13d** (111 mg, 75%) as a white powder: ^{1}H NMR ($CDCl_3$, 500 MHz) δ 9.19 (s, 1H), 7.95 (d, 1H, J = 9.1 Hz), 7.86 (d, 1H, J = 1.5 Hz), 7.42 (d, 1H, J = 7.8 Hz), 7.26 (dd, 1H, J_1 = 9.0 Hz, J_2 = 1.5 Hz), 7.19 (t, 1H, J = 7.8 Hz), 7.15 (d, 1H, J = 7.9 Hz), 7.06 (t, 1H, J = 7.6 Hz), 6.94 (t, 2H, J = 7.9 Hz), 6.66 (t, 1H, J = 7.5 Hz), 6.49 (br t, 1H), 6.13 (t, 1H, J = 5.8 Hz), 4.96 (br s, 1H), 3.43 (m, 4H), 3.37 (q, 2H, J = 6.2 Hz), 3.01 (m, 2H), 2.71 (br t, 2H), 2.32 (s, 3H), 2.22 (t, 2H, J = 7.3 Hz), 2.20 (s, 3H), 1.89 (br s, 4H), 1.71 (m, 4H), 1.64 (p, 2H, J = 7.3 Hz), 1.42 (p, 2H, J = 7.2 Hz); ^{13}C NMR ($CDCl_3$, 125 MHz) δ 174.0, 169.9, 159.6, 150.7, 147.8, 147.0, 139.6, 138.1, 133.9, 132.2,

130.6, 127.4, 127.2, 125.8, 125.5, 124.4, 124.3, 120.6, 118.5, 117.1, 116.8, 116.4, 114.9, 45.1, 39.4, 36.4, 36.3, 33.9, 31.5, 29.3, 26.4, 25.2, 25.0, 23.0, 22.6, 20.7, 13.9; *m/z* calcd for $C_{37}H_{44}ClN_5O_2$: 625.32; found 626.25 $[M+H]^+$.

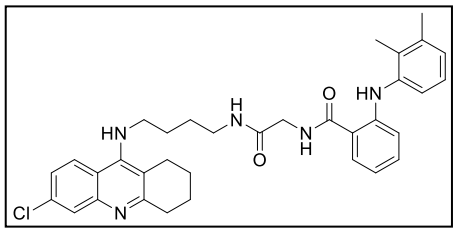

***N*-(2-((4-((6-Chloro-1,2,3,4-tetrahydroacridin-9-yl)amino)butyl)amino)-2-oxoethyl)-2-((2,3-dimethylphenyl)amino)benzamide (13e).** Compound **13e** was prepared as described for the synthesis of **10a**. The reaction of **9a** (59 mg, 0.198 mmol, 1 eq), EDAC hydrochloride (42 mg, 0.218 mmol, 1.1 eq), HOBt hydrate (33 mg, 0.218 mmol, 1.1 eq), **6b** (72 mg, 0.238 mmol, 1.2 eq), and Et_3N (50 μL, 0.357 mmol, 1.8 eq) in DMF (4 mL) yielded, after purification by flash column chromatography (SiO_2; 9:1/CH_2Cl_2:MeOH with NH_4OH (7 mL/L of solvent), R_f 0.24), **13e** (86 mg, 74%) as a pale yellow powder: ^1H NMR ($CDCl_3$, 500 MHz) δ 9.19 (s, 1H), 7.86 (d, 1H, *J* = 2.0 Hz), 7.83 (d, 1H, *J* = 9.1 Hz), 7.53 (d, 1H, *J* = 7.8 Hz), 7.29 (m, 1H), 7.24 (m, 1H), 7.22 (t, 1H, *J* = 8.5 Hz), 7.12 (d, 1H, *J* = 7.5 Hz), 7.05 (t, 1H, *J* = 7.6 Hz), 6.95 (d, 1H, *J* = 7.1 Hz), 6.87 (d, 1H, *J* = 8.4 Hz), 6.70 (m, 1H), 6.66 (t, 1H, *J* = 7.4 Hz), 4.09 (d, 2H, *J* = 5.2 Hz), 3.96 (br s, 1H), 3.44 (br t, 2H), 3.32 (q, 2H, *J* = 6.2 Hz), 3.01 (br t, 2H), 2.62 (br t, 2H), 2.29 (s, 3H), 2.15 (s, 3H), 1.89 (m, 4H), 1.64 (m, 4H); ^{13}C NMR ($CDCl_3$, 125 MHz) δ 170.2, 169.2, 159.6, 150.6, 148.0, 147.6, 139.2, 138.2, 134.0, 132.9, 131.2, 127.8, 127.4, 126.0, 125.9, 124.5, 124.4, 121.4, 118.5, 116.9, 116.2, 115.3, 114.9, 48.9, 43.7, 39.2, 34.0, 28.9, 27.0, 24.6, 22.9, 22.6, 20.6, 13.9; *m/z* calcd for $C_{34}H_{38}ClN_5O_2$: 583.27; found 584.25 $[M+H]^+$.

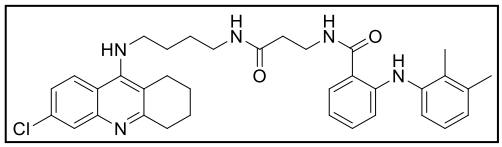

***N*-(3-((4-((6-Chloro-1,2,3,4-tetrahydroacridin-9-yl)amino)butyl)amino)-3-oxopropyl)-2-((2,3-dimethylphenyl)amino)benzamide (13f).** Compound **13f** was prepared as described for the synthesis of **10a**. The reaction of **9b** (75 mg, 0.240 mmol, 1 eq), EDAC hydrochloride (51 mg, 0.264 mmol, 1.1 eq), HOBt hydrate (40 mg, 0.264 mmol, 1.1 eq), **6b** (151 mg, 0.496 mmol, 1.2 eq), and Et_3N (60 μL, 0.433 mmol, 1.8 eq) in DMF (4 mL) yielded, after purification by flash column chromatography (SiO_2; 9:1/CH_2Cl_2:MeOH with NH_4OH (7 mL/L of solvent), R_f 0.44), **13f** (67 mg, 47%)

as a white powder: ^{1}H NMR ($CDCl_3$, 300 MHz) δ 9.30 (s, 1H), 7.85 (d, 1H, J = 2.0 Hz), 7.83 (d, 1H, J = 9.1 Hz), 7.44 (d, 1H, J = 7.8 Hz), 7.33 (br s, 1H), 7.23 (dd, 1H, J_1 = 9.1 Hz, J_2 = 2.0 Hz), 7.16 (t, 2H, J = 7.8 Hz), 7.04 (t, 1H, J = 7.7 Hz), 6.93 (d, 1H, J = 5.9 Hz), 6.91 (d, 1H, J = 7.9 Hz), 6.64 (t, 1H, J = 7.5 Hz), 6.45 (br t, 1H), 4.00 (br s, 1H), 3.70 (q, 2H, J = 5.8 Hz), 3.42 (br t, 2H), 3.28 (q, 2H, J = 6.1 Hz), 2.99 (br t, 2H), 2.61 (br t, 2H), 2.50 (t, 2H, J = 5.8 Hz), 2.30 (s, 3H), 2.18 (s, 3H), 1.87 (br s, 4H), 1.63 (m, 4H); ^{13}C NMR ($CDCl_3$, 75 MHz) δ 171.8, 169.9, 159.4, 150.7, 147.8, 147.2, 139.4, 138.1, 134.1, 132.4, 130.7, 127.6, 127.2, 125.8, 125.7, 124.5, 124.4, 120.8, 118.4, 116.9, 116.4, 116.0, 114.8, 48.9, 39.1, 35.8, 35.5, 33.8, 28.9, 27.0, 24.6, 22.8, 22.5, 20.7, 13.9; *m/z* calcd for $C_{35}H_{40}ClN_5O_2$: 597.29; found 598.20 $[M+H]^+$.

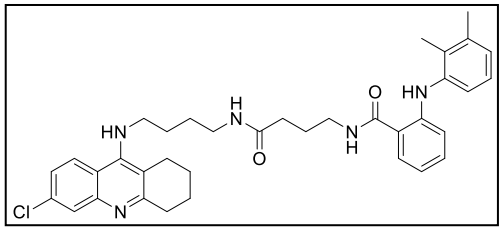

***N*-(4-((4-((6-Chloro-1,2,3,4-tetrahydroacridin-9-yl)amino)butyl)amino)-4-oxobutyl)-2-((2,3-dimethylphenyl)amino)benzamide (13g).** Compound **13g** was prepared as described for the synthesis of **10a**. The reaction of **9c** (58 mg, 0.177 mmol, 1 eq), EDAC hydrochloride (42 mg, 0.218 mmol, 1.1 eq), HOBt hydrate (33 mg, 0.218 mmol, 1.1 eq), **6b** (72 mg, 0.238 mmol, 1.2 eq), and Et_3N (50 μL, 0.357 mmol, 1.8 eq) in DMF (4 mL) yielded, after purification by flash column chromatography (SiO_2; 9:1/CH_2Cl_2:MeOH with NH_4OH (7 mL/L of solvent), R_f 0.30), **13g** (102 mg, 94%) as a white powder: ^{1}H NMR ($CDCl_3$, 500 MHz) δ 9.29 (s, 1H), 7.89 (d, 1H, J = 2.1 Hz), 7.86 (d, 1H, J = 9.1 Hz), 7.49 (dd, 1H, J_1 = 7.9 Hz, J_2 = 1.4 Hz), 7.25 (dd, 1H, J_1 = 9.0 Hz, J_2 = 2.1 Hz), 7.21 (m, 1H), 7.14 (d, 1H, J = 7.9 Hz), 7.06 (t, 1H, J = 7.7 Hz), 6.98 (br t, 1H, J = 5.5 Hz), 6.95 (d, 1H, J = 7.5 Hz), 6.92 (dd, 1H, J_1 = 7.8 Hz, J_2 = 0.7 Hz), 6.71 (m, 1H), 6.39 (br t, 1H), 4.04 (br s, 1H), 3.48 (m, 4H), 3.31 (q, 2H, J = 6.5 Hz), 3.02 (br t, 2H), 2.65 (br t, 2H), 2.31 (m, 5H), 2.18 (s, 3H), 1.96 (p, 2H, J = 6.3 Hz), 1.89 (m, 4H), 1.70 (m, 2H), 1.62 (m, 2H); ^{13}C NMR ($CDCl_3$, 125 MHz) δ 173.1, 170.3, 159.5, 150.7, 147.9, 147.2, 139.5, 138.1, 134.1, 132.4, 130.7, 127.6, 127.4, 125.8, 125.7, 124.5, 124.4, 120.8, 118.4, 116.9, 116.5, 116.2, 114.89, 49.0, 39.4, 39.2, 34.1, 33.9, 29.0, 27.1, 25.3, 24.6, 22.9, 22.6, 20.7, 13.9; *m/z* calcd for $C_{36}H_{42}ClN_5O_2$: 611.30; found 612.30 $[M+H]^+$.

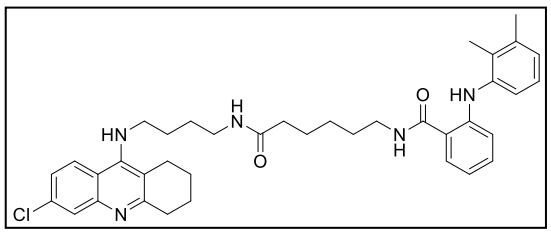

***N*-(6-((4-((6-Chloro-1,2,3,4-tetrahydroacridin-9-yl)amino)butyl)amino)-6-oxohexyl)-2-((2,3-dimethylphenyl)amino)benzamide (13h).** Compound **13h** was prepared as described for the synthesis of **10a**. The reaction of **9d** (66 mg, 0.185 mmol, 1 eq), EDAC hydrochloride (39 mg, 0.204 mmol, 1.1 eq), HOBt hydrate (31 mg, 0.204 mmol, 1.1 eq), **6b** (68 mg, 0.223 mmol, 1.2 eq), and Et_3N (51 μL, 0.367 mmol, 1.8 eq) in DMF (4 mL) yielded, after purification by flash column chromatography (SiO_2; 9:1/CH_2Cl_2:MeOH with NH_4OH (7 mL/L of solvent), R_f 0.44), **13h** (23 mg, 20%) as a pale yellow powder: ^1H NMR ($CDCl_3$, 500 MHz) δ 9.21 (s, 1H), 7.89 (d, 1H, J = 2.3 Hz), 7.87 (d, 1H, J = 9.0 Hz), 7.45 (dd, 1H, J_1 = 7.4 Hz, J_2 = 1.0 Hz), 7.27 (dd, 1H, J_1 = 9.0 Hz, J_2 = 2.1 Hz), 7.20 (td, 1H, J_1 = 7.2 Hz, J_2 = 1.0 Hz), 7.16 (d, 1H, J = 7.9 Hz), 7.06 (t, 1H, J = 7.7 Hz), 6.94 (t, 2H, J = 7.1 Hz), 6.69 (t, 1H, J = 7.3 Hz), 6.49 (t, 1H, J = 5.5 Hz), 5.79 (t, 1H, J = 5.4 Hz), 4.06 (br s, 1H), 3.47 (t, 2H), 3.44 (q, 2H, J = 6.8 Hz), 3.27 (q, 2H, J = 6.7 Hz), 3.03 (br t, 2H), 2.66 (br t, 2H), 2.32 (s, 3H), 2.20 (s, 3H), 2.18 (t, 2H, J = 7.4 Hz), 1.91 (m, 4H), 1.65 (m, 6H), 1.58 (p, 2H, J = 8.2 Hz), 1.41 (p, 2H, J = 8.0 Hz); ^{13}C NMR ($CDCl_3$, 125 MHz) δ 173.0, 169.8, 159.5, 150.7, 147.9, 147.0, 139.6, 138.1, 134.1, 132.2, 130.7, 127.4, 125.7, 125.5, 124.5, 124.4, 120.7, 118.4, 117.1, 116.8, 116.1, 114.9, 49.0, 39.3, 39.0, 36.4, 33.9, 29.2, 28.9, 27.2, 26.3, 25.0, 24.7, 22.9, 22.6, 20.7, 13.9; *m/z* calcd for $C_{38}H_{46}ClN_5O_2$: 639.33; found 640.30 $[M+H]^+$.

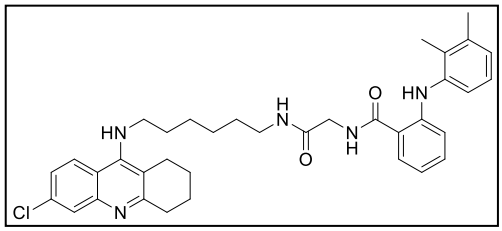

***N*-(2-((6-((6-Chloro-1,2,3,4-tetrahydroacridin-9-yl)amino)hexyl)amino)-2-oxoethyl)-2-((2,3-dimethylphenyl)amino)benzamide (13i).** Compound **13i** was prepared as described for the synthesis of **10a**. The reaction of **9a** (55 mg, 0.185 mmol, 1 eq), EDAC hydrochloride (39 mg, 0.204 mmol, 1.1 eq), HOBt hydrate (31 mg, 0.204 mmol, 1.1 eq), **6d** (74 mg, 0.223 mmol, 1.2 eq), and Et_3N (51 μL, 0.367 mmol, 1.8 eq) in DMF (4 mL) yielded, after purification by flash column chromatography (SiO_2; 9:1/CH_2Cl_2:MeOH with NH_4OH (7 mL/L of solvent), R_f 0.49), **13i** (44 mg, 38%) as a pale

yellow powder: ^{1}H NMR ($CDCl_3$, 500 MHz) δ 9.21 (s, 1H), 7.90 (d, 1H, J = 1.6 Hz), 7.89 (d, 1H, J = 5.0 Hz), 7.52 (d, 1H, J = 7.9 Hz), 7.29 (dd, 1H, J_1 = 9.0 Hz, J_2 = 2.0 Hz), 7.24 (t, 1H, J = 7.3 Hz), 7.16 (d, 1H, J = 7.8 Hz), 7.09 (t, 1H, J = 7.6 Hz), 6.99 (m, 2H), 6.90 (d, 1H, J = 8.5 Hz), 6.72 (t, 1H, J = 7.3 Hz), 6.14 (br t, 1H), 4.10 (d, 2H, J = 5.2 Hz), 3.96 (br s, 1H), 3.46 (t, 2H, J = 7.0 Hz), 3.31 (q, 2H, J = 6.6 Hz), 3.05 (br s, 2H), 2.67 (br s, 2H), 2.33 (s, 3H), 2.20 (s, 3H), 1.93 (m, 4H), 1.64 (p, 2H, J = 7.1 Hz), 1.54 (p, 2H, J = 7.4 Hz), 1.39 (m, 4H); ^{13}C NMR ($CDCl_3$, 125 MHz) δ 170.1, 169.0, 159.5, 150.8, 148.1, 147.6, 139.3, 138.1, 134.0, 132.8, 131.2, 127.8, 127.4, 126.0, 125.9, 124.6, 124.2, 121.4, 118.4, 116.8, 115.8, 115.4, 114.9, 49.4, 43.7, 39.4, 34.0, 31.6, 29.4, 26.52, 26.49, 24.6, 22.9, 22.6, 20.7, 13.9; *m/z* calcd for $C_{36}H_{42}ClN_5O_2$: 611.30; found 612.25 $[M+H]^+$.

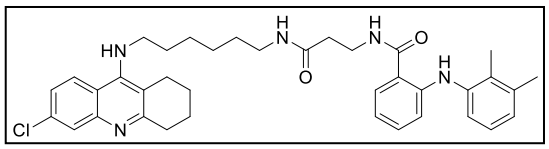

***N*-(3-((6-((6-Chloro-1,2,3,4-tetrahydroacridin-9-yl)amino)hexyl)amino)-3-oxopropyl)-2-((2,3-dimethylphenyl)amino)benzamide (13j).** Compound **13j** was prepared as described for the synthesis of **10a**. The reaction of **9b** (94 mg, 0.301 mmol, 1 eq), EDAC hydrochloride (64 mg, 0.331 mmol, 1.1 eq), HOBt hydrate (51 mg, 0.331 mmol, 1.1 eq), **6d** (130 mg, 0.391 mmol, 1.2 eq), and Et_3N (76 μL, 0.542 mmol, 1.8 eq) in DMF (4 mL) yielded, after purification by flash column chromatography (SiO_2; 9:1/CH_2Cl_2:MeOH with NH_4OH (7 mL/L of solvent), R_f 0.29), **13j** (28 mg, 15%) as a white powder: ^{1}H NMR ($CDCl_3$, 500 MHz) δ 9.32 (s, 1H), 7.90 (d, 1H, J = 2.7 Hz), 7.89 (d, 1H, J = 8.2 Hz), 7.44 (d, 1H, J = 7.8 Hz), 7.28 (dd, 1H, J_1 = 9.0 Hz, J_2 = 2.3 Hz), 7.20 (t, 1H, J = 7.5 Hz), 7.19 (m, 1H), 7.17 (d, 1H, J = 8.2 Hz), 7.08 (t, 1H, J = 7.6 Hz), 6.96 (d, 1H, J = 7.5 Hz), 6.93 (d, 1H, J = 8.5 Hz), 6.68 (t, 1H, J = 7.4 Hz), 5.86 (m, 1H), 4.01 (br s, 1H), 3.73 (q, 2H, J = 5.8 Hz), 3.47 (t, 2H, J = 7.2 Hz), 3.27 (q, 2H, J = 6.7 Hz), 3.04 (m, 2H), 2.67 (m, 2H), 2.52 (t, 2H, J = 5.8 Hz), 2.33 (s, 3H), 2.21 (s, 3H), 1.93 (m, 4H), 1.63 (p, 2H, J = 6.9 Hz), 1.52 (p, 2H, J = 7.4 Hz), 1.37 (m, 4H); ^{13}C NMR ($CDCl_3$, 125 MHz) δ 171.6, 169.8, 159.5, 150.9, 147.2, 139.5, 138.1, 134.1, 132.3, 130.8, 127.6, 127.4, 125.8, 125.6, 124.6, 124.3, 120.8, 118.3, 116.8, 116.5, 115.7, 114.8, 49.4, 39.4, 35.8, 35.6, 33.9, 31.6, 29.5, 26.6, 26.5, 24.6, 22.9, 22.6, 20.7, 13.9; *m/z* calcd for $C_{37}H_{44}ClN_5O_2$: 625.32; found 626.35 $[M+H]^+$.

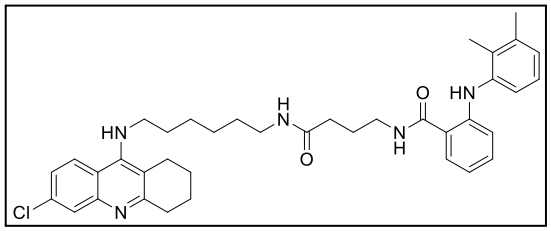

***N*-(4-((6-((6-Chloro-1,2,3,4-tetrahydroacridin-9-yl)amino)hexyl)amino)-4-oxobutyl)-2-((2,3-dimethylphenyl)amino)benzamide (13k).** Compound **13k** was prepared as described for the synthesis of **10a**. The reaction of **9c** (78 mg, 0.238 mmol, 1 eq), EDAC hydrochloride (50 mg, 0.262 mmol, 1.1 eq), HOBt hydrate (40 mg, 0.262 mmol, 1.1 eq), **6d** (95 mg, 0.285 mmol, 1.2 eq), and Et_3N (60 μL, 0.428 mmol, 1.8 eq) in DMF (4 mL) yielded, after purification by flash column chromatography (SiO_2; 9:1/CH_2Cl_2:MeOH with NH_4OH (7 mL/L of solvent), R_f 0.38), **13k** (21 mg, 13%) as a pale yellow powder: ^{1}H NMR ($CDCl_3$, 500 MHz) δ 9.33 (s, 1H), 7.90 (s, 1H), 7.89 (d, 1H, J = 9.3 Hz), 7.49 (d, 1H, J = 7.1 Hz), 7.27 (dd, 1H, J_1 = 9.1 Hz, J_2 = 2.1 Hz), 7.21 (t, 1H, J = 7.4 Hz), 7.17 (d, 1H, J = 7.9 Hz), 7.07 (t, 1H, J = 7.7 Hz), 7.02 (br t, 1H), 6.94 (t, 2H), 6.71 (t, 1H, J = 7.3 Hz), 6.19 (br t, 1H), 4.00 (br s, 1H), 3.50 (q, 2H, J = 6.2 Hz), 3.46 (t, 2H, J = 7.2 Hz), 3.26 (q, 2H, J = 6.8 Hz), 3.04 (br t, 2H), 2.66 (br t, 2H), 2.31 (m, 5H), 2.21 (s, 3H), 1.97 (p, 2H, J = 6.2 Hz), 1.92 (m, 4H), 1.64 (p, 2H, J = 7.2 Hz), 1.51 (p, 2H, J = 7.0 Hz), 1.36 (m, 4H); ^{13}C NMR ($CDCl_3$, 125 MHz) δ 173.0, 170.2, 159.5, 150.8, 148.0, 147.1, 139.6, 138.1, 134.0, 132.3, 130.7, 127.7, 127.4, 125.8, 125.6, 124.7, 124.2, 120.7, 118.3, 116.9, 116.6, 115.7, 114.8, 49.4, 43.7, 39.5, 39.4, 34.1, 34.0, 31.6, 29.5, 26.6, 26.5, 25.2, 24.6, 22.9, 22.6, 20.7, 13.9; *m/z* calcd for $C_{38}H_{46}ClN_5O_2$: 639.33; found 640.30 $[M+H]^+$.

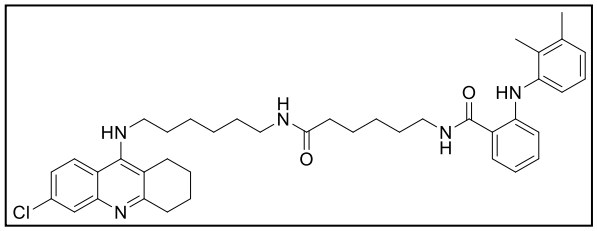

***N*-(6-((6-((6-Chloro-1,2,3,4-tetrahydroacridin-9-yl)amino)hexyl)amino)-6-oxohexyl)-2-((2,3-dimethylphenyl)amino)benzamide (13l).** Compound **13l** was prepared as described for the synthesis of **10a**. The reaction of **9d** (96 mg, 0.271 mmol, 1 eq), EDAC hydrochloride (57 mg, 0.298 mmol, 1.1 eq), HOBt hydrate (46 mg, 0.298 mmol, 1.1 eq), **6d** (108 mg, 0.325 mmol, 1.2 eq), and Et_3N (68 μL, 0.488 mmol, 1.8 eq) in DMF (4 mL) yielded, after purification by flash column chromatography (SiO_2; 9:1/CH_2Cl_2:MeOH with NH_4OH (7 mL/L of solvent), R_f 0.50), **13l** (96 mg, 53%) as a pale yellow powder: ^{1}H NMR

($CDCl_3$, 500 MHz) δ 9.24 (s, 1H), 7.88 (d, 1H, J = 9.1 Hz), 7.85 (d, 1H, J = 1.8 Hz), 7.45 (d, 1H, J = 7.8 Hz), 7.23 (dd, 1H, J_1 = 9.0 Hz, J_2 = 1.8 Hz), 7.17 (t, 1H, J = 7.4 Hz), 7.14 (d, 1H, J = 8.6 Hz), 7.04 (t, 1H, J = 7.7 Hz), 6.91 (d, 2H, J = 8.0 Hz), 6.75 (t, 1H, J = 5.3 Hz), 6.64 (t, 1H, J = 7.4 Hz), 6.02 (t, 1H, J = 5.4 Hz), 4.03 (br s, 1H), 3.41 (m, 4H), 3.19 (q, 2H, J = 6.8 Hz), 2.99 (br s, 2H), 2.63 (br s, 2H), 2.30 (s, 3H), 2.18 (s, 3H), 2.15 (t, 2H, J = 7.3 Hz), 1.88 (br s, 4H), 1.65 (p, 2H, J = 7.5 Hz), 1.60 (p, 4H, J = 7.3 Hz), 1.45 (p, 2H, J = 7.4 Hz), 1.37 (m, 4H), 1.31 (m, 2H); ^{13}C NMR ($CDCl_3$, 125 MHz) δ 173.0, 169.9, 159.5, 150.8, 148.1, 146.9, 139.6, 138.0, 133.9, 132.1, 130.6, 127.6, 127.4, 125.7, 125.5, 124.7, 124.1, 120.6, 118.4, 117.2, 116.8, 115.7, 114.8, 49.4, 39.4, 39.2, 36.4, 34.0, 31.6, 29.6, 29.2, 26.6, 26.5, 26.4, 25.1, 24.6, 22.9, 22.6, 20.7, 13.9; *m/z* calcd for $C_{40}H_{50}ClN_5O_2$: 667.37; found 668.30 $[M+H]^+$.

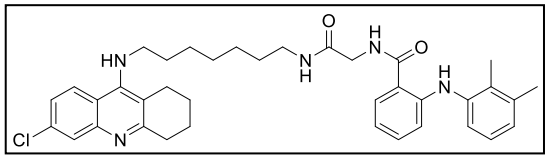

***N*-(2-((7-((6-Chloro-1,2,3,4-tetrahydroacridin-9-yl)amino)heptyl)amino)-2-oxoethyl)-2-((2,3-dimethylphenyl)amino)benzamide** (**13m**). Compound **13m** was prepared as described for the synthesis of **10a**. The reaction of **9a** (53.4 mg, 0.179 mmol, 1 eq), EDAC hydrochloride (38 mg, 0.197 mmol, 1.1 eq), HOBt hydrate (30 mg, 0.197 mmol, 1.1 eq), **6e** (74.2 mg, 0.2155 mmol, 1.2 eq), and Et_3N (45 μL, 0.323 mmol, 1.8 eq) in DMF (4 mL) yielded, after purification by flash column chromatography (SiO_2; 9:1/CH_2Cl_2:MeOH with NH_4OH (7 mL/L of solvent), R_f 0.50), **13m** (11 mg, 10%) as a white powder: ^{1}H NMR ($CDCl_3$, 500 MHz) δ 9.22 (s, 1H), 7.91 (d, 1H, J = 5.7 Hz), 7.89 (d, 1H, J = 2.8 Hz), 7.53 (d, 1H, J = 7.9 Hz), 7.28 (dd, 1H, J_1 = 9.0 Hz, J_2 = 2.8 Hz), 7.23 (t, 1H, J = 7.5 Hz), 7.15 (d, 1H, J = 7.9 Hz), 7.14 (m, 1H), 7.08 (t, 1H, J = 7.6 Hz), 6.97 (d, 1H, J = 7.4 Hz), 6.89 (d, 1H, J = 8.5 Hz), 6.70 (t, 1H, J = 7.4 Hz), 6.27 (t, 1H, J = 5.5 Hz), 4.10 (d, 2H, J = 5.2 Hz), 3.90 (very br s, 1H), 3.47 (t, 2H, J = 7.3 Hz), 3.29 (q, 2H, J = 6.8 Hz), 3.05 (br s, 2H), 2.67 (br s, 2H), 2.33 (s, 3H), 2.19 (s, 3H), 1.93 (m, 4H), 1.64 (p, 2H, J = 7.1 Hz), 1.50 (p, 2H, J = 6.7 Hz), 1.33 (m, 6H) ^{13}C NMR ($CDCl_3$, 125 MHz) δ 170.0, 168.9, 160.0, 151.0, 149.8, 147.6, 139.3, 138.1, 132.8, 132.6, 131.2, 127.8, 127.3, 126.0, 125.8, 124.6, 124.3, 121.4, 118.3, 116.8, 115.6, 115.4, 114.9, 49.5, 43.6, 39.6, 33.9, 31.7, 29.4, 28.9, 26.7, 26.6, 24.6, 22.9, 22.6, 20.7, 13.9; *m/z* calcd for $C_{37}H_{44}ClN_5O_2$: 625.32; found 626.25 $[M+H]^+$.

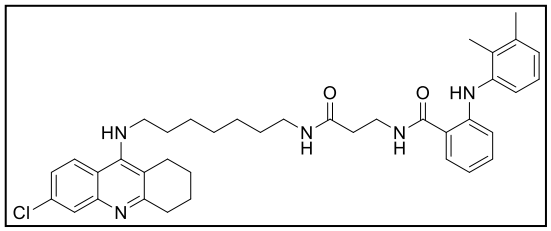

***N*-(3-((7-((6-Chloro-1,2,3,4-tetrahydroacridin-9-yl)amino)heptyl)amino)-3-oxopropyl)-2-((2,3-dimethylphenyl)amino)benzamide (13n).** Compound **13n** was prepared as described for the synthesis of **10a**. The reaction of **9b** (51 mg, 0.164 mmol, 0.86 eq), EDAC hydrochloride (40 mg, 0.209 mmol, 1.1 eq), HOBt hydrate (32 mg, 0.209 mmol, 1.1 eq), **6e** (79 mg, 0.228 mmol, 1.2 eq), and Et_3N (48 μL, 0.342 mmol, 1.8 eq) in DMF (3 mL) yielded, after purification by flash column chromatography (SiO_2; 9:1/CH_2Cl_2:MeOH with NH_4OH (7 mL/L of solvent), R_f 0.46), **13n** (61 mg, 58%) as a yellow oil: ^1H NMR ($CDCl_3$, 500 MHz) δ 9.33 (s, 1H), 7.87 (d, 1H, J = 9.0 Hz), 7.86 (d, 1H, J = 2.0 Hz), 7.45 (d, 1H, J = 7.7 Hz), 7.41 (t, 1H, J = 5.6 Hz), 7.25 (dd, 1H, J_1 = 9.0 Hz, J_2 = 2.0 Hz), 7.17 (t, 1H, J = 7.7 Hz), 7.15 (d, 1H, J = 7.6 Hz), 7.05 (t, 1H, J = 7.6 Hz), 6.93 (d, 1H, J = 7.5 Hz), 6.90 (d, 1H, J = 8.5 Hz), 6.65 (t, 1H, J = 7.3 Hz), 6.36 (t, 1H, J = 5.5 Hz), 3.98 (br s, 1H), 3.70 (q, 2H, J = 5.8 Hz), 3.44 (t, 2H, J = 6.7 Hz), 3.22 (q, 2H, J = 6.7 Hz), 3.01 (br t, 2H), 2.64 (br t, 2H), 2.50 (t, 2H, J = 5.9 Hz), 2.30 (s, 3H), 2.19 (s, 3H), 1.89 (m, 4H), 1.60 (p, 2H, J = 7.2 Hz), 1.46 (p, 2H, J = 6.7 Hz), 1.30 (m, 6H); ^{13}C NMR ($CDCl_3$, 125 MHz) δ 171.7, 169.8, 159.5, 150.8, 148.1, 147.2, 139.5, 138.0, 133.9, 132.2, 130.7, 127.7, 127.4, 125.7, 125.5, 124.7, 124.2, 120.8, 118.4, 116.8, 116.5, 115.7, 114.7, 49.5, 39.5, 35.8, 35.4, 34.0, 31.7, 29.4, 28.9, 26.8, 26.7, 24.6, 22.9, 22.6, 20.7, 13.9; *m/z* calcd for $C_{38}H_{46}ClN_5O_2$: 639.33; found 640.30 $[M+H]^+$.

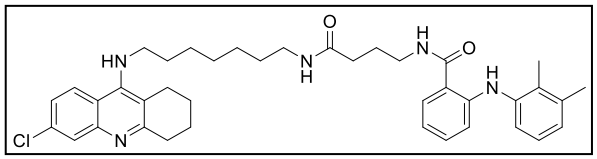

***N*-(4-((7-((6-Chloro-1,2,3,4-tetrahydroacridin-9-yl)amino)heptyl)amino)-4-oxobutyl)-2-((2,3-dimethylphenyl)amino)benzamide (13o).** Compound **13o** was prepared as described for the synthesis of **10a**. The reaction of **9c** (52 mg, 0.158 mmol, 0.87 eq), EDAC hydrochloride (38 mg, 0.200 mmol, 1.1 eq), HOBt hydrate (31 mg, 0.200 mmol, 1.1 eq), **6e** (84 mg, 0.258 mmol, 1.2 eq), and Et_3N (46 μL, 0.387 mmol, 1.8 eq) in DMF (3 mL) yielded, after purification by flash column chromatography (SiO_2; 9:1/CH_2Cl_2:MeOH with

NH_4OH (7 mL/L of solvent), R_f 0.50), **13o** (59 mg, 57%) as a yellow oil: ^1H NMR ($CDCl_3$, 500 MHz) δ 9.35 (s, 1H), 7.87 (d, 1H, J = 9.2 Hz), 7.86 (d, 1H, J = 2.1 Hz), 7.50 (d, 1H, J = 7.8 Hz), 7.39 (t, 1H, J = 7.0 Hz), 7.23 (dd, 1H, J_1 = 9.2 Hz, J_2 = 2.1 Hz), 7.17 (t, 1H, J = 7.5 Hz), 7.14 (d, 1H, J = 8.4 Hz), 7.04 (t, 1H, J = 7.6 Hz), 6.91 (d, 2H, J = 8.1 Hz), 6.66 (t, 1H, J = 7.4 Hz), 6.62 (t, 1H, J = 5.5 Hz), 4.01 (br s, 1H), 3.47 (t, 2H, J = 5.9 Hz), 3.44 (q, 2H, J = 5.4 Hz), 3.21 (q, 2H, J = 6.7 Hz), 3.00 (br t, 2H), 2.63 (br t, 2H), 2.29 (t, 2H, J = 7.2 Hz), 2.29 (s, 3H), 2.18 (s, 3H), 1.94 (p, 2H, J = 6.5 Hz), 1.88 (m, 4H), 1.60 (p, 2H, J = 7.0 Hz), 1.45 (p, 2H, J = 6.5 Hz), 1.29 (m, 6H); ^{13}C NMR ($CDCl_3$, 125 MHz) δ 173.1, 170.2, 159.4, 150.9, 148.0, 147.1, 139.6, 138.0, 134.0, 132.1, 130.6, 127.8, 127.3, 125.7, 125.5, 124.7, 124.1, 120.7, 118.3, 116.8, 116.7, 115.6, 114.7, 49.5, 39.6, 39.5, 34.1, 33.9, 31.7, 29.4, 28.9, 26.8, 26.7, 25.2, 24.6, 22.9, 22.6, 20.7, 13.9; *m/z* calcd for $C_{39}H_{48}ClN_5O_2$: 653.35; found 654.25 $[M+H]^+$.

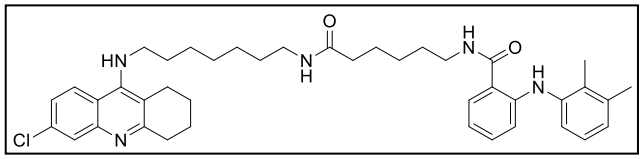

***N*-(6-((7-((6-Chloro-1,2,3,4-tetrahydroacridin-9-yl)amino)heptyl)amino)-6-oxohexyl)-2-((2,3-dimethylphenyl)amino)benzamide** (**13p**). Compound **13p** was prepared as described for the synthesis of **10a**. The reaction of **9d** (55 mg, 0.155 mmol, 0.80 eq), EDAC hydrochloride (41 mg, 0.214 mmol, 1.1 eq), HOBt hydrate (33 mg, 0.214 mmol, 1.1 eq), **6e** (81 mg, 0.233 mmol, 1.2 eq), and Et_3N (49 μL, 0.350 mmol, 1.8 eq) in DMF (3 mL) yielded, after purification by flash column chromatography (SiO_2; 9:1/CH_2Cl_2:MeOH with NH_4OH (7 mL/L of solvent), R_f 0.42), **13p** (51 mg, 48%) as a yellow oil: ^1H NMR ($CDCl_3$, 500 MHz) δ 9.23 (s, 1H), 7.89 (d, 1H, J = 9.0 Hz), 7.87 (d, 1H, J = 2.1 Hz), 7.44 (d, 1H, J = 7.1 Hz), 7.25 (dd, 1H, J_1 = 9.0 Hz, J_2 = 2.1 Hz), 7.18 (t, 1H, J = 7.5 Hz), 7.15 (d, 1H, J = 7.7 Hz), 7.05 (t, 1H, J = 7.7 Hz), 6.92 (d, 2H, J = 8.4 Hz), 6.66 (t, 1H, J = 7.4 Hz), 6.61 (t, 1H, J = 5.5 Hz), 5.85 (t, 1H, J = 5.5 Hz), 4.01 (br s, 1H), 3.46 (t, 2H, J = 7.0 Hz), 3.42 (q, 2H, J = 6.8 Hz), 3.19 (q, 2H, J = 6.7 Hz), 3.01 (m, 2H), 2.65 (m, 2H), 2.31 (s, 3H), 2.19 (s, 3H), 2.17 (t, 2H, J = 7.4 Hz), 1.90 (m, 4H), 1.68 (p, 2H, J = 7.4 Hz), 1.63 (p, 4H, J = 7.1 Hz), 1.42 (m, 4H), 1.29 (m, 6H); ^{13}C NMR ($CDCl_3$, 125 MHz) δ 172.9, 169.8, 159.5, 150.9, 148.1, 147.0, 139.6, 138.0, 133.9, 132.1, 130.6, 127.5, 127.4, 125.7, 125.5, 124.7, 124.2, 120.6, 118.4, 117.2, 116.8, 115.7, 114.8, 49.5, 39.40,

39.38, 36.4, 34.0, 31.7, 29.6, 29.2, 28.9, 26.8, 26.7, 26.4, 25.1, 24.6, 22.9, 22.6, 20.7, 13.9; *m/z* calcd for $C_{41}H_{52}ClN_5O_2$: 681.38; found 682.40 $[M+H]^+$.

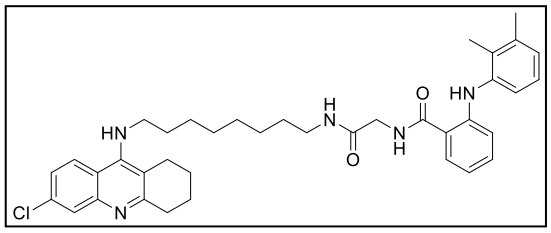

***N*-(2-((8-((6-Chloro-1,2,3,4-tetrahydroacridin-9-yl)amino)octyl)amino)-2-oxoethyl)-2-((2,3-dimethylphenyl)amino)benzamide (13q).** Compound **13q** was prepared as described for the synthesis of **10a**. The reaction of **9a** (47 mg, 0.158 mmol, 1 eq), EDAC hydrochloride (33 mg, 0.173 mmol, 1.1 eq), HOBt hydrate (27 mg, 0.173 mmol, 1.1 eq), **6f** (68 mg, 0.205 mmol, 1.2 eq), and Et_3N (40 μL, 0.284 mmol, 1.8 eq) in DMF (4 mL) yielded, after purification by flash column chromatography (SiO_2; 9:1/CH_2Cl_2:MeOH with NH_4OH (7 mL/L of solvent), R_f 0.37), **13q** (46 mg, 54%) as a pale yellow powder: ^{1}H NMR ($CDCl_3$, 500 MHz) δ 9.23 (s, 1H), 7.90 (d, 1H, *J* = 10.5 Hz), 7.88 (s, 1H), 7.56 (d, 1H, *J* = 7.9 Hz), 7.41 (t, 1H, *J* = 4.8 Hz), 7.27 (d, 1H, *J* = 9.0 Hz), 7.20 (t, 1H, *J* = 7.6 Hz), 7.15 (d, 1H, *J* = 7.8 Hz), 7.08 (t, 1H, *J* = 7.6 Hz), 6.97 (d, 1H, *J* = 7.3 Hz), 6.87 (d, 1H, *J* = 8.5 Hz), 6.66 (t, 1H, *J* = 7.6 Hz), 6.64 (t, 1H, *J* = 5.4 Hz), 4.10 (d, 2H, *J* = 5.1 Hz), 3.99 (br s, 1H), 3.46 (t, 2H, *J* = 6.7 Hz), 3.27 (q, 2H, *J* = 6.7 Hz), 3.03 (br s, 2H), 2.66 (br s, 2H), 2.32 (s, 3H), 2.18 (s, 3H), 1.92 (m, 4H), 1.62 (p, 2H, *J* = 7.0 Hz), 1.48 (br p, 2H), 1.34 (m, 2H), 1.27 (m, 6H); ^{13}C NMR ($CDCl_3$, 125 MHz) δ 170.1, 169.0, 159.5, 150.9, 148.1, 147.6, 139.3, 138.1, 134.0, 132.7, 131.2, 127.9, 127.4, 126.0, 125.8, 124.7, 124.2, 121.5, 118.4, 116.8, 115.7, 115.5, 114.8, 49.5, 43.7, 39.6, 34.0, 31.7, 29.4, 29.14, 29.07, 26.8, 26.7, 24.6, 22.9, 22.7, 20.7, 13.9; *m/z* calcd for $C_{38}H_{46}ClN_5O_2$: 639.33; found 640.35 $[M+H]^+$.

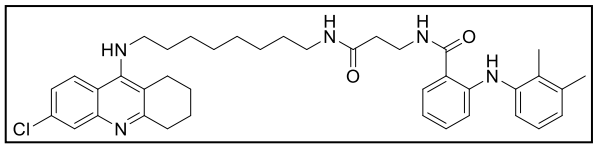

***N*-(3-((8-((6-Chloro-1,2,3,4-tetrahydroacridin-9-yl)amino)octyl)amino)-3-oxopropyl)-2-((2,3-dimethylphenyl)amino)benzamide (13r).** Compound **13r** was prepared as described for the synthesis of **10a**. The reaction of **9b** (50 mg, 0.159 mmol, 1 eq), EDAC hydrochloride (34 mg, 0.175 mmol, 1.1 eq), HOBt hydrate (27 mg, 0.175 mmol, 1.1 eq), **6f** (69 mg, 0.207 mmol, 1.2 eq), and Et_3N (40 μL, 0.286 mmol, 1.8 eq) in DMF (4 mL)

yielded, after purification by flash column chromatography (SiO_2; 9:1/CH_2Cl_2:MeOH with NH_4OH (7 mL/L of solvent), R_f 0.45), **13r** (20 mg, 20%) as a pale yellow powder: ^{1}H NMR ($CDCl_3$, 500 MHz) δ 9.32 (s, 1H), 7.90 (d, 1H, *J* = 9.0 Hz), 7.89 (d, 1H, *J* = 2.0 Hz), 7.45 (d, 1H, *J* = 7.8 Hz), 7.29 (m, 1H), 7.27 (dd, 1H, J_1 = 9.0 Hz, J_2 = 2.0 Hz), 7.20 (t, 1H, *J* = 8.0 Hz), 7.17 (d, 1H, *J* = 8.7 Hz), 7.07 (t, 1H, *J* = 7.6 Hz), 6.95 (d, 1H, *J* = 7.4 Hz), 6.92 (d, 1H, *J* = 8.5 Hz), 6.68 (t, 1H, *J* = 7.4 Hz), 6.00 (t, 1H, *J* = 5.3 Hz), 3.99 (br s, 1H), 3.72 (q, 2H, *J* = 5.8 Hz), 3.48 (t, 2H, *J* = 7.0 Hz), 3.25 (q, 2H, *J* = 6.6 Hz), 3.03 (m, 2H), 2.67 (m, 2H), 2.52 (t, 2H, *J* = 5.8 Hz), 2.33 (s, 3H), 2.21 (s, 3H), 1.92 (m, 4H), 1.64 (p, 2H, *J* = 7.4 Hz), 1.47 (br p, 2H), 1.36 (m, 4H), 1.28 (s, 4H); ^{13}C NMR ($CDCl_3$, 125 MHz) δ 171.7, 169.8, 159.5, 150.9, 148.1, 147.2, 139.6, 138.0, 134.0, 132.3, 130.8, 127.6, 127.5, 125.7, 125.6, 124.7, 124.2, 120.8, 118.4, 116.8, 116.5, 115.7, 114.8, 49.5, 39.6, 35.8, 35.5, 34.00, 33.96, 31.7, 29.5, 29.13, 29.09, 26.8, 24.6, 22.9, 22.7, 20.7, 13.9; *m/z* calcd for $C_{39}H_{48}ClN_5O_2$: 653.35; found 654.35 $[M+H]^+$.

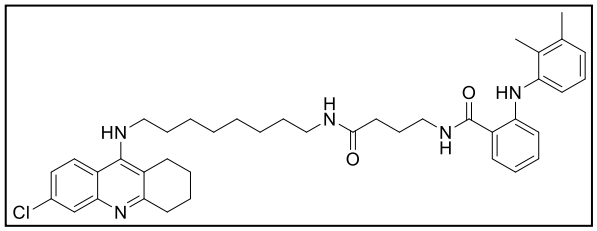

***N*-(4-((8-((6-Chloro-1,2,3,4-tetrahydroacridin-9-yl)amino)octyl)amino)-4-oxobutyl)-2-((2,3-dimethylphenyl)amino)benzamide (13s).** Compound **13s** was prepared as described for the synthesis of **10a**. The reaction of **9c** (45 mg, 0.137 mmol, 1 eq), EDAC hydrochloride (29 mg, 0.150 mmol, 1.1 eq), HOBt hydrate (23 mg, 0.150 mmol, 1.1 eq), **6f** (64 mg, 0.177 mmol, 1.2 eq), and Et_3N (34 μL, 0.247 mmol, 1.8 eq) in DMF (4 mL) yielded, after purification by flash column chromatography (SiO_2; 9:1/CH_2Cl_2:MeOH with NH_4OH (7 mL/L of solvent), R_f 0.35), **13s** (28 mg, 31%) as a pale yellow powder: ^{1}H NMR ($CDCl_3$, 500 MHz) δ 9.35 (s, 1H), 7.91 (d, 1H, *J* = 8.8 Hz), 7.92 (s, 1H), 7.49 (d, 1H, *J* = 7.2 Hz), 7.29 (m, 1H), 7.22 (t, 1H, *J* = 7.3 Hz), 7.18 (d, 1H, *J* = 7.8 Hz), 7.08 (t, 1H, *J* = 7.7 Hz), 6.99 (br t, 1H), 6.95 (m, 2H) 6.72 (t, 1H, *J* = 7.4 Hz), 6.07 (br t, 1H), 4.02 (very br s, 1H), 3.51 (p, 4H, *J* = 6.4 Hz), 3.25 (q, 2H, *J* = 6.7 Hz), 3.05 (br t, 2H), 2.68 (br t, 2H), 2.33 (m, 5H), 2.22 (s, 3H), 1.99 (m, 2H), 1.94 (m, 4H), 1.66 (p, 2H, *J* = 7.3 Hz), 1.48 (m, 2H), 1.35 (m, 2H), 1.29 (m, 6H); ^{13}C NMR ($CDCl_3$, 125 MHz) δ 172.9, 170.1, 147.2, 139.6, 138.0, 135.3, 134.7, 134.2, 132.2, 130.7, 127.6, 126.8, 125.7, 125.5, 124.7, 124.3, 120.8,

116.9, 116.6, 114.8, 49.5, 39.6, 39.5, 34.2, 34.0, 31.7, 29.5, 29.11, 29.08, 26.8, 25.1, 25.0, 24.5, 22.9, 22.6, 20.7, 13.9; *m/z* calcd for $C_{40}H_{50}ClN_5O_2$: 667.37; found 668.40 $[M+H]^+$.

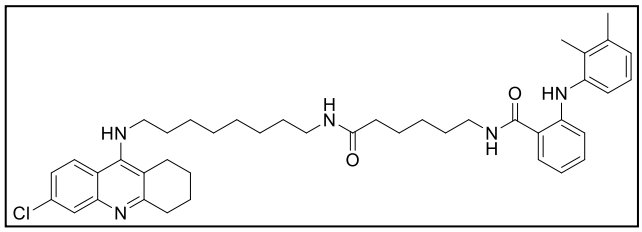

***N*-(6-((8-((6-Chloro-1,2,3,4-tetrahydroacridin-9-yl)amino)octyl)amino)-6-oxohexyl)-2-((2,3-dimethylphenyl)amino)benzamide (13t).** Compound **13t** was prepared as described for the synthesis of **10a**. The reaction of **9d** (48 mg, 0.137 mmol, 1 eq), EDAC hydrochloride (29 mg, 0.152 mmol, 1.1 eq), HOBt hydrate (23 mg, 0.152 mmol, 1.1 eq), **6f** (65 mg, 0.180 mmol, 1.2 eq), and Et_3N (34 μL, 0.244 mmol, 1.8 eq) in DMF (4 mL) yielded, after purification by flash column chromatography (SiO_2; 9:1/CH_2Cl_2:MeOH with NH_4OH (7 mL/L of solvent), R_f 0.29), **13t** (80 mg, 84%) as a pale yellow powder: ^{1}H NMR ($CDCl_3$, 500 MHz) δ 9.23 (s, 1H), 7.92 (d, 1H, J = 7.7 Hz), 7.91 (d, 1H, J = 1.9 Hz), 7.45 (d, 1H, J = 7.3 Hz), 7.28 (dd, 1H, J_1 = 9.0 Hz, J_2 = 1.9 Hz), 7.21 (t, 1H, J = 7.3 Hz), 7.17 (d, 1H, J = 7.9 Hz), 7.07 (t, 1H, J = 7.6 Hz), 6.94 (m, 2H), 6.69 (t, 1H, J = 7.2 Hz), 6.44 (br t, 1H), 5.62 (br t, 1H), 4.10 (very br s, 1H), 3.51 (t, 2H, J = 7.1 Hz), 3.45 (q, 2H, J = 6.3 Hz), 3.22 (q, 2H, J = 6.7 Hz), 3.05 (br t, 2H), 2.67 (br t, 2H), 2.33 (s, 3H), 2.21 (s, 3H), 2.20 (t, 2H, J = 7.4 Hz), 1.93 (m, 4H), 1.69 (m, 6H), 1.45 (p, 4H, J = 7.1 Hz), 1.38 (br p, 2H), 1.30 (m, 6H); ^{13}C NMR ($CDCl_3$, 125 MHz) δ 172.8, 169.8, 162.5, 151.2, 147.0, 144.0, 139.6, 138.0, 132.1, 130.7, 127.4, 125.7, 125.5, 124.7, 124.3, 120.7, 118.9, 118.1, 117.2, 116.8, 116.6, 115.5, 114.9, 49.5, 39.44, 39.38, 36.5, 31.7, 30.9, 29.6, 29.2, 29.12, 29.06, 26.74, 26.71, 26.4, 25.0, 24.5, 22.9, 22.5, 20.7, 13.9; *m/z* calcd for $C_{42}H_{54}ClN_5O_2$: 695.40; found 696.45 $[M+H]^+$.

2.6.2. Biochemical and computational methods

2.6.2.1. *In vitro* AChE assay

Compounds were dissolved in sodium phosphate (dibasic) buffer ((125 μL), 0.1 M, pH 8.0 (adjusted at rt)), and a five-fold dilution was performed. To the solution of inhibitors was added AChE cocktail (50 μL, containing 0.08 U/mL (~0.29 nM) AChE (final concentration) (Sigma-Aldrich cat #C2888 from eel) in sodium phosphate (dibasic) buffer

(0.1 M, pH 8.0 (adjusted at rt)). The mixture of inhibitor and enzyme was incubated for 10 min before initiation with 5,5'-dithiobis(2-nitrobenzoic acid) (DTNB) (50 μL, 0.25 mM final concentration) and acetylthiocholine (ATC) (0.5 mM final concentration) in phosphate buffer. The reaction was monitored at 412 nm taking measurements every 30 s for 30 min. Data was corrected with the negative control (no ATC) and normalized to the positive control (no inhibitor) using the initial rates (first 2-5 min). All assays were performed at least in triplicate. The resulting curve rate versus concentration of inhibitor was fitted to a sigmoidal curve, and IC_{50} values were calculated using KaleidaGraph 4.1.1. Three representative examples of IC_{50} curves are provided in Fig. 2.3. All IC_{50} values are provided in Table 2.1.

2.6.2.2. Studies of the mode of inhibition

Non-competitive inhibition was determined by incubating four concentrations of inhibitor (0, 0.2, 1, and 5 μM) with AChE (as described above). The enzymatic reaction was then initiated by the addition of various concentrations of ATC (62.5, 250, 500, and 1000 μM). The rates of the reactions were calculated using the first 2 min of the reaction and plotted on a Lineweaver-Burk plot. Separate lines were drawn for each concentration of inhibitor, and observation of intersection on the negative side of the *x* axis indicated non-competitive inhibition. A representative plot is provided in Fig. 2.4.

2.6.2.3. *In vitro* AChE ROS inactivation assay

In the wells of a 96-well plate, horseradish peroxidase (0.25 μM), H_2O_2 (100 μM), AChE (0.08 U/mL, ~0.29 nM), compound (25 μM – 13 pM), and diethylenetriaminepentaacetic acid (DETAPAC) (100 μM) were dissolved in acetate buffer (pH 6.0) (50 mM) and incubated at 37 °C for 30 min. *Note*: all concentrations are reported as final concentrations. To the above solution, a mixture of ATC (0.5 mM) and DTNB (0.25 mM) in sodium phosphate (dibasic) buffer (50 mM, pH 7.4 (adjusted at rt)) was added. Reaction rates were monitored at 25 °C for 20 min taking measurements every 30 s, and rates were calculated using the initial rate (first 2-5 min). Total reaction volume was 200 μL. Rates were normalized to the reaction without compounds and plotted in KaleidaGraph 4.1.1 to

calculate the IC_{50}. Three representative examples of IC_{50} curves are provided in Fig. 2.3. All IC_{50} values are provided in Table 2.1.

2.6.2.4. Molecular modeling

Molecular docking studies were run on an Intell Premium 4 CPU (3.19 GHz, 0.99 GB of RAM, Windows XP Professional (Version 2002)) using the modeling program AutoDock 4.2 (2009. The Scripps Research Institute. 10550 North Torrey Pines Road, La Jolla, CA 92037. http://autodock.scripps.edu). Additionally, the program Cygwin (version 1.7. http://www.cygwin.com) was used to properly run the Autogrid and AutoDock applications. The crystal structure of AChE from *Torpedo californica* in complex with tacrine (PDB ID: 1ACJ, 2.8 Å resolution) was first edited in PyMOL (http://www.pymol.org, (PyMOL Molecular Graphics System, version 1.1r1, Schrödinger, LLC)) by manually removing all H_2O molecules. The tacrine molecule was also removed from the active site. The enzyme was then loaded into AutoDock where all polar hydrogens were added and Kollman charges were assigned. The various ligands were prepared in ChemBio3D Ultra 12.0 (http://www.cambridgesoft.com), and then loaded into AutoDock. The scoring grid for AutoDock was centered approximately in between the CAS and PAS (x-center: 4.795, y-center: 66.845, z-center: 72.226). The grid size was selected to be 60×60×60 points with a spacing between grid points of 0.375 Å. A Lamarckian genetic search algorithm was run 100 times using 150 population size and a maximum number of energy evaluations of 2,500,000, while the rest of the docking study parameters were kept at their default quantity. After the docking was finished, conformations that were shown to be the in the largest cluster or most thermodynamically stable were examined in PyMOL. All docking figures were made in PyMOL (Fig. 2.5).

2.7. References

(1) Green, K. D.; Porter, V. R.; Zhang, Y.; Garneau-Tsodikova, S. *Biochemistry* **2010**, *49*, 6219-6227.
(2) Green, K. D.; Fridman, M.; Garneau-Tsodikova, S. *Chembiochem* **2009**, *10*, 2191-2194.
(3) Kim, A. R.; Rylett, R. J.; Shilton, B. H. *Biochemistry* **2006**, *45*, 14621-14631.

(4) Petersen, R. C.; Thomas, R. G.; Grundman, M.; Bennett, D.; Doody, R.; Ferris, S.; Galasko, D.; Jin, S.; Kaye, J.; Levey, A.; Pfeiffer, E.; Sano, M.; van Dyck, C. H.; Thal, L. J. *N Engl J Med* **2005**, *352*, 2379-2388.
(5) Courtney, C.; Farrell, D.; Gray, R.; Hills, R.; Lynch, L.; Sellwood, E.; Edwards, S.; Hardyman, W.; Raftery, J.; Crome, P.; Lendon, C.; Shaw, H.; Bentham, P. *Lancet* **2004**, *363*, 2105-2115.
(6) McGeer, P. L.; Schulzer, M.; McGeer, E. G. *Neurology* **1996**, *47*, 425-432.
(7) McGeer, P. L.; McGeer, E. G. *Neurobiol Aging* **2007**, *28*, 639-647.
(8) McGeer, P. L.; Rogers, J.; McGeer, E. G. *J Alzheimers Dis* **2006**, *9*, 271-276.
(9) Szekely, C. A.; Town, T.; Zandi, P. P. *Subcell Biochem* **2007**, *42*, 229-248.
(10) Joo, Y.; Kim, H. S.; Woo, R. S.; Park, C. H.; Shin, K. Y.; Lee, J. P.; Chang, K. A.; Kim, S.; Suh, Y. H. *Mol Pharmacol* **2006**, *69*, 76-84.
(11) Camps, P.; Formosa, X.; Munoz-Torrero, D.; Petrignet, J.; Badia, A.; Clos, M. V. *J Med Chem* **2005**, *48*, 1701-1704.
(12) Alonso, D.; Dorronsoro, I.; Rubio, L.; Munoz, P.; Garcia-Palomero, E.; Del Monte, M.; Bidon-Chanal, A.; Orozco, M.; Luque, F. J.; Castro, A.; Medina, M.; Martinez, A. *Bioorg Med Chem* **2005**, *13*, 6588-6597.
(13) Butini, S.; Guarino, E.; Campiani, G.; Brindisi, M.; Coccone, S. S.; Fiorini, I.; Novellino, E.; Belinskaya, T.; Saxena, A.; Gemma, S. *Bioorg Med Chem Lett* **2008**, *18*, 5213-5216.
(14) Shao, D.; Zou, C.; Luo, C.; Tang, X.; Li, Y. *Bioorg Med Chem Lett* **2004**, *14*, 4639-4642.
(15) Rodriguez-Franco, M. I.; Fernandez-Bachiller, M. I.; Perez, C.; Hernandez-Ledesma, B.; Bartolome, B. *J Med Chem* **2006**, *49*, 459-462.
(16) Muraoka, S.; Miura, T. *Life Sci* **2009**, *84*, 272-277.
(17) Muraoka, S.; Miura, T. *Life Sci* **2003**, *72*, 1897-1907.
(18) Thomas, T.; Nadackal, T. G.; Thomas, K. *Neuroreport* **2001**, *12*, 3263-3267.
(19) Inestrosa, N. C.; Alvarez, A.; Perez, C. A.; Moreno, R. D.; Vicente, M.; Linker, C.; Casanueva, O. I.; Soto, C.; Garrido, J. *Neuron* **1996**, *16*, 881-891.
(20) Bartolini, M.; Bertucci, C.; Cavrini, V.; Andrisano, V. *Biochem Pharmacol* **2003**, *65*, 407-416.
(21) Du, D. M.; Carlier, P. R. *Curr Pharm Des* **2004**, *10*, 3141-3156.
(22) Hu, M. K.; Wu, L. J.; Hsiao, G.; Yen, M. H. *J Med Chem* **2002**, *45*, 2277-2282.
(23) Carlier, P. R.; Chow, E. S.; Han, Y.; Liu, J.; El Yazal, J.; Pang, Y. P. *J Med Chem* **1999**, *42*, 4225-4231.
(24) Ellman, G. L.; Courtney, K. D.; Andres, V., Jr.; Feather-Stone, R. M. *Biochem Pharmacol* **1961**, *7*, 88-95.
(25) Fernandez-Bachiller, M. I.; Perez, C.; Campillo, N. E.; Paez, J. A.; Gonzalez-Munoz, G. C.; Usan, P.; Garcia-Palomero, E.; Lopez, M. G.; Villarroya, M.; Garcia, A. G.; Martinez, A.; Rodriguez-Franco, M. I. *ChemMedChem* **2009**, *4*, 828-841.
(26) Rydberg, E. H.; Brumshtein, B.; Greenblatt, H. M.; Wong, D. M.; Shaya, D.; Williams, L. D.; Carlier, P. R.; Pang, Y. P.; Silman, I.; Sussman, J. L. *J Med Chem* **2006**, *49*, 5491-5500.
(27) Fang, L.; Kraus, B.; Lehmann, J.; Heilmann, J.; Zhang, Y.; Decker, M. *Bioorg Med Chem Lett* **2008**, *18*, 2905-2909.

(28) Harel, M.; Schalk, I.; Ehret-Sabatier, L.; Bouet, F.; Goeldner, M.; Hirth, C.; Axelsen, P. H.; Silman, I.; Sussman, J. L. *Proc Natl Acad Sci U S A* **1993**, *90*, 9031-9035.
(29) da Silva, C. H.; Campo, V. L.; Carvalho, I.; Taft, C. A. *J Mol Graph Model* **2006**, *25*, 169-175.
(30) Pang, Y. P.; Quiram, P.; Jelacic, T.; Hong, F.; Brimijoin, S. *J Biol Chem* **1996**, *271*, 23646-23649.
(31) Johnson, G.; Moore, S. W. *Biochem Biophys Res Commun* **1999**, *258*, 758-762.
(32) Alvarez, A.; Opazo, C.; Alarcon, R.; Garrido, J.; Inestrosa, N. C. *J Mol Biol* **1997**, *272*, 348-361.
(33) Reyes, A. E.; Perez, D. R.; Alvarez, A.; Garrido, J.; Gentry, M. K.; Doctor, B. P.; Inestrosa, N. C. *Biochem Biophys Res Commun* **1997**, *232*, 652-655.

Note:
This chapter is adapted from a published article: Bornstein, J. J.; **Eckroat, T. J.**; Houghton, J. L.; Jones, C. K.; Green, K. D.; Garneau-Tsodikova, S. *Med Chem Commun* **2011**, *2*, 406-412.

Authors' contribution:
TJE, JJB, CKJ, and JLH synthesized all compounds.
KDG performed all biochemical assays.
CKJ and TJE performed molecular modeling.
JLH, TJE, JJB, CKJ, KDG, and SGT analyzed data and wrote manuscript.

Chapter 3

Investigation of the role of linker moieties in bifunctional tacrine hybrids

3.1. Abstract

Alzheimer's disease (AD) is a complex neurological disorder with multiple inter-connected factors playing roles in the onset and progression of the disease. One strategy currently being explored for the development of new therapeutics for AD involves linking tacrine, a known acetylcholinesterase (AChE) inhibitor, to another drug to create bifunctional hybrids. The role and influence on activity of the linker moiety in these hybrids remains ill-defined. In this study, three series of 6-chlorotacrine with linkers varying in terminal functional group and length were synthesized, evaluated for AChE inhibition, and compared to tacrine and 6-chlorotacrine-mefenamic acid hybrids. Out of the compounds with terminal amine, methyl, and hydroxyl moieties tested, several highly potent molecules (low nanomolar IC_{50} values) comprised of linkers with terminal amines were identified. These 6-chlorotacrine with linkers were significantly more potent than tacrine alone and were often more potent than similar 6-chlorotacrine-mefenamic acid hybrids.

3.2. Introduction

Alzheimer's disease (AD), the 6th leading cause of death in the USA, is a progressive dementia whose symptoms include cognitive dysfunction, psychiatric and behavioral disturbances, and difficulties in performing tasks of daily living. In contrast to other major causes of death such as HIV, stroke, breast cancer, and heart disease, which have shown decreases in overall mortality over the past decade, the number of deaths due to AD has risen over 66%.[1,2] Although the exact underlying cause of the disease is unknown, several factors are thought to play a role in the onset and progression of AD. These include plaque deposits in the brain due to the amyloid-β (Aβ) peptide, neurofibrillary tangles due to

irregular phosphorylation of Tau protein, dyshomeostasis and miscompartmentalization of the metal ions copper, iron, and zinc, inflammation and oxidative stress from reactive oxygen species (ROS), and decreased cholinergic transmission and acetylcholine (ACh) levels. Current treatments for AD are largely centered on increasing ACh levels in the brain through the inhibition of acetylcholinesterase (AChE). In fact, four out of the five approved drugs for AD are acetylcholinesterase inhibitors (AChEis). These include tacrine (**1**) (Fig. 3.1A), donepezil, rivastigmine, and galantamine. There is evidence that AChEis are moderately successful in AD treatment.[3,4] However, as highlighted by clinical studies of donepezil, it has been suggested that AChEis may not be cost-effective and new approaches should be sought.[5,6] In addition, the current treatments for AD are only able to treat symptoms of the disease and do little to stop or reverse the progression.

The development of new therapeutics to combat the multifactorial nature of AD is clearly an important research endeavor, and one approach to this end is the multitarget approach of hybrid drugs. In AD, this approach is based on the unique structural and biochemical properties of AChE. AChE is known to possess two binding sites: the catalytic active site (CAS) and the peripheral anionic site (PAS) connected by a gorge that is about 20 Å long.[7-10] In addition, AChE is known to be found entangled in the Aβ plaque, and the enzyme likely accelerates the formation of stable Aβ aggregates through interactions with the PAS.[11,12] Also found in the plaque are metal ions and ROS. Metal chelators and ROS scavengers have shown promise in the treatment of AD.[13] A popular strategy over the past 15 years has been to link a known AChEi with another compound capable of binding to the PAS and/or exerting other properties that are beneficial to the treatment of AD to create a bifunctional or multifunctional hybrid compound. The AChEi moiety of the resulting hybrid serves to direct the molecule to the CAS of AChE so the other moiety can interact with the PAS to increase potency, disrupt Aβ aggregation, chelate metals, and/or scavenge ROS. Although the use of tacrine has been severely limited since its inception due to hepatotoxicity,[14] it is often the AChEi of choice as a starting point for designing multifunctional hybrids due to its AChE inhibitory properties and the ease and low costs at which synthetic precursors, such as the 9-chloro derivative[15] that is susceptible to nucleophilic substitution for generating linked compounds, can be generated.

By linking tacrine with another compound to create a multifunctional hybrid, it is possible to not only greatly increase potency towards AChE inhibition but also to attack the multifactorial nature of AD. For example, a heptylene-linked tacrine dimer was shown to be 150-fold more potent than tacrine[16] by binding to the enzyme such that one tacrine moiety was positioned in the CAS and the other was positioned in the PAS.[8] An inhibitor of this type has the potential to disrupt AChE-mediated Aβ aggregation as mentioned above. As another example, tacrine-8-hydroxyquinoline hybrids were shown to be potent AChEis and antioxidants with low cell toxicity and the ability to complex copper ions, as well as the predicted ability to disrupt AChE-mediated Aβ aggregation.[17] The best compound from this series showed a remarkable 700-fold greater potency towards human AChE than tacrine. To date, there have been roughly fifty tacrine hybrids that have been synthesized, tested, and reported in the literature.

We recently synthesized and tested two series of 6-chlorotacrine-mefenamic acid hybrids (**11a-f** and **13f-h**, **13j-l**, **13n-p**) (Fig. 3.1A).[18] Mefenamic acid (**2**) is a NSAID with the ability to inactivate AChE in the presence of peroxidases,[19] decrease the occurrence of free-radicals, attenuate Aβ peptide-induced neurotoxicity, and improve cognitive impairments.[20] The best compounds from these series contained an 8-10 atom linker between the 6-chlorotacrine and mefenamic acid moieties and displayed low nanomolar or subnanomolar IC_{50} values for AChE under normal and ROS conditions. Many of these hybrids showed improvement in potency in our assays over a 1:1 mixture of tacrine and mefenamic acid, which seems to indicate a benefit to linking the two molecules as was originally hypothesized.

To further investigate the role of the linker itself, we report herein on the inhibition of AChE by 1:1 mixtures of 6-chlorotacrine with linkers **6b-i** and mefenamic acid or 6-chlorotacrine with linkers **6b-e** and mefenamic acid with linkers **9b-d**. These mixtures closely resemble hybrids **11a-f** and **13f-h**, **13j-l**, **13n-p** as they are essentially the hybrid lacking the final amide bond. In addition, we have synthesized new types of 6-chlorotacrine derivatives, resembling previously published tacrine with linkers, which vary in their terminal functional group to include $-CH_3$ and -OH. Despite the abundance

of tacrine hybrids in the literature, there remains little precedent for testing the inhibitory properties of 6-chlorotacrine with linkers by themselves. Our results should elucidate more clearly the role of the linker portion of the tacrine hybrid molecules and the benefit, if any, of linking together AChEis and other small molecules.

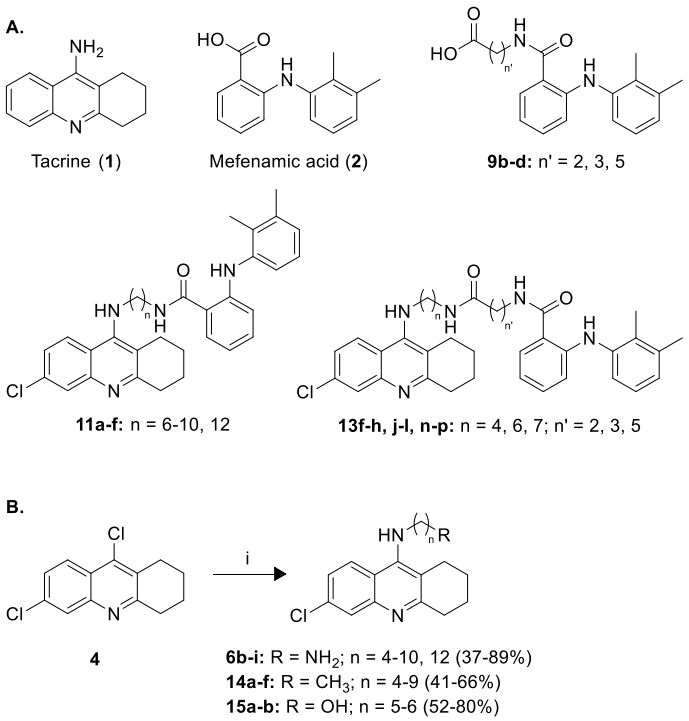

Fig. 3.1. A. Structures of tacrine (**1**), mefenamic acid (**2**), mefenamic acid with linkers (**9b-d**), and 6-chlorotacrine-mefenamic acid hybrids (**11a-f** and **13f-h**, **13j-l**, **13n-p**). **B.** Synthetic scheme for the preparation of 6-chlorotacrine amine linkers (**6b-i**), methyl linkers (**14a-f**), and hydroxyl linkers (**15a-b**). *Reagents and conditions*: (i) $H_2N(CH_2)_nNH_2$ (3-4 eq) or $H_2N(CH_2)_nCH_3$ (3-4 eq) or $H_2N(CH_2)_nOH$ (3 eq), 1-pentanol, Δ.

3.3. Results and discussion

3.3.1. Synthesis

The synthetic approach to the generation of our new 6-chlorotacrine derivatives is illustrated in Figure 3.1B. The 6-Cl substitution on the tacrine core was chosen because we have previously discovered that it increases binding potency for AChE when compared to its non-chlorinated counterpart,[18] a result that has also been observed in other studies.[21-24] In addition, the 6-Cl moiety may decrease the occurrence of unwanted side effects by increasing selectivity for AChE over butyrylcholinesterase (BChE).[25] Our new molecules contain various terminal functional groups connected to 6-chlorotacrine via a hydrophobic linker moiety of varying length and were synthesized from the starting compound 6,9-dichlorotacrine (**4**) using a nucleophilic aromatic substitution reaction in 1-pentanol. Compounds **6b** and **6d-i** with terminal amine groups were prepared as we previously described.[18] Compound **6c**, also with a terminal amine group, was prepared from **4** by substitution with cadaverine in 89% yield. Derivatives **14a-f** with terminal methyl groups were prepared from **4** by substitution with various alkyl amines in yields ranging from 41% to 66%. Compounds

15a and **15b** with terminal hydroxyl moieties were prepared from **4** by substitution with 5-amino-1-pentanol and 6-amino-1-hexanol in 80% and 52% yield, respectively.

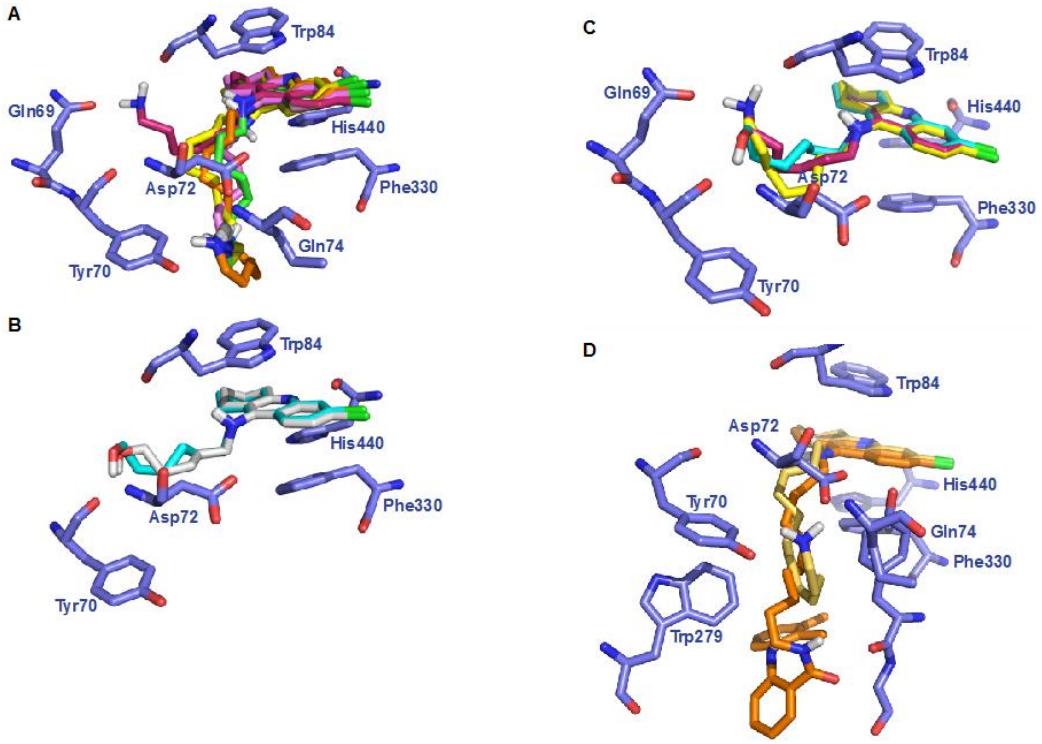

Fig. 3.2. A selection of linker molecules docked in *Tc*AChE showing **A.** the interaction of 6-chlorotacrine amine linkers **6d** (magenta), **6f** (pink), **6g** (green), **6h** (yellow), and **6i** (orange) with residues Trp84, Phe330, and His440 near the CAS and Gln69, Tyr70, Asp72, and Gln74 near the PAS, **B.** the interaction of 6-chlorotacrine hydroxyl linkers **15a** (white) and **15b** (turquoise) with residues Trp84, Phe330, and His440 and Tyr70 and Asp72, **C.** a comparison of the binding of 6-carbon amine linker **6d** (magenta), 6-carbon methyl linker **14c** (yellow), and 6-carbon hydroxyl linker **15b** (turquoise) showing the proximity of the terminal functional group to Gln69, Tyr70, and Asp72, and **D.** a comparison of the binding of 6-chlorotacrine-mefenamic acid hybrid **11f** (orange) and 12-carbon amine linker **6i** (yellow) showing the proximity of the mefenamic acid moiety of **11f** with Tyr70, Trp279, and Tyr334 near the PAS and the terminal amine group of **6i** with Tyr70, Asp72, and Gln74. Oxygen, nitrogen, hydrogen, and chlorine atoms are shown in red, blue, white, and green, respectively.

3.3.2. Biochemical evaluation

3.3.2.1. Molecular modeling

We performed molecular modeling experiments using AutoDock and a tacrine-complexed AChE structure (PDB code: 1ACJ[26]). We constructed models of several 6-chlorotacrine linkers (Fig. 3.2A-D), and, although results remain speculative in the absence of crystallographic data, they can be used in an effort to rationalize the inhibition data described in the remainder of this manuscript. Our goal was to compare the predicted

interactions of 6-chlorotacrine linkers of different lengths with the same terminal functional group, 6-chlorotacrine linkers of the same length with different terminal functional groups, and 6-chlorotacrine linkers with their mefenamic acid counterpart.

All models constructed predict that the 6-chlorotacrine portion of the molecules would be situated in the CAS of AChE with the quinoline ring system stacked between Trp84 and Phe330 (Fig. 3.2A-D). This is consistent with our previous modeling studies of tacrine-mefenamic acid hybrids[18] as well as other docking studies of tacrine-based molecules with *Tc*AChE.[24,27]

Table 3.1. Inhibition of *Ee*AChE activity by 6-chlorotacrine with linkers generated in this study.

Compound[a]	R	n	IC_{50} (nM)	ROS IC_{50} (nM)
1			52.4 ± 7.3[b]	183 ± 21[b]
6b	NH_2	4	38.0 ± 3.7	65.8 ± 8.9
6c	NH_2	5	51.0 ± 9.4	938 ± 96
6d	NH_2	6	11.1 ± 0.7	7.85 ± 2.91
6e	NH_2	7	5.37 ± 0.71	15.1 ± 2.8
6f	NH_2	8	1.14 ± 0.27	293 ± 91
6g	NH_2	9	0.604 ± 0.143	1.22 ± 0.23
6h	NH_2	10	0.932 ± 0.220	2.18 ± 0.27
6i	NH_2	12	0.648 ± 0.060	1.44 ± 0.37
14a	CH_3	4	26.3 ± 9.5	43.2 ± 7.8
14b	CH_3	5	65.3 ± 10.0	26.2 ± 6.0
14c	CH_3	6	16.0 ± 3.0	2.03 ± 0.11
14d	CH_3	7	19.6 ± 2.6	7.95 ± 2.72
14e	CH_3	8	2.27 ± 0.20	16.9 ± 2.2
14f	CH_3	9	5.17 ± 0.32	252 ± 29
15a	OH	5	72.5 ± 18.1	1520 ± 137
15b	OH	6	42.4 ± 10.8	2.47 ± 0.47

[a] See Fig. 3.1 for chemical structures. [b] These values were previously reported and are used here for comparison.[18]

3.3.2.2. AChE inhibition

To evaluate the potential cholinesterase inhibitory activity of our 6-chlorotacrine derivatives **6b-i**, **14a-f**, and **15a**,**b**, their individual IC_{50} and ROS IC_{50} values were determined against AChE from *Electrophorus electricus* (*Ee*AChE) (Fig. 3.3A-D and Table 3.1). IC_{50} and ROS IC_{50} values were also established for 1:1 combinations of **6b-i** with mefenamic acid (**2**) as well as **6b-e** with mefenamic acid derivatives **9b-d** (Table 3.2). Methods reported by Ellman[28] and Muraoka and Miura[19] were used to determine these various inhibitory constants. Our newly tested compounds were compared to a tacrine (**1**) standard, which had an IC_{50} = 52.4 ± 7.3 nM and a ROS IC_{50} = 183 ± 21 nM (Table 3.1). The IC_{50} value for tacrine is in good agreement with literature values for *Ee*AChE, which range from about 40 to 300 nM.[29-31] Our newly tested compounds were also compared to a 1:1 equimolar mixture of tacrine (**1**) and mefenamic acid (**2**) standard, which had an IC_{50} = 68.7 ± 3.8 nM and a ROS IC_{50} = 83.9 ± 0.4 nM (Table 3.2). Finally,

when applicable, our newly tested compounds were compared to similar literature compounds. However, a direct comparison was not possible because, while the Ellman method has been widely employed in the literature to determine AChE IC_{50} values of tacrine and tacrine hybrids, there is considerable variation in enzyme source. Indirect comparison based on inhibitory activity of the compound of interest relative to its tacrine standard was employed for this reason.

*Effect of terminal functional group and linker length on EeAChE inhibitory activity of derivatives **6b-i, 14a-f, and 15a,b***. Without exception, 6-chlorotacrine derivatives **6b-i**, **14a-f**, and **15a**,**b** all showed lower or comparable IC_{50} values when compared to tacrine (Table 3.1). IC_{50} values ranged from 0.604 ± 0.143 nM to 51.0 ± 9.4 nM for derivatives **6b-i** with terminal amine functionalities and 2.27 ± 0.20 nM to 65.3 ± 10.0 for derivatives **14a-f** with terminal methyl groups, while compounds **15a** and **15b** with terminal hydroxyl moieties had IC_{50} values of 72.5 ± 18.1 nM and 42.4 ± 10.8 nM, respectively. Compounds **6b**,**d**,**e**,**g-i** with terminal amines, **14a-e** with terminal methyl groups, and **15b** with a terminal hydroxyl group all gave lower ROS IC_{50} values than tacrine (183 ± 21 nM) (Table 3.1) or a 1:1/tacrine:mefenamic acid mixture (83.9 ± 0.4 nM) (Table 3.2). ROS IC_{50} values ranged from 1.22 ± 0.23 nM to 938 ± 96 nM for **6b-i** and 2.03 ± 0.11 nM to 252 ± 29 nM for **14a-f**, while compounds **15a** and **15b** had ROS IC_{50} values of 1520 ± 137 nM and 2.47 ± 0.47 nM, respectively. Overall, compounds **6g-i** (n = 9, 10, 12) with terminal amines were the most potent of the derivatives tested. With IC_{50} values <1 nM and ROS IC_{50} values <2.5 nM, these compound were over 50-fold more potent than tacrine and 30-fold more potent than the 1:1/ tacrine:mefenamic acid mixture in terms of IC_{50} and ROS IC_{50} values, respectively.

Molecular modeling shows the methylene portion of compounds **6d** and **6f-i** was predicted to extend up the AChE gorge allowing the terminal amine group to interact with residues near the PAS (Fig. 3.2A). The terminal amine of **6f-i** is positioned such that it indicates the formation of hydrogen bonds with Tyr70, Asp72, and Gln74. The flexibility of the linker allows for a large amount of folding and little variation in the position of the terminal amine among these different linker lengths, which may be

responsible for the similar IC_{50} values among these linkers. Interestingly, **6d** shows an alternative positioning in AChE with hydrogen bonds to Gln69 and Trp84. This may be a function of the shorter length of the linker not allowing it to reach the same position as its longer counterparts, and the decreased number of hydrogen bonds may be responsible for the >10-fold increase in IC_{50} value when compared to **6f-i**. The methylene portion of **15a** and **15b** was also predicted to extend up the AChE gorge allowing the terminal hydroxyl group to interact with residues near the PAS (Fig. 3.2B). The terminal hydroxyl group of **15a** and **15b** is positioned such that it hydrogen bonds to Tyr70 and Asp72.

In the literature, there have been structurally similar tacrine with linkers synthesized and tested. Recanatini et al. have previously synthesized and reported an IC_{50} value against human erythrocyte AChE for **14c**.[21] Our IC_{50} value is in good agreement with this previously reported value as in our hands **14c** provided a 3-fold increase in potency over tacrine while the previously reported value represented a 19-fold increase. Other groups have synthesized and reported IC_{50} values against *Ee*AChE for tacrine derivatives with terminal amine functionalities similar to **6b** ($n = 4$),[29,32] **6c** ($n = 5$),[29] **6d** ($n = 6$),[32,33] and **6f** ($n = 8$),[29,32] but lacking the 6-chloro substituent. Overall the IC_{50} values reported were similar to those that we present here, with the exception of **6f** ($n = 8$), which we observed to be 50-fold more potent than tacrine compared to a roughly 13-fold increase for Fang et. al.'s compound[29] relative to tacrine. This result can be attributed to the 6-chloro substituent, which is known to increase inhibitory activity. Similarly, Carlier et al. have synthesized and reported IC_{50} values against rat brain AChE for tacrine derivatives with terminal amine groups similar to **6e-i** ($n = 7$-10, 12) also lacking the 6-chloro substituent.[34] While all of their linkers showed minimal (<2.5-fold) increases in potency compared to tacrine, all of the similar compounds reported herein showed significant increase in potency compared to tacrine with most being over 80-fold more potent. Again, this difference could be attributed to the 6-chloro substituent. Also, Korabecny et al. have synthesized and reported IC_{50} values against human AChE for tacrine compounds with terminal methyl functionalities similar to compounds **14a-f** with a 7-methoxy in place of the 6-chloro substituent.[35] All of their compounds showed minimal (<5-fold) increases in

potency compared to tacrine, and the same was true for most of the comparable compounds reported here with the exception of **14e** and **14f**, which showed 20- and 10-fold increases in potency when compared to tacrine, respectively. Again, these differences can likely be attributed to the 6-chloro substituent present in our molecules.

Among the $n = 5$ linkers, there was no major difference in functional group in terms of IC_{50} values, as there was <2-fold difference between compounds **6c**, **14b**, and **15a**. However, in terms of ROS IC_{50} values, compound **14b** with a terminal methyl was over 30-fold more potent than compound **6c** with a terminal amine, and over 50-fold more potent than derivative **15a** with a terminal hydroxyl. Among the $n = 6$ linkers, **6d** and **14c** had similar potencies in terms of IC_{50} values, both of which were about 4-fold more potent than **15b**. In terms of ROS IC_{50} values, **14c** (CH_3) and **15b** (OH) had similar potencies, both of which were about 4-fold more potent than **6d** (NH_2). Compound **14c** seems to be positioned such that its terminal methyl group is somewhere between the amine functionality of **6d** and hydroxyl group of **15b** (Fig. 3.2C). In comparing these $n = 6$ linkers, all were within 4-fold of each other in terms of IC_{50} and ROS IC_{50}, and their similar docking results would suggest little reason to expect a large difference in potency. Among the $n = 4$, 7, 8, and 9 linkers, there was <4-fold difference between **6b**, **e**, and **f** and **14a**, **d**, and **e** in terms of IC_{50} values. However, **6g** was almost 10-fold more potent than **14f**. In terms of ROS IC_{50}, among the $n = 4$, 7, 8, and 9 linkers, there was <2-fold difference between **6b** and **6e** and **14a** and **14d**. However, **14e** was 17-fold more potent than **6f**, while **6g** was over 200-fold more potent than **14f**. Overall these results show little difference between terminal functional groups of 6-chlorotacrine derivatives in IC_{50} values except for compounds having 9 methylene groups between the 6-chlorotacrine moiety and the terminal functionality. However, there is greater variability between functional groups in ROS IC_{50} values with significant differences in linkers with 5, 8, and 9 methylene groups.

We have previously reported that a linker length of 8-10 atoms between the two parent molecules in tacrine-mefenamic acid hybrids is optimal for AChE inhibition.[18] When comparing the number of atoms between the amine of the 6-chlorotacrine moiety and the

terminal functional group of the linker, our current results are close to or consistent with this finding. Among the linkers with terminal amines, compounds **6g-i** with $n = 9$, 10, and 12 were the most potent in terms of IC_{50} and ROS IC_{50} values. Among the linkers with terminal methyls, compounds **14e** and **14f** with $n = 8$ and 9 were the most potent in terms of IC_{50} values, while compounds **14c** and **14d** with $n = 6$ and 7 were the most potent in terms of ROS IC_{50} values.

To determine the mode of inhibition of our 6-chlorotacrine with linkers, we used a subset of our most potent compounds comprised of **6d**, **6g**, **14c**, and **15b** (Fig. 3.3A-D(inset)). We observed a non-competitive mode of inhibition for these compounds, which is consistent with what was previously observed with tacrine-mefenamic acid hybrids[18] and tacrine-ferulic acid hybrids.[29]

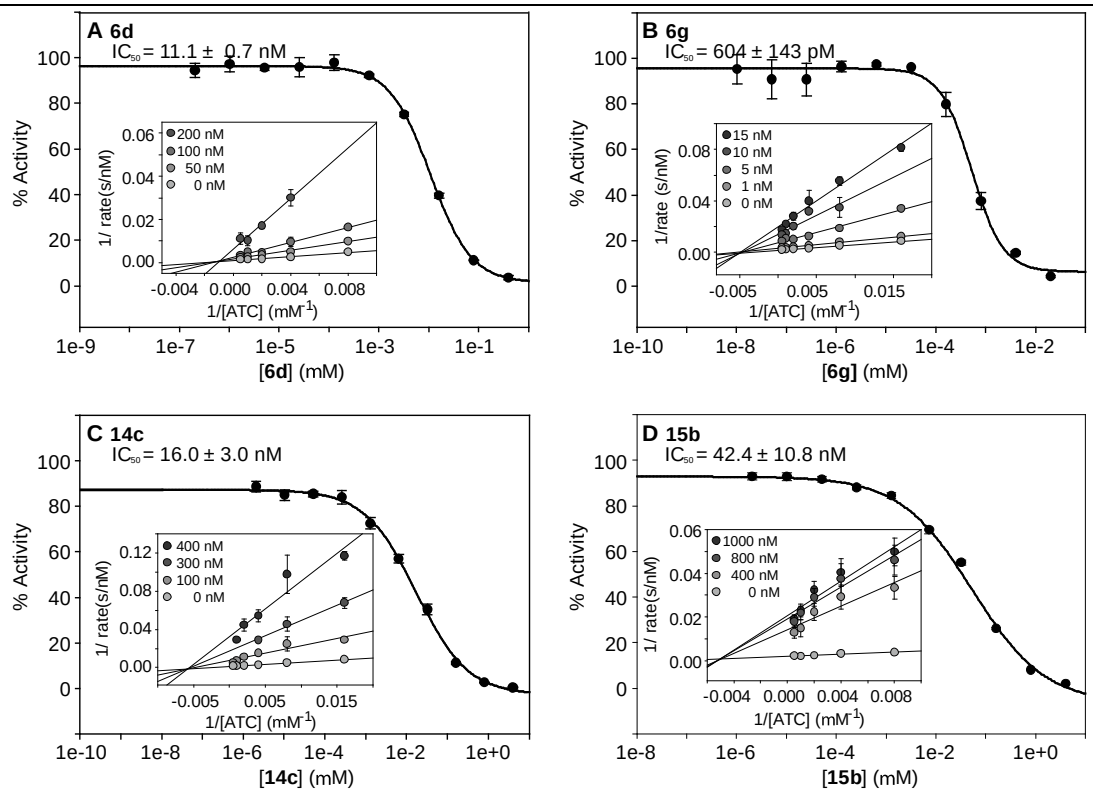

Fig. 3.3. Representative examples of IC_{50} curves (**A**-**D**) for selected 6-chlorotacrine with linkers (compounds **6d**, **6g**, **14c**, and **15b**). Inset in panels **A**-**D** are representative plots showing the non-competitive inhibition with respect to acetylthiocholine (ATC) for compounds **6d**, **6g**, **14c**, and **15b** using various concentrations of inhibitor and ATC.

Table 3.2. Comparison of inhibition of *Ee*AChE activity by combination of 6-chlorotacrine with linkers with mefenamic acid (**2**) or **9b-d** and by covalently linked 6-chlorotacrine-mefenamic acid hybrids.

	1:1 Mixture of 6-chlorotacrine derivative with linkers and mefenamic acid analogs						Covalently linked 6-chlorotacrine-mefenamic acid hybrids[b]			
Cmpds[a]	R	n	n'	IC_{50} (nM)	ROS IC_{50} (nM)	Cmpds[a]	n	n'	IC_{50} (nM)	ROS IC_{50} (nM)
1 + **2**				68.7 ± 3.8[b]	83.9 ± 0.4[b]					
6b + **2**	NH_2	4		59.2 ± 4.7	61.3 ± 11.1					
6b + **9b**	NH_2	4	2	44.1 ± 8.9	6.64 ± 0.86	**13f**	4	2	2470 ± 98	33.0 ± 9.3
6b + **9c**	NH_2	4	3	11.4 ± 3.5	40.9 ± 8.1	**13g**	4	3	13.6 ± 1.8	12.4 ± 1.8
6b + **9d**	NH_2	4	5	51.8 ± 16.7	210 ± 88	**13h**	4	5	37.4 ± 9.4	0.299 ± 0.067
6c + **2**	NH_2	5		51.1 ± 11.5	915 ± 93					
6c + **9b**	NH_2	5	2	103 ± 33	298 ± 33					
6c + **9c**	NH_2	5	3	109 ± 22	328 ± 18					
6c + **9d**	NH_2	5	5	38.1 ± 7.3	596 ± 80					
6d + **2**	NH_2	6		24.7 ± 5.9	70.4 ± 12.3	**11a**	6		7230 ± 187	1.02 ± 0.36
6d + **9b**	NH_2	6	2	5.02 ± 1.56	13.1 ± 2.7	**13j**	6	2	1.14 ± 0.31	2.96 ± 0.41
6d + **9c**	NH_2	6	3	2.99 ± 0.23	10.8 ± 2.2	**13k**	6	3	41.7 ± 11.5	15.6 ± 1.5
6d + **9d**	NH_2	6	5	8.30 ± 1.05	14.1 ± 5.0	**13l**	6	5	2.94 ± 0.45	7.39 ± 1.51
6e + **2**	NH_2	7		2.60 ± 0.71	20.5 ± 3.0	**11b**	7		1380 ± 340	29.8 ± 4.0
6e + **9b**	NH_2	7	2	8.38 ± 1.29	4.20 ± 0.53	**13n**	7	2	6.67 ± 1.82	10.0 ± 1.6
6e + **9c**	NH_2	7	3	7.17 ± 1.42	22.7 ± 3.1	**13o**	7	3	7.91 ± 0.69	6.55 ± 1.66
6e + **9d**	NH_2	7	5	4.55 ± 0.94	7.85 ± 1.83	**13p**	7	5	11.1 ± 1.1	13.4 ± 3.9
6f + **2**	NH_2	8		23.8 ± 8.5	81.8 ± 7.4	**11c**	8		0.495 ± 0.064	1.49 ± 0.30
6g + **2**	NH_2	9		0.544 ± 0.080	2.22 ± 0.45	**11d**	9		6.94 ± 0.66	6.72 ± 0.78
6h + **2**	NH_2	10		1.23 ± 0.20	2.22 ± 0.47	**11e**	10		0.776 ± 0.108	1.85 ± 0.11
6i + **2**	NH_2	12		0.493 ± 0.099	2.74 ± 0.71	**11f**	12		2360 ± 830	16.2 ± 1.8
14a + **2**	CH_3	4		60.9 ± 15.2	68.0 ± 10.9					
14b + **2**	CH_3	5		53.8 ± 11.9	10.9 ± 3.9					
14c + **2**	CH_3	6		36.2 ± 7.4	2.85 ± 0.40					
14d + **2**	CH_3	7		19.3 ± 3.4	3.31 ± 0.48					
14e + **2**	CH_3	8		16.0 ± 4.4	42.6 ± 7.8					
14f + **2**	CH_3	9		4.17 ± 0.33	284 ± 32					
15a + **2**	OH	5		64.3 ± 15.3	513 ± 69					
15b + **2**	OH	6		35.1 ± 7.9	1.96 ± 0.34					

[a] See Fig. 3.1 for chemical structures. [b] These values were previously reported and are used here for comparison.[18]

*Effect of combining 6-chlorotacrine with linkers (series **6**, **14**, **15**) with mefenamic acid (**2**) or mefenamic acid with linkers (series **9**) on EeAChE inhibitory activity*. After examining the effect of linker length and terminal functional group in our 6-chorotacrine derivatives with linkers on their activity, we wanted to determine if combining these compounds with mefenamic acid in a 1:1 equimolar mixture could increases their potency in either of the AChE inhibition assays. We first compared **6b-i** to 1:1 equimolar mixtures of **6b-i** and mefenamic acid (**2**) (**6b-i** + **2**) (Table 3.2). The 1:1 mixtures of compounds displayed IC_{50} values ranging from 0.493 ± 0.099 nM to 59.2 ± 4.7 nM and ROS IC_{50}

values ranging from 2.22 ± 0.45 nM to 915 ± 93 nM. Overall, there was little difference in terms of IC_{50} and ROS IC_{50} values between compounds **6b-i** and **6b-i** + **2**. There was <2.5-fold difference in IC_{50} and ROS IC_{50} values between the corresponding compounds from these two series in most cases with the exceptions being **6d**, which was 9-fold more potent in ROS IC_{50} than **6d** + **2**, and **6f**, which was 21-fold more potent in IC_{50} but 3.5-fold less potent in ROS IC_{50} than **6f** + **2**.

We next explored the effect of adding an equimolar equivalent of **2** to derivatives **14a-f** and **15a**,**b**. Mixtures of **14a-f** + **2** displayed IC_{50} values ranging from 4.17 ± 0.33 nM to 60.9 ± 15.2 nM and ROS IC_{50} values ranging from 2.85 ± 0.40 nM to 284 ± 32 nM. Overall, there was little difference in terms of IC_{50} and ROS IC_{50} values between derivatives **14a-f** and **14a-f** + **2**. There was <2.5-fold difference in IC_{50} and ROS IC_{50} values between the corresponding compounds from these two series in most cases with the exception of **14e**, which was 7-fold more potent in IC_{50} than **14e** + **2**. Similarly, equimolar mixtures of **15a** + **2** and **15b** + **2** displayed IC_{50} values of 64.3 ± 15.3 nM and 35.1 ± 7.9 nM, respectively, and ROS IC_{50} values of 513 ± 69 nM and 1.96 ± 0.34 nM. Overall, there was little difference in terms of IC_{50} and ROS IC_{50} values between **15a** or **15b** and **15a** + **2** or **15b** + **2**. There was <3-fold difference in IC_{50} and ROS IC_{50} values between the corresponding compounds from these two series in all cases.

We also investigated 1:1 equimolar mixtures of compounds **6b-e** and **9b-d** in combinations that provided total linker length in the ideal range identified. These 1:1 mixtures displayed IC_{50} values ranging from 2.99 ± 0.23 nM to 109 ± 22 nM and ROS IC_{50} values ranging from 4.20 ± 0.53 nM to 596 ± 80 nM. Here again, there was overall little difference in terms of IC_{50} and ROS IC_{50} values between compounds **6b-e** and **6b-e** + **9b-d**. There was <3-fold difference in IC_{50} and ROS IC_{50} values between the corresponding compounds from these two series in most cases with the exceptions of **6b**, which was 10-fold less potent in ROS IC_{50} than **6b** + **9b**, **6d**, which was 4-fold less potent in IC_{50} than **6d** + **9c**, and **6e**, which was 3.6-fold less potent in ROS IC_{50} than **6e** + **9b**. Together, these results indicate that adding mefenamic acid or its analogs to 6-chlorotacrine with

linkers (series **6**, **14**, **15**) *in trans* has little to no effect on the activity of the latter compounds.

Is a covalent linkage between tacrine and mefenamic acid required for optimal EeAChE inhibition? As mentioned previously, we have recently synthesized and tested *in vitro* two series of 6-chlorotacrine-mefenamic acid hybrids **11a-f** and **13f-h**, **13j-l**, **13n-p** (Fig. 3.1).[18] In order to elucidate the benefit, if any, of covalently linking 6-chlorotacrine and mefenamic acid, we decided to compare our previously published IC_{50} and ROS IC_{50} values for **11a-f** and **13f-h**, **13j-l**, **13n-p** with the values obtained in the current study for **6d-i** (Table 3.1) and the corresponding combination **6d-i** + **2** and **6b**,**d**,**e** + **9b-d** (Table 3.2).

We first compared **6d-i** to **11a-f**, and observed that in all cases compounds **6d-i** displayed more potent or comparable IC_{50} values than that for the linked counterparts **11a-f**. For example, **6i** was over 3600-fold more potent than **11f**, while **6h** and **11e** were nearly identical in potency. However, the difference in ROS IC_{50} values between compounds **6d-i** and **11a-f** is not as well defined. In two out of the six combinations tested, the 6-chlorotacrine covalently linked to mefenamic acid (series **11**) displayed more potent ROS IC_{50} values than the 6-chlorotacrine derivatives with a terminal amine linker. For example, **11c** was almost 200-fold more potent than **6f**. Of the remaining four combinations tested, 6-chlorotacrine derivatives with terminal amines displayed more potent ROS IC_{50} values in three instances. This is evidenced by **6i**, which was 11-fold more potent than **11f**. The remaining combination **6h** and **11e** displayed nearly equal potencies. 6-Chlorotacrine-mefenamic acid hybrid **11f** was predicted to bind with the methylene linker extending up the AChE gorge and the mefenamic acid moiety in close proximity to Tyr70, Trp279, and Tyr334 (Fig. 3.2D). The methylene linker portion of **11f** was predicted to be much more linear than the linker portion of **6i**, which folds back on itself allowing the terminal amine to form potential hydrogen bonds with Tyr70, Asp72, and Gln74. This ability to fold may be a result of the decreased steric bulk at the linker terminus (amine vs mefenamic acid). The potential hydrogen bonds of **6i** may be responsible for the over 3600-fold increase in potency in terms of IC_{50} when compared to hybrid **11f**. However, the difference between **6i** and **11f** is much less dramatic in terms of

ROS IC_{50}. This is likely because of the suspected ability of mefenamic acid to deactivate AChE through a free-radical mechanism, which we have discussed previously.[18]

Overall, these results indicate that derivatives **6d-i** are equal to or more potent than the covalently linked counterparts **11a-f** in terms of IC_{50}, which is consistent with the results observed for tacrine-ferulic acid hybrids where the linkers with terminal amines used and the linked hybrids were equally more potent than tacrine in terms of *Ee*AChE IC_{50}.[29] Altogether, this may indicate that the additional moiety in an amine-linked tacrine hybrid may not obviously affect the extent of AChE activity, and the linker alone may be responsible for the increase in inhibitory potency. However, there does not seem to be a clear trend between the linkers alone and the linked counterparts in terms of ROS IC_{50}, which potentially indicates the importance of the covalent linkage for additional different activity of hybrid molecules.

We next compared **6d-i** + **2** to **11a-f**. Again, in most cases, **6d-i** + **2** displayed more potent IC_{50} values than the linked counterparts **11a-f**. For example, **6i** + **2** was over 4700-fold more potent than the linked counterpart **11f**. The lone exceptions were **11c** and **11e**, which were more potent or comparable to the combination of **6f** + **2** and **6h** + **2**, respectively. As observed above for **6d-i**, the difference in ROS IC_{50} values between **6d-i** + **2** and **11a-f** was not as well defined. Out of the six combinations tested, the 6-chlorotacrine derivatives with a terminal amine linker plus mefenamic acid was more potent in two cases, the linked counterpart was more potent in two cases, and there was nearly equal potency in two cases. For example, **11c** was 55-fold more potent than **6f** + **2**. However, **6i** + **2** was 6-fold more potent than **11f**. Also, **6h** + **2** and **11e** displayed nearly equal inhibitory activity. Overall, these results indicate that combinations of 6-chlorotacrine with linkers with terminal amines and mefenamic acid are usually more potent than the linked counterparts in terms of IC_{50}, but there does not seem to be a clear trend between the linkers plus mefenamic acid and the linked counterparts in terms of ROS IC_{50}.

Finally, we compared **6b**,**d**,**e** + **9b-d** to **13f-h**, **13j-l**, **13n-p**. In most cases, **6b**,**d**,**e** + **9b-d**

displayed equal or more potent IC_{50} values than **13f-h**, **13j-l**, **13n-p**. For example, **6b** + **9b** was 56-fold more potent than **13f**, while **6e** + **9c** and **13o** were equally potent. However, the difference in ROS IC_{50} values between 6-chlorotacrine derivatives with terminal amine linkers plus mefenamic acid with linkers **6b**,**d**,**e** + **9b-d** and the linked counterparts **13f-h**, **13j-l**, **13n-p** showed the opposite trend. In most cases, compounds **13f-h**, **13j-l**, **13n-p** displayed equal or more potent ROS IC_{50} values than mixtures of **6b**,**d**,**e** + **9b-d**. For example, **13h** and **13o** were 6-fold and 3.5-fold more potent than **6b** + **9d** and **6e** + **9c**, respectively. Overall, these results indicate that 6-chlorotacrine amine with linkers plus mefenamic acid with linkers **6b**,**d**,**e** + **9b-d** are generally more potent than the linked counterparts **13f-h**, **13j-l**, **13n-p** in terms of IC_{50}, but the linked counterparts **13f-h**, **13j-l**, **13n-p** are generally more potent in terms of ROS IC_{50}.

3.4. Conclusion

Three series of 6-chlorotacrine derivatives were synthesized and evaluated in AChE inhibition assays. These compounds, which differed in terminal functional groups (-NH_2, -CH_3, -OH) and length (n = 4-12), appeared to be acting as non-competitive *Ee*AChE inhibitors in biochemical assays, creating some discrepancy with modeling studies. The amine group was determined to be the best terminal functional group in terms of IC_{50} and ROS IC_{50}. Compounds **6g-i** (n = 9, 10, 12) were the most potent compounds tested as they had IC_{50} values <1 nM and ROS IC_{50} values <2.5 nM and were over 50-fold more potent than tacrine and 30-fold more potent than the 1:1/tacrine:mefenamic acid mixture in terms of IC_{50} and ROS IC_{50} values, respectively. The linker length of the most potent compounds in the amine and methyl series was determined to be around 8-12 atoms, which is consistent with our previous studies of tacrine-mefenamic acid hybrids.

The 6-chlorotacrine with linkers were also evaluated in a 1:1 equimolar mixture with mefenamic acid or mefenamic acid linkers, and results indicated little difference in terms of IC_{50} and ROS IC_{50} when compared to the 6-chlorotacrine with linkers themselves. 6-Chlorotacrine derivatives with terminal amines alone and in a 1:1 mixture with mefenamic acid or mefenamic acid linkers were found, in general, to be equally potent or, in many cases, more potent than the linked counterpart tacrine–mefenamic acid hybrid in terms of

IC_{50}. In terms of ROS IC_{50}, linked compounds **13f-h**, **13j-l**, **13n-p** outperformed their unlinked counterparts. However, in general the ROS IC_{50} trend was less well defined, and no generalization could be made. These results indicate that the mefenamic acid moiety in an amine-linked tacrine-mefenamic acid hybrid may not contribute to AChE inhibition in the absence of ROS, and the linker alone may be responsible for the increase in potency relative to tacrine. However, in the presence of ROS, there may be some advantage to amine-linked tacrine-mefenamic acid hybrids. While these results do not present an overwhelming advantage to the linked compounds, they do not discount the benefit of linking tacrine with an additional moiety to create tacrine hybrids, a strategy that has been widely used in the literature.

An essential characteristic of any AD drug is the ability to cross the blood-brain barrier (BBB). The parallel artificial membrane permeation assay (PAMPA-BBB) described by Di et al.[36] provides a high-throughput, high success means of predicting passive BBB permeation. Using this assay, tacrine-melatonin, tacrine-8-hydroxyquinoline, and pyrano[3,2-*c*]quinoline-6-chlorotacrine hybrids have all been predicted to cross the BBB.[17,23,37] Based on these results, we predict that our structurally similar tacrine-mefenamic acid hybrids and tacrine linkers will show comparable PAMPA-BBB results, and experiments to verify this will be performed in the near future. We also envision future mutational and structural studies aimed to confirm the interactions of our inhibitors with AChE predicted by our molecular modeling. There is literature precedent for purification and crystallization of *Tc*AChE in complex with tacrine and other compounds.[26,38-44] We therefore expect to use molecular replacement for our future structural work. In addition, studies aimed at synthesizing and further exploring the importance of covalent linkage in multifunctional compounds with AChE inhibition, ROS scavenging, metal chelation, and prevention of Aβ aggregation properties are currently underway in our laboratory.

3.5. Materials and instrumentation

All reagents were purchased from Sigma-Aldrich (St. Louis, MO, USA) and used without further purification. Compounds **9b-d**, **11a-f**, **13f-h**, **13j-l**, **13n-p**, **4**, **6b**, and **6d-i** were

prepared as previously described.[18] Reactions were monitored by TLC (Merck, Silica gel 60 F_{254}). Visualization was achieved using one or more of the following methods: UV absorption by fluorescence quenching, a cerium-molybdate stain ($(NH_4)_2Ce(NO_3)_6$ (5 g), $(NH_4)_6Mo_7O_{24}•4H_2O$ (120 g), H_2SO_4 (80 mL), H_2O (720 mL)), a ninhydrin stain (ninhydrin (1.5 g), *n*-butanol (100 mL), AcOH (3 mL)), a $KMnO_4$ stain ($KMnO_4$ (1.5 g), K_2CO_3 (10 g), NaOH (1.25 mL 10%), H_2O (200 mL)), a bromocresol green stain (bromocresol green (0.04 g), EtOH (100 mL, absolute), slowly drip NaOH (0.1 M) until the solution just turns pale blue), or Dragendorff's reagent (solution A: $BiNO_3$ (0.17 g) in AcOH (2 mL), H_2O (8 mL); solution B: KI (4 g) in AcOH (10 mL) and H_2O (20 mL). Solutions A and B were mixed and diluted to 100 mL with H_2O). Compounds were purified by SiO_2 flash chromatography (Dynamic Adsorbents Inc., Flash Silica Gel 32-63u). ^1H NMR and ^{13}C NMR spectra were recorded on a Varian 400 or 500 MHz spectrometer. Liquid chromatography mass spectrometry (LCMS) was performed on a Shimadzu LCMS-2019EV equipped with a SPD-20AV UV-Vis detector and a LC-20AD liquid chromatograph. Analyses by UV-Vis assays were done on a multimode SpectraMax M5 plate reader using 96-well plates (Fisher Scientific). Molecular modeling was performed using AutoDock 4.2 and Cygwin 1.7.

3.6. Methods

3.6.1. Chemical methods

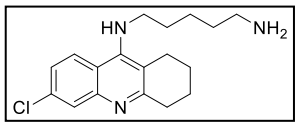

3.6.1.1. Preparation of *N*[1]-(6-chloro-1,2,3,4-tetrahydroacridin-9-yl)pentane-1,5-diamine (6c). 6,9-Dichloro-1,2,3,4-tetrahydroacridine (**4**) (300 mg, 1.19 mmol, 1 eq), cadaverine (0.56 mL, 4.76 mmol, 4 eq), and 1-pentanol (2.5 mL) were combined and heated to reflux for 48 h. The reaction was cooled to rt, diluted with CH_2Cl_2 (50 mL), and washed with 10% aq. KOH (2x50 mL), H_2O (2x50 mL), and brine (50 mL). The organic layer was dried ($MgSO_4$), filtered, and concentrated under reduced pressure to afford the crude product, which was purified by flash column chromatography (SiO_2; 7:3/CH_2Cl_2:MeOH with NH_4OH (7 mL/L of solvent), R_f 0.12) to afford **6c** (338 mg, 89%) as a yellow oil: ^1H NMR ($CDCl_3$, 400 MHz) δ 7.77 (d, 1H, J = 2.2 Hz), 7.76 (d, 1H, J = 9.0 Hz), 7.13 (dd, 1H, J_1 = 9.0 Hz, J_2 = 2.2 Hz), 3.87 (br s, 1H), 3.24 (t, 2H, J = 7.2 Hz),

2.91 (br t, 2H), 2.61 (br s, 2H), 2.53 (br t, 2H), 2.24 (br s, 2H), 1.79 (p, 4H, J = 3.3 Hz), 1.54 (p, 2H, J = 7.3 Hz), 1.35-1.42 (m, 2H), 1.26-1.33 (m, 2H) (Fig. 3.4); ^{13}C NMR ($CDCl_3$, 100 MHz) δ 159.5, 150.5, 148.1, 133.7, 127.5, 124.5, 124.0, 118.3, 115.7, 49.3, 41.6, 34.0, 32.7, 31.5, 24.5, 24.1, 22.8, 22.6 (Fig. 3.5); *m/z* calcd for $C_{18}H_{24}ClN_3$: 317.17; found 318.05 $[M+H]^+$.

3.6.1.2. General procedure for attachment of alkyl amine linkers to 6-chlorotacrine

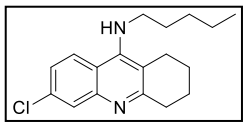

6-Chloro-*N*-pentyl-1,2,3,4-tetrahydroacridin-9-amine (14a). 6,9-Dichloro-1,2,3,4-tetrahydroacridine (**4**) (410 mg, 1.625 mmol, 1 eq), pentylamine (750 μL, 6.5 mmol, 4 eq), and 1-pentanol (1 mL) were combined and heated to reflux for 24 h. The reaction was cooled to rt, diluted with CH_2Cl_2 (50 mL), and washed with 10% aq. KOH (2x50 mL), H_2O (2x50 mL), and brine (50 mL). The organic layer was dried ($MgSO_4$), filtered, and concentrated under reduced pressure to afford the crude product, which was purified by flash column chromatography (SiO_2; 9.9:0.1/EtOAc:MeOH with NH_4OH (7 mL/L of solvent), R_f 0.33 (EtOAc)). Further purification by flash column chromatography (SiO_2; 19:1/CH_2Cl_2:MeOH with NH_4OH (7 mL/L of solvent)) removed remaining impurities and gave **14a** (250 mg, 51%) as a brown oil: ^{1}H NMR ($CDCl_3$, 400 MHz) δ 7.86 (d, 1H, J = 9.0 Hz), 7.85 (d, 1H, J = 2.2 Hz), 7.23 (dd, 1H, J_1 = 9.0 Hz, J_2 = 2.2 Hz), 3.91 (br s, 1H), 3.44 (td, 2H, J_1 = 7.0 Hz, J_2 = 3.2 Hz), 3.00 (br t, 2H), 2.63 (br t, 2H), 1.89 (p, 4H, J = 3.5 Hz), 1.63 (p, 2H, J = 7.2 Hz), 1.39-1.28 (m, 4H), 0.88 (t, 3H, J = 7.2 Hz) (Fig. 3.6); ^{13}C NMR ($CDCl_3$, 100 MHz) δ 159.6, 150.9, 148.4, 133.9, 127.7, 124.7, 124.2, 118.5, 115.8, 49.7, 34.2, 31.6, 29.2, 24.6, 23.0, 22.8, 22.5, 14.1 (Fig. 3.7); *m/z* calcd for $C_{18}H_{23}ClN_2$: 302.12; found 302.15 $[M+H]^+$.

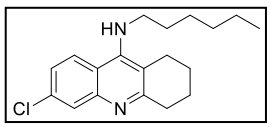

6-Chloro-*N*-hexyl-1,2,3,4-tetrahydroacridin-9-amine (14b). Compound **14b** was prepared as described for the synthesis of **14a**. The reaction of 6,9-dichloro-1,2,3,4-tetrahydroacridine (**4**) (361 mg, 1.4 mmol, 1 eq), hexylamine (750 μL, 5.7 mmol, 4 eq), and 1-pentanol (1 mL) yielded, after purification by flash column chromatography (SiO_2; 9.9:0.1/EtOAc:MeOH with NH_4OH (7 mL/L of solvent), R_f 0.32 (EtOAc)) and further purification by flash column chromatography (SiO_2; 19:1/CH_2Cl_2:MeOH with NH_4OH (7 mL/L of solvent)), **14b** (190

mg, 42%) as a light brown solid: ^{1}H NMR ($CDCl_3$, 400 MHz) δ 7.86 (d, 1H, J = 8.5 Hz), 7.85 (d, 1H, J = 2.5 Hz), 7.22 (dd, 1H, J_1 = 9.0 Hz, J_2 = 2.2 Hz), 3.92 (br s, 1H), 3.44 (t, 2H, J = 7.2 Hz), 3.00 (br t, 2H), 2.63 (br t, 2H), 1.88 (p, 4H, J = 3.2 Hz), 1.62 (p, 2H, J = 7.6 Hz), 1.40-1.21 (m, 6H), 0.86 (t, 3H, J = 6.8 Hz) (Fig. 3.8); ^{13}C NMR ($CDCl_3$, 100 MHz) δ 159.5, 150.8, 148.2, 133.8, 127.5, 124.6, 124.0, 118.4, 115.6, 49.6, 34.0, 31.7, 31.5, 26.5, 24.5, 22.9, 22.6, 22.5, 13.9 (Fig. 3.9); *m/z* calcd for $C_{19}H_{25}ClN_2$: 316.17; found 317.15 $[M+H]^+$.

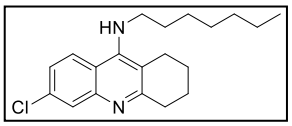

6-Chloro-*N*-heptyl-1,2,3,4-tetrahydroacridin-9-amine (14c). Compound **14c** was prepared as described for the synthesis of **14a**. The reaction of 6,9-dichloro-1,2,3,4-tetrahydroacridine (**4**) (95 mg, 0.375 mmol, 1 eq), heptylamine (178 μL, 1.3 mmol, 3.5 eq), and 1-pentanol (1 mL) yielded, after purification by flash column chromatography (SiO_2; 9.9:0.1/EtOAc:MeOH with NH_4OH (7 mL/L of solvent), R_f 0.29 (EtOAc)) and further purification by flash column chromatography (SiO_2; 19:1/CH_2Cl_2:MeOH with NH_4OH (7 mL/L of solvent)), **14c** (50 mg, 41%) as a light brown solid: ^{1}H NMR ($CDCl_3$, 400 MHz) δ 7.89 (d, 1H, J = 9.0 Hz), 7.88 (d, 1H, J = 1.8 Hz), 7.26 (dd, 1H, J_1 = 9.0 Hz, J_2 = 2.2 Hz), 3.48 (t, 2H, J = 7.2 Hz), 3.02 (br t, 2H), 2.66 (br t, 2H), 1.91 (p, 4H, J = 3.3 Hz), 1.65 (p, 2H, J = 7.2 Hz), 1.44-1.23 (m, 8H), 0.88 (t, 3H, J = 6.8 Hz) (Fig. 3.10); ^{13}C NMR ($CDCl_3$, 100 MHz) δ 159.4, 150.8, 148.1, 133.9, 127.5, 124.6, 124.1, 118.4, 115.6, 49.6, 34.0, 31.8, 31.7, 29.0, 26.8, 24.5, 22.9, 22.6, 22.5, 14.0 (Fig. 3.11); *m/z* calcd for $C_{20}H_{27}ClN_2$: 330.19; found 331.20 $[M+H]^+$.

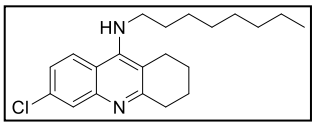

6-Chloro-*N*-octyl-1,2,3,4-tetrahydroacridin-9-amine (14d). Compound **14d** was prepared as described for the synthesis of **14a**. The reaction of 6,9-dichloro-1,2,3,4-tetrahydroacridine (**4**) (384 mg, 1.51 mmol, 1 eq), octylamine (1 mL, 6.1 mmol, 4 eq), and 1-pentanol (1 mL) yielded, after purification by flash column chromatography (SiO_2; 9.9:0.1/EtOAc:MeOH with NH_4OH (7 mL/L of solvent), R_f 0.36 (EtOAc)) and further purification by flash column chromatography (SiO_2; 19:1/CH_2Cl_2:MeOH with NH_4OH (7 mL/L of solvent)), **14d** (342 mg, 66%) as a light brown solid: ^{1}H NMR ($CDCl_3$, 400 MHz) δ 7.80 (d, 1H, J =

2.2 Hz), 7.79 (d, 1H, J = 9.3 Hz), 7.15 (dd, 1H, J_1 = 9.0 Hz, J_2 = 2.2 Hz), 3.88 (br s, 1H), 3.37 (t, 2H, J = 7.2 Hz), 2.93 (br t, 2H), 2.56 (br t, 2H), 1.82 (p, 4H, J = 3.1 Hz), 1.55 (p, 2H, J = 7.2 Hz), 1.34-1.15 (m, 10H), 0.84 (t, 3H, J = 6.7 Hz) (Fig. 3.12); ^{13}C NMR ($CDCl_3$, 100 MHz) δ 159.4, 150.7, 148.1, 133.7, 127.5, 124.6, 123.8, 118.3, 115.5, 49.5, 34.0, 31.69, 31.66, 29.2, 29.1, 26.8, 24.5, 22.9, 22.54, 22.48, 14.0 (Fig. 3.13); *m/z* calcd for $C_{21}H_{29}ClN_2$: 344.20; found 345.10 $[M+H]^+$.

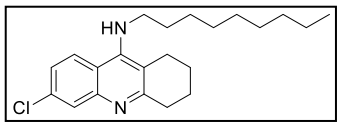

6-Chloro-*N*-nonyl-1,2,3,4-tetrahydroacridin-9-amine (14e). Compound **14e** was prepared as described for the synthesis of **14a**. The reaction of 6,9-dichloro-1,2,3,4-tetrahydroacridine (**4**) (55 mg, 0.22 mmol, 1 eq), nonylamine (160 μL, 0.88 mmol, 4 eq), and 1-pentanol (1 mL) yielded, after purification by flash column chromatography (SiO_2; 9.9:0.1/EtOAc:MeOH with NH_4OH (7 mL/L of solvent), R_f 0.38 (EtOAc)) and further purification by flash column chromatography (SiO_2; 19:1/CH_2Cl_2:MeOH with NH_4OH (7 mL/L of solvent)), **14e** (37 mg, 46%) as a light brown solid: ^{1}H NMR ($CDCl_3$, 500 MHz) δ 7.90 (d, 1H, J = 9.1 Hz), 7.88 (d, 1H, J = 2.0 Hz), 7.27 (dd, 1H, J_1 = 9.1 Hz, J_2 = 2.0 Hz), 3.95 (br s, 1H), 3.48 (t, 2H, J = 7.2 Hz), 3.03 (br t, 2H), 2.67 (br t, 2H), 1.92 (br p, 4H, J = 3.1 Hz), 1.65 (p, 2H, J = 7.4 Hz), 1.38 (p, 2H, J = 7.3 Hz), 1.32-1.26 (m, 10H), 0.88 (t, 3H, J = 6.8 Hz) (Fig. 3.14); ^{13}C NMR ($CDCl_3$, 100 MHz) δ 158.5, 151.3, 134.5, 126.3, 124.7, 124.3, 118.3, 117.7, 114.8, 49.4, 33.1, 31.8, 31.7, 29.4, 29.3, 29.2, 26.8, 24.4, 22.8, 22.6, 22.3, 14.1 (Fig. 3.15); *m/z* calcd for $C_{22}H_{31}ClN_2$: 358.22; found 360.95 $[M+H]^+$.

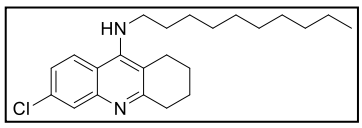

6-Chloro-*N*-decyl-1,2,3,4-tetrahydroacridin-9-amine (14f). Compound **14f** was prepared as described for the synthesis of **14a**. The reaction of 6,9-dichloro-1,2,3,4-tetrahydroacridine (**4**) (400 mg, 1.59 mmol, 1 eq), decylamine (1.3 mL, 6.4 mmol, 4 eq), and 1-pentanol (1 mL) yielded, after purification by flash column chromatography (SiO_2; 9.9:0.1/EtOAc:MeOH with NH_4OH (7 mL/L of solvent), R_f 0.45 (EtOAc)) and further purification by flash column chromatography (SiO_2; 19:1/CH_2Cl_2:MeOH with NH_4OH (7 mL/L of solvent)), **14f** (328 mg, 55%) as a light brown solid: ^{1}H NMR ($CDCl_3$, 400 MHz) δ 7.75 (d, 1H, J = 2.2 Hz), 7.71 (d, 1H, J = 9.1 Hz), 7.06 (dd, 1H, J_1 = 9.1 Hz, J_2 = 2.2 Hz),

3.84 (br s, 1H), 3.29 (t, 2H, J = 7.4 Hz), 2.87 (br t, 2H), 2.47 (br t, 2H), 1.74 (br p, 4H), 1.48 (p, 2H, J = 7.4 Hz), 1.24-1.12 (m, 14H), 0.76 (t, 3H, J = 6.4 Hz) (Fig. 3.16); ^{13}C NMR ($CDCl_3$, 100 MHz) δ 159.2, 150.6, 148.0, 133.6, 127.3, 124.5, 123.7, 118.2, 115.3, 49.4, 33.9, 31.8, 31.6, 29.41, 29.39, 29.23, 29.18, 26.8, 24.4, 22.8, 22.6, 22.5, 14.0 (Fig. 3.17); *m/z* calcd for $C_{23}H_{33}ClN_2$: 372.23; found 375.15 $[M+H]^+$.

3.6.1.3. General procedure for attachment of amino alcohol linkers to 6-chlorotacrine

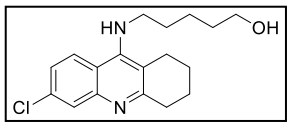

5-((6-Chloro-1,2,3,4-tetrahydroacridin-9-yl)amino)pentan-1-ol (15a). 6,9-Dichloro-1,2,3,4-tetrahydroacridine (**5**) (252 mg, 1 mmol, 1 eq), 5-amino-1-pentanol (310 mg, 3 mmol, 3 eq), and 1-pentanol (1 mL) were combined and heated to reflux for 24 h. The reaction was cooled to rt, diluted with CH_2Cl_2 (50 mL), and washed with 10% aq. KOH (2x50 mL), H_2O (2x50 mL), and brine (50 mL). The organic layer was dried ($MgSO_4$), filtered, and concentrated under reduced pressure to afford the crude product, which was purified by flash column chromatography (SiO_2; 9:1/CH_2Cl_2:MeOH with NH_4OH (7 mL/L of solvent), R_f 0.34) to give **15a** (261 mg, 80%) as a brown solid: ^{1}H NMR ($CDCl_3$, 400 MHz) δ 7.859 (d, 1H, J = 9.0 Hz), 7.856 (d, 1H, J = 2.2 Hz), 7.21 (dd, 1H, J_1 = 9.0 Hz, J_2 = 2.2 Hz), 4.15 (very br s, 1H), 3.65 (t, 2H, J = 6.3 Hz), 3.48 (t, 2H, J = 7.2 Hz), 3.05 (very br s, 1H), 2.99 (br t, 2H), 2.62 (br t, 2H), 1.87 (p, 4H, J = 3.4 Hz), 1.68 (p, 2H, J = 7.4 Hz), 1.59 (p, 2H, J = 7.1 Hz), 1.47 (p, 2H, J = 6.8 Hz) (Fig. 3.18); ^{13}C NMR ($CDCl_3$, 100 MHz) δ 159.0, 151.3, 147.4, 134.4, 126.8, 124.8, 124.4, 118.1, 115.5, 62.3, 49.5, 33.6, 32.4, 31.5, 24.6, 23.3, 22.9, 22.5 (Fig. 3.19); *m/z* calcd for $C_{18}H_{23}ClN_2O$: 318.15; found 319.00 $[M+H]^+$.

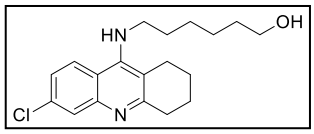

6-((6-Chloro-1,2,3,4-tetrahydroacridin-9-yl)amino)hexan-1-ol (15b). Compound **15b** was prepared as described for the synthesis of **15a**. The reaction of 6,9-dichloro-1,2,3,4-tetrahydroacridine (**4**) (252 mg, 1 mmol, 1 eq), 6-amino-1-hexanol (352 mg, 3 mmol, 3 eq), and 1-pentanol (1 ml) yielded, after purification by flash column chromatography (SiO_2; 9:1 CH_2Cl_2:MeOH with NH_4OH (7 mL/L of solvent), R_f 0.40), **15b** (172 mg, 52%) as a brown solid: ^{1}H NMR ($CDCl_3$, 400 MHz) δ 7.870 (d, 1H, J = 2.2 Hz), 7.867 (d, 1H, J = 9.0 Hz), 7.24 (dd, 1H, J_1 = 9.0 Hz, J_2 = 2.2 Hz), 3.99 (very br s, 1H), 3.63 (t, 2H, J = 6.5

Hz), 3.47 (t, 2H, *J* = 7.4 Hz), 3.01 (br t, 2H), 2.64 (br t, 2H), 2.48 (very br s, 1H), 1.89 (p, 4H, *J* = 3.2 Hz), 1.66 (p, 2H, *J* = 7.1 Hz), 1.56 (p, 2H, *J* = 6.7 Hz), 1.40 (p, 4H, *J* = 3.9 Hz) (Fig. 3.20); ^{13}C NMR ($CDCl_3$, 100 MHz) δ 158.7, 151.3, 147.1, 134.4, 126.4, 124.7, 124.3, 117.9, 115.2, 62.4, 49.3, 33.3, 32.5, 31.6, 26.6, 25.5, 24.4, 22.8, 22.4 (Fig. 3.21); *m/z* calcd for $C_{19}H_{25}ClN_2O$: 332.17; found 333.10 $[M+H]^+$.

3.6.2. Biochemical and computational methods

3.6.2.1. *In vitro* AChE assay

Compounds were dissolved in sodium phosphate (dibasic) buffer ((125 μL), 0.1 M, pH 8.0 (adjusted at rt)), and a five-fold dilution was performed. To the solution of inhibitors was added AChE cocktail (50 μL, containing 0.08 U/mL (~0.29 nM) AChE (final concentration) (Sigma-Aldrich cat #C2888 from eel) in sodium phosphate (dibasic) buffer (0.1 M, pH 8.0 (adjusted at rt)). The mixture of inhibitor and enzyme was incubated for 10 min before initiation with 5,5'-dithiobis(2-nitrobenzoic acid) (DTNB) (50 μL, 0.25 mM final concentration) and acetylthiocholine (ATC) (0.5 mM final concentration) in phosphate buffer. The reaction was monitored at 412 nm taking measurements every 30 s for 30 min. Data was corrected with the negative control (no ATC) and normalized to the positive control (no inhibitor) using the initial rates (first 2-5 min). All assays were performed at least in triplicate. The resulting curve rate versus concentration of inhibitor was fitted to a sigmoidal curve, and IC_{50} values were calculated using KaleidaGraph 4.1.1. Four representative examples of IC_{50} curves are provided in Fig. 3.3A-D. All IC_{50} values are provided in Tables 3.1 and 3.2.

3.6.2.2. Studies of the mode of inhibition

Non-competitive inhibition was determined by incubating four concentrations of inhibitor (0, 0.2, 1, and 5 μM) with AChE (as described above). The enzymatic reaction was then initiated by the addition of various concentrations of ATC (62.5, 250, 500, and 1000 μM). The rates of the reactions were calculated using the first 2 min of the reaction and plotted on a Lineweaver-Burk plot. Separate lines were drawn for each concentration of inhibitor, and observation of intersection on the negative side of the *x* axis indicated non-competitive inhibition. Representative plots are provided in Fig. 3.3A-D(inset).

3.6.2.3. *In vitro* AChE ROS inactivation assay

In the wells of a 96-well plate, horseradish peroxidase (0.25 μM), H_2O_2 (100 μM), AChE (0.08 U/mL, ~0.29 nM), compound (25 μM – 13 pM), and diethylenetriaminepentaacetic acid (DETAPAC) (100 μM) were dissolved in acetate buffer (pH 6.0) (50 mM) and incubated at 37 °C for 30 min. *Note*: all concentrations are reported as final concentrations. To the above solution, a mixture of ATC (0.5 mM) and DTNB (0.25 mM) in sodium phosphate (dibasic) buffer (50 mM, pH 7.4 (adjusted at rt)) was added. Reaction rates were monitored at 25 °C for 20 min taking measurements every 30 s, and rates were calculated using the initial rate (first 2-5 min). Total reaction volume was 200 μL. Rates were normalized to the reaction without compounds and plotted in KaleidaGraph 4.1.1 to calculate the IC_{50}. Four representative examples of IC_{50} curves are provided in Fig. 3.3A-D. All IC_{50} values are provided in Tables 3.1 and 3.2.

3.6.2.4. Molecular modeling

Molecular docking studies were run on an Intell Premium 4 CPU (3.19 GHz, 0.99 GB of RAM, Windows XP Professional (Version 2002)) using the modeling program AutoDock 4.2 (2009. The Scripps Research Institute. 10550 North Torrey Pines Road, La Jolla, CA 92037. http://autodock.scripps.edu). Additionally, the program Cygwin (version 1.7. http://www.cygwin.com) was used to properly run the Autogrid and AutoDock applications. The crystal structure of AChE from *Torpedo californica* in complex with tacrine (PDB ID: 1ACJ, 2.8 Å resolution) was first edited in PyMOL (http://www.pymol.org, (PyMOL Molecular Graphics System, version 1.1r1, Schrödinger, LLC)) by manually removing all H_2O molecules. The tacrine molecule was also removed from the active site. The enzyme was then loaded into AutoDock where all polar hydrogens were added and Kollman charges were assigned. The various ligands were prepared in ChemBio3D Ultra 12.0 (http://www.cambridgesoft.com), and then loaded into AutoDock. The scoring grid for AutoDock was centered approximately in between the CAS and PAS (x-center: 4.795, y-center: 66.845, z-center: 72.226). The grid size was selected to be 60×60×60 points with a spacing between grid points of 0.375 Å. A Lamarckian genetic search algorithm was run 100 times using 250 population size and a maximum number of

energy evaluations of 2,500,000, while the rest of the docking study parameters were kept at their default quantity. After the docking was finished, conformations that were shown to be the in the largest cluster or most thermodynamically stable were examined in PyMOL. All docking figures were made in PyMOL (Fig. 3.2).

3.7. References

(1) Burns, A.; Iliffe, S. *BMJ* **2009**, *338*, 467-471.
(2) Thies, W.; Bleiler, L. *Alzheimers Dement* **2011**, *7*, 208-244.
(3) Black, S. E.; Doody, R.; Li, H.; McRae, T.; Jambor, K. M.; Xu, Y.; Sun, Y.; Perdomo, C. A.; Richardson, S. *Neurology* **2007**, *69*, 459-469.
(4) Rountree, S. D.; Chan, W.; Pavlik, V. N.; Darby, E. J.; Siddiqui, S.; Doody, R. S. *Alzheimers Res Ther* **2009**, *1*, 7.
(5) Petersen, R. C.; Thomas, R. G.; Grundman, M.; Bennett, D.; Doody, R.; Ferris, S.; Galasko, D.; Jin, S.; Kaye, J.; Levey, A.; Pfeiffer, E.; Sano, M.; van Dyck, C. H.; Thal, L. J. *N Engl J Med* **2005**, *352*, 2379-2388.
(6) Courtney, C.; Farrell, D.; Gray, R.; Hills, R.; Lynch, L.; Sellwood, E.; Edwards, S.; Hardyman, W.; Raftery, J.; Crome, P.; Lendon, C.; Shaw, H.; Bentham, P. *Lancet* **2004**, *363*, 2105-2115.
(7) Dvir, H.; Silman, I.; Harel, M.; Rosenberry, T. L.; Sussman, J. L. *Chem Biol Interact* **2010**, *187*, 10-22.
(8) Rydberg, E. H.; Brumshtein, B.; Greenblatt, H. M.; Wong, D. M.; Shaya, D.; Williams, L. D.; Carlier, P. R.; Pang, Y. P.; Silman, I.; Sussman, J. L. *J Med Chem* **2006**, *49*, 5491-5500.
(9) Bourne, Y.; Radic, Z.; Kolb, H. C.; Sharpless, K. B.; Taylor, P.; Marchot, P. *Chem Biol Interact* **2005**, *157-158*, 159-165.
(10) Pang, Y. P.; Quiram, P.; Jelacic, T.; Hong, F.; Brimijoin, S. *J Biol Chem* **1996**, *271*, 23646-23649.
(11) Inestrosa, N. C.; Alvarez, A.; Perez, C. A.; Moreno, R. D.; Vicente, M.; Linker, C.; Casanueva, O. I.; Soto, C.; Garrido, J. *Neuron* **1996**, *16*, 881-891.
(12) Bartolini, M.; Bertucci, C.; Cavrini, V.; Andrisano, V. *Biochem Pharmacol* **2003**, *65*, 407-416.
(13) Jomova, K.; Vondrakova, D.; Lawson, M.; Valko, M. *Mol Cell Biochem* **2010**, *345*, 91-104.
(14) Ames, D. J.; Bhathal, P. S.; Davies, B. M.; Fraser, J. R. E. *Lancet* **1988**, *331*, 887.
(15) Hu, M. K.; Wu, L. J.; Hsiao, G.; Yen, M. H. *J Med Chem* **2002**, *45*, 2277-2282.
(16) Carlier, P. R.; Han, Y. F.; Chow, E. S.; Li, C. P.; Wang, H.; Lieu, T. X.; Wong, H. S.; Pang, Y. P. *Bioorg Med Chem* **1999**, *7*, 351-357.
(17) Fernandez-Bachiller, M. I.; Perez, C.; Gonzalez-Munoz, G. C.; Conde, S.; Lopez, M. G.; Villarroya, M.; Garcia, A. G.; Rodriguez-Franco, M. I. *J Med Chem* **2010**, *53*, 4927-4937.
(18) Bornstein, J. J.; Eckroat, T. J.; Houghton, J. L.; Jones, C. K.; Green, K. D.; Garneau-Tsodikova, S. *Med Chem Commun* **2011**, *2*, 406-412.
(19) Muraoka, S.; Miura, T. *Life Sci* **2009**, *84*, 272-277.

(20) Joo, Y.; Kim, H. S.; Woo, R. S.; Park, C. H.; Shin, K. Y.; Lee, J. P.; Chang, K. A.; Kim, S.; Suh, Y. H. *Mol Pharmacol* **2006**, *69*, 76-84.
(21) Recanatini, M.; Cavalli, A.; Belluti, F.; Piazzi, L.; Rampa, A.; Bisi, A.; Gobbi, S.; Valenti, P.; Andrisano, V.; Bartolini, M.; Cavrini, V. *J Med Chem* **2000**, *43*, 2007-2018.
(22) Alonso, D.; Dorronsoro, I.; Rubio, L.; Munoz, P.; Garcia-Palomero, E.; Del Monte, M.; Bidon-Chanal, A.; Orozco, M.; Luque, F. J.; Castro, A.; Medina, M.; Martinez, A. *Bioorg Med Chem* **2005**, *13*, 6588-6597.
(23) Rodriguez-Franco, M. I.; Fernandez-Bachiller, M. I.; Perez, C.; Hernandez-Ledesma, B.; Bartolome, B. *J Med Chem* **2006**, *49*, 459-462.
(24) Fernandez-Bachiller, M. I.; Perez, C.; Campillo, N. E.; Paez, J. A.; Gonzalez-Munoz, G. C.; Usan, P.; Garcia-Palomero, E.; Lopez, M. G.; Villarroya, M.; Garcia, A. G.; Martinez, A.; Rodriguez-Franco, M. I. *ChemMedChem* **2009**, *4*, 828-841.
(25) Camps, P.; Formosa, X.; Munoz-Torrero, D.; Petrignet, J.; Badia, A.; Clos, M. V. *J Med Chem* **2005**, *48*, 1701-1704.
(26) Harel, M.; Schalk, I.; Ehret-Sabatier, L.; Bouet, F.; Goeldner, M.; Hirth, C.; Axelsen, P. H.; Silman, I.; Sussman, J. L. *Proc Natl Acad Sci U S A* **1993**, *90*, 9031-9035.
(27) da Silva, C. H.; Campo, V. L.; Carvalho, I.; Taft, C. A. *J Mol Graph Model* **2006**, *25*, 169-175.
(28) Ellman, G. L.; Courtney, K. D.; Andres, V., Jr.; Feather-Stone, R. M. *Biochem Pharmacol* **1961**, *7*, 88-95.
(29) Fang, L.; Kraus, B.; Lehmann, J.; Heilmann, J.; Zhang, Y.; Decker, M. *Bioorg Med Chem Lett* **2008**, *18*, 2905-2909.
(30) de Los Rios, C.; Egea, J.; Marco-Contelles, J.; Leon, R.; Samadi, A.; Iriepa, I.; Moraleda, I.; Galvez, E.; Garcia, A. G.; Lopez, M. G.; Villarroya, M.; Romero, A. *J Med Chem* **2010**, *53*, 5129-5143.
(31) Marco-Contelles, J.; Leon, R.; de los Rios, C.; Samadi, A.; Bartolini, M.; Andrisano, V.; Huertas, O.; Barril, X.; Luque, F. J.; Rodriguez-Franco, M. I.; Lopez, B.; Lopez, M. G.; Garcia, A. G.; Carreiras Mdo, C.; Villarroya, M. *J Med Chem* **2009**, *52*, 2724-2732.
(32) Chen, Y.; Sun, J.; Fang, L.; Liu, M.; Peng, S.; Liao, H.; Lehmann, J.; Zhang, Y. *J Med Chem* **2012**, *55*, 4309-4321.
(33) Chen, X.; Zenger, K.; Lupp, A.; Kling, B.; Heilmann, J.; Fleck, C.; Kraus, B.; Decker, M. *J Med Chem* **2012**, *55*, 5231-5242.
(34) Carlier, P. R.; Chow, E. S.; Han, Y.; Liu, J.; El Yazal, J.; Pang, Y. P. *J Med Chem* **1999**, *42*, 4225-4231.
(35) Korabecny, J.; Musilek, K.; Holas, O.; Binder, J.; Zemek, F.; Marek, J.; Pohanka, M.; Opletalova, V.; Dohnal, V.; Kuca, K. *Bioorg Med Chem Lett* **2010**, *20*, 6093-6095.
(36) Di, L.; Kerns, E. H.; Fan, K.; McConnell, O. J.; Carter, G. T. *Eur J Med Chem* **2003**, *38*, 223-232.
(37) Camps, P.; Formosa, X.; Galdeano, C.; Munoz-Torrero, D.; Ramirez, L.; Gomez, E.; Isambert, N.; Lavilla, R.; Badia, A.; Clos, M. V.; Bartolini, M.; Mancini, F.; Andrisano, V.; Arce, M. P.; Rodriguez-Franco, M. I.; Huertas, O.; Dafni, T.; Luque, F. J. *J Med Chem* **2009**, *52*, 5365-5379.
(38) Sussman, J. L.; Harel, M.; Frolow, F.; Varon, L.; Toker, L.; Futerman, A. H.; Silman, I. *J Mol Biol* **1988**, *203*, 821-823.

(39) Sussman, J. L.; Harel, M.; Frolow, F.; Oefner, C.; Goldman, A.; Toker, L.; Silman, I. *Science* **1991**, *253*, 872-879.
(40) Paz, A.; Roth, E.; Ashani, Y.; Xu, Y.; Shnyrov, V. L.; Sussman, J. L.; Silman, I.; Weiner, L. *Protein Sci* **2012**, *21*, 1138-1152.
(41) Bartolucci, C.; Stojan, J.; Yu, Q. S.; Greig, N. H.; Lamba, D. *Biochem J* **2012**, *444*, 269-277.
(42) Paz, A.; Xie, Q.; Greenblatt, H. M.; Fu, W.; Tang, Y.; Silman, I.; Qiu, Z.; Sussman, J. L. *J Med Chem* **2009**, *52*, 2543-2549.
(43) Harel, M.; Sonoda, L. K.; Silman, I.; Sussman, J. L.; Rosenberry, T. L. *J Am Chem Soc* **2008**, *130*, 7856-7861.
(44) Harel, M.; Hyatt, J. L.; Brumshtein, B.; Morton, C. L.; Wadkins, R. M.; Silman, I.; Sussman, J. L.; Potter, P. M. *Chem Biol Interact* **2005**, *157-158*, 153-157.

Note:
This chapter is adapted from a published article: **Eckroat, T. J.**; Green, K. D.; Reed, R. A.; Bornstein, J. J.; Garneau-Tsodikova, S. *Bioorg Med Chem* **2013**, *21*, 3614-3623.

Authors' contribution:
TJE, RAR, and JJB synthesized all compounds.
TJE, RAR, JJB, and KDG performed all biochemical assays.
TJE and Christopher K. Jones performed molecular modeling.
TJE and SGT analyzed data and wrote manuscript.

3.8. Appendix

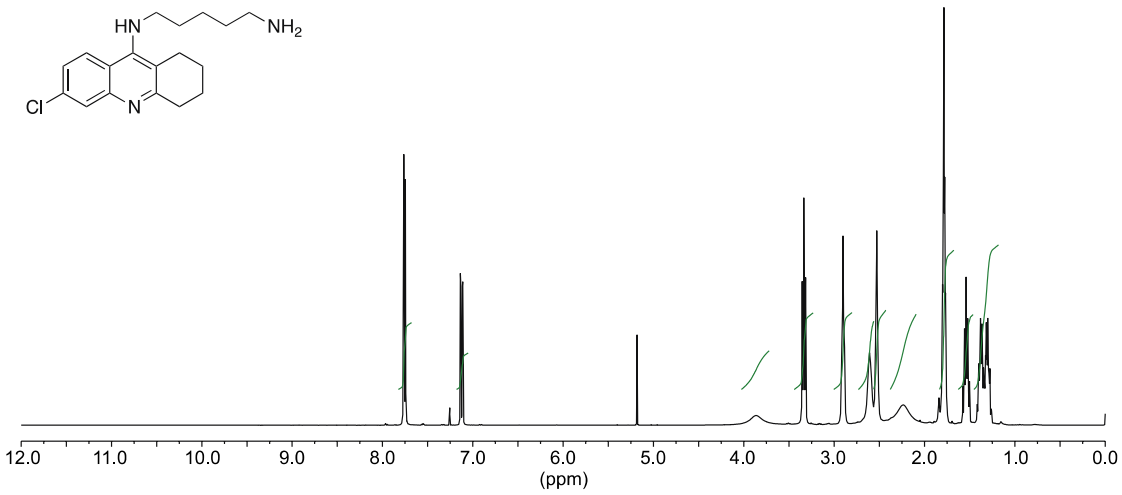

Fig. 3.4. ^{1}H NMR in $CDCl_3$ for compound **6c**.

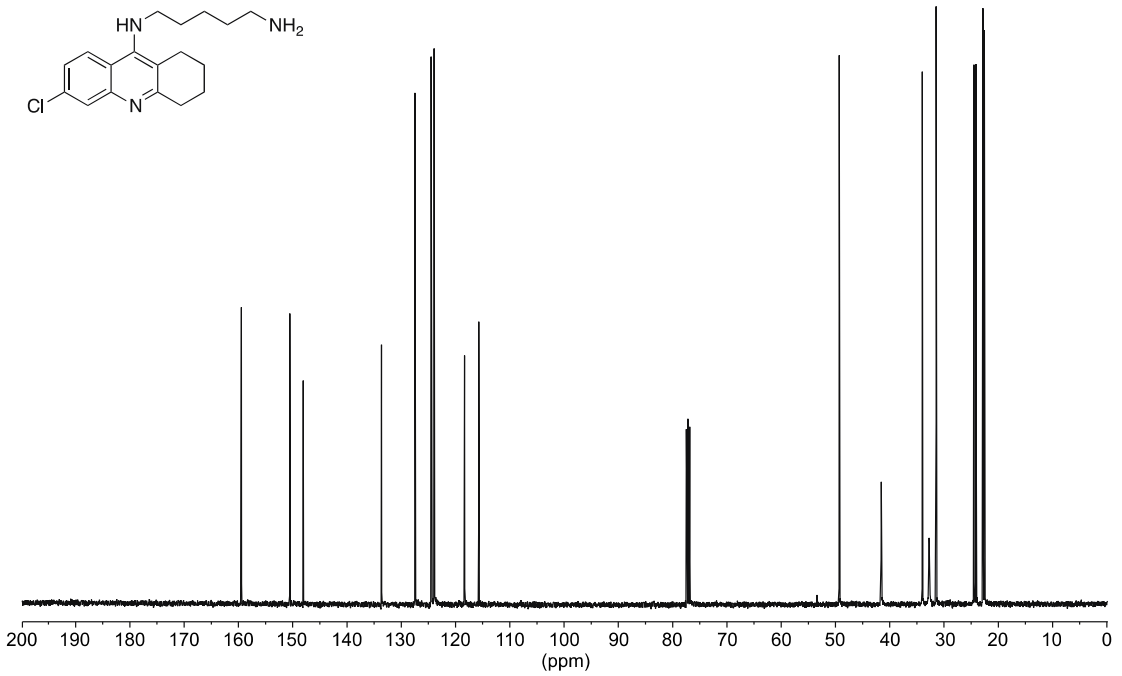

Fig. 3.5. ^{13}C NMR in $CDCl_3$ for compound **6c**.

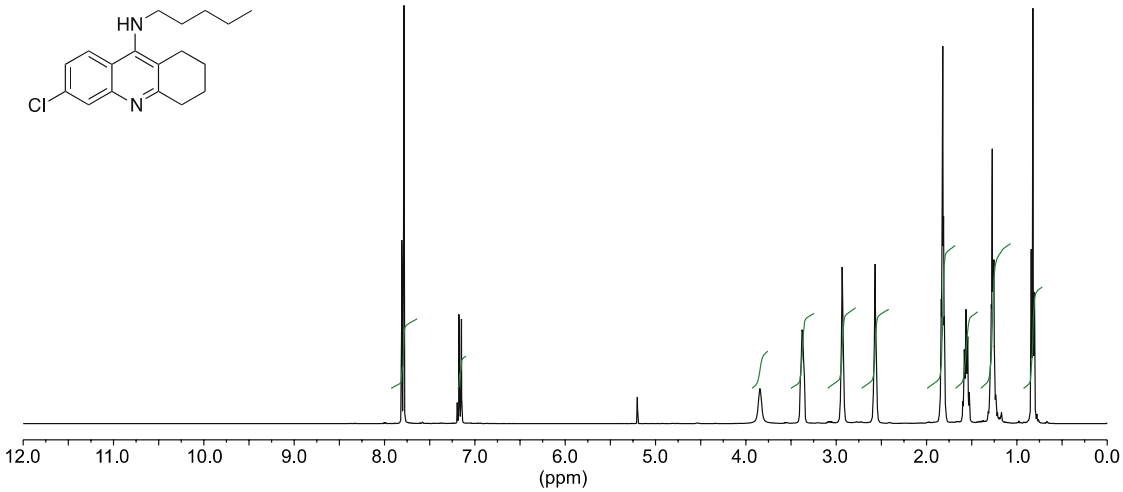

Fig. 3.6. ^{1}H NMR in $CDCl_3$ for compound **14a**.

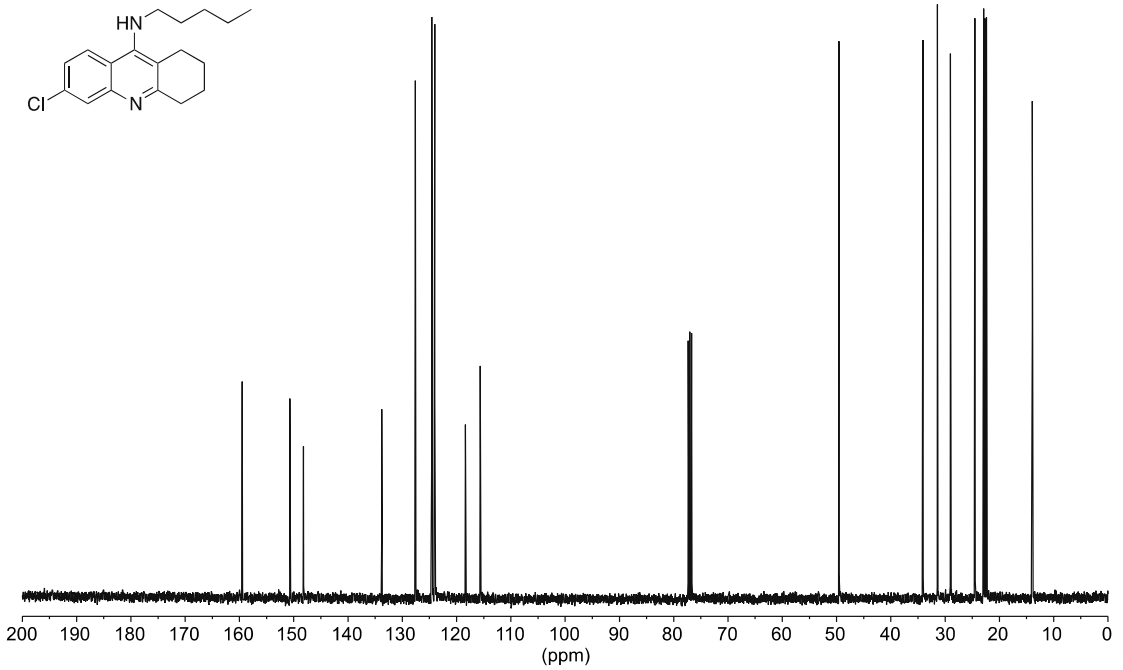

Fig. 3.7. ^{13}C NMR in $CDCl_3$ for compound **14a**.

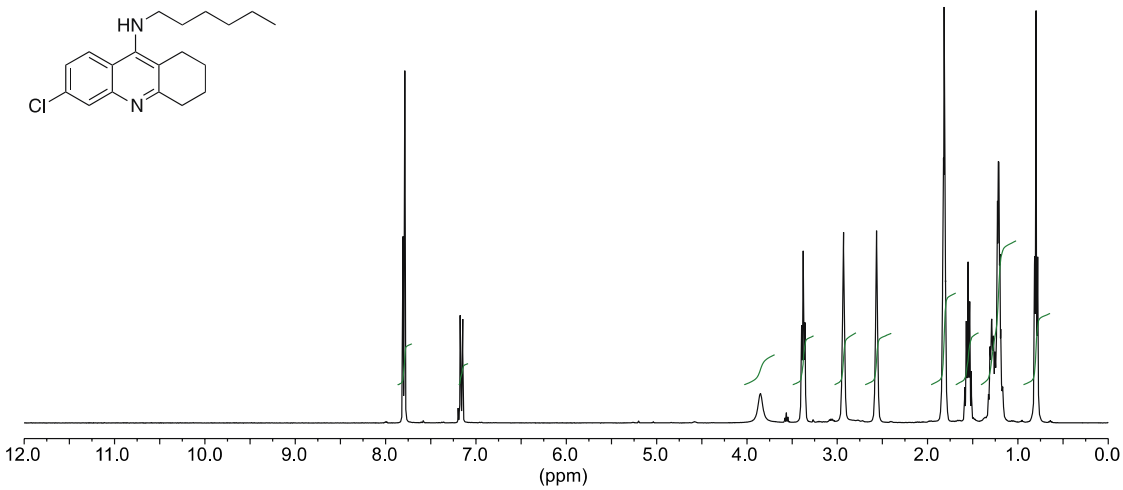

Fig. 3.8. ^{1}H NMR in $CDCl_3$ for compound **14b**.

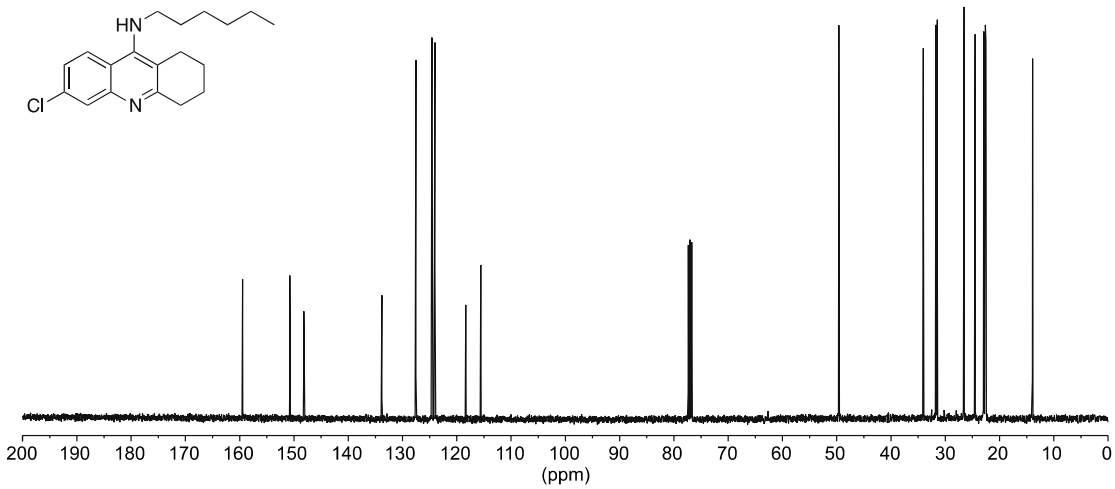

Fig. 3.9. ^{13}C NMR in $CDCl_3$ for compound **14b**.

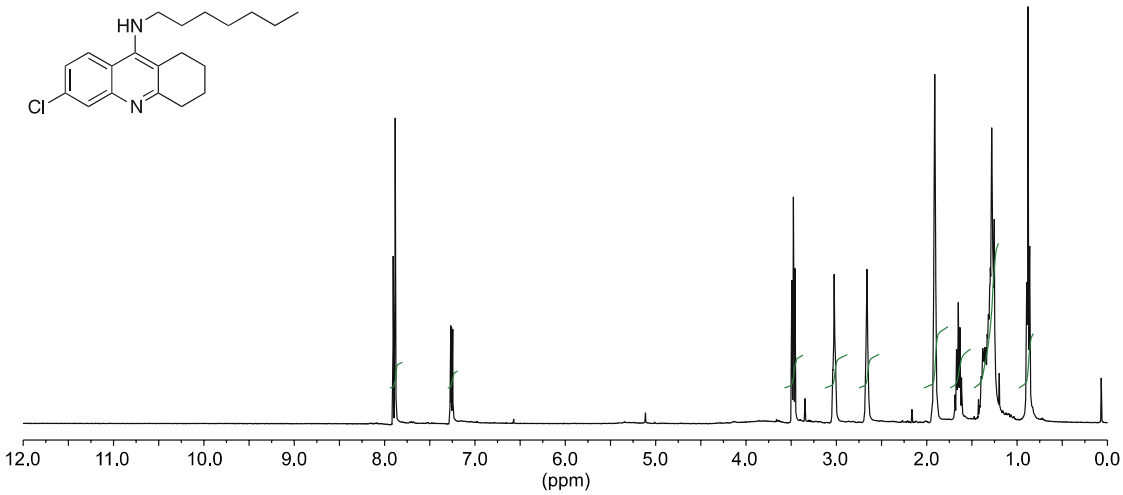

Fig. 3.10. ^{1}H NMR in $CDCl_3$ for compound **14c**.

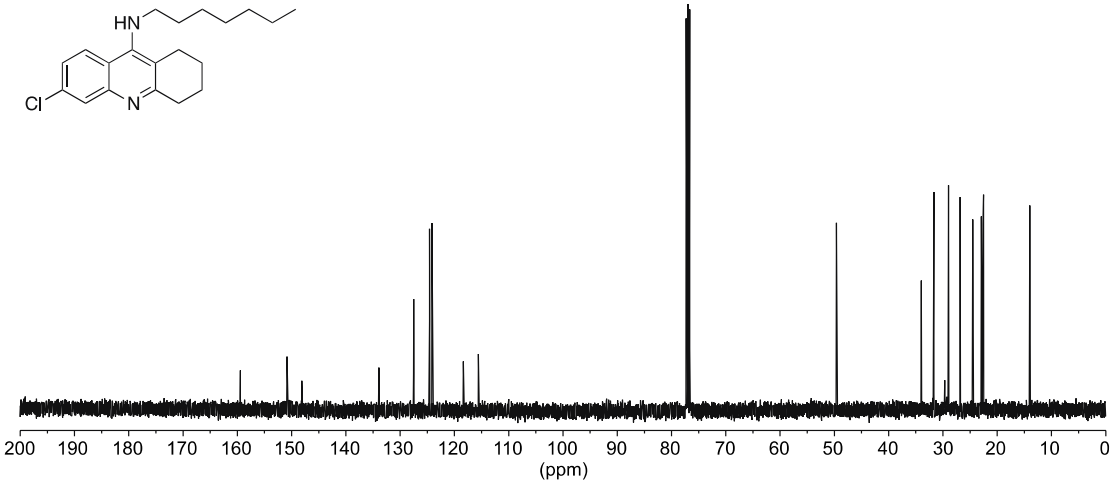

Fig. 3.11. ^{13}C NMR in $CDCl_3$ for compound **14c**.

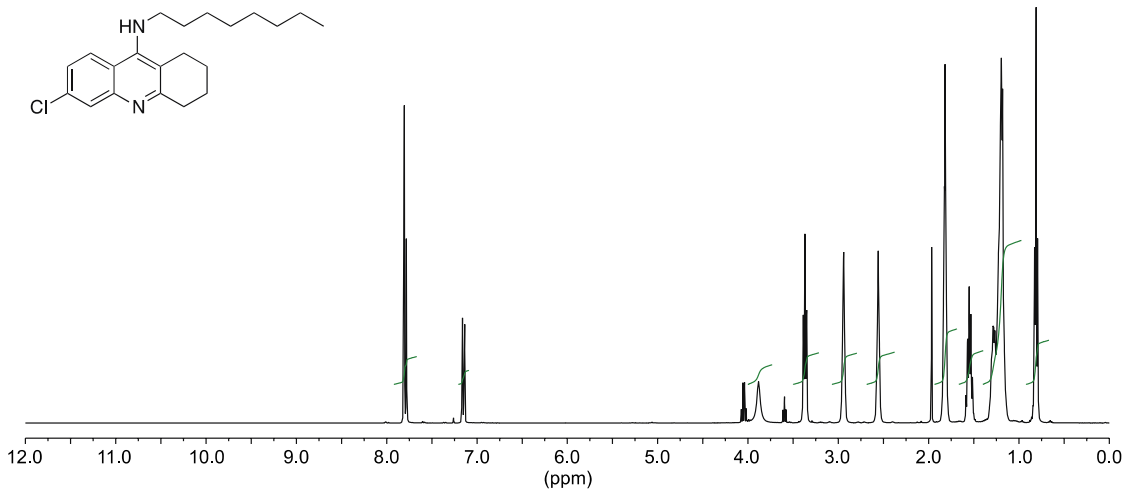

Fig. 3.12. ^{1}H NMR in $CDCl_3$ for compound **14d**.

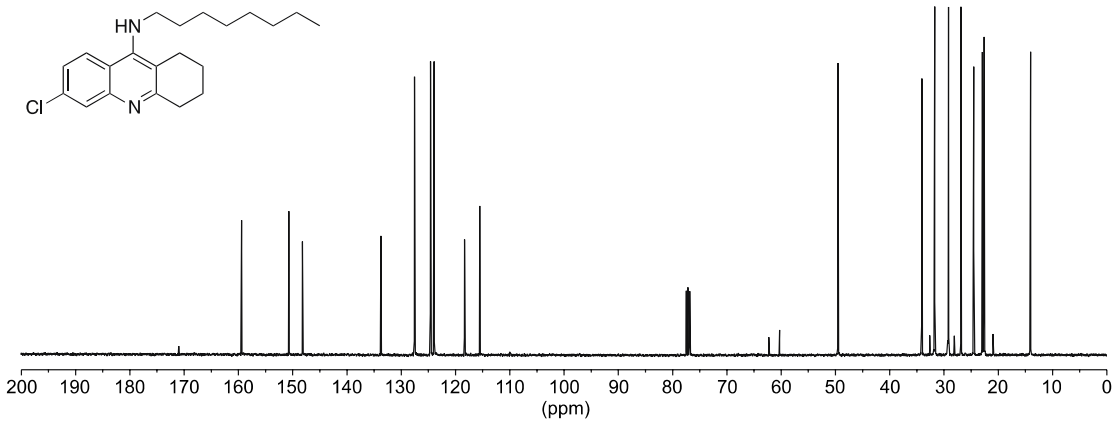

Fig. 3.13. ^{13}C NMR in $CDCl_3$ for compound **14d**.

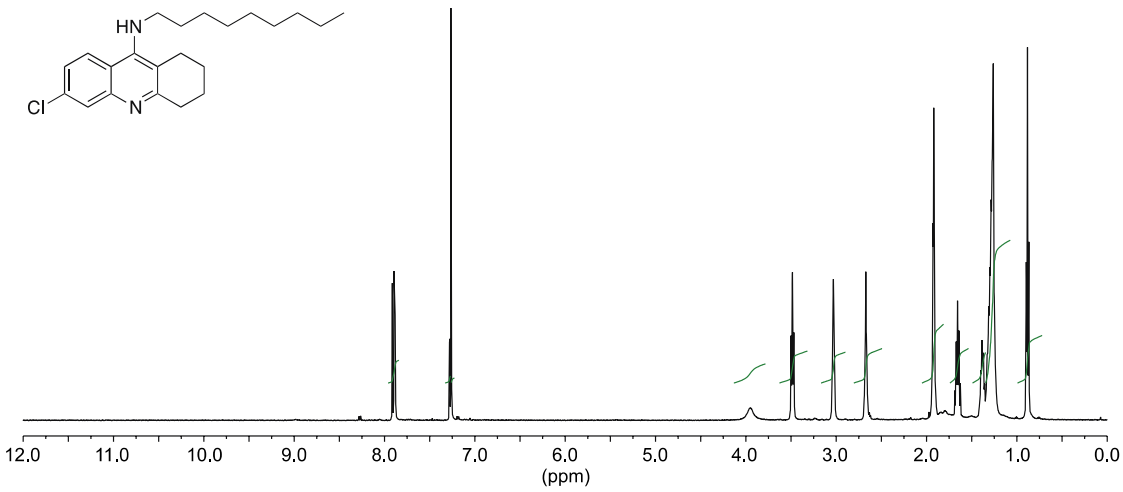

Fig. 3.14. ^{1}H NMR in $CDCl_3$ for compound **14e**.

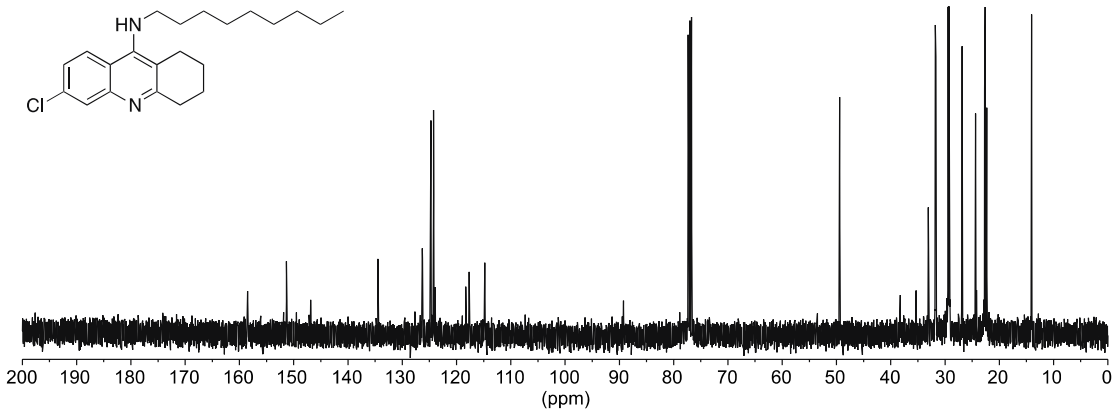

Fig. 3.15. ^{13}C NMR in $CDCl_3$ for compound **14e**.

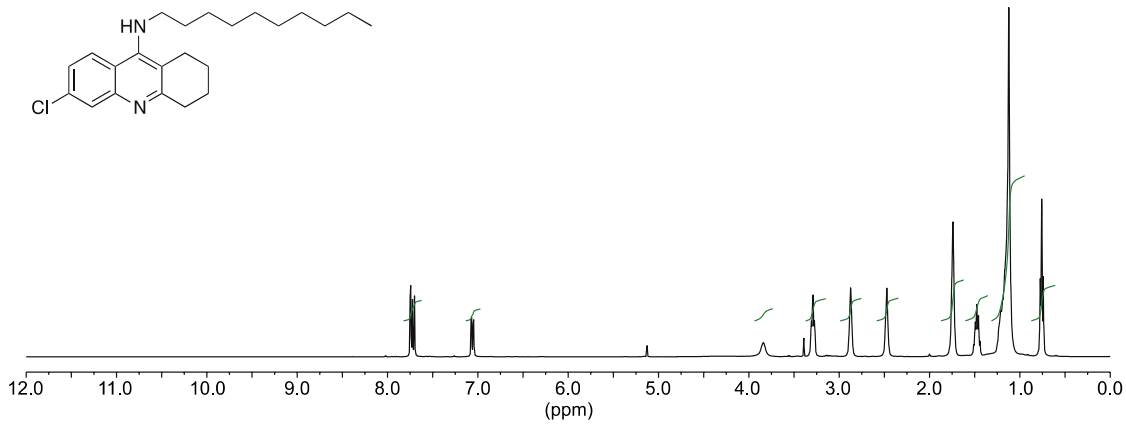

Fig. 3.16. ^{1}H NMR in $CDCl_3$ for compound **14f**.

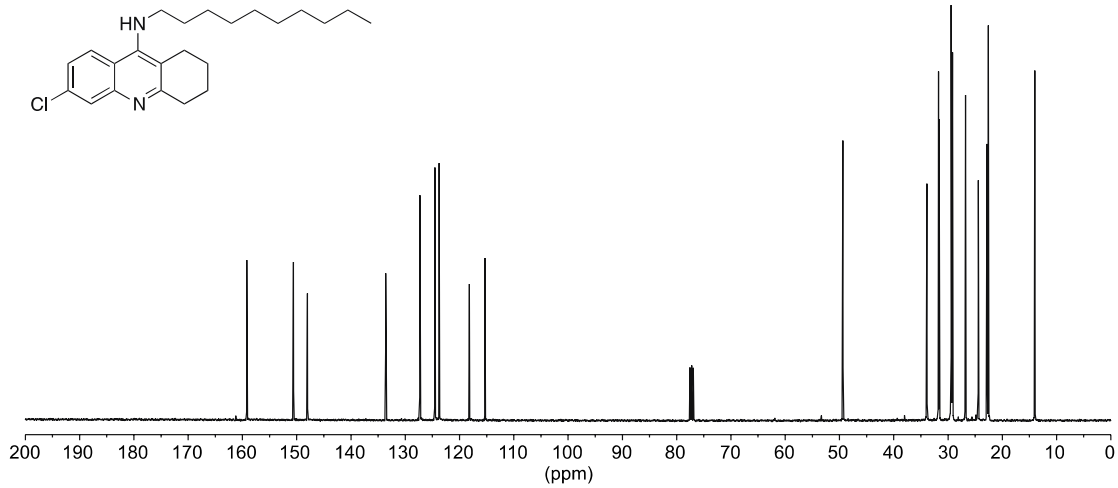

Fig. 3.17. ^{13}C NMR in $CDCl_3$ for compound **14f**.

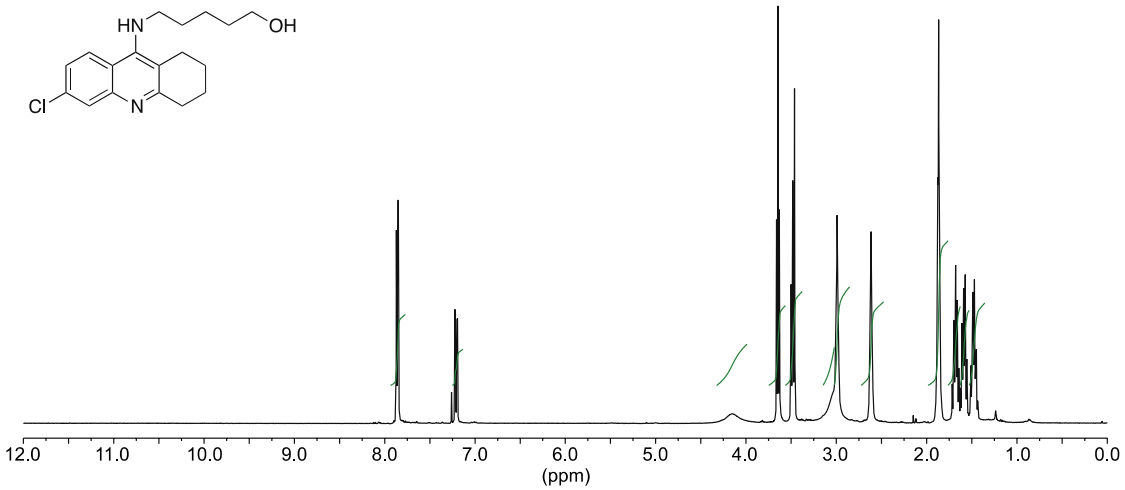

Fig. 3.18. ^{1}H NMR in $CDCl_3$ for compound **15a**.

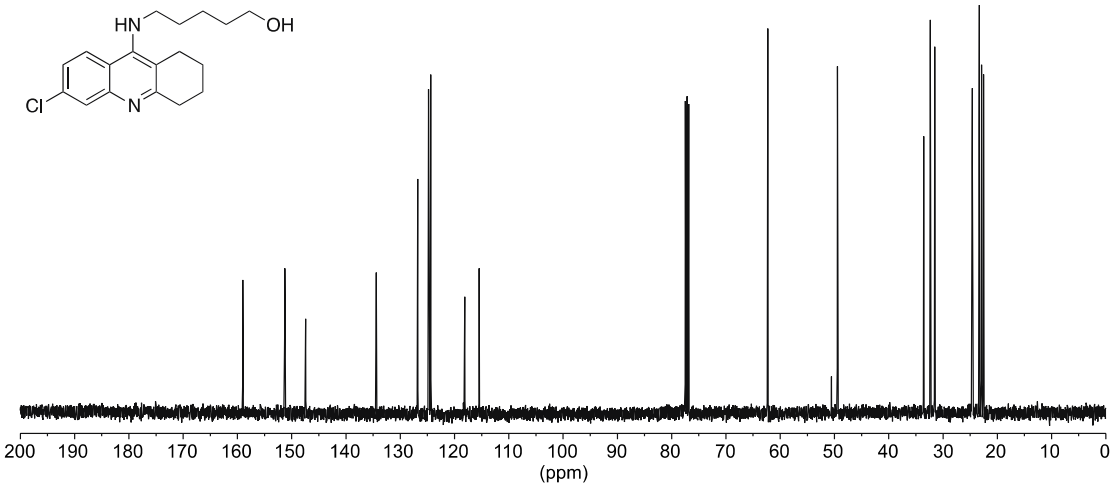

Fig. 3.19. ^{13}C NMR in $CDCl_3$ for compound **15a**.

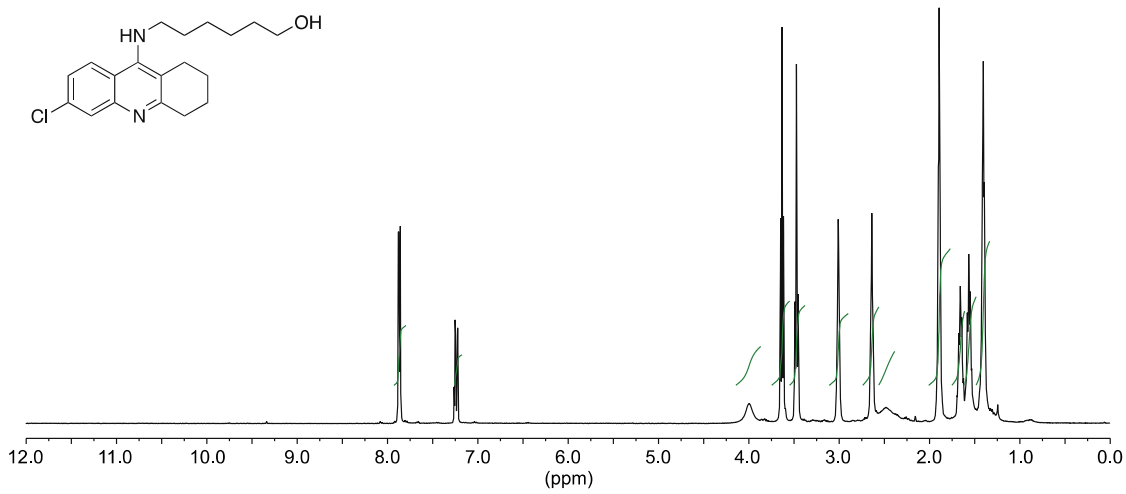

Fig. 3.20. ^{1}H NMR in $CDCl_3$ for compound **15b**.

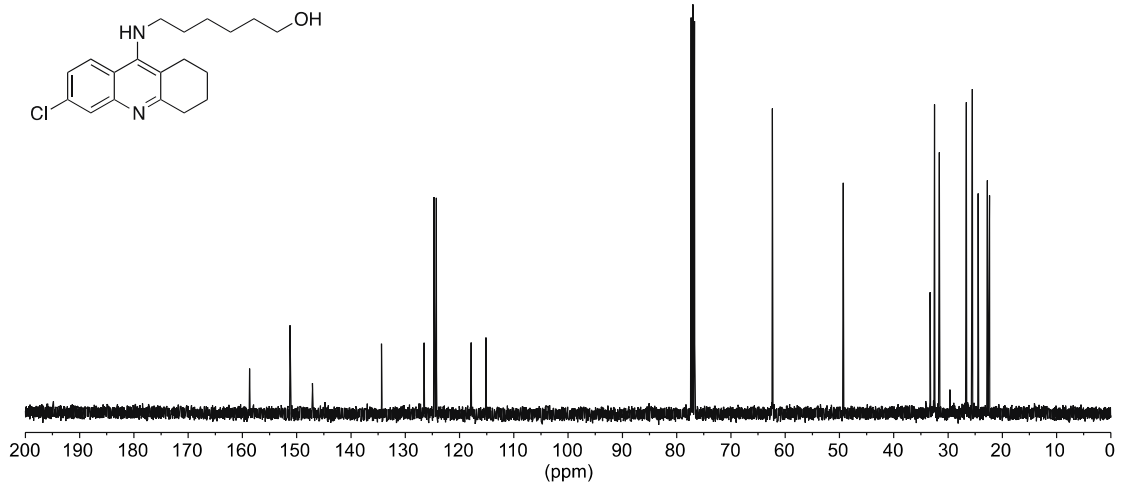

Fig. 3.21. ^{13}C NMR in $CDCl_3$ for compound **15b**.

Chapter 4

A novel hybrid of 6-chlorotacrine and metal-amyloid-β modulator for inhibition of acetylcholinesterase and metal-induced amyloid-β aggregation

4.1. Abstract

The number of people suffering from Alzheimer's disease (AD) is expected to increase dramatically in the coming decades. Currently, acetylcholinesterase inhibitors (AChEis) provide some relief of cognitive symptoms, while newer approaches, such as amyloid-β (Aβ)-targeted metal chelation, offer potential hope for slowing and/or reversing disease progression. This work details the synthesis and biochemical evaluation of a novel hybrid of 6-chlorotacrine and a metal-Aβ modulator that chemically combines an AChEi and an Aβ-targeted metal chelator into a single molecule. This hybrid shows potent inhibition of AChE under various conditions, interaction with Cu^{2+} and Zn^{2+}, control of metal-free and metal-induced Aβ aggregate assembly, and disaggregation of preformed metal-free and metal-associated Aβ aggregates. As such, the hybrid described herein represents a promising, new multifunctional compound for AD studies.

4.2. Introduction

Alzheimer's disease (AD) is an age-related, neurodegenerative disorder estimated to affect over 5 million people in the United States alone.[1] AD is progressive and ultimately fatal with symptoms ranging from cognitive dysfunction to psychiatric and behavioral disturbances. As the population ages, the prevalence of AD is expected to increase dramatically in the coming years and place an increasing burden on society. Many pathological hallmarks of the disease have been documented, yet the exact cause remains unknown. Current treatments for AD act mainly by inhibiting acetylcholinesterase (AChE).

While these acetylcholinesterase inhibitors (AChEis) are moderately effective in treating cognitive symptoms, they are incapable of stopping or reversing disease progression.[2]

Tacrine was the first AChEi approved by the FDA.[3] Though its clinical use has been limited by hepatotoxicity,[4] tacrine remains an important starting point in research towards developing new drugs for AD due to its straightforward synthesis and comparatively low cost.[5,6] In fact, tacrine hybrids, bifunctional molecules where tacrine has been chemically linked to another molecule with beneficial anti-AD properties, have been well characterized in the literature. For example, tacrine-8-hydroxyquinoline hybrids, tacrine-ferulic acid hybrids, and tacrine-mefenamic acid hybrids have all shown promising results.[7-11] The role of the linker in inhibitory activity of these hybrids towards AChE has also been investigated.[12]

The presence and possible role of amyloid-β (Aβ) peptide aggregates in the brains of AD patients has been well documented.[13-17] These aggregates provide an interesting pharmacological target in that drugs capable of disrupting already formed Aβ aggregates or preventing Aβ aggregation may be capable of halting or inverting the progression of AD.[14,16] While AChE and butyrylcholinesterase (BChE) are important in AD because they control acetylcholine (ACh) levels, they also interact with Aβ.[18-20] Structurally, AChE consists of a catalytic active site (CAS) and a peripheral anionic site (PAS) connected by a 20 Å gorge.[21-23] AChE is known to promote Aβ aggregation through interaction at the PAS, and it is often found entangled in Aβ plaques along with BChE.[18,24] Thus, tacrine hybrids with the ability to simultaneously bind to the CAS and PAS by virtue of a chemical linker spanning the active site gorge have the potential to disrupt Aβ aggregation.[25,26]

Metal ions, such as Cu^{2+} and Zn^{2+}, are known to interact with Aβ peptides and promote their aggregation, which has been suggested to be involved in neurotoxicity.[27-33] Given this fact, small molecules for modulation of metal-Aβ interaction and reactivity have been developed. For example, N^1,N^1-dimethyl-N^4-(pyridin-2-yl-methyl)benzene-1,4-diamine

(**17**, Fig. 4.1) has shown the ability to chelate Cu^{2+} and Zn^{2+} and interact with Aβ, effectively regulating metal-induced Aβ aggregation and neurotoxicity *in vitro* and in human neuroblastoma cells.[34] We reasoned that chemically linking an AChEi with the metal-Aβ modulator **17** would create a hybrid molecule (**19**, Fig. 4.1) potentially capable of multifunctionality (inhibition of AChE at the CAS, prevention of AChE-Aβ interaction by blocking the PAS, as well as alteration of the interaction between metal ions and Aβ with subsequent moderation of the reactivity of metal-associated Aβ species). Herein, we describe the design, synthesis, and initial biochemical evaluation of such a hybrid (**19**, Fig. 4.1).

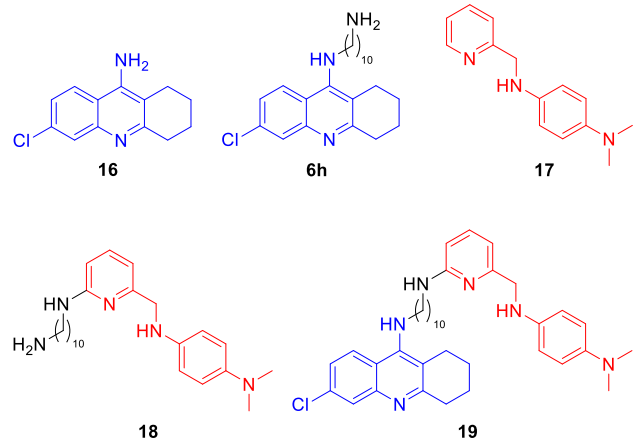

Fig. 4.1. Structures of 6-chlorotacrine (**16**), 6-chlorotacrine linker (**6h**), N^1,N^1-dimethyl-N^4-(pyridin-2-ylmethyl)benzene-1,4-diamine, metal-Aβ modulator (**17**), metal-Aβ modulator linker (**18**), and hybrid of 6-chlorotacrine-metal-Aβ modulator (**19**).

4.3. Results and discussion

4.3.1. Hybrid design and synthesis

Hybrid **19** (Fig. 4.1) was designed to contain an AChEi moiety (blue), a linker region (black), and a metal-Aβ modulating moiety (red). 6-Chlorotacrine (**16**), which was chosen as the AChEi moiety, has shown potent inhibition of AChE[5] and has been incorporated into other AChE-directed hybrid molecules with favorable results.[9] For comparison in biochemical studies, compound **16** was prepared by heating 2-amino-4-chlorobenzonitrile and cyclohexanone in the presence of anhydrous $ZnCl_2$ (Fig. 4.2A), as previously reported.[5,6] A decamethylene linker region was chosen due to its appropriate length to span the gorge of AChE and produce a compound capable of simultaneously interacting with the CAS and PAS.[9] This linker moiety was attached to 6-chlorotacrine to give analog **6h** as previously reported.[9] Compound **17** was chosen as the metal-Aβ modulating moiety because of its ability to chelate metal ions (*i.e.*, Cu^{2+} and Zn^{2+}) as well as effectively interact with Aβ, and it was prepared as established in previous procedures.[34] For comparison in

biochemical studies, metal-Aβ modulator linker **18** was prepared from 6-bromo-2-pyridinecarboxaldehyde *via* reductive amination with *N*,*N*-dimethyl-*p*-phenylenediamine followed by subsequent nucleophilic displacement of the bromo substituent by 1,10-diaminodecane (Fig. 4.2B). Hybrid **19** was prepared using a copper-catalyzed Ullmann-type reaction between **6h** and the cyclic ethylene acetal-protected form of 6-bromo-2-pyridinecarboxaldehyde. Subsequent deprotection and reductive amination with *N*,*N*-dimethyl-*p*-phenylenediamine gave the desired target hybrid **19** in 8% overall yield (Fig. 4.2C).

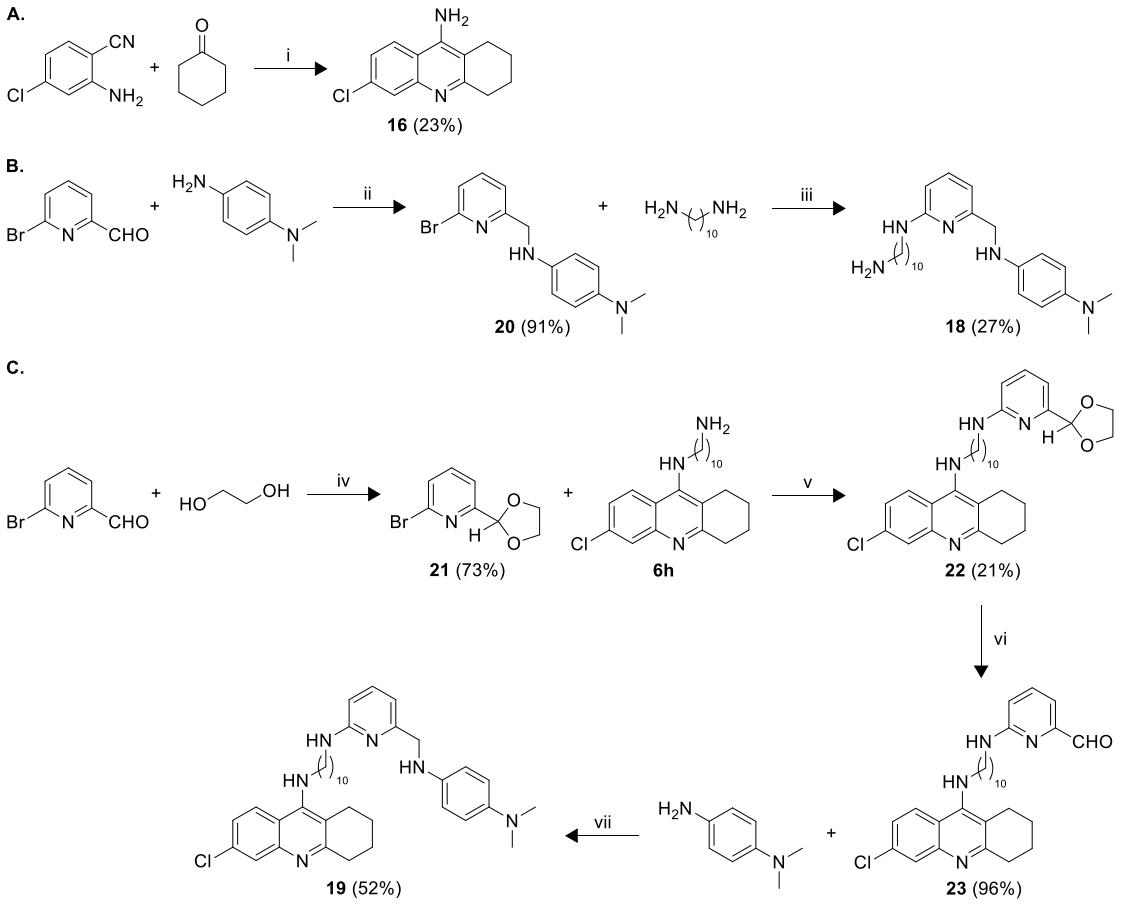

Fig. 4.2. Synthetic schemes for the preparation of **A.** 6-chlorotacrine (**16**), **B.** metal-Aβ modulator linker (**18**), and **C.** hybrid of 6-chlorotacrine-metal-Aβ modulator (**19**). *Reagents and conditions*: (i) $ZnCl_2$ (2.2 eq), Δ. (ii) a) EtOH, Δ. b) $NaBH_4$ (5.4 eq), Δ. (iii) 1-pentanol, Δ. (iv) MsOH (0.33 eq), toluene, Δ. (v) CuI (0.05 eq), L-proline (0.10 eq), K_2CO_3 (0.15 eq), 10:1/DMSO:H_2O, 90 °C. (vi) 2:1/MeCN:aq. HCl, 60 °C. (vii) a) EtOH, Δ. b) $NaBH_4$ (6.7 eq), 0 °C to rt.

4.3.2. Biochemical evaluation

4.3.2.1. AChE inhibition

The AChE inhibitory properties of compounds **6h** and **16-19** were assessed against AChE from *Electrophorus electricus* (*Ee*AChE) using the well-established Ellman method[35] to determine IC_{50} (Table 4.1). We previously tested tacrine with AChE (Table 4.1).[9] However, since 6-chlorotacrine (**16**) is 25-fold more potent than tacrine itself, herein, we used it as the standard against which we compare all compounds. 6-Chlorotacrine (**16**) presented potent inhibition of AChE with an $IC_{50} = 2.41 \pm 0.48$ nM, which is in good agreement with the literature value.[36] The IC_{50} of compound **6h** has recently been reported,[12] and it also exhibited potent AChE inhibition. Metal-Aβ modulator **17** showed very poor inhibition ($IC_{50} > 200$ μM), which was expected given that it was not originally designed to interact with AChE. Introduction of the 1,10-diaminodecane moiety to **17**, however, provides a remarkable increase (>200-fold) in potency ($IC_{50} = 757 \pm 279$ nM for **18**). Hybrid **19** was observed to have an $IC_{50} = 2.37 \pm 0.29$ nM, identical to that of **16**. Many tacrine hybrids reported in the literature showed an increase in potency compared to their parent compound. While this is not the case for **19** because the parent 6-chlorotacrine (**16**) is already highly potent, this compound is still of interest given its potential for metal chelation and Aβ interaction. In addition, the IC_{50} value of **19** is within the range reported for structurally similar metal/Aβ-targeted tacrine hybrids in the literature.[37-40]

The AChE inhibitory properties of compounds **6h** and **16-19** were also assessed using a method described by Muraoka and Miura[41] to determine IC_{50} in the presence of reactive oxygen species (ROS IC_{50}, Table 4.1). Inflammation and oxidative stress from ROS are thought to play a role in AD, and tacrine-mefenamic acid hybrids have shown an increase in potency towards AChE in the presence of ROS, which may be beneficial for anti-AD compounds.[9] As such, we aimed to establish if the compounds of interest in this study displayed similar results. Unfortunately, only metal-Aβ modulator **17** showed a significant increase in potency in the presence of ROS. Although, even with this increase, **17** remains a relatively poor inhibitor. In the case of **18** and hybrid **19**, there was actually a reduction in potency. Compounds **16** and **6h** indicated virtually no change between IC_{50} and ROS IC_{50}. To investigate the effect on enzyme inhibition of covalent linkage between

the AChEi, linker, and metal-Aβ modulating moieties of hybrid **19**, we examined combinations of molecules (**6h** + **17**, **16** + **18** in 1:1 equimolar mixtures) in our inhibition assays (Table 4.1). Results indicate that covalent linkage is not essential for hybrid **19** in terms of IC_{50} as the values for **19**, **6h** + **17**, and **16** + **18** were nearly identical. Similar results have been observed for tacrine-mefenamic acid hybrids.[9,12] Interestingly, in terms of ROS IC_{50}, covalent linkage may actually be detrimental for hybrid **19** as it was outperformed by both mixtures in this assay. However, covalent linkage may still be beneficial for simultaneous delivery of all components of the hybrid to the same location in the brain.

4.3.2.2. BChE inhibition

BChE is also commonly associated with characteristic Aβ plaques. Thus, inhibition of BChE from equine serum (*es*BChE) by compounds **6h** and **16-19** was also tested (Table 4.1). With an $IC_{50} = 2.41 \pm 0.52$ nM against BChE, 6-chlorotactine (**16**) showed inhibitory effect identical to that of AChE (2.41 ± 0.48 nM). Compounds **6h** and **18** were found to be less active towards BChE than AChE with IC_{50} values of 13.6 ± 3.0 nM (13-fold diminution) and >200 μM, respectively. Meanwhile, as observed with AChE, compound **17** exhibited no inhibitory activity with BChE, and hybrid **19** demonstrated similar inhibition towards BChE ($IC_{50} = 2.01 \pm 0.12$ nM) and AChE ($IC_{50} = 2.37 \pm 0.29$ nM).

As with AChE, the inhibitory effect of compounds **6h** and **16-19** on BChE was also examined under a ROS environment (Table 4.1). With the exception of compounds **16** and **18**, the introduction of ROS seemed to have little effect on the inhibition of BChE. Compound **16** showed *ca.* 75-fold reduction in activity, while compound **18** displayed vastly improved inhibitory properties ($IC_{50} = 0.162 \pm 0.049$ nM) suggesting that, in the absence of the tacrine moiety, the oxidized form(s) of compound **18** may block enzymatic turnover of BChE with an increased efficiency compared to other compounds. As with AChE, the covalent bond linkage requirement for inhibitory activity was investigated. While an equimolar combination of compounds **16** + **18** showed no improvement in inhibitory activity for BChE, an equimolar mixture of compounds **6h** + **17** presented a 59-fold increase in activity over hybrid **19**. In the presence of ROS, equimolar mixtures of compounds **16** + **18** and **6h** + **17** yielded values 2.5-fold and 125-fold better,

respectively, than those observed for the covalently linked hybrid **19**. Although the covalent link seems to have an adverse effect upon the inhibitory activity of BChE, it still may be purposeful in transporting both components to the same site in the brain. It is important to note that the current linker has been optimized for AChE and not BChE.

Table 4.1. Inhibition of *Ee*AChE and *es*BChE activity by compounds **6h** and **16-19** and effect of M^{2+} and Aβ on IC_{50} of hybrid **19** under various conditions.

	*Ee*AChE		*es*BChE	
Compound[a]	IC_{50} (nM)	ROS IC_{50} (nM)	IC_{50} (nM)	ROS IC_{50} (nM)
Tacrine[b]	52.4 ± 7.3	183 ± 21	ND[f]	ND
16	2.41 ± 0.48	1.86 ± 0.37	2.41 ± 0.52	188 ± 43
6h[c]	0.932 ± 0.220	2.18 ± 0.27	13.6 ± 3.0	2.18 ± 0.27
17	>200 μM	1858 ± 235	>200 μM	>200 μM
18	757 ± 279	1906 ± 490	>200 μM	0.162 ± 0.049
19	2.37 ± 0.29	96.5 ± 24.3	2.01 ± 0.12	1.51 ± 0.18
6h + **17**[d]	0.544 ± 0.123	1.13 ± 0.33	0.034 ± 0.007	0.012 ± 0.003
16 + **18**[d]	1.61 ± 0.19	1.93 ± 0.24	2.85 ± 0.71	0.604 ± 0.223
Conditions[e]	*Ee*AChE		*es*BChE	
Effect of M^{2+} on IC_{50} (nM) of hybrid 19				
	$CuCl_2$	$ZnCl_2$	$CuCl_2$	$ZnCl_2$
a	75.4 ± 12.4	2.46 ± 0.55	1.78 ± 0.22	0.713 ± 0.065
b	144 ± 11	2.08 ± 0.37	8.14 ± 1.00	1.28 ± 0.08
c	4.14 ± 0.43	6.99 ± 2.26	6.09 ± 0.54	2.76 ± 0.22
Effect of Aβ on IC_{50} (nM) of hybrid 19				
d	14.4 ± 5.2		0.554 ± 0.138	
e	2003 ± 647		1.02 ± 0.21	
f	7.26 ± 2.40		3.70 ± 0.48	
Effect of M^{2+} and Aβ on IC_{50} (nM) of hybrid 19				
	$CuCl_2$	$ZnCl_2$	$CuCl_2$	$ZnCl_2$
g	82.8 ± 8.3	8.80 ± 0.84	4.52 ± 1.54	2.38 ± 0.49
h	8.87 ± 1.22	9.42 ± 1.49	23.0 ± 3.2	4.70 ± 0.94
i	182 ± 66	111 ± 30	65.4 ± 6.7	41.5 ± 8.4

[a] See Fig. 4.1 for chemical structures. [b,c] These values were previously reported and are used here for comparison.[9,12] [d] Tested as 1:1 equimolar mixture. [e] Conditions: (a) Dilute hybrid **19**, add AChE (or BChE), wait 10 min, add M^{2+}, wait 10 min, and initiate reaction. (b) Dilute hybrid **19**, add M^{2+}, wait 10 min, add AChE (or BChE), wait 10 min, and initiate reaction. (c) Dilute hybrid **19**, add mixture of AChE (or BChE) and M^{2+}, wait 10 min, and initiate reaction. (d) Dilute hybrid **19**, add AChE (or BChE), wait 10 min, add Aβ, wait 10 min, and initiate reaction. (e) Dilute hybrid **19**, add Aβ, wait 10 min, add AChE (or BChE), wait 10 min, and initiate reaction. (f) Dilute hybrid **19**, add mixture of AChE (or BChE) and Aβ, wait 10 min, and initiate reaction. (g) Dilute hybrid **19**, add AChE (or BChE), wait 10 min, add Aβ treated with M^{2+} for 2 min, wait 10 min, and initiate reaction. (h) Dilute hybrid **19**, add Aβ treated with M^{2+} for 2 min, wait 10 min, add AChE (or BChE), wait 10 min, and initiate reaction. (i) Dilute hybrid **19**, add mixture of AChE (or BChE), Aβ, and M^{2+}, wait 10 min, and initiate reaction. [f] ND = not determined.

4.3.2.3. Effect of metals and Aβ on AChE inhibition

As previously mentioned, AChE is often found to be entangled in Aβ plaques, and aggregation of Aβ is promoted through binding at the PAS of AChE.[18,24] Additionally, metal ions, such as Cu^{2+} and Zn^{2+}, have been observed to interact with Aβ and promote peptide aggregation.[27-31] Composed of tacrine and a metal-Aβ modulating moiety, hybrid **19** was envisioned to interact with AChE, Aβ, and Cu^{2+}/Zn^{2+} simultaneously within the complex environment of an AD brain. However, interaction with Aβ and Cu^{2+}/Zn^{2+} could potentially be detrimental to the ability of **19** to function as an AChEi. The ability of hybrid **19** to inhibit AChE in the presence of M^{2+} (Cu^{2+} or Zn^{2+}) and Aβ was examined (Table 4.1). It is important to note that, although other tacrine-derived hybrids have been shown to successfully coinhibit cholinesterases and Aβ aggregation,[37-40] to our knowledge, the effects of metals and Aβ on cholinesterase inhibition have not been studied for these compounds. Various conditions (a-i, Table 4.1) were tested as it was anticipated that the order of interaction with AChE, Aβ, and M^{2+} could affect the IC_{50} of **19**. For example, **19** could potentially interact with AChE before being exposed to M^{2+} (condition a), with M^{2+} before being exposed to AChE (condition b), or with AChE and M^{2+} simultaneously (condition c). Similarly, **19** could interact with AChE before being exposed to Aβ (condition d), with Aβ before being exposed to AChE (condition e), or with AChE and Aβ simultaneously (condition f). Finally, **19** could interact with AChE before being exposed to Aβ treated with M^{2+} (condition g), with Aβ treated with M^{2+} before being exposed to AChE (condition h), or with AChE, Aβ, and M^{2+} simultaneously (condition i).

In general, hybrid **19** retained good inhibition of AChE in the presence of M^{2+} and Aβ. With only one exception, **19** showed an $IC_{50} < 200$ nM under all conditions tested. The lone exception (condition e, Table 4.1) occurred when **19** was exposed to Aβ for 10 min before introduction of AChE. Under these conditions, **19** indicated a nearly 850-fold reduction in potency ($IC_{50} = 2003 \pm 647$ nM), which was not unexpected given that interaction of **19** with Aβ could likely lead to a complex that simply cannot fit into the AChE binding site as before. Only slight increases in IC_{50} were seen in the presence of Aβ in other cases (conditions d and f).

Hybrid **19** showed moderate reduction in potency in the presence of Cu^{2+} in two cases (conditions a and b, Table 4.1) but virtually no change under condition c. Similar to the case seen with Aβ, the largest reduction in potency was seen when **19** was exposed to Cu^{2+} for 10 min before introduction of AChE (condition b). However, in contrast to the case seen with Aβ, the reduction was only around 60-fold (IC_{50} = 144 ± 11 nM). Interestingly, **19** presented essentially no change in IC_{50} in the presence of Zn^{2+} under the conditions tested (conditions a-c, Table 4.1).

Hybrid **19** exhibited varying IC_{50} values in the presence of M^{2+} and Aβ simultaneously (conditions g-i, Table 4.1). A moderate reduction in potency was indicated when **19** interacted with AChE before being exposed to Cu^{2+}-treated Aβ (IC_{50} = 82.8 ± 8.3 nM), but this effect was not seen with Zn^{2+}-treated Aβ samples (condition g). Only slight increases in IC_{50} were visible when **19** interacted with Cu^{2+}/Zn^{2+}-treated Aβ before being exposed to AChE (condition h). These results are interesting given the observation for condition e (described above) and may indicate that compound **19** interacts differently with Aβ and M^{2+}-treated Aβ. Moderate reductions in potency were observed when **19** interacted with AChE, Aβ, and M^{2+} simultaneously (condition i). In the presence of AChE/Aβ/Cu^{2+}, hybrid **19** showed a nearly 80-fold reduction (IC_{50} = 182 ± 66 nM). In the presence of AChE/Aβ/Zn^{2+}, the reduction was nearly 50-fold (IC_{50} = 111 ± 30 nM). The case of AChE/Aβ/Zn^{2+} should be noted in that, of all the conditions tested with Zn^{2+} present, it was the only one that showed a significant change in IC_{50}.

The fact that **19** maintains much of its inhibition potential when exposed to M^{2+}-treated Aβ prior to AChE, but not when exposed to Aβ prior to AChE, may have implications for future *in vivo* studies. However, it is difficult to predict the order of interaction between these components in complex living systems. Regardless, the results described above indicate that hybrid **19** remains a relatively potent AChEi when interacting with M^{2+} and Aβ.

4.3.2.4. Effect of metals and Aβ on BChE inhibition

The effects of Cu^{2+}, Zn^{2+}, Aβ, and M^{2+}-treated Aβ on BChE inhibition were also tested (Table 4.1). In general, hybrid **19** maintained good inhibition of BChE, never losing more than 32-fold activity when compared to compound alone. Interestingly, with BChE, Cu^{2+} never increased the IC_{50} value by more than 4-fold (conditions a-c), while with AChE, the presence of Cu^{2+} increased the IC_{50} value by up to 60-fold. On the other hand, Zn^{2+} actually improved the inhibitory activity by *ca.* 3-fold ($IC_{50} = 0.713 \pm 0.065$) when added to the inhibitor-BChE complex (condition a). Similarly, the addition of Aβ to the inhibitor-BChE complex (condition d) resulted in a 4-fold increase in inhibitory activity ($IC_{50} = 0.554 \pm 0.138$ nM) when compared to hybrid **19**. In addition, a slight increase in inhibitory activity was seen when BChE was added to the Zn^{2+}-inhibitor or Aβ-inhibitor complex (conditions b and e), but no relative change was observed when Zn^{2+} and BChE or Aβ and BChE were added simultaneously (conditions c and f).

Larger shifts in BChE IC_{50} values were seen when hybrid **19** was tested in the presence of M^{2+} and Aβ simultaneously (conditions g-i, Table 4.1). While the effect on inhibition was minimal when Cu^{2+}/Zn^{2+}-treated Aβ was added to the inhibitor-BChE complex (condition g), the inhibitory activity of hybrid **19** was decreased 11-fold ($IC_{50} = 23.0 \pm 3.2$ nM) when it interacted with Cu^{2+}-treated Aβ before being exposed to BChE (condition h). However, this same effect was not seen when **19** interacted with Zn^{2+}-treated Aβ before being exposed to BChE. The worst perturbation of activity arose when hybrid **19** interacted with BChE, Aβ, and M^{2+} simultaneously (condition i). In the presence of BChE/Aβ/Cu^{2+}, hybrid **19** showed a 32-fold reduction in inhibitory activity ($IC_{50} = 65.4 \pm 6.7$ nM). In the presence of BChE/Aβ/Zn^{2+}, the reduction was 21-fold ($IC_{50} = 41.5 \pm 8.4$nM). Overall, while the inhibition of BChE by hybrid **19** is disturbed in the presence of Aβ and metal species, the resulting change is less severe than that observed with AChE.

4.3.2.5. Metal binding

The ability of compounds **16**, **6h**, **18**, and **19** to bind Cu^{2+} and Zn^{2+} was studied by UV-Visible (UV-Vis) and nuclear magnetic resonance (NMR) spectroscopy (Fig. 4.3 A-D).

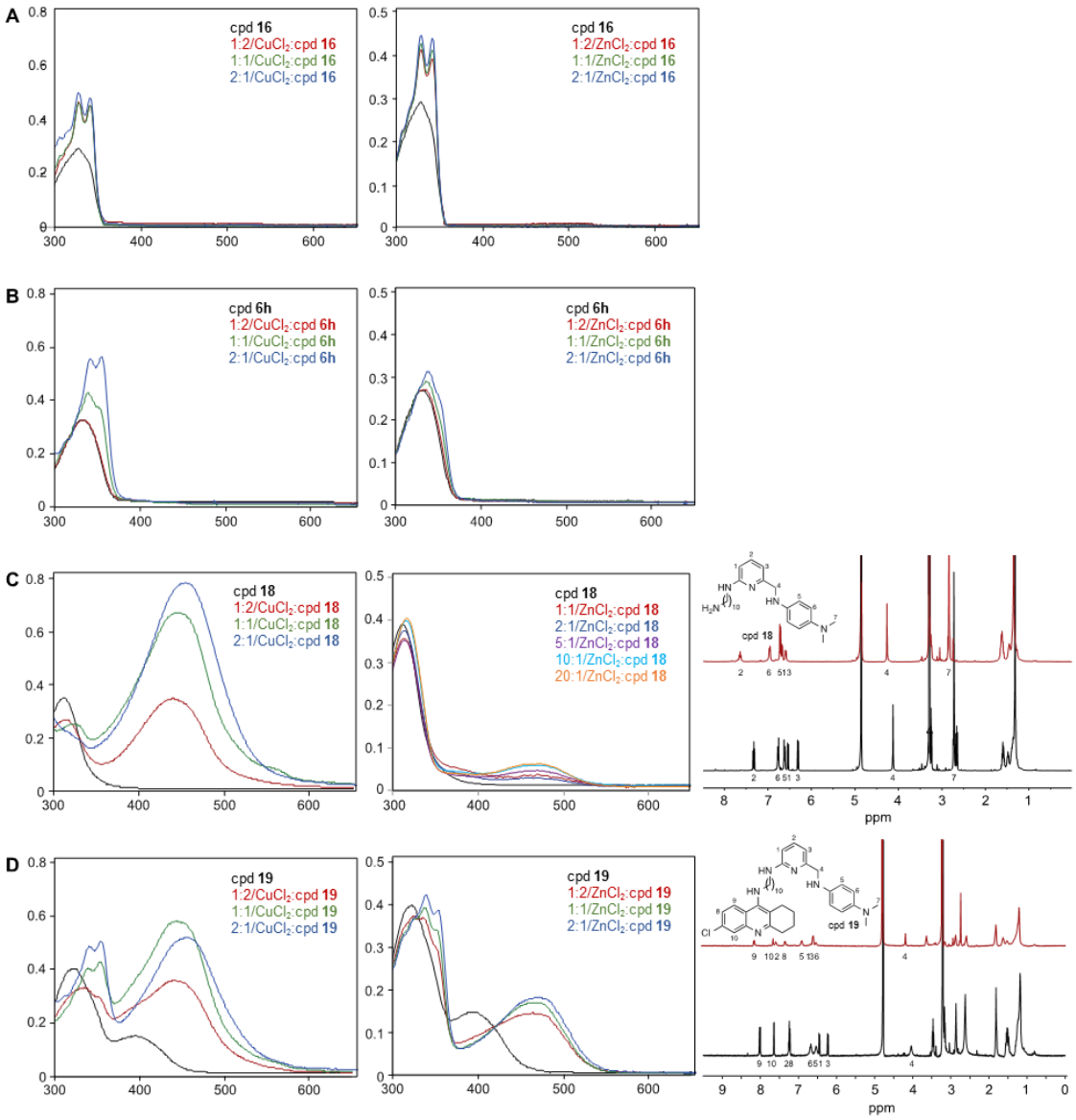

Fig. 4.3. Metal binding studies of **A.** cpd **16**, **B.** cpd **6h**, **C.** cpd **18**, and **D.** cpd **19** with $CuCl_2$ (left) or $ZnCl_2$ (middle) by UV-Vis. Conditions: [compound] = 40 μM; [$CuCl_2$ or $ZnCl_2$] = 20-800 μM; 30 min incubation (4 h for Zn^{2+} binding for cpd **18**); rt. **C** and **D.** right panel = Zn^{2+} binding of **18** or **19** by ^1H NMR. NMR spectra of **18** or **19** (black, 2.0 mM) with $ZnCl_2$ (red, 3.2 mM) in CD_3OD at rt.

The Cu^{2+} and Zn^{2+} binding properties of compound **17** were previously reported.[34,42] New optical bands were observed in the UV-Vis spectra of compounds **16** and **6h** upon the addition of $CuCl_2$ or $ZnCl_2$, suggesting that these compounds were able to interact with Cu^{2+}/Zn^{2+} (Fig. 4.3A and B). More importantly, compound **18** and hybrid **19**, which were designed as metal chelators, showed promising metal binding properties. Upon incubation of $CuCl_2$ with ligand (**18** or **19**) in EtOH, new optical bands (*ca.* 450 nm and 440 nm for

18 and **19**, respectively) were indicated, implicating complex formation *via* metal chelation (Fig. 4.3C and D). Moreover, **18** or **19** treated with $ZnCl_2$ displayed a new optical band at *ca.* 440 nm suggesting Zn^{2+} binding (Fig. 4.3C and D). In addition, ^{1}H NMR investigation was used to examine possible interaction between compound **18** or **19** and Zn^{2+}. Distinguishable downfield chemical shifts of the pyridyl, methylene, and aromatic protons were seen in the resulting spectrum of **18** or **19** when incubated with Zn^{2+} (Fig. 4.3C and D, right panel). This suggests that both compounds are able to bind Zn^{2+} through the N-donor atoms on the pyridine ring and amino group.

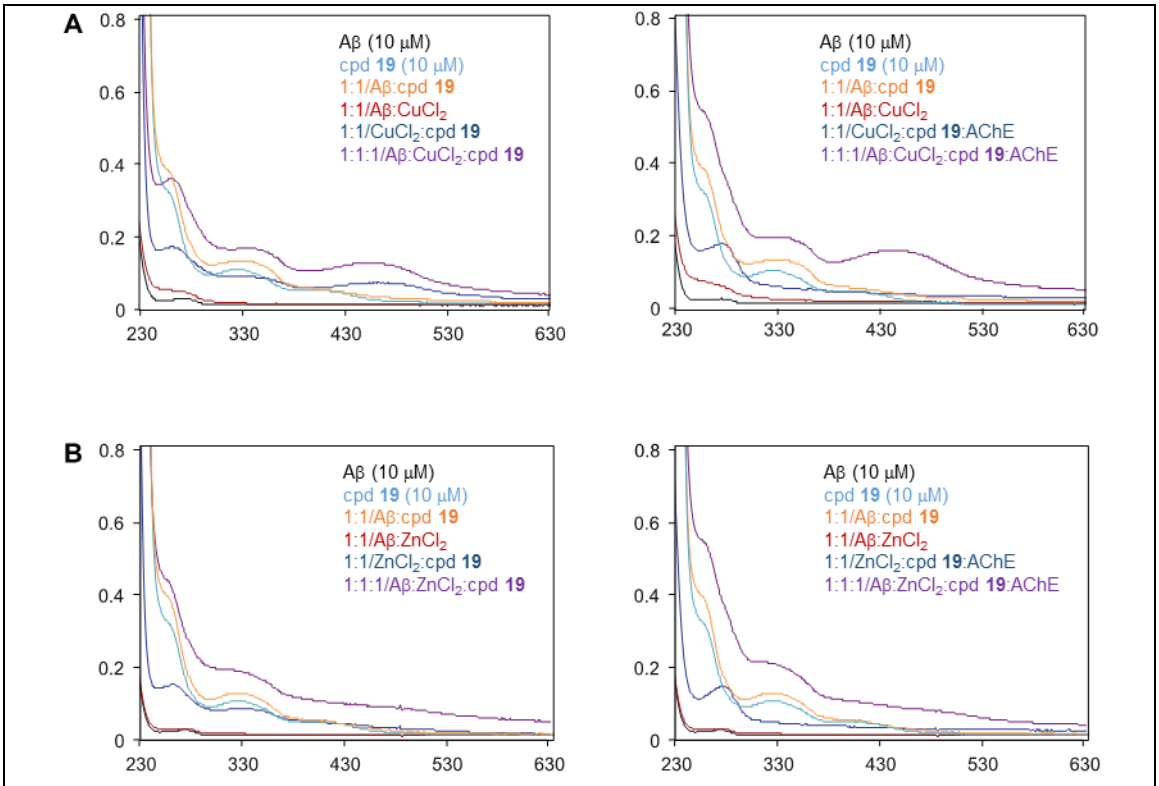

Fig. 4.4. Metal binding studies of **19** with **A.** $CuCl_2$ or **B.** $ZnCl_2$ in the absence and presence of Aβ and/or AChE at pH 6.6 (Cu^{2+}) and 7.4 (Zn^{2+}), monitored by UV-Vis. Spectra of Aβ, **19**, [Aβ + **19**], [Aβ + MCl_2], [MCl_2 + **19**], and [Aβ + MCl_2 + **19** ± AChE] are depicted in black, light blue, orange, red, dark blue, and purple, respectively. Conditions: [Aβ] = 10 μM; [$CuCl_2$ or $ZnCl_2$] = 10 μM; [AChE] = 10 μM; [**19**] = 10 μM (5% v/v DMSO); 20 mM HEPES, pH 6.6 (Cu^{2+}) and 7.4 (Zn^{2+}), 150 mM NaCl; rt.

Furthermore, the interaction of hybrid **19** with Cu^{2+}/Zn^{2+} was examined by UV-Vis in the presence of Aβ with or without AChE (Fig. 4.4A and B). For solutions containing Aβ and Cu^{2+} or Zn^{2+} with or without AChE, optical changes upon addition of **19** were similar to those observed from the samples containing **19** incubated with Cu^{2+} or Zn^{2+} alone, which

implies that **19** has the ability to interact with Cu^{2+} or Zn^{2+} in the presence of Aβ and AChE. While other metal/Aβ-targeted tacrine hybrids have shown the ability to bind biometals,[8,37] this is the first instance where a tacrine-metal chelator hybrid has been shown to bind Cu^{2+} or Zn^{2+} in the presence of Aβ and AChE. Overall, the UV-Vis and NMR results demonstrate Cu^{2+} and Zn^{2+} interaction of compounds **16**, **6h**, **18**, and **19**, as well as the potential interaction of **19** with Cu^{2+} and Zn^{2+} surrounded by Aβ and AChE. These results may correlate to the reactivity of the compounds towards metal-Aβ species *in vitro* (*vide infra*).

4.3.2.6. Aβ aggregation inhibition

In addition to examining the AChE inhibitory activity and metal binding properties of hybrid **19**, its influence, compared to compounds **6h** and **16-18**, on metal-free and metal-induced $A\beta_{1-40}$ aggregation in the absence and presence of AChE was studied *in vitro*. Two different Aβ aggregation studies were carried out: inhibition (Fig. 4.5A) and disaggregation (Fig. 4.6A). The distribution of various-sized Aβ species in both experiments was analyzed by gel electrophoresis followed by Western blotting with an anti-Aβ antibody (6E10), and morphologies of the resulting Aβ species were identified by transmission electron microscopy (TEM).

The inhibition experiment was conducted to determine whether compounds **6h** and **16-19** were able to control the formation of metal-free and metal-associated Aβ aggregates in the absence and presence of AChE (Fig. 4.5A-C). Aβ species having a dispersion of molecular weight (MW) were observed with both metal-free and metal-treated conditions with and without AChE upon treatment with hybrid **19** (Fig. 4.5B, lanes 6). Noticeable differences in the MW distribution of the generated Aβ species were indicated between Cu^{2+}-treated and Zn^{2+}-treated samples with and without AChE upon incubation with **19** (Fig. 4.5B, lanes 6). In addition, TEM analysis of metal-free and metal-induced Aβ species with and without AChE upon treatment with hybrid **19** displayed a mixture of amorphous and structured peptide species distinct from those of untreated samples (Fig. 4.5C). Metal/ Aβ-targeted tacrine hybrids have been shown to inhibit self-induced and

AChE-induced Aβ aggregation in previous studies.[37-39,43,44] However, there exists little precedent for demonstrating modulation of metal-associated Aβ species among these hybrids making the results seen with **19** unique.

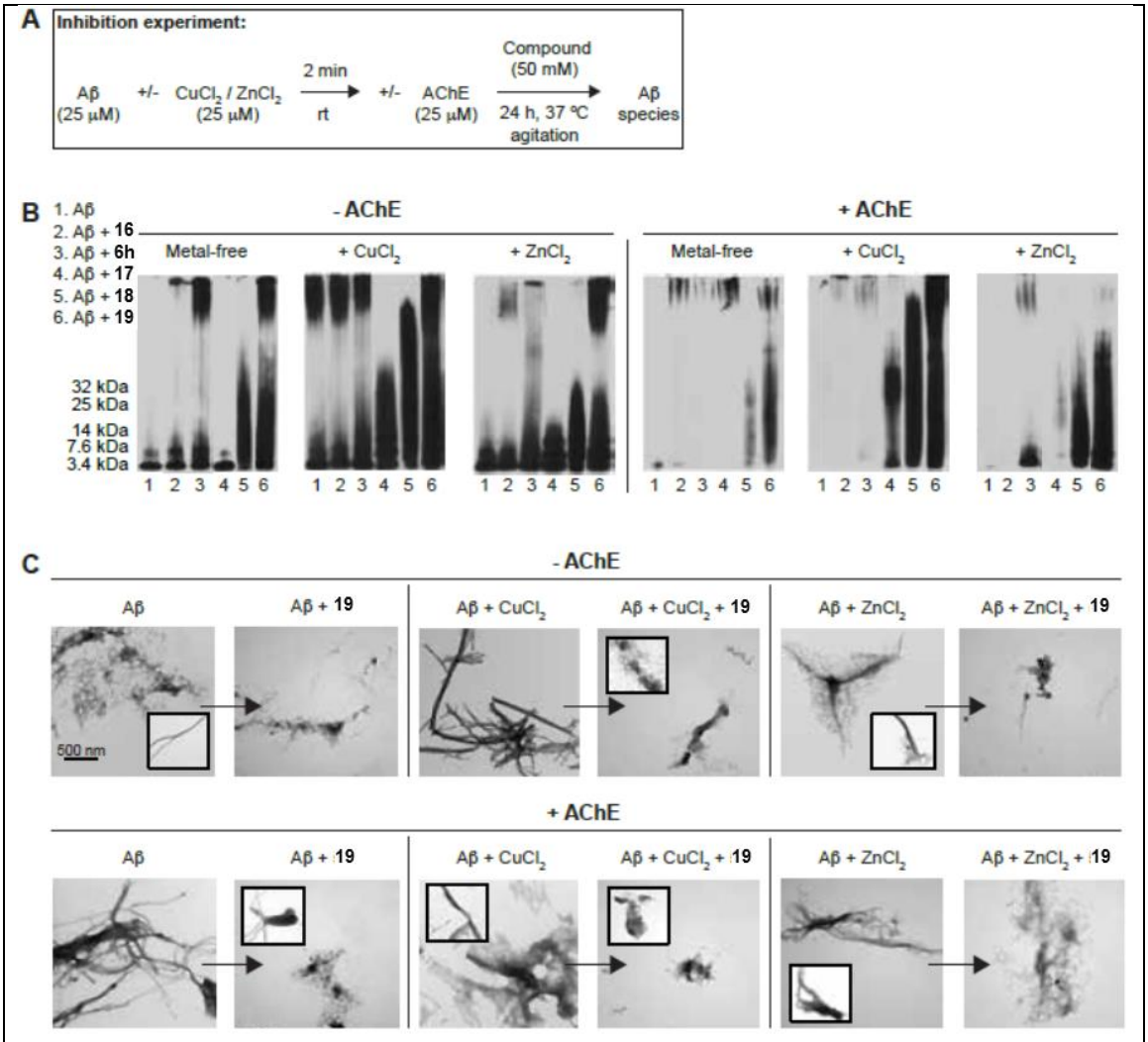

Fig. 4.5. *In vitro* studies of the influence of **6h** and **16**-**19** on metal-free and metal-associated $A\beta_{1-40}$ aggregation with and without AChE. **A.** Scheme of the inhibition experiment. **B.** Visualization of various-sized Aβ species in the absence (left) and presence (right) of AChE by gel electrophoresis with Western blot (anti-Aβ antibody, 6E10). **C.** TEM images of the 24 h incubated samples. Conditions: [Aβ] = 25 μM; [$CuCl_2$ or $ZnCl_2$] = 25 μM; [AChE] = 25 μM; [compound] = 50 μM; pH 6.6 (for Cu^{2+} samples) or 7.4 (for metal-free and Zn^{2+} samples); 24 h incubation; 37 °C; constant agitation.

The reactivity of metal-Aβ modulator linker **18**, which has the same metal chelation moiety and linker region as **19** minus the AChEi moiety, towards both metal-free and metal-involved Aβ aggregation with and without AChE was similar to that of **19** (Fig.

4.5B, lanes 5 and 6). However, metal-Aβ modulator **17**, which lacks the linker region and AChEi moiety, showed distinguishable reactivity with metal-treated samples with and without AChE compared to metal-free samples resulting in Aβ species that have MW ≤ 32 kDa (Fig. 4.5B, lanes 4).[34] Comparing the results across all compounds of interest, the presence of the linker region in compounds **6h**, **18**, and **19** gave greater reactivity towards metal-free and metal-associated Aβ species with and without AChE (Fig. 4.5B, **6h**/**19** *versus* **16** and **18**/**19** *versus* **17**). These results suggest the importance of the linker region, possibly by virtue of the increased hydrophobicity that it lends, for Aβ reactivity. Overall, hybrid **19** displayed the desired multifunctionality by presenting varying degrees of regulatory activity towards metal-free and metal-mediated Aβ aggregation with and without AChE *in vitro*. This activity may result from combined properties of metal chelation, Aβ interaction, and hydrophobicity.

4.3.2.7. Disaggregation of Aβ aggregates

Disaggregation of preformed Aβ aggregates by other tacrine-derived hybrids has, to our knowledge, not been reported. Here, the disaggregation experiment was performed to assess the ability of compounds **6h** and **16**-**19** to disassemble preformed metal-free and metal-associated $A\beta_{1\text{-}40}$ aggregates in the absence and presence of AChE (Fig. 4.6A and B). Similar to the results from the inhibition experiment, a wide array of both metal-free and metal-induced Aβ species in the absence of AChE were observed upon treatment with hybrid **19** (Fig. 4.6B, lanes 6). However, in the presence of AChE, diverse-sized Aβ species generated by incubation with **19** were only visualized under metal-involved conditions. Also, as before, Aβ species having variable MW were detected between Cu^{2+}- and Zn^{2+}-treated samples with and without AChE upon treatment with **19** (Fig. 4.6B, lanes 6). The overall reactivity of **18** towards preformed metal-free and metal-mediated Aβ aggregates with and without AChE was similar to that of **19** (Fig. 4.6B, lanes 5). Relative to **19**, samples containing Aβ and **17** presented a smaller range of MW in both metal-free and metal-treated cases with and without AChE. (Fig. 4.6B, lanes 4). Analogous to the inhibition results, compounds containing the linker region were shown to have greater reactivity towards metal-free and metal-associated Aβ aggregates in the absence and presence of

AChE (Fig. 4.6B, in particular, **17** *versus* **18**). Taken together, these results suggest that hybrid **19**, in addition to being able to modulate the formation of metal-free and metal-induced Aβ aggregates with and without AChE, has the ability to impact preformed metal-free and metal-triggered Aβ aggregates with and without AChE to different extents.

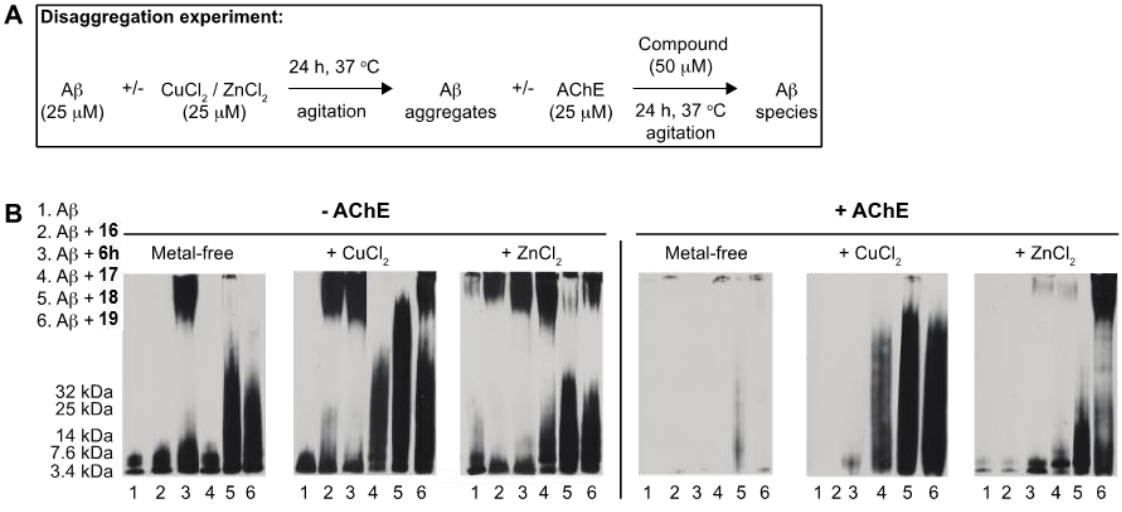

Fig. 4.6. Disaggregation studies using **6h** and **16-19** with and without AChE. **A.** Scheme of the disaggregation experiment. **B.** Visualization of various-sized $A\beta_{1\text{-}40}$ species in the absence (left) and presence (right) of AChE by gel electrophoresis with Western blot (anti-Aβ antibody, 6E10). Conditions: [Aβ] = 25 μM; [$CuCl_2$ or $ZnCl_2$] = 25 μM; [AChE] = 25 μM [compound] = 50 μM; pH 6.6 (for Cu^{2+} samples) or 7.4 (for metal-free and Zn^{2+} samples); 24 h incubation; 37 °C; constant agitation.

4.3.2.8. Molecular modeling

Molecular modeling was performed in an effort to visualize the interactions of hybrid **19** with AChE and Aβ. Modeling was performed with GOLD[45] using AChE from *Torpedo californica* (*Tc*AChE) and $A\beta_{1\text{-}40}$ (PDB codes: 1ACJ[46] and 2LFM,[47] respectively). Hybrid **19** was docked into the tacrine binding site of an energy optimized $A\beta_{1\text{-}40}$-*Tc*AChE complex, and the first-ranked conformation is shown (Fig. 4.7A and B).

The energy optimized $A\beta_{1\text{-}40}$-*Tc*AChE complex showed a close association between the two components (Fig. 4.7A). As expected, the 6-chlorotacrine moiety of **19** was positioned in the CAS of the enzyme with the quinoline ring system stacked between W84 and F330 and the nitrogen of the quinoline ring in close proximity to H440 (Fig. 4.7B). The linker region of **19** was positioned such that it extended from the CAS to the PAS of the

enzyme by spanning the gorge region. These modeling results are consistent with previous docking studies on tacrine-based linkers and hybrids with *Tc*AChE.[9,12,48,49] Of more interest is the predicted binding of the metal chelator moiety of **19** and its potential interactions with Aβ. This moiety was predicted to bind near the PAS of AChE and in close proximity to H6, H13, and H14 of $A\beta_{1\text{-}40}$ (Fig. 4.7B). These residues are known to be important for interaction of M^{2+} with Aβ.[27-31,50] In addition, N-donor atoms from the pyridine ring and amino group of the metal chelator moiety of **19** were predicted to be in the correct geometry to coordinate M^{2+}.

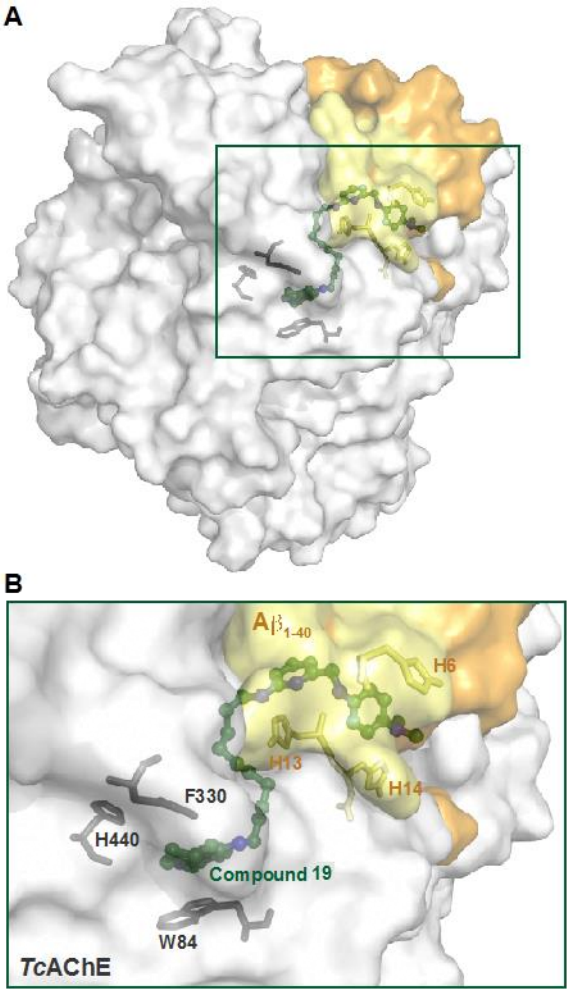

Fig. 4.7. Hybrid **19** docked with $A\beta_{1\text{-}40}$-*Tc*AChE complex. **A.** Interaction of **19** with *Tc*AChE (grey) and $A\beta_{1\text{-}40}$ (yellow/orange). **B.** Close-up of important interactions between **19** and W84, H440, and F330 (grey) from *Tc*AChE and H6, H13, and H14 (yellow) from $A\beta_{1\text{-}40}$. Carbon and nitrogen atoms of **19** are shown in green and blue, respectively.

4.3.2.9. Blood-brain barrier permeability

An essential characteristic for any anti-AD compound is the ability to cross the blood-brain barrier (BBB) and gain access to the central nervous system (CNS). BBB permeability for compounds **6h** and **16-19** was first predicted based on the calculated values of Lipinski's rules and logBB (Table 4.2), which suggested that they might be able to cross the BBB.[30,51,52] Along with this theoretical prediction, the potential BBB penetration of **6h** and **16-19** was verified by an *in vitro* parallel artificial membrane permeability-BBB (PAMPA-BBB) assay (Table 4.2).[34,53] Permeability values ($-\log P_e$) of **6h** and **16-19** were measured to be

5.1 ± 0.1 (for **16**, **6h**, and **18**), 4.0 ± 0.1 (for **17**),[34] and 4.8 ± 0.1 (for **19**). Based on empirical classification of known BBB permeable molecules (*e.g.*, verapamil), our chemical scaffolds (in particular, hybrid **19**) could potentially be BBB permeable. Similar results have been seen in this type of assay with tacrine-8-hydroxyquinoline hybrids and pyrano[3,2-*c*]quinoline-6-chlorotacrine hybrids.[8,38] However, the PAMPA-BBB prediction only takes into account passive diffusion across the BBB. Permeability is likely more complex given the enzymes and efflux transporters (*e.g.*, P-glycoprotein) that are known to prevent xenobiotic entry into the CNS, and future studies will aim to elucidate how hybrid **19** interacts with these biochemical barriers.

Table 4.2. Values (MW, *c*log*P*, HBA, HBD, PSA, logBB, and -logP_e) for compounds **6h** and **16**-**19**.

Calculation[a]	Cpd **16**	Cpd **6h**	Cpd **17**[b]	Cpd **18**	Hybrid **19**	Lipinski's rules and others
MW	233	388	227	398	613	500
*c*log*P*	4.08	7.76	1.76	5.10	10.7	≤ 5.0
HBA	2	3	3	5	6	≤ 10
HBD	2	3	1	4	3	≤ 5.0
PSA	38.9	50.9	28.2	66.2	65.1	≤ 90
logBB	0.174	0.555	-0.0197	-0.0744	0.785	> 0.3 (readily cross the BBB)
						< -1.0 (poor brain distribution)
-logP_e[c]	5.1 ± 0.1	5.1 ± 0.1	4.0 ± 0.1	5.1 ± 0.1	4.8 ±0.1	
CNS+/-	CNS+	CNS+	CNS+	CNS+	CNS+	-logP_e < 5.4 (CNS+)
prediction[d]						-logP_e > 5.7 (CNS-)

[a] MW: molecular weight; *c*log*P*: calculated logarithm of the octanol-H_2O partition coefficient; HBA: hydrogen bond acceptor; HBD: hydrogen bond donor; PSA: polar surface area; logBB: -0.0148 x PSA + 0.152 x *c*log*P* + 0.130. [b] The values for cpd **17** were previously reported.[34] [c] The values of -logP_e were obtained using the parallel artificial membrane permeability assay adapted for blood-brain barrier (PAMPA-BBB). [d] CNS+/- prediction: prediction of compound penetration to the central nervous system (CNS).

4.4. Conclusion

In conclusion, a novel hybrid **19** of 6-chlorotacrine and metal-Aβ modulator has been synthesized and evaluated *in vitro*. This compound showed potent inhibition of both AChE and BChE, and this potent inhibition was largely retained in the presence of ROS, M^{2+}, and Aβ. Additionally, **19** showed the ability to bind Cu^{2+} and Zn^{2+}, and it was able to effectively modulate the assembly of metal-free and metal-induced Aβ aggregates in the presence and absence of AChE. Furthermore, this compound presented the ability to transform preformed metal-free and metal-associated Aβ aggregates with and without

AChE. Molecular modeling predicted that **19** was able to simultaneously interact with the CAS and PAS of AChE and with histidine residues known to be involved in M^{2+} binding in the Aβ peptide. A PAMPA-BBB assay predicted the BBB penetrability of **19**. Together, these results make hybrid **19** a worthy candidate for additional studies. As both a tacrine-8-hydroxyquinoline hybrid and a tacrine-melatonin hybrid have shown the ability to decrease Aβ deposits using an *in vivo* mouse model,[11,54] similar results would be anticipated for hybrid **19**. However, due to the hepatotoxicity associated with tacrine, the next generation of hybrids capable of disaggregating metal-free and metal-triggered preformed Aβ aggregates as well as inhibiting cholinesterases and Aβ aggregation for *in vivo* studies will be composed of other currently used AD treatments, such as donepezil and galantamine. The synthesis and *in vitro* studies of such hybrids are currently underway in our laboratories.

4.5. Materials and instrumentation

Compounds **6h**[9] and **17**[34] were prepared as previously reported. $A\beta_{1-40}$ (DAEFRHDSGYEVHHQKLVFFAEDVGSNKGAIIGLMVGGVV) was purchased from Anaspec (Fremont, CA). All reagents for chemical synthesis were purchased from Sigma-Aldrich (St. Louis, MO) and used without further purification. Reactions were monitored by TLC (Merck, Silica gel 60 F_{254}). Visualization was achieved using the following methods: UV absorption by fluorescence quenching or a ninhydrin stain (ninhydrin (1.5 g), *n*-butanol (100 mL), AcOH (3 mL)). Compounds were purified by SiO_2 flash chromatography (Dynamic Adsorbents Inc., Flash Silica Gel 32-63u). ^{1}H and ^{13}C NMR spectra were recorded on a Bruker Avance™ DPX 500 or Varian 400 MHz spectrometer. Liquid chromatography mass spectrometry (LCMS) was performed on a Shimadzu LCMS-2019EV equipped with a SPD-20AV UV-Vis detector and a LC-20AD liquid chromatograph. HRMS was performed on a Micromass AutoSpec Ultima Magnetic sector mass spectrometer. Optical spectra for metal binding studies were obtained using an Agilent 8453 UV-Vis spectrophotometer. Analyses by UV-Vis assays (determination of IC_{50} values and parallel artificial membrane permeability assay for blood-brain barrier penetration (PAMPA-BBB)) were carried out on a multimode SpectraMax M5 plate reader (Molecular Devices, Sunnyvale, CA) using 96-well plates

(Fisher Scientific). Transmission electron microscopy (TEM) images were recorded on a Philips CM-100 transmission electron microscope (Microscopy and Image Analysis Laboratory, University of Michigan, Ann Arbor, MI). Molecular modeling was performed using Sybyl-X and GOLD.[45]

4.6. Methods

4.6.1. Chemical methods

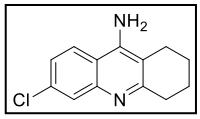

4.6.1.1. Preparation of 6-chloro-1,2,3,4-tetrahydroacridin-9-amine (16). The known compound **16** was prepared in a manner similar to those previously established in the literature.[5,6] Briefly, 2-amino-4-chlorobenzonitrile (382 mg, 2.5 mmol, 1 eq), cyclohexanone (1.26 mL, 12.2 mmol, 4.9 eq), and anhydrous $ZnCl_2$ (750 mg, 5.5 mmol, 2.2 eq) were combined and heated at 125 °C for 3 h. The reaction mixture was cooled to rt and treated with H_2O (50 mL). The remaining solid was collected by vacuum filtration, treated with 1 M aq. NaOH (50 mL), and heated to reflux for 16 h. The reaction mixture was then cooled to rt and extracted with $CHCl_3$ (3 x 50 mL). The combined organic layers were washed with brine (50 mL), dried ($MgSO_4$), filtered, and concentrated under reduced pressure to afford a crude yellow solid, which was purified by flash column chromatography (SiO_2, 9:1/EtOAc:MeOH, R_f 0.15) to yield **16** (135 mg, 23%) as an off-white solid: ^{1}H NMR ($(CD_3)_2SO$, 400 MHz) δ 8.18 (d, 1H, J = 9.0 Hz), 7.62 (d, 1H, J = 2.0 Hz), 7.28 (dd, 1H, J_1 = 9.0 Hz, J_2 = 2.0 Hz,), 6.48 (s, 2H), 2.81 (t, 2H, J = 5.4 Hz), 2.53 (t, 2H, J = 5.5 Hz), 1.81 (m, 4H); ^{13}C NMR ($(CD_3)_2SO$, 100 MHz) δ 158.8, 148.3, 147.0, 132.4, 126.4, 124.2, 122.7, 115.6, 109.4, 33.5, 23.6, 22.5, 22.4; LRMS *m/z* calcd for $C_{13}H_{13}ClN_2$: 232.08; found 233.00 $[M+H]^+$.

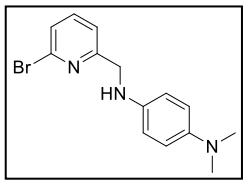

4.6.1.2. Preparation of N^1-((6-bromopyridin-2-yl)methyl)-N^4,N^4-dimethylbenzene-1,4-diamine (20). 6-Bromo-2-pyridinecarboxaldehyde (1 g, 5.38 mmol, 1 eq), *N*,*N*-dimethyl-*p*-phenylenediamine (733 mg, 5.38 mmol, 1 eq), and EtOH (40 mL) were combined and heated to reflux for 1 h. The reaction was cooled to rt, and $NaBH_4$ (1.1 g, 28.8 mmol, 5.4 eq) was added. The reaction was again heated to reflux for 1 h before being cooled to rt, quenched with H_2O (100 mL), and extracted with Et_2O (3 x 50 mL).

The combined organic layers were washed with brine (100 mL), dried ($MgSO_4$), filtered, and concentrated under reduced pressure to afford a crude brown oil, which was purified by flash column chromatography (SiO_2, 1:1/hexanes:EtOAc, R_f 0.43) to yield **20** (1.5 g, 91%) as a brown solid: ^{1}H NMR ($CDCl_3$, 400 MHz) δ 7.48 (t, 1H, *J* = 7.7 Hz), 7.35 (d, 1H, *J* = 7.8 Hz), 7.32 (d, 1H, *J* = 7.6 Hz), 6.76-6.58 (m, 4H), 4.41 (br s, 2H), 2.83 (br s, 6H); ^{13}C NMR ($CDCl_3$, 100 MHz) δ 161.5, 144.3, 141.6, 139.9, 139.1, 126.3, 120.3, 115.8, 114.5, 50.1, 42.2; LRMS *m/z* calcd for $C_{14}H_{16}BrN_3$: 305.05; found 305.75 $[M+H]^+$.

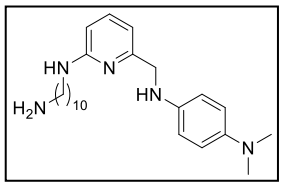

4.6.1.3. Preparation of N^1-((6-((10-aminodecyl)amino)pyridin-2-yl)methyl)-N^4,N^4-dimethylbenzene-1,4-diamine (18). Compound **20** (136 mg, 0.443 mmol, 1 eq), 1,10-diaminodecane (305 mg, 1.77 mmol, 4 eq), and 1-pentanol (2 mL) were combined and heated to reflux for 14 h. The reaction was cooled to rt, diluted with CH_2Cl_2 (50 mL), and washed with 10% aq. KOH (2 x 50 mL), H_2O (2 x 50 mL), and brine (50 mL). The organic layer was dried ($MgSO_4$), filtered, and concentrated under reduced pressure to afford a crude yellow oil, which was purified by flash column chromatography (SiO_2, 7:3/CH_2Cl_2:MeOH with NH_4OH (7 mL/L of solvent), R_f 0.76). Further purification by flash column chromatography (SiO_2, 9:1/CH_2Cl_2:MeOH with NH_4OH (7 mL/L of solvent), R_f 0.23) removed remaining impurities and gave **18** (47 mg, 27%) as a dark yellow solid: ^{1}H NMR ($CDCl_3$, 400 MHz) δ 7.36 (t, 1H, *J* = 7.9 Hz), 6.73 (d, 2H, *J* = 8.8 Hz), 6.65 (d, 2H, *J* = 8.8 Hz), 6.58 (d, 1H, *J* = 7.3 Hz), 6.23 (d, 1H, *J* = 8.2 Hz), 4.56 (br t, 1H, *J* = 5.1 Hz), 4.19 (s, 2H), 3.22 (q, 2H, *J* = 6.6 Hz), 2.80 (s, 6H), 2.68 (t, 2H, *J* = 7.0 Hz), 1.61 (p, 2H, *J* = 7.2 Hz), 1.46-1.36 (m, 4H), 1.29 (s, 10H) (Fig. 4.8); ^{13}C NMR ($CDCl_3$, 100 MHz) δ 158.8, 157.4, 144.2, 141.0, 138.1, 116.0, 114.6, 110.4, 104.1, 50.4, 42.5, 42.4, 42.2, 33.5, 29.7, 29.63, 29.62, 29.53, 29.49, 27.2, 27.0 (Fig. 4.9); HRMS *m/z* calcd for $C_{24}H_{39}N_5$: 397.3205; found 398.3260 $[M+H]^+$.

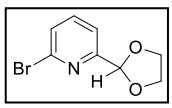

4.6.1.4. Preparation of 2-bromo-6-(1,3-dioxolan-2-yl)pyridine (21). The known compound **21** was prepared by following a modified protocol of previously reported procedures.[55,56] A solution of 6-bromo-2-pyridinecarboxaldehyde (2.0 g, 10.8 mmol, 1 eq), ethylene glycol (1.2 mL, 21.5 mmol, 2 eq), and methanesulfonic acid

(230 μL, 3.55 mmol, 0.33 eq) in toluene (65 mL) was heated to reflux in a Dean-Stark apparatus for 24 h prior to being cooled to rt and neutralized with saturated aq. $NaHCO_3$. The organic layer was separated and the aqueous phase was extracted with Et_2O (3 x 50 mL). The combined organic layers were washed with H_2O (3 x 50 mL) and brine (50 mL), dried ($MgSO_4$), filtered, and concentrated under reduced pressure to afford a crude yellow oil, which was purified by flash column chromatography (SiO_2, 1:1/hexanes:EtOAc, R_f 0.66) to yield **21** (1.81 g, 73%) as a pale yellow oil: ^{1}H NMR ($CDCl_3$, 500 MHz) δ 7.49 (t, 1H. J = 7.7 Hz), 7.38 (d, 1H, J = 7.3 Hz), 7.35 (d, 1H, J = 7.9 Hz), 5.68 (s, 1H), 4.06-3.99 (m, 2H), 3.97-3.90 (m, 2H); ^{13}C NMR ($CDCl_3$, 125 MHz) δ 158.3, 141.3, 139.0, 128.2, 119.3, 102.5, 65.4.

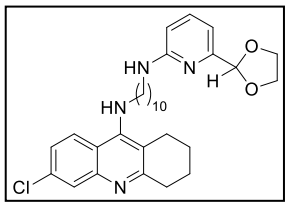

4.6.1.5. Preparation of N^1-(6-(1,3-dioxolan-2-yl)pyridin-2-yl)-N^{10}-(6-chloro-1,2,3,4-tetrahydroacridin-9-yl)decane-1,10-diamine (22). Compound **21** (500 mg, 2.17 mmol, 1 eq), compound **6h** (1.25 g, 3.23 mmol, 1.5 eq), CuI (21 mg, 0.109 mmol, 0.05 eq), L-proline (25 mg, 0.217 mmol, 0.10 eq), K_2CO_3 (45 mg, 0.326 mmol, 0.15 eq), DMSO (8 mL), and H_2O (800 μL) were combined and stirred at 90 °C for 47 h. The reaction was cooled to rt, diluted with H_2O (150 mL), and extracted with CH_2Cl_2 (3 x 50 mL). The combined organic layers were washed with H_2O (3 x 50 mL) and brine (50 mL), dried ($MgSO_4$), filtered, and concentrated under reduced pressure to afford a crude brown oil, which was purified by flash column chromatography (SiO_2, 49:1/CH_2Cl_2:MeOH with NH_4OH (7 mL/L of solvent) to 19:1/CH_2Cl_2:MeOH with NH_4OH (7 mL/L of solvent), R_f 0.41 (9:1/CH_2Cl_2:MeOH with NH_4OH (7 mL/L of solvent))) to yield **22** (249 mg, 21%) as a yellow oil: ^{1}H NMR ($CDCl_3$, 400 MHz) δ 7.84 (d, 1H, J = 9.0 Hz), 7.83 (s, 1H), 7.39 (t, 1H, J = 7.8 Hz), 7.20 (dd, 1H, J_1 = 9.0 Hz, J_2 = 1.4 Hz), 6.73 (d, 1H, J = 7.3 Hz), 6.29 (d, 1H, J = 8.4 Hz), 5.63 (s, 1H), 4.65 (br t, 1H, J = 5.0 Hz), 4.13-4.05 (m, 2H), 4.02-3.96 (m, 2H), 3.94 (br s, 1H), 3.42 (br t, 2H), 3.15 (q, 2H, J = 6.6 Hz), 2.97 (br t, 2H), 2.60 (br t, 2H), 1.85 (br p, 4H), 1.59 (p, 2H, J = 7.0 Hz), 1.54 (p, 2H, J = 7.3 Hz), 1.32-1.29 (m, 4H), 1.23 (br s, 8H); ^{13}C NMR ($CDCl_3$, 100 MHz) δ 159.4, 158.8, 155.4, 150.8, 148.1, 138.0, 133.8, 127.5, 124.6, 124.0, 118.4, 115.6, 108.9, 106.0, 103.6, 65.3, 49.6, 42.3, 34.0, 31.7, 29.42, 29.38, 29.27, 29.26, 27.0, 26.8, 24.5, 22.9, 22.6; LRMS *m/z* calcd for $C_{31}H_{41}ClN_4O_2$:

536.29; found 537.35 $[M+H]^+$.

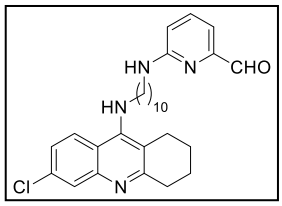

4.6.1.6. Preparation of 6-((10-((6-chloro-1,2,3,4-tetrahydroacridin-9-yl)amino)decyl)amino)picolinaldehyde (23). A solution of compound **22** (91 mg, 0.170 mmol) in MeCN (2.2 mL) and 2 M aq. HCl (1.1 mL) was stirred at 60 °C for 23 h. The reaction was cooled to rt, slowly quenched with saturated aq. $NaHCO_3$, and extracted with CH_2Cl_2 (3 x 25 mL). The combined organic layers were washed with brine (50 mL), dried ($MgSO_4$), filtered, and concentrated under reduced pressure to yield **23** (81 mg, 96%) as a yellow oil, which was used without any further purification: ^{1}H NMR ($CDCl_3$, 400 MHz) δ 9.82 (s, 1H), 7.85 (d, 1H, J = 9.1 Hz), 7.84 (s, 1H), 7.48 (t, 1H, J = 7.8 Hz), 7.20 (dd, 1H, J_1 = 9.1 Hz, J_2 = 1.9 Hz), 7.15 (d, 1H, J = 7.2 Hz), 6.53 (d, 1H, J = 8.4 Hz), 4.86 (br t, 1H), 4.03-3.97 (m, 1H), 3.43 (t, 2H, J = 7.2 Hz), 3.27 (q, 2H, J = 6.7 Hz), 2.98 (br t, 2H), 2.61 (br t, 2H), 1.85 (br p, 4H), 1.62 (p, 2H, J = 7.2 Hz), 1.57 (p, 2H, J = 7.4 Hz), 1.34-1.30 (m, 4H), 1.24 (br s, 8H); ^{13}C NMR ($CDCl_3$, 100 MHz) δ 193.8, 159.4, 159.1, 151.3, 150.9, 148.0, 137.8, 133.9, 127.4, 124.7, 124.1, 118.3, 115.6, 112.0, 111.5, 49.6, 42.1, 34.0, 31.8, 29.5, 29.4, 29.31, 29.28, 27.0, 26.9, 24.6, 22.9, 22.6; LRMS *m/z* calcd for $C_{29}H_{37}ClN_4O$: 492.27; found 493.20 $[M+H]^+$.

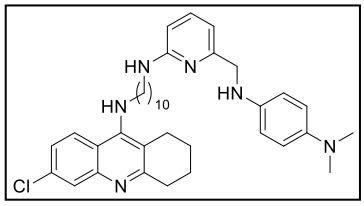

4.6.1.7. Preparation of N^1-((6-((10-((6-chloro-1,2,3,4-tetrahydroacridin-9-yl)amino)decyl)amino)pyridin-2-yl)methyl)-N^4,N^4-dimethylbenzene-1,4-diamine (19). To a solution of compound **23** (64 mg, 0.129 mmol, 1 eq) in EtOH (2.5 mL) was added *N*,*N*-dimethyl-*p*-phenylenediamine (18 mg, 0.129 mmol, 1 eq). The reaction mixture was heated to reflux for 1 h and cooled to 0 °C prior to addition of $NaBH_4$ (33 mg, 0.864 mmol, 6.7 eq). The reaction mixture was stirred at 0 °C for 5 min, warmed to rt, and stirred for an additional 30 min before quenching with H_2O (10 mL) and extracting with Et_2O (3 x 10 mL). The combined organic layers were dried ($MgSO_4$), filtered, and concentrated under reduced pressure to afford a crude yellow oil, which was purified by flash column chromatography (SiO_2, 19:1/CH_2Cl_2:MeOH with NH_4OH (7 mL/L of solvent), R_f 0.20) to yield **19** (41 mg, 52%) as a yellow oil: ^{1}H NMR ($CDCl_3$, 400

MHz) δ 7.888 (d, 1H, J = 1.5 Hz), 7.886 (d, 1H, J = 8.8 Hz), 7.35 (t, 1H, J = 7.7 Hz), 7.25 (dd, 1H, J_1 = 8.8 Hz, J_2 = 1.5 Hz), 6.73 (d, 2H, J = 8.6 Hz), 6.64 (d, 2H, J = 8.6 Hz), 6.58 (d, 1H, J = 7.3 Hz), 6.22 (d, 1H, J = 8.3 Hz), 4.56 (br t, 1H, J = 4.9 Hz), 4.19 (s, 2H), 3.97 (br s, 1H), 3.47 (t, 2H, J = 7.0 Hz), 3.22 (q, 2H, J = 6.6 Hz), 3.02 (br t, 2H), 2.80 (s, 6H), 2.65 (br t, 2H), 1.90 (br p, 4H), 1.64 (p, 2H, J = 7.1 Hz), 1.61 (p, 2H, J = 7.4 Hz), 1.39-1.35 (m, 4H), 1.29 (s, 9H) (Fig. 4.10); ^{13}C NMR ($CDCl_3$, 100 MHz) δ 159.5, 158.7, 157.4, 150.9, 148.2, 144.1, 141.0, 138.1, 134.0, 127.6, 124.7, 124.2, 118.5, 115.9, 115.7, 114.6, 110.4, 104.1, 50.3, 49.7, 42.44, 42.36, 34.1, 31.9, 29.7, 29.5, 29.44, 29.39, 27.2, 27.0, 24.6, 23.0, 22.7 (Fig. 4.11); HRMS *m/z* calcd for $C_{37}H_{49}ClN_6$: 612.3707; found 613.3600 $[M+H]^+$.

4.6.2. Biochemical, biophysical, and computational methods

4.6.2.1. *In vitro* AChE and BChE assay

Compounds of interest were dissolved in sodium phosphate (dibasic) buffer ((100 μL), 0.1 M, pH 8.0 adjusted at rt). AChE was added to the solution of inhibitors (50 μL, containing 0.08 U/mL (~0.29 nM) AChE (final concentration) (Sigma-Aldrich cat #C2888 from eel) in sodium phosphate (dibasic) buffer (100 mM, pH 8.0 adjusted at rt)). The mixture of inhibitor and enzyme was incubated for 10 min before initiation with a DTNB:acetylthiocholine (ATC) (0.25 mM:0.5 mM final concentration, respectively) mixture (50 μL) in phosphate buffer (100 mM, pH 8.0 adjusted at rt). The reaction was monitored at 412 nm taking measurements every 30 sec for 20 min on a SpectraMax M5 plate reader. Data was corrected with the negative control (no ATC) and normalized to the positive control (no inhibitor) using the initial rates (first 2-5 min). All assays were performed in triplicate. The data was fitted to a Hill-plot and IC_{50} values calculated using KaleidaGraph 4.1.1. All IC_{50} values are reported in Table 4.1. All butyrylcholinesterase (BChE) experiments were performed using identical conditions substituting butyrylthiocholine (BTC) for ATC.

4.6.2.2. *In vitro* AChE and BChE ROS inactivation assay

In the wells of a 96-well plate, horseradish peroxidase (0.25 μM), H_2O_2 (100 μM), AChE (0.08 U/mL, ~0.29 nM), inhibitors (25 μM to 13 pM), and DETAPAC (100 μM) were

dissolved in sodium acetate buffer (50 mM, pH 6.0 adjusted at rt) and incubated at 37 °C for 30 min. *Note*: all concentrations are reported as final concentrations. A DTNB:acetylthiocholine (ATC) (0.25 mM:0.5 mM final concentration, respectively) mixture in sodium phosphate (dibasic) buffer (50 mM, pH 7.4 adjusted at rt) was added to the AChE/inhibitor solution to initiate the reactions. The crude data was processed to obtain IC_{50} values as described in section 4.6.2.1. All IC_{50} values are reported in Table 4.1. BChE experiments were done in an identical manner substituting BTC for ATC.

4.6.2.3. Metal binding studies by UV-Vis and NMR spectroscopy

The interaction of compounds **6h** and **16-19** with 0.5-2 eq of Cu^{2+} or Zn^{2+} in EtOH was monitored by UV-Vis ([compound] = 40 μM (1% v/v final DMSO concentration); incubation for 30 min (4 h for Zn^{2+} binding for cpd **18**); rt) (Fig. 4.3). Metal binding properties of compound **19** in the presence of Aβ and/or AChE were also studied by UV-Vis (Fig. 4.4). Aβ (10 μM) was treated for 2 min with $CuCl_2$ or $ZnCl_2$ (10 μM) in HEPES (20 mM, pH 6.6 (for Cu^{2+}) or pH 7.4 (for Zn^{2+})) and NaCl (150 mM). AChE (10 μM) was added to the solution containing Aβ and Cu^{2+} or Zn^{2+}. The resulting sample was incubated for 5 min at rt and treated with compound **19** (10 μM, 5% v/v final DMSO concentration) followed by 5 min incubation. For comparison, optical spectra of the samples generated from incubation of compound **19** (10 μM) with $CuCl_2$ or $ZnCl_2$ (10 μM) for 5 min were measured. The interaction of compounds **18** and **19** with $ZnCl_2$ was observed by ^1H NMR (Fig. 4.3C,D). Compound **18** or **19** (2 mM) was dissolved in CD_3OD and treated with 1 eq of $ZnCl_2$. The resulting solution was incubated for 30 min prior to NMR measurement. Sequentially, 0.2 eq of $ZnCl_2$ was added to this solution until no further change in the NMR spectrum or precipitation was observed.

4.6.2.4. Aβ peptide experiments

To aliquot the $Aβ_{1-40}$ (1 mg), it was completely dissolved with the NH_4OH provided by the supplier, split into 5 aliquots, lyophilized, and stored at -80 °C. For assays, $Aβ_{1-40}$ solutions were prepared by addition of NH_4OH (10 μL, 1% v/v, aq) to the above aliquots followed by dilution with ddH_2O to obtain *ca.* 200 μM as determined by UV-Vis (280 nm, rt). For

both inhibition and disaggregation experiments (Fig. 4.5A and 4.6A), the buffer solution (20 μM HEPES, pH 6.6 (for Cu^{2+}) or pH 7.4 (for metal-free and Zn^{2+}), 150 μM NaCl) was used. For the inhibition experiment, Aβ (25 μM) was first treated with either $CuCl_2$ or $ZnCl_2$ (25 μM) for 2 min at rt followed by addition and incubation of AChE (25 μM) for 5 min (only for AChE-indicated samples). The resulting samples were then incubated with compounds **6h** and **16-19** (50 μM, 1% v/v final DMSO concentration) at 37 °C for 24 h with constant agitation. For the disaggregation experiment, Aβ (25 μM) was first incubated with $CuCl_2$ or $ZnCl_2$ (25 μM) at 37 °C for 24 h with constant agitation. The samples were then treated sequentially with AChE (25 μM, only for AChE-indicated samples) for 5 min followed by addition of compounds **6h** and **16-19** (50 μM; 1% v/v final DMSO concentration). These resulting solutions were incubated for an additional 24 h at 37 °C with constant agitation.

4.6.2.5. Gel electrophoresis with Western blotting

The Aβ peptide experiments (described in section 4.6.2.4) were analyzed by gel electrophoresis with Western blotting using anti-Aβ antibody (6E10) (Fig. 4.5B and Fig. 4.6B).[34,57] Various Aβ species generated by both inhibition and disaggregation experiments were separated by a 10-20% Tris-tricine gel (Invitrogen). The gel was transferred to a nitrocellulose membrane and blocked for 2 h with BSA (Sigma, 3% w/v) dissolved in Tris-buffered saline (TBS, Fisher) containing 0.1% Tween-20 (TBS-T, Sigma). The membrane was treated with 6E10 (1:2000; 2% BSA in TBS-T, Covance, Princeton, NJ) overnight at 4 °C with gentle agitation and probed with a horseradish peroxidase-conjugated goat anti-mouse secondary antibody (1:5000; Cayman Chemical, Ann Arbor, MI) in 2% BSA in TBS-T solution for 1 h at rt. The protein bands were visualized by using the ThermoScientific Supersignal West Pico Chemiluminescent Substrate (Fisher).

4.6.2.6. Transmission electron microscopy (TEM)

TEM samples were prepared following a previously reported method.[34,57] Glow-discharged grids (Formar/Carbon 300-mesh, Electron Microscopy Sciences, Hatfield, PA) were treated with the samples (5 μL) from either the inhibition or disaggregation experiment for

2 min at rt. Excess sample was removed with filter paper. The grids were washed five times with ddH_2O, stained with uranyl acetate (1% w/v, ddH_2O, 5 μL) for 1 min, and dried for 15 min at rt. A Philips CM-100 transmission electron microscope (80 kV, 25000x magnification) was used for obtaining TEM images of the samples (Fig. 4.5C).

4.6.2.7. Effect of metals and Aβ peptide on AChE and BChE inhibition

The AChE inhibitor **19** (10 μM to 5 pM) was dissolved in phosphate buffer (100 μL, 100 mM final concentration, pH 8.0 adjusted at rt), and one of three conditions was followed. Conditions (a), (d), and (g): AChE (25 μL, 0.08 U/mL final concentration) was added to the inhibitor solutions (100 μL) and incubated for 10 min prior to addition of $CuCl_2$ or $ZnCl_2$ or Aβ peptide (25 μL, 10 μM final concentration). After 10 min, the reactions were initialized with a DTNB:ATC (0.25 mM:0.5 mM final concentration, respectively) mixture (50 μL) in phosphate buffer (100 mM final concentration, pH 8.0 adjusted at rt). Conditions (b), (e), and (h): $CuCl_2$ or $ZnCl_2$ or Aβ peptide (25 μL, 10 μM final concentration) was added to the inhibitor solutions (100 μL) and incubated for 10 min prior to addition AChE (0.08 U/mL final concentration). After 10 min, the reactions were initialized with a DTNB:ATC (0.25 mM:0.5 mM final concentration, respectively) mixture (50 μL) in phosphate buffer (100 mM final concentration, pH 8.0 adjusted at rt). Conditions (c), (f), and (i): A mixture (50 μL) of AChE (0.08 U/mL final concentration) and $CuCl_2$ or $ZnCl_2$ or Aβ peptide (10 μM final concentration) (50 μL total) was added to the inhibitor solutions (100 μL). After 10 min, the reactions were initialized with a DTNB:ATC (0.25 mM:0.5 mM final concentration, respectively) mixture (50 μL) in phosphate buffer (100 mM final concentration, pH 8.0 adjusted at rt). IC_{50} values were determined as previously described (section 4.6.2.1) and are reported in Table 4.1. Outside of using BTC in lieu of ATC, all BChE experiments were performed as AChE experiments.

4.6.2.8. Molecular modeling

Compound **19** was built using the Sybyl-X software and minimized to 0.01 kcal/mol by the Powell method, using Gasteiger-Hückel charges and the Tripos force fields. The coordinates of AChE from *Torpedo californica* (*Tc*AChE) and $A\beta_{1\text{-}40}$ were downloaded

from the Protein Data Bank website (PDB codes: 1ACJ and 2LFM, respectively). The H_2O molecules and all other ligands were removed from the two proteins. Hydrogen atoms were added, and the energy of both proteins was minimized separately using the Amber force fields with Amber charges. The energy-optimized ligand (compound **19**) was then docked into the tacrine binding site in the energy minimized tacrine-free *Tc*AChE using GOLD.[45] The parameters were set as the default values for GOLD. The maximum distance between hydrogen bond donors and acceptors for hydrogen bonding was set to 3.5 Å. After docking, the first-ranked conformation of compound **19** was merged into the corresponding tacrine-free *Tc*AChE (to determine the proper binding area for $A\beta_{1\text{-}40}$ binding).

The energy-optimized Aβ was then docked close to the surface of *Tc*AChE using GOLD. A distance constraint was applied between the H6 residue of $A\beta_{1\text{-}40}$ and the Q74 of *Tc*AChE (that was chosen due to its vicinity to the metal-chelator portion of compound **19** in the compound **19**-*Tc*AChE complex). Here again, the parameters were set as the default values for GOLD. The maximum distance between hydrogen bond donors and acceptors for hydrogen bonding was set to 3.5 Å. After docking, the first-ranked conformation of $A\beta_{1\text{-}40}$ was merged into the corresponding tacrine-free *Tc*AChE. The new $A\beta_{1\text{-}40}$-*Tc*AChE complex was subsequently subjected to energy minimization using the Amber force fields with Amber charges. During the energy minimization, the structure of $A\beta_{1\text{-}40}$ and residues within a 7 Å radius were allowed to move. The remaining residues were kept frozen in order to save calculation time. The energy minimization was performed using the Powell method with a 0.05 kcal/mol energy gradient convergence criterion and a distance dependent dielectric function.

Finally, compound **19** was docked into the tacrine binding site in the obtained energy optimized $A\beta_{1\text{-}40}$-*Tc*AChE complex as described above. The first-ranked conformation of compound **19** was merged into the tacrine-free $A\beta_{1\text{-}40}$-*Tc*AChE complex (Fig. 4.7).

4.6.2.9. Parallel artificial membrane permeability assay adapted for blood-brain barrier (PAMPA-BBB)

Previously reported protocols with modification using the PAMPA Explorer kit (Pion, Inc.) were applied to our PAMPA-BBB experiment.[34,53,58,59] Each stock solution of the compounds was diluted to a final concentration of 10 μM (1% v/v final DMSO concentration) with pH 7.4 Prisma HT buffer (Pion). The resulting solution (200 μL) was added to each of the wells of the donor plate (number of replicates per sample = 12). The BBB-1 lipid (Pion formulation, 5 μL) was used to coat the polyvinylidene fluoride (PDVF, 0.45 μM) filter membrane on the acceptor plate. The acceptor plate was placed on the top of the donor plate generating a "sandwich," and each well of the acceptor plate was filled with the brain sink buffer (200 μL, Pion). The sandwich was incubated at rt for 4 h without stirring. A microplate reader was used to obtain the optical spectra (250-500 nm) of the solutions in the reference, acceptor, and donor plates. The $-\log P_e$ for each compound was calculated using the PAMPA Explorer software c. 3.5 (Pion). CNS+/– assignment was determined in comparison to compounds identified previously.[53,58,59] Compounds categorized as CNS+ have the ability to permeate through the BBB and target the CNS. Compounds categorized as CNS– have poor permeability through the BBB, and, therefore, their bioavailability into the CNS is considered to be minimal. All values (MW, *c*log*P*, HBA, HBD, PSA, logBB, and $-\log P_e$) for compounds **6h** and **16-19** are reported in Table 4.2.

4.7. References

(1) Thies, W.; Bleiler, L. *Alzheimers Dement* **2013**, *9*, 208-245.
(2) Schliebs, R.; Arendt, T. *J Neural Transm* **2006**, *113*, 1625-1644.
(3) Davis, K. L.; Powchik, P. *Lancet* **1995**, *345*, 625-630.
(4) Ames, D. J.; Bhathal, P. S.; Davies, B. M.; Fraser, J. R. E. *Lancet* **1988**, *331*, 887.
(5) Recanatini, M.; Cavalli, A.; Belluti, F.; Piazzi, L.; Rampa, A.; Bisi, A.; Gobbi, S.; Valenti, P.; Andrisano, V.; Bartolini, M.; Cavrini, V. *J Med Chem* **2000**, *43*, 2007-2018.
(6) da Costa, J. S.; Pisoni, D. S.; da Silva, C. B.; Petzhold, C. L.; Russowsky, D.; Ceschi, M. A. *J Braz Chem Soc* **2009**, *20*, 1448-1454.
(7) Fang, L.; Kraus, B.; Lehmann, J.; Heilmann, J.; Zhang, Y.; Decker, M. *Bioorg Med Chem Lett* **2008**, *18*, 2905-2909.

(8) Fernandez-Bachiller, M. I.; Perez, C.; Gonzalez-Munoz, G. C.; Conde, S.; Lopez, M. G.; Villarroya, M.; Garcia, A. G.; Rodriguez-Franco, M. I. *J Med Chem* **2010**, *53*, 4927-4937.
(9) Bornstein, J. J.; Eckroat, T. J.; Houghton, J. L.; Jones, C. K.; Green, K. D.; Garneau-Tsodikova, S. *Med Chem Commun* **2011**, *2*, 406-412.
(10) Chen, Y.; Sun, J.; Fang, L.; Liu, M.; Peng, S.; Liao, H.; Lehmann, J.; Zhang, Y. *J Med Chem* **2012**, *55*, 4309-4321.
(11) Antequera, D.; Bolos, M.; Spuch, C.; Pascual, C.; Ferrer, I.; Fernandez-Bachiller, M. I.; Rodriguez-Franco, M. I.; Carro, E. *Neurobiol Dis* **2012**, *46*, 682-691.
(12) Eckroat, T. J.; Green, K. D.; Reed, R. A.; Bornstein, J. J.; Garneau-Tsodikova, S. *Bioorg Med Chem* **2013**, *21*, 3614-3623.
(13) Hardy, J. A.; Higgins, G. A. *Science* **1992**, *256*, 184-185.
(14) Wang, Y. J.; Zhou, H. D.; Zhou, X. F. *Drug Discov Today* **2006**, *11*, 931-938.
(15) Haass, C.; Selkoe, D. J. *Nat Rev Mol Cell Biol* **2007**, *8*, 101-112.
(16) Jakob-Roetne, R.; Jacobsen, H. *Angew Chem Int Ed Engl* **2009**, *48*, 3030-3059.
(17) Kurz, A.; Perneczky, R. *J Alzheimers Dis* **2011**, *24 Suppl 2*, 61-73.
(18) Inestrosa, N. C.; Alvarez, A.; Perez, C. A.; Moreno, R. D.; Vicente, M.; Linker, C.; Casanueva, O. I.; Soto, C.; Garrido, J. *Neuron* **1996**, *16*, 881-891.
(19) Alvarez, A.; Alarcon, R.; Opazo, C.; Campos, E. O.; Munoz, F. J.; Calderon, F. H.; Dajas, F.; Gentry, M. K.; Doctor, B. P.; De Mello, F. G.; Inestrosa, N. C. *J Neurosci* **1998**, *18*, 3213-3223.
(20) De Ferrari, G. V.; Canales, M. A.; Shin, I.; Weiner, L. M.; Silman, I.; Inestrosa, N. C. *Biochemistry* **2001**, *40*, 10447-10457.
(21) Dvir, H.; Silman, I.; Harel, M.; Rosenberry, T. L.; Sussman, J. L. *Chem Biol Interact* **2010**, *187*, 10-22.
(22) Rydberg, E. H.; Brumshtein, B.; Greenblatt, H. M.; Wong, D. M.; Shaya, D.; Williams, L. D.; Carlier, P. R.; Pang, Y. P.; Silman, I.; Sussman, J. L. *J Med Chem* **2006**, *49*, 5491-5500.
(23) Bourne, Y.; Radic, Z.; Kolb, H. C.; Sharpless, K. B.; Taylor, P.; Marchot, P. *Chem Biol Interact* **2005**, *157-158*, 159-165.
(24) Bartolini, M.; Bertucci, C.; Cavrini, V.; Andrisano, V. *Biochem Pharmacol* **2003**, *65*, 407-416.
(25) Musial, A.; Bajda, M.; Malawska, B. *Curr Med Chem* **2007**, *14*, 2654-2679.
(26) Mehta, M.; Adem, A.; Sabbagh, M. *Int J Alzheimers Dis* **2012**, *2012*, 728983.
(27) Pithadia, A. S.; Lim, M. H. *Curr Opin Chem Biol* **2012**, *16*, 67-73.
(28) Faller, P.; Hureau, C. *Dalton Trans* **2009**, 1080-1094.
(29) Drew, S. C.; Barnham, K. J. *Acc Chem Res* **2011**, *44*, 1146-1155.
(30) Scott, L. E.; Orvig, C. *Chem Rev* **2009**, *109*, 4885-4910.
(31) Savelieff, M. G.; Lee, S.; Liu, Y.; Lim, M. H. *ACS Chem Biol* **2013**, *8*, 856-865.
(32) Hureau, C. *Coord Chem Rev* **2012**, *256*, 2164-2174.
(33) Hureau, C.; Dorlet, P. *Coord Chem Rev* **2012**, *256*, 2175-2187.
(34) Choi, J. S.; Braymer, J. J.; Nanga, R. P.; Ramamoorthy, A.; Lim, M. H. *Proc Natl Acad Sci U S A* **2010**, *107*, 21990-21995.
(35) Ellman, G. L.; Courtney, K. D.; Andres, V., Jr.; Feather-Stone, R. M. *Biochem Pharmacol* **1961**, *7*, 88-95.

(36) Gregor, V. E.; Emmerling, M. R.; Lee, C.; Moore, C. J. *Bioorg Med Chem Lett* **1992**, *2*, 861-864.
(37) Mao, F.; Huang, L.; Luo, Z.; Liu, A.; Lu, C.; Xie, Z.; Li, X. *Bioorg Med Chem* **2012**, *20*, 5884-5892.
(38) Camps, P.; Formosa, X.; Galdeano, C.; Munoz-Torrero, D.; Ramirez, L.; Gomez, E.; Isambert, N.; Lavilla, R.; Badia, A.; Clos, M. V.; Bartolini, M.; Mancini, F.; Andrisano, V.; Arce, M. P.; Rodriguez-Franco, M. I.; Huertas, O.; Dafni, T.; Luque, F. J. *J Med Chem* **2009**, *52*, 5365-5379.
(39) Luo, W.; Li, Y. P.; He, Y.; Huang, S. L.; Tan, J. H.; Ou, T. M.; Li, D.; Gu, L. Q.; Huang, Z. S. *Bioorg Med Chem* **2011**, *19*, 763-770.
(40) Fernandez-Bachiller, M. I.; Perez, C.; Monjas, L.; Rademann, J.; Rodriguez-Franco, M. I. *J Med Chem* **2012**, *55*, 1303-1317.
(41) Muraoka, S.; Miura, T. *Life Sci* **2009**, *84*, 272-277.
(42) Braymer, J. J.; Merrill, N. M.; Lim, M. H. *Inorg Chim Acta* **2012**, *380*, 261-268.
(43) Wang, Y.; Wang, F.; Yu, J. P.; Jiang, F. C.; Guan, X. L.; Wang, C. M.; Li, L.; Cao, H.; Li, M. X.; Chen, J. G. *Bioorg Med Chem* **2012**, *20*, 6513-6522.
(44) Pi, R.; Mao, X.; Chao, X.; Cheng, Z.; Liu, M.; Duan, X.; Ye, M.; Chen, X.; Mei, Z.; Liu, P.; Li, W.; Han, Y. *PLoS One* **2012**, *7*, e31921.
(45) Verdonk, M. L.; Cole, J. C.; Hartshorn, M. J.; Murray, C. W.; Taylor, R. D. *Proteins* **2003**, *52*, 609-623.
(46) Harel, M.; Schalk, I.; Ehret-Sabatier, L.; Bouet, F.; Goeldner, M.; Hirth, C.; Axelsen, P. H.; Silman, I.; Sussman, J. L. *Proc Natl Acad Sci U S A* **1993**, *90*, 9031-9035.
(47) Vivekanandan, S.; Brender, J. R.; Lee, S. Y.; Ramamoorthy, A. *Biochem Biophys Res Commun* **2011**, *411*, 312-316.
(48) Fernandez-Bachiller, M. I.; Perez, C.; Campillo, N. E.; Paez, J. A.; Gonzalez-Munoz, G. C.; Usan, P.; Garcia-Palomero, E.; Lopez, M. G.; Villarroya, M.; Garcia, A. G.; Martinez, A.; Rodriguez-Franco, M. I. *ChemMedChem* **2009**, *4*, 828-841.
(49) da Silva, C. H.; Campo, V. L.; Carvalho, I.; Taft, C. A. *J Mol Graph Model* **2006**, *25*, 169-175.
(50) Alies, B.; Bijani, C.; Sayen, S.; Guillon, E.; Faller, P.; Hureau, C. *Inorg Chem* **2012**, *51*, 12988-13000.
(51) Lipinski, C. A.; Lombardo, F.; Dominy, B. W.; Feeney, P. J. *Adv Drug Deliv Rev* **2001**, *46*, 3-26.
(52) Clark, D. E.; Pickett, S. D. *Drug Discov Today* **2000**, *5*, 49-58.
(53) Di, L.; Kerns, E. H.; Fan, K.; McConnell, O. J.; Carter, G. T. *Eur J Med Chem* **2003**, *38*, 223-232.
(54) Spuch, C.; Antequera, D.; Isabel Fernandez-Bachiller, M.; Isabel Rodriguez-Franco, M.; Carro, E. *Neurotox Res* **2010**, *17*, 421-431.
(55) Landa, A.; Minkkila, A.; Blay, G.; Jorgensen, K. A. *Chemistry* **2006**, *12*, 3472-3483.
(56) Hamon, F.; Largy, E.; Guedin-Beaurepaire, A.; Rouchon-Dagois, M.; Sidibe, A.; Monchaud, D.; Mergny, J. L.; Riou, J. F.; Nguyen, C. H.; Teulade-Fichou, M. P. *Angew Chem Int Ed Engl* **2011**, *50*, 8745-8749.
(57) Hindo, S. S.; Mancino, A. M.; Braymer, J. J.; Liu, Y.; Vivekanandan, S.; Ramamoorthy, A.; Lim, M. H. *J Am Chem Soc* **2009**, *131*, 16663-16665.
(58) Avdeef, A.; Bendels, S.; Di, L.; Faller, B.; Kansy, M.; Sugano, K.; Yamauchi, Y. *J Pharm Sci* **2007**, *96*, 2893-2909.

(59) *Pion, Inc. BBB protocol and test compounds,* **2009**.

Note:
This chapter is adapted from a published article: Kochi, A.*; **Eckroat, T. J.***; Green, K. D.; Mayhoub, A. S.; Lim, M. H.; Garneau-Tsodikova, S. *Chem Sci* **2013**, *4*, 4137-4145.
*Denotes equal contribution.

Authors' contribution:
TJE synthesized all compounds.
AK performed all metal binding, Aβ, and blood-brain barrier experiments.
KDG performed all enzyme inhibition assays.
ASM performed molecular modeling.
TJE, AK, KDG, ASM, MHL, and SGT analyzed data and wrote manuscript.

4.8 Appendix

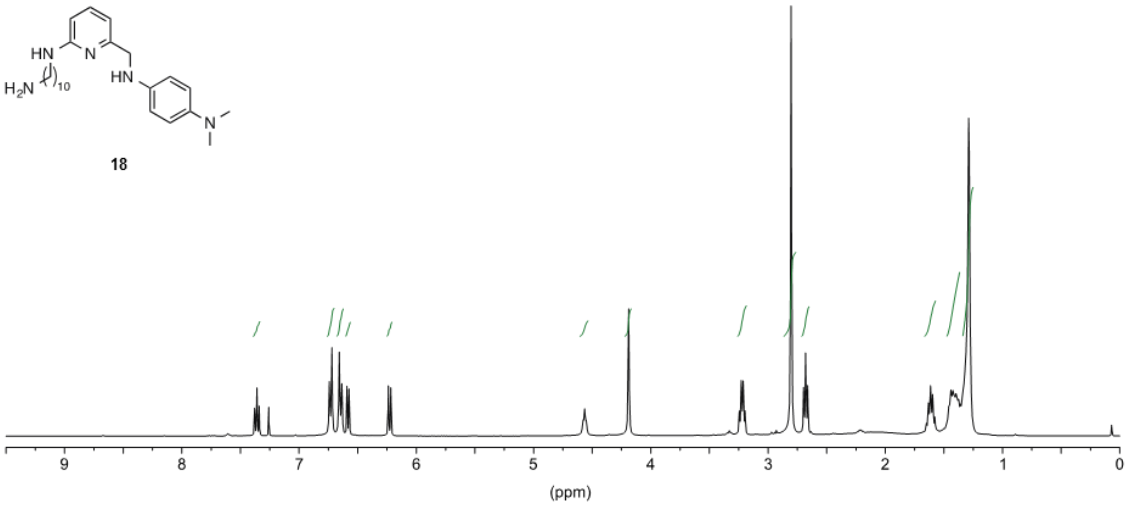

Fig. 4.8. ^{1}H NMR in $CDCl_3$ for compound **18**.

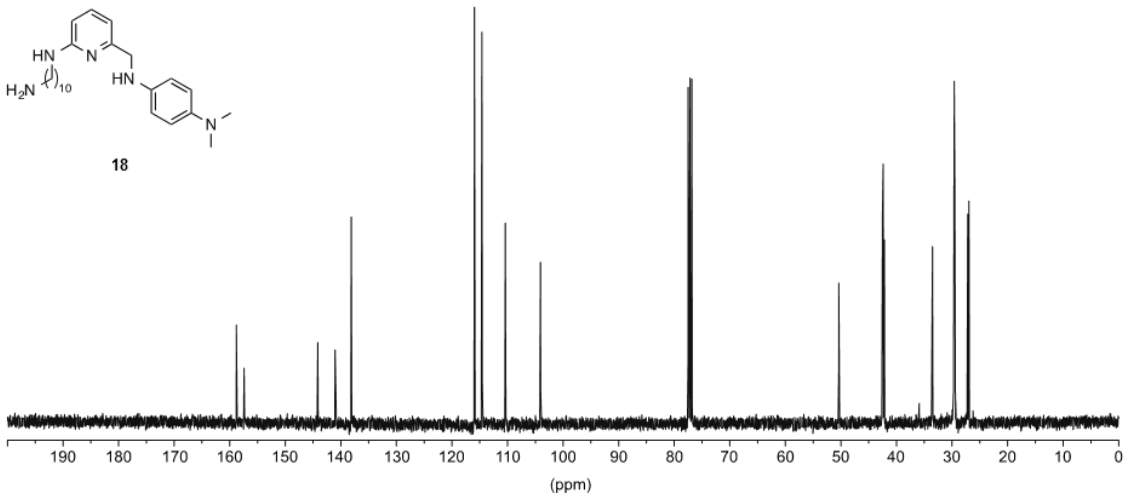

Fig. 4.9. ^{13}C NMR in $CDCl_3$ for compound **18**.

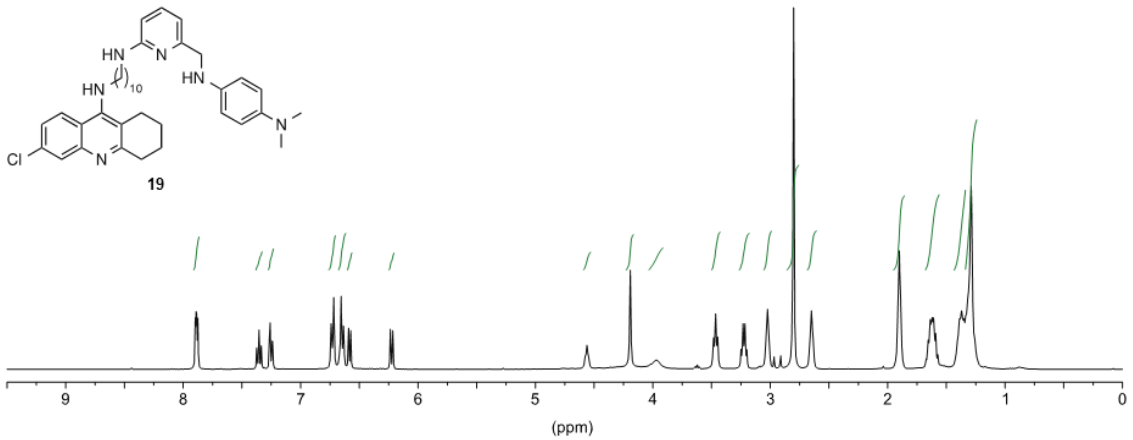

Fig. 4.10. ^{1}H NMR in $CDCl_3$ for compound **19**.

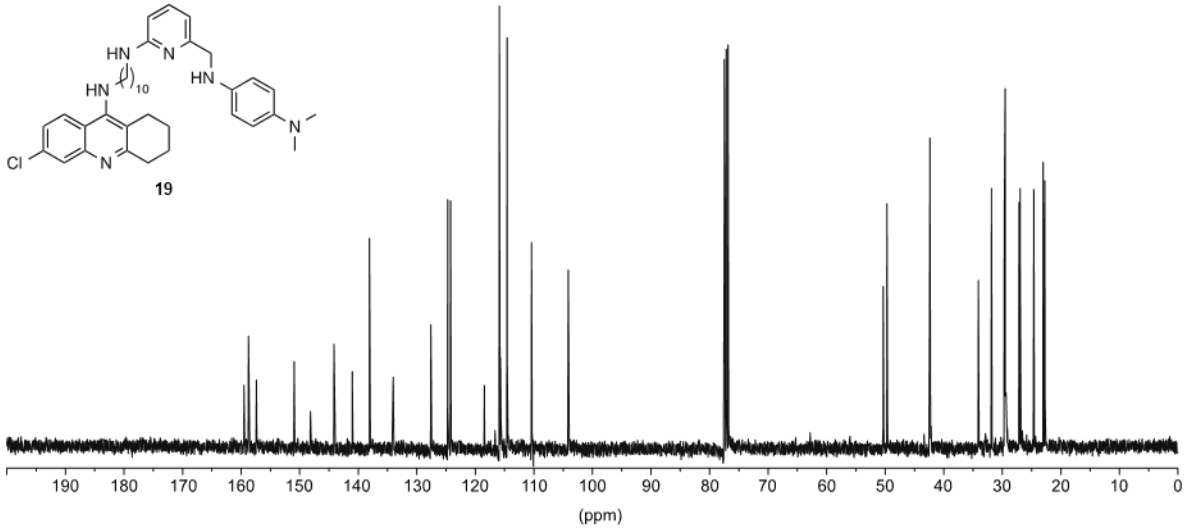

Fig. 4.11. ^{13}C NMR in $CDCl_3$ for compound **19**.

Chapter 5

Future directions

The worked described in this dissertation represents a significant contribution to the multifunctional hybrid approach for the treatment of AD. In chapter 2, novel series of tacrine- and 6-chlorotacrine-mefenamic acid hybrids were synthesized and evaluated for AChE inhibition under standard conditions and in the presence of ROS. Several highly potent AChEis with low nanomolar IC_{50} values were identified. As intended, many compounds from these series showed improvement in IC_{50} in the presence of ROS. These results have never been seen in a tacrine hybrid before, and the improved IC_{50} in the presence of ROS may have unique *in vivo* implications. The most potent compound identified was **13m** (IC_{50} = 0.418 ± 0.025 nM, ROS IC_{50} = 0.009 ± 0.003 nM), which exhibited >100-fold increase in potency under standard conditions and >20,000-fold increase in the presence of ROS when compared to tacrine (**1**). This compound represents one of the most potent tacrine hybrids described to date.

Further study of tacrine-mefenamic acid hybrids is warranted. It was hypothesized the formation of a nitrogen radical on the mefenamic acid moiety was responsible for the increases in potency in the presence of ROS. To further test this idea, analogs could be synthesized that prevent the formation of this radical. It is anticipated that such analogs would not show the dramatic increases in potency in the presence of ROS. Initial synthesis of several *N*-methylated analogs has already been accomplished. Surprisingly, these analogs still remain highly potent in the presence of ROS (data not shown) indicating that factors other than formation of a nitrogen radical on the mefenamic acid moiety may be responsible for the increase in potency. Further studies will aim to more fully elucidate this interaction.

Additional studies of **13m**, the most potent tacrine-mefenamic acid hybrid identified, are needed to further explore its potential as an anti-AD compound. For example, it remains to be seen if **13m** is also a potent inhibitor of BChE, which may be important for an anti-AD compound as described in chapter 4. Also, while modeling studies suggested that **13m** was capable of interacting with and blocking with the PAS, this remains to be proven experimentally. The propidium displacement assay, which has been successfully used to determine the ability of tacrine-melatonin hybrids to interact with the PAS,[1] could be used for this purpose. Additionally, because of its suspected ability to block the PAS, **13m** could be tested for its ability to inhibit AChE-induced Aβ aggregation using an assay that has been well-established in the literature.[1-4] Beyond that, **13m** could be tested for drug-like properties, such as BBB permeability and metabolic stability, and optimized as needed. An optimized version of **13m** could then be evaluated in whole cell viability and neuroprotection assays to determine toxicity, therapeutic safety range, and ability to protect cells from oxidative stress and Aβ-induced toxicities. Ultimately, favorable results in these assays may lead to studies using animal models of AD.

In chapter 3, three series of 6-chlorotacrine with linkers varying in terminal functional group and length were synthesized, evaluated for AChE inhibition, and compared to tacrine and 6-chlorotacrine-mefenamic acid hybrids. Several highly potent molecules (low nanomolar IC_{50} values) comprised of linkers with terminal amines were identified. Additionally, the need for covalent linkage of mefenamic acid in regards to AChE inhibition was investigated. Results suggest that the mefenamic acid moiety in an amine-linked tacrine-mefenamic acid hybrid may not contribute to AChE inhibition under standard conditions, and the linker moiety alone may be responsible for the increase in potency relative to tacrine. However, in the presence of ROS, there may be some advantage to covalent linkage of the mefenamic acid moiety in amine-linked tacrine-mefenamic acid hybrids. This study represents the first extensive study of the linker moiety and requirement for covalent linkage in tacrine hybrids. The methodology used in this study will be employed in future work to more fully elucidate the need for covalent linkage in other multifunctional hybrids for AD.

In chapter 4, 6-chlorotacrine-metal-Aβ modulator hybrid **19** was synthesized and evaluated *in vitro*. Hybrid **19** displayed potent inhibition of AChE (IC_{50} = 2.37 ± 0.29 nM) and BChE (IC_{50} = 2.01 ± 0.12 nM). Potent inhibition was largely retained in the presence of ROS, Cu^{2+}/Zn^{2+}, and Aβ. Testing of inhibition in the presence of ROS, Cu^{2+}/Zn^{2+}, and Aβ has never been previously reported for a tacrine hybrid. Additionally, **19** showed remarkable multifunctionality through interaction with Cu^{2+}/Zn^{2+}, control of metal-free and metal-induced Aβ aggregate assembly, and disaggregation of preformed metal-free and metal-associated Aβ aggregates, while PAMPA-BBB predicted the BBB penetrability of **19**. Hybrid **19** represents one of the few tacrine hybrids designed to specifically target the interplay of AChE/Aβ/metals, and no other tacrine hybrids have been tested in the aggregation and disaggregation assays described in this work. Together, these results make hybrid **19** a worthy candidate for additional studies, and future directions will largely focus on further understanding and improving the properties of this compound.

First, the length of the linker in **19** will be optimized for AChE inhibition and AChE/Aβ/metal interaction. As mentioned in chapter 4, the linker length was chosen based on the results seen with tacrine-mefenamic acid hybrids. However, it remains to be seen if the decamethylene linker gives optimal results for **19** in the biochemical assays used. Analogs with shorter and longer linker lengths will be synthesized and tested for this reason. Also, the structure activity relationship (SAR) between **19** and Aβ will be established. The -$N(CH_3)_2$ group of **19** will be replaced with -$NHCH_3$, -NH_2, and -H groups to determine how the degree of methylation affects the interaction of the hybrid with Aβ species. It has been previously established in the literature that the -$N(CH_3)_2$ group is essential for Aβ interaction when the metal-Aβ modulating moiety **17** is tested alone.[5] However, it remains to be established if the same is true in the hybrid molecule, but it is anticipated that analogs with greater degrees of methylation will show greater interaction with Aβ peptide. It is also remains to be seen how the degree of methylation affects AChE/BChE inhibition, although it is anticipated that the effects will be minimal given the predicted binding of the compound. Syntheses of the required hybrids are in various stages

of completion, and similar biochemical, biophysical, and computational methods as employed previously will be used to determine this SAR.

Additionally, the drug-like properties of hybrid **19** will be improved. For example, it is anticipated that replacing the polymethylene linker with a polyethylene glycol linker of similar length will decrease lipophilicity and increase overall aqueous solubility of the compound. Replacement of the pyridine ring of **19** with a pyrimidine ring is another possible modification with anticipated similar effects. Increased aqueous solubility may provide better performance in biochemical assays (e.g. quantifying interaction of **19** with Cu^{2+}/Zn^{2+}) in the short-term, and better performance in whole cell or animal studies in the long-term. Syntheses of these hybrids are in preliminary and planning stages. As another example, through collaboration with Dr. Mayland Chang (University of Notre Dame), we have found that **19** is susceptible to metabolism primarily through *N*-dealkylation (data not shown). Chemical strategies to combat this metabolism are currently being devised. In addition, while PAMPA-BBB predicted **19** should be BBB permeable via passive diffusion, it remains to be established whether **19** is a substrate for active transport into or P-glycoprotein efflux from the CNS. Hybrid **19** will be assessed in cell-based *in vitro* assays for BBB permeability to more accurately predict access to the CNS and chemical modifications will be made as needed. An optimized version of **19** could then be evaluated in whole cell viability and neuroprotection assays, ultimately progressing to animal studies if favorable results are obtained.

Another possible direction includes replacement of the 6-chlorotacrine moiety of hybrid **19** with donepezil. While the initial biochemical characterization of **19** was very promising, this hybrid may ultimately fail in more advanced studies because it contains 6-chlorotacrine as the core AChEi, which, as described previously, is hepatotoxic and clinically irrelevant. It is anticipated that replacement of the 6-chlorotacrine moiety of hybrid **19** with a donepezil moiety will create a second generation hybrid with similar biochemical properties and multifunctionality that might ultimately be better suited for future *in vivo* studies. The synthesis of a donepezil moiety with a suitable linkage point has been completed. However, chemically linking this moiety with the metal-Aβ modulating moiety

17 has posed some synthetic difficulties, and various strategies are being tested. Similar biochemical, biophysical, and computational methods as employed previously will be used to determine proper linker length and overall properties of this donepezil-metal-Aβ modulator hybrid.

Finally, if the donepezil hybrid proposed above is successful, metal-Aβ modulator moieties distinct from **17** will be sought for incorporation into novel donepezil-metal-Aβ modulator hybrids. One such metal-Aβ modulator is myricetin, a naturally occurring flavonoid with multiple metal chelation sites that has been shown to modulate production of metal-triggered Aβ aggregates, disassemble structured metal-Aβ aggregates, and modulate metal-Aβ toxicity in human neuroblastoma cells.[6] It is anticipated that a donepezil-myricetin hybrid may show additional beneficial properties for AD, among them AChE/BChE inhibition. Synthesis of this hybrid is in preliminary and planning stages. Similar biochemical, biophysical, and computational methods as employed previously will be used to determine proper linker length and overall properties of this donepezil-myricetin hybrid.

References

(1) Fernandez-Bachiller, M. I.; Perez, C.; Campillo, N. E.; Paez, J. A.; Gonzalez-Munoz, G. C.; Usan, P.; Garcia-Palomero, E.; Lopez, M. G.; Villarroya, M.; Garcia, A. G.; Martinez, A.; Rodriguez-Franco, M. I. *ChemMedChem* **2009**, *4*, 828-841.

(2) Rydberg, E. H.; Brumshtein, B.; Greenblatt, H. M.; Wong, D. M.; Shaya, D.; Williams, L. D.; Carlier, P. R.; Pang, Y. P.; Silman, I.; Sussman, J. L. *J Med Chem* **2006**, *49*, 5491-5500.

(3) Bartolini, M.; Bertucci, C.; Cavrini, V.; Andrisano, V. *Biochem Pharmacol* **2003**, *65*, 407-416.

(4) Bartolini, M.; Bertucci, C.; Bolognesi, M. L.; Cavalli, A.; Melchiorre, C.; Andrisano, V. *Chembiochem* **2007**, *8*, 2152-2161.

(5) Choi, J. S.; Braymer, J. J.; Nanga, R. P.; Ramamoorthy, A.; Lim, M. H. *Proc Natl Acad Sci U S A* **2010**, *107*, 21990-21995.

(6) DeToma, A. S.; Choi, J. S.; Braymer, J. J.; Lim, M. H. *Chembiochem* **2011**, *12*, 1198-1201.